A class of mixed finite element methods based on the Helmholtz decomposition in computational mechanics

DISSERTATION

zur Erlangung des akademischen Grades
doctor rerum naturalium (Dr. rer. nat.)
im Fach Mathematik

eingereicht an der
Mathematisch-Naturwissenschaftlichen Fakultät
der Humboldt-Universität zu Berlin

von

Dipl.-Math. Mira Schedensack

Präsident der Humboldt-Universität zu Berlin
Prof. Dr. Jan-Hendrik Olbertz

Dekan der Mathematisch-Naturwissenschaftlichen Fakultät
Prof. Dr. Elmar Kulke

Gutachter:
1. Prof. Dr. Carsten Carstensen, Humboldt-Universität zu Berlin
2. Prof. Dr. Daniele Boffi, Università degli Studi di Pavia
3. Prof. Dr. Daya Reddy, University of Cape Town

Tag der Verteidigung: 25. Juni 2015

Zusammenfassung

Die Konstruktion nichtkonformer Finite-Elemente-Methoden (FEMn) für die numerische Behandlung partieller Differentialgleichungen aus der Mechanik geht bis in die 1960er Jahre zurück und ist motiviert durch robuste Diskretisierungen für fast-inkompressible Materialien in der Festkörpermechanik, durch punktweise divergenzfreie Ansatzfunktionen in der Strömungslehre und durch einfachere Ansatzräume für Probleme höherer Ordnungen wie das biharmonische Problem für die Kirchhoff-Platte in der Strukturmechanik. Eine natürliche Verallgemeinerung auf höhere Polynomgrade, die die wesentlichen Eigenschaften der Diskretisierungen erhält, ist bisher nicht gelungen.

Diese Dissertation verallgemeinert die nichtkonformen FEMn nach Morley und Crouzeix und Raviart durch neue gemischte Formulierungen für das Poisson-Problem, die Stokes-Gleichungen, die Navier-Lamé-Gleichungen der linearen Elastizität und m-Laplace-Gleichungen der Form $(-1)^m \Delta^m u = f$ für beliebiges $m = 1, 2, 3, \ldots$ Diese Formulierungen beruhen auf Helmholtz-Zerlegungen, die ein unstrukturiertes Vektorfeld zerlegen in ein Gradienten- und ein Rotationsfeld. Die neuen Formulierungen gestatten die Verwendung von Ansatzräumen beliebigen Polynomgrades und ihre Diskretisierungen stimmen für den niedrigsten Polynomgrad mit den genannten nicht-konformen FEMn überein. Auch für höhere Polynomgrade ergeben sich robuste Diskretisierungen für fast-inkompressible Materialien und Approximationen für die Lösungen der Stokes-Gleichungen, die punktweise die Masse erhalten. Dieser Ansatz erlaubt außerdem eine Verallgemeinerung der nichtkonformen FEMn von der Poisson- und der biharmonischen Gleichung auf m-Laplace-Gleichungen für beliebiges $m \geq 3$. Ermöglicht wird dies durch eine neue Helmholtz-Zerlegung für tensorwertige Funktionen. Die in dieser Dissertation vorgestellten neuen Diskretisierungen lassen sich nicht nur für beliebiges m einheitlich implementieren, sondern sie erlauben auch Ansatzräume niedrigster Ordnung, beispielsweise stückweise affine Polynome für beliebiges m.

Hat eine Lösung der betrachteten Probleme Singularitäten, so beeinträchtigt dies in der Regel die Konvergenz so stark, dass höhere Polynomgrade in den Ansatzräumen auf uniformen Gittern dieselbe Konvergenzrate zeigen wie niedrigere Polynomgrade. Deshalb sind gerade für höhere Polynomgrade in den Ansatzräumen adaptiv generierte Gitter unabdingbar. Neben der A-priori- und der A-posteriori-Analysis werden in dieser Dissertation optimale Konvergenzraten für adaptive Algorithmen für die neuen Diskretisierungen des Poisson-Problems, der Stokes-Gleichungen und der m-Laplace-Gleichung bewiesen. Diese werden auch in den numerischen Beispielen dieser Dissertation empirisch nachgewiesen.

Abstract

The construction of non-conforming finite element methods (FEMs) for the numerical treatment of partial differential equations arising in mechanics dates back to the 1960s and is motivated by robust discretizations for almost incompressible materials in solid mechanics, by pointwise divergence-free ansatz functions in fluid mechanics, and by low-order ansatz spaces for higher-order problems as the biharmonic problem for the Kirchhoff plate in structural mechanics. A natural generalization to higher polynomial degrees which preserves the inherent properties of the discretizations is not known so far.

This thesis generalizes the non-conforming FEMs of Morley and Crouzeix and Raviart by novel mixed formulations for the Poisson problem, the Stokes equations, the Navier-Lamé equations of linear elasticity, and mth-Laplace equations of the form $(-1)^m \Delta^m u = f$ for arbitrary $m = 1, 2, 3, \ldots$ These formulations are based on Helmholtz decompositions which decompose an unstructured vector field into a gradient and a curl. The new formulations allow for ansatz spaces of arbitrary polynomial degree and its discretizations coincide with the mentioned non-conforming FEMs for the lowest polynomial degree. Also for higher polynomial degrees, this results in robust discretizations for almost incompressible materials and approximations of the solution of the Stokes equations with pointwise mass conservation. Furthermore this approach also allows for a generalization of the non-conforming FEMs for the Poisson problem and the biharmonic equation to mth-Laplace equations for arbitrary $m \geq 3$. A new Helmholtz decomposition for tensor-valued functions enables this. The discretizations presented in this thesis allow not only for a uniform implementation for arbitrary m, but they also allow for lowest-order ansatz spaces, e.g., piecewise affine polynomials for arbitrary m.

The presence of singularities usually affects the convergence such that higher polynomial degrees in the ansatz spaces show the same convergence rate on uniform meshes as lower polynomial degrees. Therefore adaptive mesh-generation is indispensable especially for ansatz spaces of higher polynomial degree. Besides the a priori and a posteriori analysis, this thesis proves optimal convergence rates for adaptive algorithms for the new discretizations of the Poisson problem, the Stokes equations, and mth-Laplace equations. This is also demonstrated in the numerical experiments of this thesis.

Contents

1. Introduction

Non-conforming finite element methods (FEMs) play an important role in computational mechanics. They allow the discretization of partial differential equations (PDEs) for incompressible fluid flows modelled in the Stokes equations, for almost incompressible materials in linear elasticity, and for low polynomial degrees in the ansatz spaces for the Kirchhoff plate problem. A generalization to higher polynomial degrees which also transfers the desirable properties of the scheme, however, has been an open question. This thesis introduces novel formulations based on Helmholtz-type decompositions along with their discretizations of arbitrary (globally fixed) polynomial degree for the Poisson equation, for higher-order equations of the form $(-1)^m \Delta^m u = f$, for the Stokes equations, and for the Navier-Lamé equations of linear elasticity. For the lowest-order polynomial degree, discrete Helmholtz decompositions of Arnold and Falk [1989] and Carstensen et al. [2013c, 2014b] prove equivalence of the novel discretizations to the known famous non-conforming FEMs of Crouzeix and Raviart [1973] for the Poisson and Stokes equations and the Morley FEM [Morley, 1968] for the biharmonic problem $\Delta^2 u = f$. In the context of the novel (mixed) formulations, these discretizations appear to be conforming. The new generalization to higher polynomial degrees proposed in this thesis appears to be natural in the sense that the inherent properties of the lowest order discretization carry over to higher polynomial ansatz spaces, namely an inf-sup condition, the conformity of the method, and a crucial projection property (also known as integral mean property of the non-conforming interpolation operator).

In this introduction, the idea of the novel FEMs of this thesis shall be briefly sketched for the Poisson equation $-\Delta u = f$. The Helmholtz decomposition (also called Hodge decomposition)

$$L^2(\Omega;\mathbb{R}^2) = \nabla H_0^1(\Omega) \oplus \operatorname{Curl} H^1(\Omega)$$

(which is orthogonal) allows a characterization of the set of gradients of $H_0^1(\Omega)$ functions as

$$\nabla H_0^1(\Omega) = (\operatorname{Curl} H^1(\Omega))^{\perp_{L^2(\Omega)}}$$

and so characterizes the gradient of the solution of the Poisson equation by

$$-\operatorname{div} p = f \qquad \text{and} \qquad p \perp_{L^2(\Omega)} \operatorname{Curl} H^1(\Omega). \tag{1.1}$$

The first equality in (1.1) is discretized with the help of a function $\varphi \in H(\operatorname{div},\Omega)$ that fulfils $-\operatorname{div}\varphi = f$. Then p is characterized by

$$(\varphi - p) \perp_{L^2(\Omega)} \nabla H_0^1(\Omega) \qquad \text{and} \qquad p \perp_{L^2(\Omega)} \operatorname{Curl} H^1(\Omega)$$

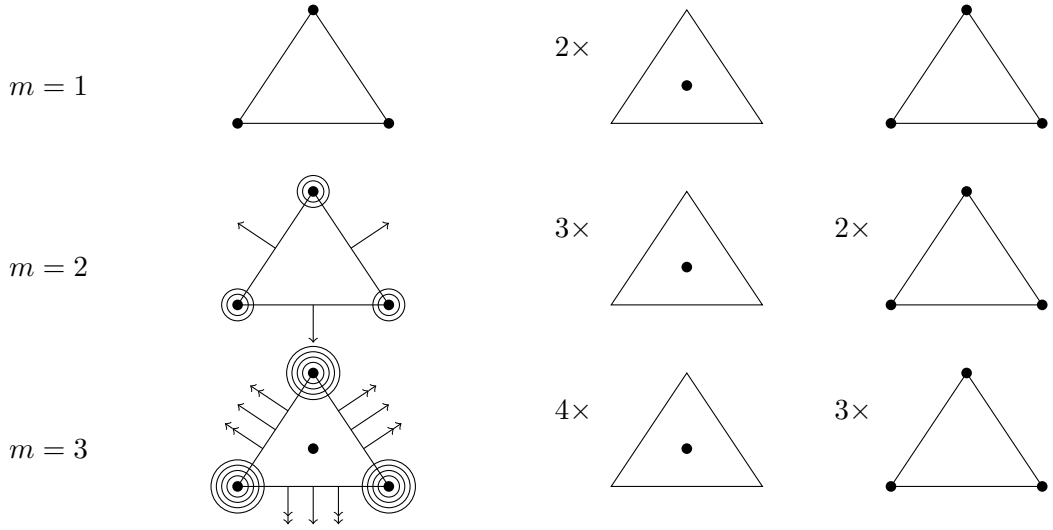

Figure 1.1.: Lowest order standard conforming [Ciarlet, 1978, Ženíšek, 1970] and novel FEMs for the problem $(-1)^m \Delta^m u = f$ for $m = 1, 2, 3$.

and is known as the Helmholtz projection of φ. The discrete problem then is to decompose φ (more precisely, the L^2 projection of φ to piecewise polynomials of degree $\leq k$) in p_h with

$$p_h \perp_{L^2(\Omega)} \operatorname{Curl}(P_{k+1}(\mathcal{T}) \cap H^1(\Omega)) \tag{1.2}$$

and some $\operatorname{Curl} \alpha_h$. For the lowest order case $k = 0$, it turns out that the orthogonality in (1.2) implies that p_h is a non-conforming gradient of a Crouzeix-Raviart function [Crouzeix and Raviart, 1973]. Therefore, the new discretization generalizes this FEM to higher polynomial ansatz spaces.

The difference to standard mixed FEMs is that they do not use the orthogonality (1.1) for the discretization, but rather ask for $p_h = \nabla_h u_h$ for some u_h and some *discrete gradient* ∇_h [Huang and Xu, 2012], e.g., $(p_h, q_h)_{L^2(\Omega)} = -(u_h, \operatorname{div} q_h)_{L^2(\Omega)}$ for all q_h in the mixed ansatz space. In the FEMs proposed in this thesis, (1.2) means that p_h is a gradient in a *discrete orthogonal* sense.

A similar approach as for the Poisson problem is possible for mth-Laplace equations of the form

$$(-1)^m \Delta^m u = f. \tag{1.3}$$

Standard conforming FEMs require ansatz spaces in $H_0^m(\Omega)$. To circumvent those high regularity requirements and resulting complicated finite elements, non-standard methods are of high interest [Morley, 1968, Engel et al., 2002, Brenner, 2012]. The novel Helmholtz decomposition of Chapter 6 decomposes any (tensor-valued) L^2 function in an mth derivative and a symmetric part of a Curl. This ansatz generalizes Crouzeix and Raviart [1973] and Morley [1968] to $m \geq 3$ and higher polynomial

```
function SYSTEM_MATRIX = computeSystemMatrix(m,A1,B1,B2)

nComponents = (1+m);
nX = size(A1,1); % dimension of scalar-valued discontinous P_k space
A = sparse(nComponents*nX,nComponents*nX);
for j=0:nComponents-1;
    A(j*nX+(1:nX),j*nX+(1:nX)) = nchoosek(m,j) * A1; end
nY=size(B1,2);  % dimension of scalar-valued continous P_{k+1} space
B = sparse(nComponents*nX,(nComponents-1)*nY);
for j=0:nComponents-2
    B(j*nX+(1:nX),j*nY+(1:nY)) = nchoosek(m-1,j) * B1;
    B((j+1)*nX+(1:nX),j*nY+(1:nY)) = nchoosek(m-2,j) * B2; end
SYSTEM_MATRIX = [A,B;B',sparse(size(B,2),size(B,2))];
```

Figure 1.2.: Assembling of system matrix for $(-1)^m \Delta^m u = f$ for arbitrary m.

ansatz spaces (see Subsections 3.1.3 and 6.4.3). The direct approximation of $D^m u$ instead of u enables low order discretizations; only first derivatives appear in the symmetric part of the Curl and so the lowest order approach only requires piecewise affine functions. In contrast to that, even interior penalty methods require piecewise quadratic [Brenner, 2012] resp. piecewise cubic [Gudi and Neilan, 2011] functions for $m = 2$ resp. $m = 3$. Mnemonic diagrams in Figure 1.1 illustrate lowest-order standard conforming FEMs and the lowest-order novel FEMs proposed in this thesis for $m = 1, 2, 3$. Since the proposed new FEMs differ only in the number of components in the ansatz spaces, an implementation of one single program, which runs for arbitrary order, is possible. This is demonstrated in Figure 1.2 with the following notation. Let `A1` denote the standard global mass matrix of scalar discontinous piecewise P_k functions and `B1` and `B2` the matrices which represent the bilinear forms $(\bullet, -\partial_y \bullet)_{L^2(\Omega)}$ and $(\bullet, \partial_x \bullet)_{L^2(\Omega)}$ with discrete ansatz spaces of scalar discontinuous piecewise P_k functions and standard continuous piecewise P_{k+1} Lagrange finite element functions. The code from Figure 1.2 illustrates the assembly of the system matrix for mth-Laplace equations for arbitrary $m \in \mathbb{N}$.

The presence of singularities for non-convex domains usually yields the same sub-optimal convergence rate for any polynomial degree. This motivates adaptive mesh-generation strategies, which recover the optimal convergence rates.

The computation of φ appears as a practical difficulty, because φ needs to be defined through integration of f. If f has some simple structure, e.g., f is polynomial, this can be done manually, while for more complicated f, a numerical integration of f has to be employed, but is possible in parallel. Another possible drawback of the new FEMs is that the gradient of the solution ∇u is approximated, but not the solution u itself. This excludes an obvious generalization to partial differential equations where u itself appears.

Historical overview

The Helmholtz decomposition is a classical tool in both theoretical and numerical analysis of physical problems, such as Maxwell's equations [Monk, 2003], fluid problems [Girault and Raviart, 1986], and continuum mechanics [Carstensen and Dolzmann, 1998, Beirão da Veiga et al., 2007]. Discrete Helmholtz decompositions were invented for the analysis of non-conforming FEMs for the Reissner-Mindlin plate [Arnold and Falk, 1989] and further utilized in the a posteriori and optimality analysis of non-conforming FEMs [Becker et al., 2010, Carstensen et al., 2013c, 2014b] and in the analysis of adaptive algorithms and preconditioning for mixed FEMs [Huang and Xu, 2012, Arnold et al., 1997, Brezzi et al., 1991]. Falk and Mercier [1977] employed a Helmholtz decomposition similar as in this thesis for the discretization of the Bingham problem (without mentioning mixed or non-conforming FEMs at all) and so introduced the non-conforming FEM of Carstensen, Reddy, and Schedensack [2014e].

The history of non-conforming FEMs dates back to the engineering literature of the 1960s [Adini and Clough, 1961, Morley, 1968] where the objective was to obtain low-order discretizations for the biharmonic problem (1.3) for $m = 2$. Crouzeix and Raviart [1973] introduced the piecewise affine non-conforming FEM paired with a piecewise constant discontinuous pressure approximation for the Stokes problem. Many possible generalizations of that scheme to higher polynomial degrees have been proposed. All those generalizations are either based on a modification of the classical concept of degrees of freedom [Fortin and Soulie, 1983, Fortin, 1985, Stoyan and Baran, 2006], are restricted to odd polynomial degrees [Crouzeix and Falk, 1989, Arnold and Brezzi, 1985], or employ an enrichment by additional bubble-functions [Maubach and Rabier, 2003, Matthies and Tobiska, 2005].

Non-standard methods are an attractive approach for the discretization of higher-order PDEs. Wang and Xu [2013] introduced non-conforming FEMs that generalize the FEMs of Crouzeix and Raviart [1973] and Morley [1968] to $2m$-th-order elliptic equations in $\mathbb{R}^n$ for $n \geq m \geq 1$. Discontinuous Galerkin methods, such as interior penalty methods, appear as a promising approach for fourth-order [Engel et al., 2002, Brenner, 2012] and sixth-order [Gudi and Neilan, 2011] problems.

The a priori analysis of mixed FEMs has been well-established since Brezzi [1974] and nowadays is a standard part of textbooks [Boffi et al., 2013]. The a posteriori analysis of non-standard FEMs traces back to Dari et al. [1996], Alonso [1996], and Carstensen [1997]; a unifying approach can be found in [Carstensen, 2005]. The notion of medius analysis for non-conforming FEMs, which denotes the usage of a posteriori techniques to derive a priori error estimates, was recently introduced by Gudi [2010]. This technique was also employed in Carstensen, Peterseim, and Schedensack [2012], Carstensen, Köhler, Peterseim, and Schedensack [2014d], Carstensen, Gallistl, and Schedensack [2015], Carstensen and Schedensack [2014], and Carstensen, Gallistl, and Schedensack [2014c] in the context of the Poisson problem, the Stokes equations, the Navier-Lamé equations, eigenvalue approximations, and mixed FEMs.

In the last decade, optimal convergence rates for FEMs based on local mesh adaptation have been established [Stevenson, 2007, Cascon et al., 2008]. These works employ that newest-vertex bisection does not result in an overrefinement Binev et al. [2004]. For non-conforming FEMs, optimal convergence rates were proved by Becker et al. [2010], Rabus [2010], Becker and Mao [2011], Carstensen et al. [2013c], Hu and Xu [2013], Carstensen and Rabus [2012], and Hu et al. [2012] for the Poisson problem, the Stokes equations, the Navier-Lamé equations of linear elasticity, and the biharmonic problem. While the first proofs of optimal convergence rates for non-conforming FEMs employed the discrete Helmholtz decomposition, later works circumvented this and used transfer operators instead [Hu and Xu, 2013, Hu et al., 2012] and [Carstensen, Gallistl, and Schedensack, 2013b, Kreuzer and Schedensack, 2014]. The recent work of Carstensen et al. [2014a] presents an axiomatic framework for optimal convergence rates of adaptive algorithms. This is generalized in the ongoing work of Carstensen and Rabus [2015] to algorithms with separate marking.

Principal results

This thesis defines new FEMs for the Poisson problem, the Stokes equations, the Navier-Lamé equations of linear elasticity, and mth-Laplace equations of the form $(-1)^m\Delta^m u = f$ for arbitrary (fixed) polynomial degrees. For the first time, this ansatz creates a framework, in which the non-conforming FEMs of Crouzeix and Raviart [1973] and Morley [1968] appear in a natural hierarchy. The important projection property of the non-conforming interpolation operator carries over to higher polynomial degrees and thus the novel FEMs allow for the proof of optimal convergence rates of an adaptive algorithm. Since the efficient and reliable error estimator involves a data approximation term without a multiplicative power of the mesh-size, the adaptive algorithm is based on separate marking. The medius analysis and generalizations to rectangular meshes and 3D problems are illustrated for the Poisson equation.

Conforming FEMs which fulfil the divergence-free condition $\operatorname{div} u = 0$ in the Stokes equations pointwise are complicated [Scott and Vogelius, 1985, Guzmán and Neilan, 2014] and therefore the divergence-free condition is usually incorporated through a saddle-point formulation for common conforming FEMs [Boffi et al., 2013]. However, the new discretization of this thesis approximates Du with pointwise trace-free functions and thus generalizes the non-conforming FEM of Crouzeix and Raviart [1973] to higher polynomial degrees. The corresponding adaptive algorithm is proved to converge with optimal rates.

Since the symmetric part of the gradient has a non-trivial kernel on the space of the P_1 non-conforming method of Brenner and Sung [1992] based on the finite element functions of Crouzeix and Raviart [1973], the discretization of the Navier-Lamé equations of linear elasticity with these functions is restricted to the pure Dirichlet problem, where the weak formulation with the symmetric part of the

gradient is equivalent to a formulation that involves the full gradient. The proposed FEM in this thesis incorporates the symmetry through a saddle-point formulation and thus allows mixed boundary conditions. The resulting discretizations are proved to be locking free. A reliable and efficient error estimator is suggested for an adaptive algorithm.

For mth-Laplace equations, the Helmholtz decomposition for tensor-valued functions of Theorem 6.15 is the point of departure for the new FEMs proposed in this thesis. While conforming FEMs require high polynomial degrees for the ansatz spaces, the new approach of the novel FEMs allows even for lowest order ansatz spaces. Moreover, a uniform analysis and implementation for all $m \in \mathbb{N}$ is possible. Optimal convergence rates for an adaptive algorithm are proved.

Numerical experiments underline the quasi-optimal convergence of the adaptive algorithms in all applications, also for linear elasticity, where the proof is not possible due to the missing projection property.

Structure of the thesis

The remaining parts of this thesis are organized as follows. Chapter 2 defines notation and recalls some results employed in this thesis. Chapter 3 introduces the novel formulation and discretizations for the Poisson equation $-\Delta u = f$. Besides its a priori, a posteriori, and medius error analysis, that chapter discusses possible generalizations (e.g., mixed boundary conditions, rectangular finite elements, extension to 3D). The quasi-optimality of an adaptive algorithm is proved in Section 3.5, while Section 3.7 is devoted to numerical experiments for the new discretizations. Chapter 4 introduces the novel formulation and its discretizations together with its a priori and a posteriori error analysis for the Stokes equations. Optimal convergence rates of an adaptive algorithm are proved in Section 4.3 and are numerically investigated in Section 4.4. Chapter 5 is devoted to the discretizations of the Navier-Lamé equations of linear elasticity and the Stokes equations with symmetric gradient. Section 5.3 introduces different possible choices of ansatz spaces. While Section 5.4 proves efficiency and reliability of an error estimator, the discretization of the symmetry disables the proof of optimal convergence rates of the adaptive algorithm. Those are, however, observed in the numerical experiments from Section 5.6. Chapter 6 proves a Helmholtz decomposition for tensor-valued functions. Based on this decomposition, a new formulation and its discretizations for (1.3) are presented in Section 6.4. Optimal convergence rates of an adaptive algorithm are proved in Section 6.6 and numerically observed in Section 6.7. The tables of Appendix A summarize the utilized notation. Appendix B comments the Software for the numerical experiments, which is attached on the data medium in Appendix C.

Conclusions and outlook

This thesis introduces new FEMs based on the Helmholtz decomposition for four problems from computational mechanics and covers the a priori and a posteriori error analysis. Optimal convergence rates for the adaptive algorithms are proved for the Poisson problem, the Stokes equations, and mth-Laplace equations. The optimality of an adaptive algorithm for linear elasticity is numerically observed. How to overcome the difficulties in the proof of quasi-orthogonality (see Subsection 5.4.2), remains as an open question.

The construction and investigation of iterative solvers (e.g., multigrid methods) are beyond the scope of this thesis and are left for future research.

The numerical benchmark examples deal with right-hand sides f, for which the right-hand side φ of the proposed FEMs can be computed by an integration. In practice, an automatic computation of φ (e.g., by numerical integration) has to be developed and the error analysis for such a perturbed φ has to be done. For smooth φ, the a priori analysis leads to convergence rates of the same order as the best-approximation. However, the numerical experiments for the higher-order problems suggest that the magnitude of the error heavily depends on the choice of φ. This motivates further investigations of the question how to choose φ to reduce this size in an optimal way.

Since the Helmholtz decompositions do not involve lower-order terms, it is a completely open question how one could modify the proposed methods for problems with lower-order terms. The generalization to nonlinear problems, e.g., obstacle problems, is a further challenging open question and will be the objective of future research.

Acknowledgement

The author thanks Professor C. Carstensen for the supervision of this thesis. Moreover, the author thankfully acknowledges the support of the Berlin Mathematical School (BMS), the Deutsche Forschungsgemeinschaft (DFG), the support by the Chinesisch-Deutsches Zentrum (project "The Adaptive Finite Element Method for the Fourth Order Problem", grant no. GZ578), and by the Indian Department of Science and Technology (DST) (National programme on differential equations) which enabled the participation in several workshops. The author thanks Professor S. Brenner for the possibility to participate in the IMA Special Workshop "WhAM! A Research Collaboration Workshop for Women in Applied Mathematics: Numerical Partial Differential Equations and Scientific Computing".

2. Preliminaries

This chapter introduces notation on Lebesgue and Sobolev spaces in Section 2.1 and on triangulations in Section 2.2. Frequently used results are recalled in Section 2.3. A comprehensive summary of the notation can be found in the tables of Appendix A. The notation on tensor-valued functions used in Chapter 6 is stated in Section 6.1.

Throughout this thesis, the notation $a \lesssim b$ abbreviates the estimate $a \leq Cb$ with generic constant $C < \infty$ independent of the mesh-size; $a \approx b$ abbreviates $a \lesssim b \lesssim a$.

2.1. Function spaces and operators

This thesis employs standard notation on Lebesgue and Sobolev spaces [Evans, 2010]. Let $(\omega, \mathfrak{A}, \mu)$ be a measure space with $\omega \subseteq \mathbb{R}^n$. Given some μ-measurable function $f : \omega \to \mathbb{R}$, let $\int_\omega f \, d\mu$ denote the Lebesgue integral of f. If for some $k, m \in \mathbb{N}$ the components of $f : \omega \to X \subseteq \mathbb{R}^{k\times m}$ are μ-measurable, then $\int_\omega f \, d\mu$ denotes the component-wise Lebesgue integral.

Definition 2.1. Assume $\mu(\omega) < \infty$. Given a μ-measurable function $f : \omega \to X$, let

$$\fint_\omega f \, d\mu = \mu(\omega)^{-1} \int_\omega f \, d\mu$$

denote the integral mean of f over ω. ♦

The L^2 seminorm of a function $f : \omega \to X \subseteq \mathbb{R}^{k\times m}$ reads

$$\|f\|_{L^2(\omega)} := \left(\int_\omega |f|^2 \, d\mu \right)^{1/2},$$

where $|f|$ denotes the pointwise Frobenius norm of f. The space of (equivalence classes of) square integrable functions $f : \omega \to X \subseteq \mathbb{R}^{k\times m}$ (up to equality almost everywhere) is denoted by $L^2(\omega; X)$ and $L^2(\omega) := L^2(\omega; \mathbb{R})$. Furthermore, let $L^2_0(\omega; X) = \{f \in L^2(\omega; X) \mid \int_\omega f \, d\mu = 0\}$ denote the subset of functions with vanishing integral and set $L^2_0(\Omega) = L^2_0(\Omega; \mathbb{R})$. Let $L^\infty(\omega)$ denote the set of essentially bounded measurable functions $f : \omega \to \mathbb{R}$ and let

$$(f, g)_{L^2(\Omega)} := \int_\omega f : g \, d\mu$$

denote the L^2 scalar product of $f, g \in L^2(\omega; X)$ with the scalar product $A : B = \sum_{j=1}^k \sum_{\ell=1}^m A_{j\ell} B_{j\ell}$ for all $A, B \in \mathbb{R}^{k\times m}$. For a Lebesgue-measurable set $\omega \subseteq \mathbb{R}^n$

and a Lebesgue-measurable function $f : \omega \to X \subseteq \mathbb{R}^{k\times m}$, the integral with respect to the n-dimensional Lebesgue measure reads $\int_\omega f\,dx$, while the integral over an $(n-1)$-dimensional hyper-surface $\Gamma \subseteq \omega$ with respect to the $(n-1)$-dimensional Hausdorff measure is denoted by $\int_\Gamma f\,ds$. The k-dimensional Hausdorff measure of a set $\omega \subseteq \mathbb{R}^n$ is denoted by $\mathrm{meas}_k(\omega)$. For a closed subspace $\Sigma \subseteq L^2(\omega;X)$, the operator $\Pi_\Sigma : L^2(\omega;X) \to \Sigma$ denotes the L^2 projection onto Σ.

Given $\omega \subseteq \mathbb{R}^n$, the set of infinitely differentiable functions $f : \omega \to X$ is denoted by $C^\infty(\omega;X)$ and the subset of functions with compact support is denoted by $C_c^\infty(\omega;X)$; $C^\infty(\omega)$ and $C_c^\infty(\omega)$ abbreviate $C^\infty(\omega;\mathbb{R})$ and $C_c^\infty(\omega;\mathbb{R})$. The partial derivative of f with respect to the multi-index $\alpha \in \mathbb{N}_0^n$ of length $|\alpha| := \sum_{j=1}^n \alpha_j$ reads

$$\frac{\partial^{|\alpha|} f}{\partial x^\alpha} := \frac{\partial^{|\alpha|} f}{\partial x_1^{\alpha_1} \dots \partial x_n^{\alpha_n}}.$$

For a bounded open Lipschitz domain $\omega \subseteq \mathbb{R}^n$, a function $f \in L^2(\omega)$ is called ℓ times weakly differentiable with respect to the multi-index α with length $|\alpha| = \ell$, if there exists some $g \in L^2(\omega)$ such that

$$\int_\omega f\,\frac{\partial^{|\alpha|}\varphi}{\partial x^\alpha}\,dx = (-1)^\ell \int_\omega g\varphi\,dx \qquad \text{for all } \varphi \in C_c^\infty(\omega).$$

The function $\partial^{|\alpha|} f/\partial x^\alpha := g$ is called ℓ-th weak derivative with respect to α. Let $\partial f/\partial x_k$ abbreviate $\partial^{|\alpha|} f/\partial x^\alpha$ for $\alpha_k = 1$ and $\alpha_j = 0$ for all $j \in \{1,\dots,n\} \setminus \{k\}$. Define the Sobolev spaces

$$H^m(\omega) := \{f \in L^2(\omega) \mid \forall \alpha \in \mathbb{N}_0^n \text{ with } |\alpha| \le m\ \exists \partial^{|\alpha|} f/\partial x^\alpha \in L^2(\omega)\}$$

and for a vector space $X \subseteq \mathbb{R}^{k\times N}$ define $H^m(\omega;X) := \{f \in L^2(\Omega;X) \mid f_{j\ell} \in H^m(\omega) \text{ for all } j = 1,\dots,k \text{ and } \ell = 1,\dots,N\}$. Define the Sobolev norm

$$\|f\|_{H^m(\omega)} := \left(\sum_{j=1}^k \sum_{\ell=1}^N \sum_{|\alpha|\le m} \left\| \partial^{|\alpha|} f_{j\ell}/\partial x^\alpha \right\|_{L^2(\omega)}^2 \right)^{1/2}.$$

The trace theorem of Lions and Magenes [1972] and Grisvard [1985] proves the existence of a (continuous) trace operator $T : H^m(\Omega) \to \prod_{j=0}^{m-1} L^2(\partial\Omega)$ with $(Tu)_j = \partial^j u/\partial\nu^j$ for all $j \in \{0,\dots,m-1\}$ and $u \in H^m(\Omega) \cap C^\infty(\Omega)$. For ease of reading, $(\partial^j u/\partial\nu^j)|_\Gamma$ abbreviates $((Tu)_j)|_\Gamma$ for all $\Gamma \subseteq \partial\Omega$. Let $H^{1/2}(\Gamma) := \{v \in L^2(\Gamma) \mid \exists u \in H^1(\Omega) \text{ with } v = u|_\Gamma\}$ denote the space of traces of $H^1(\Omega)$-functions on Γ. Given $\Gamma \subseteq \partial\Omega$ define

$$H_\Gamma^m(\Omega) := \{v \in H^m(\Omega) \mid (\partial^j u/\partial\nu^j)|_\Gamma = 0 \text{ for all } j = 0,\dots,m-1\}$$

and $H_0^m(\Omega) := H_{\partial\Omega}^m(\Omega)$. Let $H^{-1}(\Omega)$ denote the dual of $H_0^1(\Omega)$ and $\langle \bullet, \bullet \rangle_{H^{-1}}$ the duality pairing of $H^{-1}(\Omega)$ and $H_0^1(\Omega)$.

Differential operators. For sufficiently smooth $f : \omega \to \mathbb{R}^m$, the first (weak) derivative of f is denoted by Df. If $m = 1$, then $\nabla f := (Df)^\top$ denotes the gradient of f and $D^2 f$ the Hessian matrix. If $m = n$, the divergence of f reads $\operatorname{div} f := \sum_{j=1}^n \partial f_j / \partial x_j$. For $\sigma : \omega \to \mathbb{R}^{n\times n}$, the divergence is applied row-wise, i.e., $\operatorname{div} \sigma := (\operatorname{div} \sigma_{1\bullet}, \dots, \operatorname{div} \sigma_{n\bullet})^\top$. The Laplacian reads $\Delta := \operatorname{div} \nabla$. If, for $f \in L^2(\omega;\mathbb{R}^n)$ there exists a function $g : \omega \to \mathbb{R}$ with

$$\int_\omega f \cdot \nabla \varphi \, dx = -\int_\omega \varphi g \, dx \qquad \text{for all } \varphi \in C_c^\infty(\omega),$$

then f is said to have the weak divergence $\operatorname{div} f := g$. The subset of $L^2(\omega)$ of all functions with weak divergence in $L^2(\omega)$ reads

$$H(\operatorname{div},\omega) := \{f \in L^2(\omega;\mathbb{R}^n) \mid \exists \operatorname{div} f \text{ and } \operatorname{div} f \in L^2(\omega)\}.$$

Furthermore,

$$\begin{aligned} H(\operatorname{div},\omega;\mathbb{R}^{n\times n}) &:= \{f \in L^2(\omega;\mathbb{R}^{n\times n}) \mid \exists \operatorname{div} f \text{ and } \operatorname{div} f \in L^2(\omega;\mathbb{R}^n)\},\\ H(\operatorname{div},\omega;\mathbb{S}) &:= H(\operatorname{div},\omega;\mathbb{R}^{n\times n}) \cap L^2(\Omega;\mathbb{S}) \end{aligned}$$

for the vector space of symmetric matrices $\mathbb{S} \subseteq \mathbb{R}^{n\times n}$ from Appendix A.

Definition 2.2. For $v \in H^1(\omega)$, $w \in H^1(\omega;\mathbb{R}^2)$, and $f \in H^1(\omega;\mathbb{R}^{2\times 2})$, define the Curl of a function by $\operatorname{Curl} v := (\partial v/\partial x_2, -\partial v/\partial x_1)$,

$$\operatorname{Curl} w := \begin{pmatrix} -\partial w_1/\partial x_2 & \partial w_1/\partial x_1 \\ -\partial w_2/\partial x_2 & \partial w_2/\partial x_1 \end{pmatrix},$$

and $\operatorname{curl} w := -\partial w_1/\partial x_2 + \partial w_2/\partial x_1$, and

$$\operatorname{curl} f := \begin{pmatrix} -\partial f_{11}/\partial x_2 + \partial f_{12}/\partial x_1 \\ -\partial f_{21}/\partial x_2 + \partial f_{22}/\partial x_1 \end{pmatrix}. \qquad \blacklozenge$$

A definition of the Curl in three space dimensions is given in Section 3.6, while the Curl for arbitrary tensor-valued functions can be found in Definition 6.5.

2.2. Triangulations and refinements

A shape-regular triangulation $\mathcal{T}$ of a bounded open Lipschitz domain $\Omega \subseteq \mathbb{R}^2$ is a set of closed triangles $T \in \mathcal{T}$ such that $\overline{\Omega} = \bigcup \mathcal{T}$ and any two distinct triangles are either disjoint or share exactly one common edge or one vertex. Let $\mathcal{N}(T)$ denote the vertices of a triangle $T \in \mathcal{T}$ and $\mathcal{E}(T)$ the edges. Let $\mathcal{N} := \mathcal{N}(\mathcal{T}) := \bigcup_{T\in\mathcal{T}} \mathcal{N}(T)$ denote the set of vertices of $\mathcal{T}$ and $\mathcal{E} := \mathcal{E}(\mathcal{T}) := \bigcup_{T\in\mathcal{T}} \mathcal{E}(T)$ the set of edges. For an edge $E \in \mathcal{E}$, define the patch $\omega_E := \operatorname{int}(\bigcup\{T \in \mathcal{T} \mid E \in \mathcal{E}(T)\})$. Any edge $E \in \mathcal{E}$ is associated with a fixed orientation of the unit normal ν_E on E (and $\tau_E = (0,-1;1,0)\nu_E$ denotes the unit tangent on E). On the boundary, ν_E is the

outer unit normal of Ω, while for interior edges $E \not\subseteq \partial\Omega$, the orientation is fixed through the choice of the triangles $T_+ \in \mathcal{T}$ and $T_- \in \mathcal{T}$ with $E = T_+ \cap T_-$ and $\nu_E := \nu_{T_+}|_E$ is the outer normal of T_+ on E. In this situation, $[v]_E := v|_{T_+} - v|_{T_-}$ denotes the jump across E. For an edge $E \subseteq \partial\Omega$ on the boundary, the jump across E reads $[v]_E := v$. For $T \in \mathcal{T}$, let

$$P_k(T;\mathbb{R}^m) := \left\{ v : T \to \mathbb{R}^m \;\middle|\; \begin{array}{l} \forall j = 1,\dots,m \text{ the } j\text{-th component} \\ \text{of } v \text{ is a polynomial of total degree} \le k \end{array} \right\};$$
$$P_k(\mathcal{T};\mathbb{R}^m) := \{ v : \Omega \to \mathbb{R}^m \mid \forall T \in \mathcal{T} :\ v|_T \in P_k(T;\mathbb{R}^m) \}$$

denote the set of piecewise polynomials and $P_k(\mathcal{T}) := P_k(\mathcal{T};\mathbb{R})$. For a triangle $T = \operatorname{conv}\{a,b,c\} \in \mathcal{T}$, let φ_a, φ_b, and $\varphi_c \in P_1(T)$ denote the barycentric coordinates, i.e., $\varphi_z(y) = 1$, if $y = z$, while $\varphi_z(y) = 0$ for $y \in \{a,b,c\} \setminus \{z\}$. Let

$$\Pi_k := \Pi_{P_k(\mathcal{T};\mathbb{R}^m)} : L^2(\Omega;\mathbb{R}^m) \to P_k(\mathcal{T};\mathbb{R}^m)$$

abbreviate the L^2 projection onto piecewise polynomials of degree $\le k$. Given a triangle $T \in \mathcal{T}$, let $h_T := (\operatorname{meas}_2(T))^{1/2}$ denote the square root of the area of T and let $h_{\mathcal{T}} \in P_0(\mathcal{T})$ denote the piecewise constant mesh-size with $h_{\mathcal{T}}|_T := h_T$ for all $T \in \mathcal{T}$. For an edge $E \in \mathcal{E}$, let h_E denote the length of E.

For piecewise polynomial functions $v \in P_k(\mathcal{T})$ or $v \in P_k(\mathcal{T};\mathbb{R}^2)$ (resp. $v \in P_k(\mathcal{T};\mathbb{R}^2)$ or $v \in P_k(\mathcal{T};\mathbb{R}^{2\times 2})$) the $\mathcal{T}$-piecewise differential operators D_{NC} and $\operatorname{Curl}_{\mathrm{NC}}$ (resp. $\operatorname{div}_{\mathrm{NC}}$ and $\operatorname{curl}_{\mathrm{NC}}$) exist and are defined by the $\mathcal{T}$-piecewise action of the respective differential operator, e.g., $(D_{\mathrm{NC}}v)|_T = D(v|_T)$ for all $T \in \mathcal{T}$. The piecewise Hessian matrix is denoted by $D^2_{\mathrm{NC}}v$.

The oscillations of $f \in L^2(\Omega;\mathbb{R}^m)$ read $\operatorname{osc}(f,\mathcal{T}) := \|h_{\mathcal{T}}(f - \Pi_0 f)\|_{L^2(\Omega)}$.

For a set of triangles $\mathcal{M} \subseteq \mathcal{T}$, let $\| \bullet \|_{\mathcal{M}}$ abbreviate

$$\| \bullet \|_{\mathcal{M}} := \sqrt{\sum_{T\in\mathcal{M}} \| \bullet \|^2_{L^2(T)}}.$$

Adaptive mesh refinement. Let $\mathcal{T}_0$ denote some initial shape-regular triangulation of Ω, such that each triangle $T \in \mathcal{T}$ is equipped with a refinement edge $E_T \in \mathcal{E}(T)$. We assume that $\mathcal{T}_0$ fulfils the following initial condition.

Definition 2.3 (initial condition)**.** All $T, K \in \mathcal{T}_0$ with $T \cap K = E \in \mathcal{E}$ and with refinement edges $E_T \in \mathcal{E}(T)$ and $E_K \in \mathcal{E}(K)$ satisfy: If $E_T = E$, then $E_K = E_T$. If $E_K = E$, then $E_T = E_K$. ⧫

The newest-vertex bisection relies on the bisection of triangles. The bisection of a triangle bisects the refinement edge of the triangle and creates in this way two new triangles. The arrangement of the refinement edges of the newly created triangles is depicted in Figure 2.1.

Definition 2.4 (admissible triangulations)**.** Given an initial triangulation $\mathcal{T}_0$, the set of admissible triangulations $\mathbb{T}$ is defined as the set of all regular triangulations which can be created from $\mathcal{T}_0$ by newest-vertex bisection [Stevenson, 2008]. ⧫

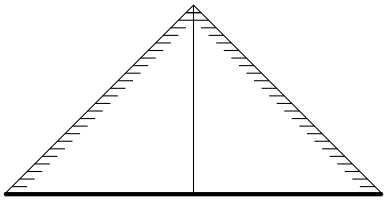

Figure 2.1.: Bisection of a triangle. The refinement edge of the bisected triangle is depicted in thick; the refinement edges of the newly created triangles are highlighted with ⊔⊔⊔.

The adaptive algorithm involves the overlay of two triangulations.

Definition 2.5 (overlay)**.** Let $\mathcal{T}, \mathcal{T}_\star \in \mathbb{T}$ be two admissible triangulations. The overlay $\mathcal{T} \otimes \mathcal{T}_\star \in \mathbb{T}$ is defined by

$$\mathcal{T} \otimes \mathcal{T}_\star := \{T \in \mathcal{T} \cup \mathcal{T}_\star \mid \exists K \in \mathcal{T}, K_\star \in \mathcal{T}_\star \text{ with } T \subseteq K \cap K_\star\}.$$

♦

2.3. Frequently used results

This section recalls some theorems used in this thesis and starts with the well-known weighted Young inequality.

Lemma 2.6 (Young inequality)**.** *Any $\varepsilon > 0$ and $a, b \in \mathbb{R}$ satisfy*

$$ab \leq \frac{a^2}{2\varepsilon} + \frac{\varepsilon b^2}{2}.$$

Proof. This follows from the binomial formula. ■

The following trace inequality of [Brenner and Scott, 2008, p. 282] estimates the L^2 norm of the trace of a function on the boundary of a triangle T by the L^2 norm of the function and its gradient on T.

Theorem 2.7 (trace inequality, [Brenner and Scott, 2008])**.** *Let T be a triangle. There exists $C_{\mathrm{tr}} > 0$ such that any $v \in H^1(T)$ satisfies*

$$\|v\|_{L^2(\partial T)} \leq C_{\mathrm{tr}}(h_T^{-1/2}\|v\|_{L^2(T)} + h_T^{1/2}\|\nabla v\|_{L^2(T)}).$$ ■

Let $(X, \|\bullet\|_X)$ and $(Y, \|\bullet\|_Y)$ be two Hilbert spaces and $a : X \times X \to \mathbb{R}$, $b : X \times Y \to \mathbb{R}$ continuous bilinear forms and $F \in X^\star$, $G \in Y^\star$. Consider the problem: Find $(u, y) \in X \times Y$ such that

$$\begin{aligned} a(u, v) + b(v, y) &= F(v) && \text{for all } v \in X, \\ b(u, z) &= G(z) && \text{for all } z \in Y. \end{aligned} \tag{2.1}$$

The following well-known theorem of Brezzi [1974] proves existence and uniqueness of solutions of the saddle-point problem (2.1).

Theorem 2.8 (Brezzi's splitting lemma). *Define* $Z := \{w \in X \mid b(w, \bullet) = 0\}$. *If*

$$\|y\|_Y \lesssim \sup_{v \in X\setminus\{0\}} \frac{b(v,y)}{\|v\|_X} \qquad \text{for all } y \in Y,$$

$$\|u\|_X \lesssim \sup_{v \in Z\setminus\{0\}} \frac{a(u,v)}{\|v\|_X} \qquad \text{for all } u \in Z,$$

$$\|v\|_X \lesssim \sup_{u \in Z\setminus\{0\}} \frac{a(u,v)}{\|u\|_X} \qquad \text{for all } v \in Z,$$

then problem (2.1) *has a unique solution* $(u, y) \in X \times Y$ *and it satisfies*

$$\|u\|_X + \|y\|_Y \lesssim \|F\|_{X^\star} + \|G\|_{Y^\star}.$$ ■

The following tr-dev-div lemma is contained in Brezzi and Fortin [1991, Proposition 3.1 in Section IV.3] and Carstensen and Dolzmann [1998, Lemma 4.1]. The deviatoric part $\mathrm{dev}A$ of a matrix $A \in \mathbb{R}^{2\times 2}$ is defined by $\mathrm{dev}A = A - (1/2)\mathrm{tr}(A)I_{2\times 2}$ (see Appendix A).

Lemma 2.9 (tr-dev-div lemma). *Let* $\tau \in H(\mathrm{div}, \Omega; \mathbb{R}^{2\times 2})$ *with* $\int_\Omega \mathrm{tr}(\tau)\, dx = 0$ *or let* $\Gamma \subseteq \partial\Omega$ *with* $\mathrm{meas}_1(\Gamma) > 0$ *and* $\tau \in H(\mathrm{div}, \Omega; \mathbb{R}^{2\times 2})$ *with* $(\tau\nu)|_\Gamma = 0$. *Then it satisfies*

$$\|\tau\|_{L^2(\Omega)} \lesssim \|\mathrm{dev}\,\tau\|_{L^2(\Omega)} + \|\mathrm{div}\,\tau\|_{L^2(\Omega)}.$$

The constant hidden in $\lesssim$ *depends on* Γ *and* Ω.

Proof. If $\tau \in H(\mathrm{div}, \Omega; \mathbb{R}^{2\times 2})$ with $\int_\Omega \mathrm{tr}(\tau)\, dx = 0$, the proof is contained in Brezzi and Fortin [1991, Proposition 3.1 in Section IV.3]. Since

$$\Sigma_0 := \{\tau \in H(\mathrm{div}, \Omega; \mathbb{R}^{2\times 2}) \mid (\tau\nu)|_\Gamma = 0\}$$

is a closed subspace of $H(\mathrm{div}, \Omega; \mathbb{R}^{2\times 2})$ that does not contain the constant tensor $I_{2\times 2}$, the second statement follows from [Carstensen and Dolzmann, 1998, Lemma 4.1]. ■

The following theorem proves that the symmetric part of the gradient defines a norm on $H^1_{\Gamma_D}(\Omega; \mathbb{R}^2)$. This proves the well-posedness of the Navier-Lamé equations in Chapter 5.

Theorem 2.10 (Korn's inequality, [Brenner and Scott, 2008]). *Let* $\Gamma_D \subseteq \partial\Omega$ *with positive measure. There exists a constant* $C_{\mathrm{Korn}} < \infty$ *such that any* $v \in H^1_{\Gamma_D}(\Omega; \mathbb{R}^2)$ *satisfies*

$$\|Dv\|_{L^2(\Omega)} \le C_{\mathrm{Korn}} \|\varepsilon(v)\|_{L^2(\Omega)}.$$ ■

The next theorem is used in Chapter 6 in the proof that $\|\operatorname{sym}\operatorname{Curl}\bullet\|_{L^2(\Omega)}$ defines a norm.

For $n, m \in \mathbb{N}$, $m \leq n$, and indices $1 \leq k \leq m$, $1 \leq s \leq n$ and a multi-index $\kappa \in \{(1,0),(0,1)\}$ let $a_{k,s,\kappa} \in \mathbb{R}$ and consider some operators $(N_k)_{k=1,\dots,m}$, $N_k : H^1(\Omega;\mathbb{R}^n) \to L^2(\Omega)$,

$$N_k v = \sum_{s=1}^{n} \sum_{\kappa=(1,0),(0,1)} a_{k,s,\kappa} D^\kappa v_s \qquad \text{for all } v = (v_1,\dots,v_n) \in H^1(\Omega;\mathbb{R}^n).$$

The following theorem summarizes [Nečas, 1967, Chapitre 3, Théorème 7.6] and [Nečas, 1967, Théorème 7.8] and proves the coercivity of the associated bilinear form $A : H^1(\Omega;\mathbb{R}^n) \times H^1(\Omega;\mathbb{R}^n) \to \mathbb{R}$,

$$A(v,u) := \int_\Omega \left(\sum_{k=1}^{m} N_k v N_k u \right) dx.$$

Theorem 2.11 ([Nečas, 1967]). *If, for all $\xi \in \mathbb{R}^2$, the rank of the matrix $(\mathfrak{N}_{ks}\xi)_{\substack{1\leq k\leq m\\ 1\leq s\leq n}}$ with entries*

$$\mathfrak{N}_{ks}\xi := \sum_{\kappa=(1,0),(0,1)} a_{k,s,\kappa}\xi^\kappa$$

is equal to m, then the form A is $H^1(\Omega;\mathbb{R}^m)$ coercive in the sense that

$$\|v\|^2_{H^1(\Omega)} \lesssim A(v,v) + \|v\|^2_{L^2(\Omega)}.$$ ■

3. Poisson problem

This chapter introduces the novel formulation of the Poisson problem based on the Helmholtz decomposition and its discretization together with an a priori result in Section 3.1. The equivalence with the P_1 non-conforming FEM for the lowest-order case is proved in Subsection 3.1.3. Section 3.2 summarizes some remarks and generalizations. Sections 3.3 and 3.4 are devoted to the medius analysis and the a posteriori error analysis of the FEM, while Section 3.5 proves quasi-optimality of an adaptive algorithm. Section 3.6 outlines the generalization to 3D. Section 3.7 concludes this chapter with numerical experiments.

Throughout this chapter $\Omega \subseteq \mathbb{R}^2$ is a simply connected, bounded, polygonal Lipschitz domain.

3.1. Problem formulation and discretization

This section introduces the new formulation based on the Helmholtz decomposition in Subsection 3.1.1 and its discretization in Subsection 3.1.2. Subsection 3.1.3 discusses the equivalence with the P_1 non-conforming FEM.

3.1.1. Mixed formulation of the Poisson problem

Given the simply connected, bounded, polygonal Lipschitz domain $\Omega \subseteq \mathbb{R}^2$ and $f \in L^2(\Omega)$, the Poisson model problem seeks $u \in H^1_0(\Omega)$ with

$$-\Delta u = f \text{ in } \Omega \qquad \text{and} \qquad u = 0 \text{ on } \partial\Omega. \tag{3.1}$$

The novel weak formulation is based on the classical Helmholtz decomposition, which is recalled here for completeness, cf. [Rudin, 1976].

Theorem 3.1 (Helmholtz decomposition)**.** *Any simply connected domain $\Omega \subseteq \mathbb{R}^2$ satisfies*

$$L^2(\Omega;\mathbb{R}^2) = \nabla H^1_0(\Omega) \oplus \operatorname{Curl}(H^1(\Omega) \cap L^2_0(\Omega))$$

and the sum is orthogonal with respect to the L^2 scalar product. ■

Remark 3.2. Note that for $\Omega \subseteq \mathbb{R}^2$, the definition of the Curl implies

$$H(\operatorname{Curl},\Omega) := \{\beta \in L^2(\Omega) \mid \operatorname{Curl}\beta \in L^2(\Omega)\} = H^1(\Omega). \qquad \blacklozenge$$

Define $X := L^2(\Omega;\mathbb{R}^2)$ and $Y := H^1(\Omega) \cap L^2_0(\Omega)$ and let $\varphi \in H(\operatorname{div},\Omega)$ satisfy $-\operatorname{div}\varphi = f$. The novel weak formulation of the Poisson problem (3.1) seeks $(p,\alpha) \in X \times Y$ with

$$\begin{aligned} (p,q)_{L^2(\Omega)} + (q,\operatorname{Curl}\alpha)_{L^2(\Omega)} &= (\varphi,q)_{L^2(\Omega)} \quad && \text{for all } q \in X, \\ (p,\operatorname{Curl}\beta)_{L^2(\Omega)} &= 0 && \text{for all } \beta \in Y. \end{aligned} \tag{3.2}$$

This formulation is the point of departure for the numerical approximation of ∇u in Subsection 3.1.2.

The remaining part of this subsection proves an inf-sup condition, the unique existence of solutions and the equivalence of problem (3.1) and (3.2).

Define the bilinear form $\mathcal{B} : \big(X \times Y\big) \times \big(X \times Y\big) \to \mathbb{R}$ by

$$\mathcal{B}((p,\alpha),(q,\beta)) := (p,q)_{L^2(\Omega)} + (q,\operatorname{Curl}\alpha)_{L^2(\Omega)} + (p,\operatorname{Curl}\beta)_{L^2(\Omega)} \tag{3.3}$$

for all $p,q \in X$ and all $\alpha,\beta \in Y$.

Lemma 3.3 (global inf-sup condition)**.** *The bilinear form $\mathcal{B}$ satisfies the inf-sup condition*

$$(1/5)\big(\|p\|_{L^2(\Omega)} + \|\operatorname{Curl}\alpha\|_{L^2(\Omega)}\big) \le \sup_{(q,\beta)\in(X\times Y)\setminus\{0\}} \frac{\mathcal{B}((p,\alpha),(q,\beta))}{\|q\|_{L^2(\Omega)} + \|\operatorname{Curl}\beta\|_{L^2(\Omega)}}$$

for all $(p,\alpha) \in X \times Y$.

Proof. Given $(p,\alpha) \in X \times Y$, the Helmholtz decomposition of Theorem 3.1 guarantees the existence of $(v,\gamma) \in H^1_0(\Omega) \times Y$ with

$$p = \nabla v + \operatorname{Curl}\gamma.$$

Set $q := \nabla v + \operatorname{Curl}\alpha \in X$ and $\beta := \gamma \in Y$ and, for abbreviation, $a = \|\nabla v\|_{L^2(\Omega)}$, $b = \|\operatorname{Curl}\gamma\|_{L^2(\Omega)}$ and $c = \|\operatorname{Curl}\alpha\|_{L^2(\Omega)}$. The L^2 orthogonality $\nabla H^1_0(\Omega) \perp_{L^2(\Omega)} \operatorname{Curl} Y$ implies

$$\begin{aligned} &\big(\|p\|_{L^2(\Omega)} + \|\operatorname{Curl}\alpha\|_{L^2(\Omega)}\big)\big(\|q\|_{L^2(\Omega)} + \|\operatorname{Curl}\beta\|_{L^2(\Omega)}\big) \\ &\qquad = \sqrt{a^2+b^2}\,\sqrt{a^2+c^2} + b\sqrt{a^2+b^2} + c\sqrt{a^2+c^2} + b\,c. \end{aligned}$$

Since $\sqrt{a^2+b^2} \le a+b$ and $\sqrt{a^2+c^2} \le a+c$, it follows

$$\begin{aligned} &\big(\|p\|_{L^2(\Omega)} + \|\operatorname{Curl}\alpha\|_{L^2(\Omega)}\big)\big(\|q\|_{L^2(\Omega)} + \|\operatorname{Curl}\beta\|_{L^2(\Omega)}\big) \\ &\qquad\qquad \le a^2 + b^2 + c^2 + 2ab + 2ac + 2bc. \end{aligned}$$

Three weighted Young inequalities from Lemma 2.6 (two with weights 2 and one with weight 1) yield

$$a^2 + b^2 + c^2 + 2ab + 2ac + 2bc \le 5(a^2 + (1/2)b^2 + (1/2)c^2).$$

A further application of the Young inequality reads $-(1/2)(b^2+c^2) \leq -bc$ and, hence,

$$a^2 + (1/2)b^2 + (1/2)c^2 \leq a^2 + b^2 + c^2 - bc.$$

The combination of the previous two inequalities reads

$$a^2 + b^2 + c^2 + 2ab + 2ac + 2bc \leq 5(a^2 + b^2 + c^2 - bc).$$

Note that the choice $a = 1/2$, $b = c = 1$ proves that the constant 5 is optimal. The Cauchy inequality implies

$$-bc \leq (\operatorname{Curl}\gamma, \operatorname{Curl}\alpha)_{L^2(\Omega)}.$$

On the other hand, the orthogonality $\nabla H_0^1(\Omega) \perp_{L^2(\Omega)} \operatorname{Curl} Y$ yields

$$\mathcal{B}((p,\alpha),(q,\beta)) = a^2 + (\operatorname{Curl}\gamma, \operatorname{Curl}\alpha)_{L^2(\Omega)} + b^2 + c^2.$$

The combination of the previous displayed inequalities leads to the assertion. ∎

Theorem 3.4 (existence of solutions)**.** *Given $\varphi \in H(\operatorname{div},\Omega)$, there exists a unique solution $(p,\alpha) \in X \times Y$ to* (3.2) *and it satisfies $p = \nabla u$ for the solution $u \in H_0^1(\Omega)$ of* (3.1) *and*

$$\|p\|^2_{L^2(\Omega)} + \|\operatorname{Curl}\alpha\|^2_{L^2(\Omega)} = \|\varphi\|^2_{L^2(\Omega)}. \tag{3.4}$$

Proof. Given $(q,\beta) \in X \times Y$ with $\mathcal{B}((p,\alpha),(q,\beta)) = 0$ for all $(p,\alpha) \in X \times Y$, the choice $\alpha = 0$ proves $q = -\operatorname{Curl}\beta$. The choice $\alpha = \beta$ then leads to $(q,\beta) = 0$. Therefore, the inf-sup condition of Lemma 3.3 and the theorem of Banach-Nečas-Babuška [Di Pietro and Ern, 2012, Theorem 1.1] yield the unique existence of a solution to (3.2).

The second equation of (3.2) and the Helmholtz decomposition from Theorem 3.1 imply the existence of $\widetilde{u} \in H_0^1(\Omega)$ with $p = \nabla\widetilde{u}$. Let $v \in H_0^1(\Omega)$. Then

$$(p, \nabla v)_{L^2(\Omega)} = (\varphi, \nabla v)_{L^2(\Omega)} = (f, v)_{L^2(\Omega)}$$

and, hence, $\widetilde{u}$ solves (3.1).

The L^2 orthogonality of p and $\operatorname{Curl}\alpha$ implies (3.4). ∎

3.1.2. Discretization

Let $\mathcal{T}$ be a regular triangulation of Ω and define

$$X_h(\mathcal{T}) := P_k(\mathcal{T};\mathbb{R}^2),$$
$$Y_h(\mathcal{T}) := P_{k+1}(\mathcal{T}) \cap Y.$$

The discretization of (3.2) seeks $p_h \in X_h(\mathcal{T})$ and $\alpha_h \in Y_h(\mathcal{T})$ with

$$(p_h, q_h)_{L^2(\Omega)} + (q_h, \operatorname{Curl}\alpha_h)_{L^2(\Omega)} = (\varphi, q_h)_{L^2(\Omega)} \qquad \text{for all } q_h \in X_h(\mathcal{T}), \tag{3.5.a}$$
$$(p_h, \operatorname{Curl}\beta_h)_{L^2(\Omega)} = 0 \qquad \text{for all } \beta_h \in Y_h(\mathcal{T}). \tag{3.5.b}$$

Remark 3.5. Since there are no continuity conditions on $q_h \in X_h(\mathcal{T})$ and since $\operatorname{Curl} Y_h(\mathcal{T}) \subseteq X_h(\mathcal{T})$, the first equation is fulfilled in a strong form, i.e.,

$$p_h + \operatorname{Curl} \alpha_h = \Pi_k \varphi.$$

In contrast to classical finite element methods, the approximation p_h of ∇u is a gradient only in a *discrete orthogonal* sense, namely (3.5.b). For $k = 0$, Subsection 3.1.3 below proves that this *discrete orthogonal gradient property* is equivalent to being a non-conforming gradient of a Crouzeix-Raviart finite element function. The main motivation of the novel formulation is the generalization to any polynomial degree k. ⧫

Remark 3.6 (discrete inf-sup-condition)**.** The discrete inf-sup condition for the bilinear form $(\bullet, \operatorname{Curl} \bullet)_{L^2(\Omega)}$ reads

$$\|\operatorname{Curl} \beta_h\|_{L^2(\Omega)} \leq C_{\mathrm{is}} \sup_{q_h \in X_h(\mathcal{T})\setminus\{0\}} \frac{(q_h, \operatorname{Curl} \beta_h)_{L^2(\Omega)}}{\|q_h\|_{L^2(\Omega)}} .$$

Since $\operatorname{Curl} \beta_h \in X_h(\mathcal{T})$, this inf-sup-condition is satisfied with $C_{\mathrm{is}} = 1$. Brezzi's splitting lemma (Theorem 2.8) therefore leads to the unique existence of a solution to (3.5). ⧫

Define the set of *discrete orthogonal gradients*

$$W_h(\mathcal{T}) := \{q_h \in X_h(\mathcal{T}) \mid (q_h, \operatorname{Curl} \beta_h)_{L^2(\Omega)} = 0 \text{ for all } \beta_h \in Y_h(\mathcal{T})\}. \tag{3.6}$$

The following proposition explicitly states the inf-sup constant for the global inf-sup condition.

Proposition 3.7 (discrete global inf-sup condition)**.** *The bilinear form $\mathcal{B}$ from* (3.3) *satisfies the discrete inf-sup condition*

$$(1/5)\big(\|p_h\|_{L^2(\Omega)} + \|\operatorname{Curl} \alpha_h\|_{L^2(\Omega)}\big) \leq \sup_{(q_h,\beta_h)\in(X_h(\mathcal{T})\times Y_h(\mathcal{T}))\setminus\{0\}} \frac{\mathcal{B}((p_h,\alpha_h),(q_h,\beta_h))}{\|q_h\|_{L^2(\Omega)} + \|\operatorname{Curl} \beta_h\|_{L^2(\Omega)}}$$

for all $(p_h, \alpha_h) \in X_h(\mathcal{T}) \times Y_h(\mathcal{T})$.

Proof. Let $(p_h, \alpha_h) \in X_h(\mathcal{T}) \times Y_h(\mathcal{T})$. Since $W_h(\mathcal{T}) \oplus \operatorname{Curl} Y_h(\mathcal{T}) = X_h(\mathcal{T})$, there exist $(\tau_h, \gamma_h) \in W_h(\mathcal{T}) \times Y_h(\mathcal{T})$ with

$$p_h = \tau_h + \operatorname{Curl} \gamma_h.$$

Set $q_h := \tau_h + \operatorname{Curl} \alpha_h$ and $\beta_h := \gamma_h$. The claim of Proposition 3.7 then follows analogously as Lemma 3.3. ■

The first conclusion from the inf-sup condition is the unique existence of discrete solutions.

Theorem 3.8 (existence of discrete solutions)**.** *Given $\varphi \in H(\operatorname{div},\Omega)$, there exists a unique solution $(p_h,\alpha_h) \in X_h(\mathcal{T}) \times Y_h(\mathcal{T})$ to (3.5) and*

$$\|p_h\|^2 + \|\operatorname{Curl}\alpha_h\|^2 = \|\Pi_k\varphi\|^2 \leq \|\varphi\|^2. \tag{3.7}$$

Proof. This follows from the continuity of $\mathcal{B}$, the global inf-sup condition from Proposition 3.7 and the symmetry of $\mathcal{B}$ as in the proof of Theorem 3.4. Alternatively, it follows from Theorem 2.8 and the inf-sup condition from Remark 3.6. The equality (3.7) follows from the L^2 orthogonality of p_h and $\operatorname{Curl}\alpha_h$. ∎

The conformity of the method and Proposition 3.7 imply the following best-approximation result.

Theorem 3.9 (best-approximation)**.** *The solution $(p,\alpha) \in X \times Y$ to (3.2) and the discrete solution $(p_h,\alpha_h) \in X_h(\mathcal{T}) \times Y_h(\mathcal{T})$ of (3.5) satisfy*

$$\begin{aligned}&\|p-p_h\|_{L^2(\Omega)} + \|\operatorname{Curl}(\alpha-\alpha_h)\|_{L^2(\Omega)}\\ &\qquad\leq 5\Big(\min_{q_h\in X_h(\mathcal{T})}\|p-q_h\|_{L^2(\Omega)} + \min_{\beta_h\in Y_h(\mathcal{T})}\|\operatorname{Curl}(\alpha-\beta_h)\|_{L^2(\Omega)}\Big).\end{aligned}$$

Proof. The bilinear form $\mathcal{B}$ is continuous with constant 1. Lemma 3.3 and Proposition 3.7 prove that the inf-sup constant of $\mathcal{B}$ is $1/5$. Classical results on oblique projections in Hilbert spaces [Xu and Zikatanov, 2003, Theorem 2] yield the assertion. ∎

Remark 3.10. The best-approximation of Theorem 3.9 contains the term

$$\min_{\beta_h\in Y_h(\mathcal{T})}\|\operatorname{Curl}(\alpha-\beta_h)\|_{L^2(\Omega)}$$

on the right-hand side, which depends on the choice of φ. This seems to be worse than the best-approximation results for standard FEMs, which do not involve such a term. However, if φ is smooth enough, then $\operatorname{Curl}\alpha = \varphi - \nabla u$ has at least the same regularity as ∇u, and therefore the convergence rate is not diminished. On the other hand, the approximation space for p does not have any continuity restriction and so the first approximation term

$$\min_{q_h\in X_h(\mathcal{T})}\|p-q_h\|_{L^2(\Omega)} \tag{3.8}$$

is superior to the best-approximation of a standard FEM, where $p = \nabla u$ is approximated with gradients of finite element functions. However, Veeser [2014, Theorem 3.2] and the comparison results of Carstensen, Peterseim, and Schedensack [2012] prove equivalence of (3.8) and the best-approximation with gradients of a standard FEM up to some multiplicative constant. ♦

The following lemma proves a projection property. This means that for any $v \in H^1_0(\Omega)$, the best-approximation of ∇v in $X_h(\mathcal{T})$ is a *discrete orthogonal gradient* in the sense that it is orthogonal to $\operatorname{Curl} Y_h(\mathcal{T})$ and so belongs to $W_h(\mathcal{T})$ from (3.6). The projection property is the key ingredient in the a posteriori and optimality analysis of Sections 3.4–3.5.

Lemma 3.11 (projection property). *Let $q \in L^2(\Omega;\mathbb{R}^2)$ with $(q, \operatorname{Curl}\beta)_{L^2(\Omega)} = 0$ for all $\beta \in Y$ (that means that q is a gradient of a $H^1_0(\Omega)$ function). Then $\Pi_{X_h(\mathcal{T})} q \in W_h(\mathcal{T})$. If $\mathcal{T}_\star$ is an admissible refinement of $\mathcal{T}$, then $\Pi_{X_h(\mathcal{T})} W_h(\mathcal{T}_\star) \subseteq W_h(\mathcal{T})$.*

Proof. Since $\operatorname{Curl} Y_h(\mathcal{T}) \subseteq X_h(\mathcal{T})$ and $Y_h(\mathcal{T}) \subseteq Y$, any $\beta_h \in Y_h(\mathcal{T})$ satisfies

$$(\Pi_{X_h(\mathcal{T})} q, \operatorname{Curl}\beta_h)_{L^2(\Omega)} = (q, \operatorname{Curl}\beta_h)_{L^2(\Omega)} = 0.$$

A similar proof applies to $q_h \in W_h(\mathcal{T}_\star)$ and proves $\Pi_{X_h(\mathcal{T})} W_h(\mathcal{T}_\star) \subseteq W_h(\mathcal{T})$. ∎

Remark 3.12 (Schur complement). Since there is no continuity restriction in $X_h(\mathcal{T})$ between elements, the mass matrix $\mathbf{M}$, that describes (q_h, p_h) for all $p_h, q_h \in X_h(\mathcal{T})$, is block diagonal. Let $\mathbf{p}_h$ and $\mathbf{a}_h$ be the coefficient vectors for p_h and α_h, $\mathbf{M}$ and $\mathbf{B}$ the representation matrices corresponding to $(\bullet, \bullet)_{L^2(\Omega)}$ and $(\bullet, \operatorname{Curl}\bullet)_{L^2(\Omega)}$ and $\mathbf{b}$ the right-hand side vector for $(\varphi, \bullet)_{L^2(\Omega)}$. Then, the discrete system can be rewritten as

$$\begin{aligned} \mathbf{M}\mathbf{p}_h + \mathbf{B}\mathbf{a}_h &= \mathbf{b}, \\ \mathbf{B}^\top \mathbf{p}_h &= 0. \end{aligned}$$

Since $\mathbf{M}$ is block diagonal with local mass matrices as sub-blocks, it can be directly inverted. This leads to the equivalent system

$$\begin{aligned} \mathbf{B}^\top \mathbf{M}^{-1} \mathbf{B} \mathbf{a}_h &= \mathbf{B}^\top \mathbf{M}^{-1} \mathbf{b}, \\ \mathbf{p}_h &= \mathbf{M}^{-1}(\mathbf{b} - \mathbf{B}\mathbf{a}_h) \end{aligned}$$

and the dimension of $\mathbf{B}^\top \mathbf{M}^{-1} \mathbf{B}$ is the same as in a standard FEM (up to degrees of freedom on the boundary) with a comparable sparsity. The condition numbers of $\mathbf{B}^\top \mathbf{M}^{-1} \mathbf{B}$ are compared with the condition numbers of a standard P_1 conforming FEM in Subsections 3.7.1–3.7.2 in two examples. They scale in the same way and the condition numbers of $\mathbf{B}^\top \mathbf{M}^{-1} \mathbf{B}$ are approximately 2 to 10 times larger. ⧫

3.1.3. Equivalence with Crouzeix-Raviart FEM

The non-conforming finite element space of Crouzeix and Raviart [1973] reads

$$\mathrm{CR}^1_0(\mathcal{T}) := \left\{ v_{\mathrm{CR}} \in P_1(\mathcal{T}) \;\middle|\; \begin{array}{l} v_{\mathrm{CR}} \text{ is continuous at midpoints of interior edges} \\ \text{and vanishes at midpoints of boundary edges} \end{array} \right\}.$$

Since $\mathrm{CR}^1_0(\mathcal{T}) \not\subseteq H^1_0(\Omega)$ (if the triangulation consists of more than one triangle), the weak gradient of a function $v_{\mathrm{CR}} \in \mathrm{CR}^1_0(\mathcal{T})$ does not exist in general. However, the piecewise version $\nabla_{\mathrm{NC}} v_{\mathrm{CR}} \in P_0(\mathcal{T};\mathbb{R}^2)$ defined by $(\nabla_{\mathrm{NC}} v_{\mathrm{CR}})|_T := \nabla(v_{\mathrm{CR}}|_T)$ for all $T \in \mathcal{T}$ exists. The P_1 non-conforming discretization of the Poisson problem seeks $u_{\mathrm{CR}} \in \mathrm{CR}^1_0(\mathcal{T})$ with

$$(\nabla_{\mathrm{NC}} u_{\mathrm{CR}}, \nabla_{\mathrm{NC}} v_{\mathrm{CR}})_{L^2(\Omega)} = (f, v_{\mathrm{CR}})_{L^2(\Omega)} \qquad \text{for all } v_{\mathrm{CR}} \in \mathrm{CR}^1_0(\mathcal{T}). \tag{3.9}$$

The lowest-order space of Raviart-Thomas finite element functions [Raviart and Thomas, 1977] reads

$$\mathrm{RT}_0(\mathcal{T}) := \left\{ q_{\mathrm{RT}} \in H(\mathrm{div},\Omega) \;\middle|\; \begin{array}{l} \forall T \in \mathcal{T}\, \exists a_T \in \mathbb{R}^2, b_T \in \mathbb{R} \\ \text{with } q_{\mathrm{RT}}(x) = a_T + b_T x \end{array} \right\}. \tag{3.10}$$

The Raviart-Thomas functions have the property that the integration by parts formula holds for functions in $H^1_0(\Omega)$ as well as for functions in $\mathrm{CR}^1_0(\mathcal{T})$.

The following proposition proves the equivalence of the P_1 non-conforming discretization and the discretization (3.5) for $k = 0$. Note that the discretization (3.9) is a non-conforming discretization, while the discretization (3.5) is a conforming one.

Proposition 3.13 (equivalence with CR-NCFEM)**.** *Let $f \in P_0(\mathcal{T})$ be piecewise constant and let $\varphi_{\mathrm{RT}} \in \mathrm{RT}_0(\mathcal{T})$ satisfy $-\operatorname{div}\varphi_{\mathrm{RT}} = f$. Then the discrete solution $(p_h, \alpha_h) \in P_0(\mathcal{T};\mathbb{R}^2) \times (P_1(\mathcal{T}) \cap Y)$ to (3.5) for $k = 0$ and the gradient of the discrete solution $u_{\mathrm{CR}} \in \mathrm{CR}^1_0(\mathcal{T})$ to (3.9) coincide,*

$$p_h = \nabla_{\mathrm{NC}} u_{\mathrm{CR}}.$$

Proof. The crucial point is the discrete Helmholtz decomposition of Arnold and Falk [1989]

$$P_0(\mathcal{T};\mathbb{R}^2) = \nabla_{\mathrm{NC}} \mathrm{CR}^1_0(\mathcal{T}) \oplus \mathrm{Curl}(P_1(\mathcal{T}) \cap Y). \tag{3.11}$$

Since p_h is L^2 orthogonal to $\mathrm{Curl}(P_1(\mathcal{T}) \cap Y)$, this implies $p_h = \nabla_{\mathrm{NC}} \widetilde{u}_{\mathrm{CR}}$ for some $\widetilde{u}_{\mathrm{CR}} \in \mathrm{CR}^1_0(\mathcal{T})$. Let $q_h = \nabla_{\mathrm{NC}} v_{\mathrm{CR}}$ for some $v_{\mathrm{CR}} \in \mathrm{CR}^1_0(\mathcal{T})$. Then q_h is L^2 orthogonal to $\mathrm{Curl}(P_1(\mathcal{T}) \cap Y)$ and a piecewise integration by parts and (3.5) imply

$$\begin{aligned} (\nabla_{\mathrm{NC}} \widetilde{u}_{\mathrm{CR}}, \nabla_{\mathrm{NC}} v_{\mathrm{CR}})_{L^2(\Omega)} &= (p_h, q_h)_{L^2(\Omega)} = (\varphi_{\mathrm{RT}}, q_h)_{L^2(\Omega)} \\ &= (-\operatorname{div}\varphi_{\mathrm{RT}}, v_{\mathrm{CR}})_{L^2(\Omega)} = (f, v_{\mathrm{CR}})_{L^2(\Omega)}. \end{aligned}$$

Hence, $\widetilde{u}_{\mathrm{CR}} = u_{\mathrm{CR}}$ solves (3.9). ∎

Remark 3.14 (higher polynomial degrees)**.** For higher polynomial degrees $k \geq 1$, the discretization (3.5) is not equivalent to known non-conforming schemes [Fortin and Soulie, 1983, Crouzeix and Falk, 1989, Crouzeix and Raviart, 1973, Matthies and Tobiska, 2005], in the sense that $W_h(\mathcal{T}) \neq \nabla_{\mathrm{NC}} V_h(\mathcal{T})$ for those non-conforming finite element spaces $V_h(\mathcal{T})$ as proved in the following.

The dimension of $W_h(\mathcal{T})$ can be computed by $\dim(W_h(\mathcal{T})) = \dim(X_h(\mathcal{T})) - \dim(Y_h(\mathcal{T}))$. Let $\mathcal{E}(\Omega)$ denote the interior sides. Then Euler's formulae lead to

$$\begin{aligned} \mathrm{card}(\mathcal{E}) + \mathrm{card}(\mathcal{E}(\Omega)) &= 3\,\mathrm{card}(\mathcal{T}), \\ \mathrm{card}(\mathcal{E}(\Omega)) + \mathrm{card}(\mathcal{N}) &= 2\,\mathrm{card}(\mathcal{T}) + 1. \end{aligned} \tag{3.12}$$

This results in

$$\begin{aligned} \dim(W_h(\mathcal{T})) &= \operatorname{card}(\mathcal{T}) + 2\operatorname{card}(\mathcal{E}(\Omega)) && \text{for } k=1, \\ \dim(W_h(\mathcal{T})) &= 3\operatorname{card}(\mathcal{T}) + 3\operatorname{card}(\mathcal{E}(\Omega)) && \text{for } k=2, \\ \dim(W_h(\mathcal{T})) &= 6\operatorname{card}(\mathcal{T}) + 4\operatorname{card}(\mathcal{E}(\Omega)) && \text{for } k=3. \end{aligned} \tag{3.13}$$

The non-conforming piecewise quadratic finite element of Fortin and Soulie [1983] has dimension $2\operatorname{card}(\mathcal{E}(\Omega))+1$. The non-conforming piecewise cubic finite element space of Crouzeix and Falk [1989] has dimension $3\operatorname{card}(\mathcal{E}(\Omega))+\operatorname{card}(\mathcal{T})$. This leads to $W_h(\mathcal{T}) \neq \nabla_{\mathrm{NC}} V_h(\mathcal{T})$ for those finite element spaces. The non-conforming FEM space of piecewise cubic plus quartic enrichment of Crouzeix and Raviart [1973] has dimension $3\operatorname{card}(\mathcal{E}(\Omega))+3\operatorname{card}(\mathcal{T})$, but $W_h(\mathcal{T}) \neq \nabla_{\mathrm{NC}} V_h(\mathcal{T})$ because of the quartic enrichment. The non-conforming FEMs of Matthies and Tobiska [2005] have the same dimensions as in (3.13), but the enrichment of those finite element spaces $V_h(\mathcal{T})$ result in $\nabla_{\mathrm{NC}} V_h(\mathcal{T}) \not\subseteq W_h(\mathcal{T})$. ♦

3.2. Remarks

The approximation of u does not appear in the discretization (3.5) and therefore the handling of non-homogeneous boundary conditions is not immediate but possible as discussed in Subsection 3.2.1. Subsection 3.2.2 is devoted to the question of how to find a function $\varphi \in H(\operatorname{div},\Omega)$ with $-\operatorname{div}\varphi = f$. Subsection 3.2.3 generalizes the novel FEM to quadrilateral meshes and proves a new discrete Helmholtz decomposition for the Q_1 rotated non-conforming FEM of Rannacher and Turek [1992]. Subsection 3.2.4 discusses a discretization with Raviart-Thomas functions.

3.2.1. Boundary conditions

This subsection discusses inhomogeneous Dirichlet and Neumann boundary conditions. Let $\partial\Omega = \Gamma_D \cup \Gamma_N$ with $\Gamma_D \neq \emptyset$ closed, $\Gamma_D \cap \Gamma_N = \emptyset$, and each connectivity component of Γ_D has positive length. Assume that the triangulation resolves Γ_D. Define

$$H^1_\star(\Omega) := \{\beta \in Y \mid \beta \text{ is constant on each connectivity component of } \Gamma_N\}.$$

The following Helmholtz decomposition is the point of departure for the novel formulation for mixed boundary conditions, cf. Girault and Raviart [1986, Corollary 3.1].

Theorem 3.15 (Helmholtz decomposition with mixed boundary conditions)**.** *It holds*

$$L^2(\Omega;\mathbb{R}^2) = \nabla H^1_{\Gamma_D}(\Omega) \oplus \operatorname{Curl} H^1_\star(\Omega)$$

and the sum is L^2-orthogonal.

Proof. The statement of Theorem 3.15 is a consequence of [Girault and Raviart, 1986, Corollary 3.1]; the proof given here deduces this statement from the Helmholtz decomposition from Theorem 3.1.

The orthogonality follows from an integration by parts. Let $\varphi \in L^2(\Omega;\mathbb{R}^2)$ and $u \in H^1_{\Gamma_D}(\Omega)$ be the solution of

$$(\nabla u, \nabla v)_{L^2(\Omega)} = (\varphi, \nabla v)_{L^2(\Omega)} \qquad \text{for all } v \in H^1_{\Gamma_D}(\Omega).$$

Then $r := (\varphi - \nabla u) \perp_{L^2(\Omega)} \nabla H^1_{\Gamma_D}(\Omega)$; in particular $r \perp_{L^2(\Omega)} \nabla H^1_0(\Omega)$. Theorem 3.1 guarantees the existence of $\alpha \in Y$ with $r = \operatorname{Curl}\alpha$. An integration by parts implies

$$0 = (r, \nabla v)_{L^2(\Omega)} = (\operatorname{Curl}\alpha, \nabla v)_{L^2(\Omega)} = \int_{\Gamma_N} v\, \nabla\alpha \cdot \tau \, ds$$

for all $v \in H^1_{\Gamma_D}(\Omega)$. This leads to $(\alpha \cdot \tau)|_{\Gamma_N} = 0$. Hence, α is constant on each connectivity component of Γ_N. ∎

Let $H^{-1/2}(\Gamma_N)$ denote the space of generalized normal traces of $H(\operatorname{div},\Omega)$ functions and let $u_D \in H^1(\Omega)$ and $g \in H^{-1/2}(\Gamma_N)$ in the sense, that there holds $g = q\cdot\nu$ on Γ_N in the sense of distributions for some $q \in H(\operatorname{div},\Omega)$. Consider the mixed boundary value problem

$$\begin{aligned} -\Delta u &= f && \text{in } \Omega, \\ u|_{\Gamma_D} &= u_D && \text{on } \Gamma_D, \\ (\nabla u \cdot \nu)|_{\Gamma_N} &= g && \text{on } \Gamma_N. \end{aligned} \tag{3.14}$$

Let $\varphi \in H(\operatorname{div},\Omega)$ with $-\operatorname{div}\varphi = f$ additionally fulfil the boundary condition $\varphi\nu|_{\Gamma_N} = g$. Then (3.14) is equivalent to the weak formulation: Find $(p,\alpha) \in L^2(\Omega;\mathbb{R}^2) \times H^1_\star(\Omega)$ with

$$\begin{aligned} (p,q)_{L^2(\Omega)} + (q, \operatorname{Curl}\alpha)_{L^2(\Omega)} &= (\varphi, q)_{L^2(\Omega)} && \text{for all } q \in L^2(\Omega;\mathbb{R}^2), \\ (p, \operatorname{Curl}\beta)_{L^2(\Omega)} &= (\nabla u_D, \operatorname{Curl}\beta)_{L^2(\Omega)} && \text{for all } \beta \in H^1_\star(\Omega). \end{aligned}$$

Since $p = \varphi - \operatorname{Curl}\alpha \in H(\operatorname{div},\Omega)$, the equivalence follows as in Subsection 3.1.1 and with

$$\begin{aligned} (p\cdot\nu)|_{\Gamma_N} &= (\varphi\cdot\nu)|_{\Gamma_N} - (\operatorname{Curl}\alpha\cdot\nu)|_{\Gamma_N} \\ &= g - (\nabla\alpha\cdot\tau)|_{\Gamma_N} = g. \end{aligned}$$

For the discretization, define $Y_h(\mathcal{T},\Gamma_N) := P_{k+1}(\mathcal{T}) \cap H^1_\star(\Omega)$. Then the discrete formulation reads: Find $(p_h,\alpha_h) \in X_h(\mathcal{T}) \times Y_h(\mathcal{T},\Gamma_N)$ with

$$\begin{aligned} (p_h,q_h)_{L^2(\Omega)} + (q_h, \operatorname{Curl}\alpha_h)_{L^2(\Omega)} &= (\varphi, q_h)_{L^2(\Omega)} && \text{for all } q_h \in X_h(\mathcal{T}), \\ (p_h, \operatorname{Curl}\beta_h)_{L^2(\Omega)} &= (\nabla u_D, \operatorname{Curl}\beta_h)_{L^2(\Omega)} && \text{for all } \beta_h \in Y_h(\mathcal{T},\Gamma_N). \end{aligned}$$

The a priori analysis from Section 3.1 proves the best-approximation result

$$\begin{aligned} &\|\nabla u - p_h\|_{L^2(\Omega)} + \|\operatorname{Curl}(\alpha-\alpha_h)\|_{L^2(\Omega)} \\ &\qquad \le 5\Big(\min_{q_h\in X_h(\mathcal{T})} \|\nabla u - q_h\|_{L^2(\Omega)} + \min_{\beta_h \in Y_h(\mathcal{T},\Gamma_N)} \|\operatorname{Curl}(\alpha-\beta_h)\|_{L^2(\Omega)} \Big). \end{aligned}$$

Remark 3.16 (multiply connected domains)**.** If $\Omega \subseteq \mathbb{R}^2$ is a multiply connected polygonal bounded Lipschitz domain and $\partial\Omega = \Gamma_D \cup \Gamma_N$, such that all parts of Γ_D lie on the outer boundary of Ω (on the unbounded connectivity component of $\mathbb{R}^2 \setminus \Omega$), then Theorem 3.15 still holds and a discretization as above is then immediate. However, if the Dirichlet boundary Γ_D also covers parts of interior boundary, the Helmholtz decomposition of Theorem 3.15 does no longer hold: There exist harmonic functions which are constant on different parts of Γ_D and, hence, are neither in $\nabla H^1_{\Gamma_D}(\Omega)$, nor in $\operatorname{Curl} H^1_\star(\Omega)$. ♦

3.2.2. Possible constructions of φ

Let $R \in \mathbb{R}$ with $\Omega \subseteq [-R, R]^2$. Given $f \in L^2(\Omega)$, the integration

$$\varphi_1(x, y) := -\int_{-R}^{x} f(t, y)\, dt$$

leads to $\varphi = (\varphi_1, 0) \in H(\operatorname{div}, \Omega)$ with $-\operatorname{div}\varphi = f$. For $\Gamma_N \neq \emptyset$, φ has to satisfy additional boundary conditions (see Subsection 3.2.1) and, hence, the construction is more involved. The following examples illustrate a possible design of $\varphi \in H(\operatorname{div}, \Omega)$ with $-\operatorname{div}\varphi = f$ in Ω and $\varphi \cdot \nu = g$ on Γ_N as long as $\operatorname{meas}_1(\Gamma_D) > 0$. The main idea is that one component of φ can be used to satisfy boundary conditions while the other one is constructed through an integration of f to guarantee $-\operatorname{div}\varphi = f$ (plus boundary conditions on one side). In all the experiments in Section 3.7, the construction of φ is possible by this ansatz.

Example 3.17. Let Ω be as in Figure 3.1a with $\Gamma_N \subseteq \{x_0\} \times \mathbb{R}$ and Neumann datum $g \in L^2(\Gamma_N)$. For almost all $(x, y) \in \Omega$, $\varphi(x, y)$ can be defined by

$$\begin{aligned} \varphi_1(x, y) &:= g(x_0, y) - \int_{x_0}^{x} f(t, y)\, dt \qquad \text{for almost all } (x, y) \in \Omega, \\ \varphi_2(x, y) &:= 0. \end{aligned}$$ ♦

Example 3.18. Let Ω be as in Figure 3.1b with $\Gamma_N \subseteq (\{x_0\} \times \mathbb{R}) \cup (\mathbb{R} \times \{y_0\})$ and Neumann datum $g \in L^2(\Gamma_N)$. For almost all $(x, y) \in \Omega$, $\varphi(x, y)$ can be defined by

$$\begin{aligned} \varphi_1(x, y) &:= g(x_0, y) - \int_{x_0}^{x} f(t, y)\, dt, \\ \varphi_2(x, y) &:= g(x, y_0). \end{aligned}$$ ♦

Example 3.19. Let Ω be as in Figure 3.1c with $\Gamma_N \subseteq (\{x_0\} \times \mathbb{R}) \cup (\mathbb{R} \times \{y_0\}) \cup (\{x_1\} \times \mathbb{R})$ and Neumann datum $g \in L^2(\Gamma_N)$. For almost all $(x, y) \in \Omega$, $\varphi(x, y)$ can be defined as follows. Let φ_1 fulfil the boundary conditions on the vertical parts of Γ_N and let

$$\varphi_2(x, y) := g(x, y_0) - \int_{y_0}^{y} \left(f(x, t) - \frac{\partial}{\partial x}\varphi_1(x, t) \right) dt.$$ ♦

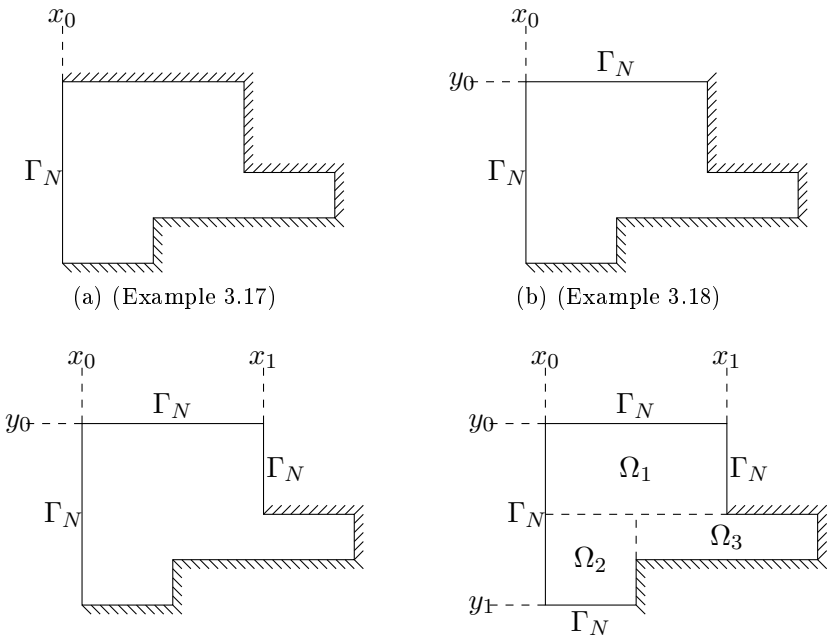

(a) (Example 3.17) (b) (Example 3.18)

(c) (Example 3.19) (d) (Example 3.20)

Figure 3.1.: The domains Ω from Examples 3.17–3.20 with Neumann boundary Γ_N and Dirichlet boundary (⊔⊔⊔).

Example 3.20. Let Ω be as in Figure 3.1d with $\Gamma_N \subseteq (\{x_0\} \times \mathbb{R}) \cup (\mathbb{R} \times \{y_0\}) \cup (\{x_1\} \times \mathbb{R}) \cup (\mathbb{R} \times \{y_1\})$ and Neumann datum $g \in L^2(\Gamma_N)$ and let Ω be decomposed in the subdomains Ω_1, Ω_2 and Ω_3 as depicted in Figure 3.1d. In the first step, let φ_1 fulfil the boundary conditions on the vertical parts of $\Gamma_N \cap \partial\Omega_1$ and define $\varphi_2|_{\Omega_1}(x,y)$ on Ω_1 for almost all $(x,y) \in \Omega_1$ by the integration

$$\varphi_2(x,y) := g(x,y_0) - \int_{y_0}^{y} \left(f(x,t) - \frac{\partial}{\partial x}\varphi_1(x,t) \right) dt.$$

In the second step, let $\varphi_2|_{\Omega_2}$ satisfy the boundary conditions on the lower horizontal part of $\Gamma_N \cap \partial\Omega_2$ and the boundary condition given through $\varphi_2|_{\Omega_1}$ on the upper horizontal part of $\partial\Omega_1 \cap \partial\Omega_2$. Define $\varphi_1|_{\Omega_2}(x,y)$ for almost all $(x,y) \in \Omega_2$ by

$$\varphi_1(x,y) := g(x_0,y) - \int_{-x_0}^{x} \left(f(t,y) - \frac{\partial}{\partial y}\varphi_2(x,t) \right) dt.$$

In the third step, $\varphi_1|_{\Omega_3}$ and $\varphi_2|_{\Omega_3}$ can be constructed as in Example 3.18 such that $\varphi_1|_{\partial\Omega_3} = \varphi_1|_{\partial\Omega_2}$ on $\partial\Omega_2 \cap \partial\Omega_3$ and $\varphi_2|_{\partial\Omega_3} = \varphi_2|_{\partial\Omega_1}$ on $\partial\Omega_1 \cap \partial\Omega_3$ and $-\operatorname{div}\varphi = f$. ♦

3.2.3. Quadrilateral finite elements

For this subsection, consider a regular partition $\mathcal{T}$ of Ω in quadrilaterals. Define for the reference rectangle $\widehat{T} = [0,1]^2$

$$Q_k(\widehat{T}) := \{v_h \in P_{2k}(\widehat{T}) \mid \exists f, g \in P_k([0,1]) :\ v_h(x,y) = f(x)g(y)\}.$$

Given $T \in \mathcal{T}$, let $\psi_T : \widehat{T} \to T$ denote the bilinear transformation from the reference rectangle to T. For consistency, let $P_{-1}([0,1]) := \{0\}$ and set

$$V_{Q,k}(\mathcal{T}) := \left\{ \beta_h \in Y \;\middle|\; \forall T \in \mathcal{T} :\ (\beta_h \circ \psi_T)|_{\widehat{T}} \in Q_k(\widehat{T}) \right\},$$

$$X_k^{\mathrm{rect}}(\widehat{T}) := \left\{ \tau_h \in L^2(\widehat{T};\mathbb{R}^2) \;\middle|\; \begin{array}{l} \exists a \in \mathbb{R}, b, c \in P_{k-2}([0,1]), d, e \in Q_{k-1}(\widehat{T}) \\ \text{ such that } \forall (\widehat{x},\widehat{y}) \in \widehat{T} \\ \tau_h(\widehat{x},\widehat{y}) = a \begin{pmatrix} -\widehat{x}^k \widehat{y}^{k-1} \\ \widehat{x}^{k-1}\widehat{y}^k \end{pmatrix} + \begin{pmatrix} \widehat{x}^k b(\widehat{y}) + d(\widehat{x},\widehat{y}) \\ \widehat{y}^k c(\widehat{x}) + e(\widehat{x},\widehat{y}) \end{pmatrix} \end{array} \right\},$$

$$X_k^{\mathrm{rect}}(\mathcal{T}) := \left\{ \tau_h \in L^2(\Omega;\mathbb{R}^2) \;\middle|\; \begin{array}{l} \forall T \in \mathcal{T}\, \exists \rho_T \in X_k^{\mathrm{rect}}(\widehat{T}) \text{ such that} \\ (\tau_h \circ \psi_T)|_{\widehat{T}} \\ \qquad = \begin{pmatrix} 0 & 1 \\ -1 & 0 \end{pmatrix} D(\psi_T^{-1})^\top \circ \psi_T \begin{pmatrix} 0 & -1 \\ 1 & 0 \end{pmatrix} \rho_T \end{array} \right\}.$$

Then a discretization with respect to the quadrilateral partition seeks $p_h \in X_k^{\mathrm{rect}}(\mathcal{T})$ and $\alpha_h \in V_{Q,k}(\mathcal{T})$ with

$$\begin{aligned} (p_h, q_h)_{L^2(\Omega)} + (q_h, \operatorname{Curl}\alpha_h)_{L^2(\Omega)} &= (\varphi, q_h)_{L^2(\Omega)} && \text{for all } q_h \in X_k^{\mathrm{rect}}(\mathcal{T}), \\ (p_h, \operatorname{Curl}\beta_h)_{L^2(\Omega)} &= 0 && \text{for all } \beta_h \in V_{Q,k}(\mathcal{T}). \end{aligned}$$

Let $\beta_h \in V_{Q,k}(\mathcal{T})$, i.e., $(\beta_h \circ \psi_T)|_{\widehat{T}} \in Q_k(\widehat{T})$. A direct calculation reveals for all $T \in \mathcal{T}$

$$\begin{aligned}((\operatorname{Curl}\beta_h)^\top \circ \psi_T)|_T &= (\nabla(\beta_h \circ \psi_T \circ \psi_T^{-1}))^\top \circ \psi_T \begin{pmatrix} 0 & 1 \\ -1 & 0 \end{pmatrix} \\ &= (\nabla(\beta_h \circ \psi_T))^\top D(\psi_T^{-1}) \circ \psi_T \begin{pmatrix} 0 & 1 \\ -1 & 0 \end{pmatrix}.\end{aligned}$$

Let $(\beta_h \circ \psi_T)(\widehat{x},\widehat{y}) = (\mathfrak{a}\widehat{x}^k + f(\widehat{x}))(\mathfrak{b}\widehat{y}^k + g(\widehat{y}))$ with $\mathfrak{a},\mathfrak{b} \in \mathbb{R}$ and $f, g \in P_{k-1}([0,1])$. Then it holds

$$\nabla(\beta_h \circ \psi_T) = \mathfrak{a}\mathfrak{b}k \begin{pmatrix} \widehat{x}^{k-1}\widehat{y}^k \\ \widehat{y}^{k-1}\widehat{x}^k \end{pmatrix} + \begin{pmatrix} \mathfrak{b}\widehat{y}^k \partial f(\widehat{x})/\partial\widehat{x} \\ \mathfrak{a}\widehat{x}^k \partial g(\widehat{y})/\partial\widehat{y} \end{pmatrix} + \begin{pmatrix} \mathfrak{a}k\widehat{x}^{k-1} g(\widehat{y}) + g(\widehat{y})\partial f(\widehat{x})/\partial\widehat{x} \\ \mathfrak{b}k\widehat{y}^{k-1} f(\widehat{x}) + f(\widehat{x})\partial g(\widehat{y})/\partial\widehat{y} \end{pmatrix}$$

and therefore

$$\begin{aligned}&(\nabla(\beta_h \circ \psi_T))^\top \begin{pmatrix} 0 & -1 \\ 1 & 0 \end{pmatrix} \\ &\quad = \left(\mathfrak{a}\mathfrak{b}k \begin{pmatrix} \widehat{y}^{k-1}\widehat{x}^k \\ -\widehat{x}^{k-1}\widehat{y}^k \end{pmatrix} + \begin{pmatrix} \mathfrak{a}\widehat{x}^k \partial g(\widehat{y})/\partial\widehat{y} \\ -\mathfrak{b}\widehat{y}^k \partial f(\widehat{x})/\partial\widehat{x} \end{pmatrix} + \begin{pmatrix} \mathfrak{b}k\widehat{y}^{k-1} f(\widehat{x}) + f(\widehat{x})\partial g(\widehat{y})/\partial\widehat{y} \\ -\mathfrak{a}k\widehat{x}^{k-1} g(\widehat{y}) - g(\widehat{y})\partial f(\widehat{x})/\partial\widehat{x} \end{pmatrix} \right)^\top \\ &\quad =: (\rho_T(\widehat{x},\widehat{y}))^\top.\end{aligned}$$

This implies $\rho_T \in X_k^{\mathrm{rect}}(\widehat{T})$ and $(\nabla(\beta_h \circ \psi_T)) = (0,1;-1,0)\rho_T$. The combination of the previous equalities leads to

$$((\operatorname{Curl}\beta_h) \circ \psi_T)|_T = \begin{pmatrix} 0 & 1 \\ -1 & 0 \end{pmatrix} D(\psi_T^{-1})^\top \circ \psi_T \begin{pmatrix} 0 & -1 \\ 1 & 0 \end{pmatrix} \rho_T.$$

Consequently, $\operatorname{Curl}\beta_h \in X_k^{\mathrm{rect}}(\mathcal{T})$. This and the conformity of the method prove as in Section 3.1 the following statements

(i) unique existence of solutions,

(ii) the best-approximation result

$$\begin{aligned}&\|p - p_h\|_{L^2(\Omega)} + \|\operatorname{Curl}(\alpha - \alpha_h)\|_{L^2(\Omega)} \\ &\qquad \lesssim \Big(\min_{q_h \in X_k^{\mathrm{rect}}(\mathcal{T})} \|p - q_h\|_{L^2(\Omega)} + \min_{\beta_h \in V_{Q,k}(\mathcal{T})} \|\operatorname{Curl}(\alpha - \beta_h)\|_{L^2(\Omega)} \Big),\end{aligned}$$

(iii) projection property

$$\Pi_{X_k^{\mathrm{rect}}(\mathcal{T})} \nabla H_0^1(\Omega) \subseteq W_h^{\mathrm{rect}}(\mathcal{T})$$

for

$$W_h^{\mathrm{rect}}(\mathcal{T}) = \{q_h \in X_k^{\mathrm{rect}}(\mathcal{T}) \mid \forall \beta_h \in V_{Q,k}(\mathcal{T}) :\ (q_h, \operatorname{Curl}\beta_h)_{L^2(\Omega)} = 0\}. \quad (3.15)$$

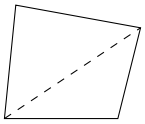

Figure 3.2.: Quadrilateral divided into two triangles.

Remark 3.21. The properties (i)–(iii) still hold for any $\widetilde{X}_h(\mathcal{T})$ with $X_k^{\mathrm{rect}}(\mathcal{T}) \subseteq \widetilde{X}_h(\mathcal{T}) \subseteq X$. ♦

The remaining part of this subsection proves the equivalence of the lowest-order rectangular discretization with the non-conforming FEM of Rannacher and Turek [1992]. To this end, define for the reference rectangle $\widehat{T}$ and the bilinear transformation $\psi_T : \widehat{T} \to T$,

$$Q^{\mathrm{rot}}(\widehat{T}) := \mathrm{span}\{1, x, y, x^2 - y^2\},$$
$$V_{\mathrm{NC}}^{\mathrm{rot}}(\mathcal{T}) := \left\{ v_h \in L^2(\Omega) \;\middle|\; \begin{array}{l} \forall T \in \mathcal{T}:\ (v_h \circ \psi_T)|_{\widehat{T}} \in Q^{\mathrm{rot}}(\widehat{T}) \text{ and} \\ \int_E v_h \, ds \text{ is continuous for all interior} \\ \text{edges } E \text{ and vanishes at boundary edges } E \end{array} \right\}. \quad (3.16)$$

The following lemma proves a relation between the cardinalities of the quadrilaterals, nodes, and interior edges of a quadrilateral partition similar to Euler's formulae (3.12). This enables a dimension argument in the proof of the discrete Helmholtz decomposition in Theorem 3.23 below.

Lemma 3.22 (Euler formula for quadrilateral partitions)**.** *Let $\mathcal{T}$ be a regular partition of Ω in quadrilaterals with edges $\mathcal{E}$, interior edges $\mathcal{E}(\Omega)$, and vertices $\mathcal{N}$. Then*

$$3\mathrm{card}(\mathcal{T}) + 1 = \mathrm{card}(\mathcal{E}(\Omega)) + \mathrm{card}(\mathcal{N}).$$

Proof. Define a triangulation $\mathcal{T}_\Delta$ of Ω in triangles by the division of each quadrilateral into two triangles as in Figure 3.2. Let $\mathcal{E}_\Delta$ denote the edges of $\mathcal{T}_\Delta$, $\mathcal{E}_\Delta(\Omega)$ the interior edges and $\mathcal{N}_\Delta$ the vertices. Then the following relations between the two partitions hold

$$\begin{aligned} \mathrm{card}(\mathcal{T}_\Delta) &= 2\mathrm{card}(\mathcal{T}), \\ \mathrm{card}(\mathcal{E}_\Delta) &= \mathrm{card}(\mathcal{E}) + \mathrm{card}(\mathcal{T}), \\ \mathrm{card}(\mathcal{E}_\Delta(\Omega)) &= \mathrm{card}(\mathcal{E}(\Omega)) + \mathrm{card}(\mathcal{T}), \\ \mathrm{card}(\mathcal{N}_\Delta) &= \mathrm{card}(\mathcal{N}). \end{aligned}$$

This and Euler's formulae for triangles (3.12) prove

$$\begin{aligned} \mathrm{card}(\mathcal{E}(\Omega)) + \mathrm{card}(\mathcal{N}) &= \mathrm{card}(\mathcal{E}_\Delta(\Omega)) - \mathrm{card}(\mathcal{T}) + \mathrm{card}(\mathcal{N}_\Delta) \\ &= 2\mathrm{card}(\mathcal{T}_\Delta) + 1 - \mathrm{card}(\mathcal{T}) \\ &= 3\mathrm{card}(\mathcal{T}) + 1. \end{aligned}$$

■

The following theorem proves that the solution space $W_h^{\mathrm{rect}}(\mathcal{T})$ from (3.15) equals the piecewise gradients of functions in $V_{\mathrm{NC}}^{\mathrm{rot}}(\mathcal{T})$ on a partition in squares.

Theorem 3.23 (discrete Helmholtz decomposition on squares)**.** *Let $\mathcal{T}$ be a regular partition of Ω in squares. Then,*

$$X_1^{\mathrm{rect}}(\mathcal{T}) = \nabla_{\mathrm{NC}} V_{\mathrm{NC}}^{\mathrm{rot}}(\mathcal{T}) \oplus \operatorname{Curl} V_{Q,1}(\mathcal{T})$$

and the decomposition is L^2 orthogonal.

Remark 3.24. The L^2-orthogonality

$$\nabla_{\mathrm{NC}} V_{\mathrm{NC}}^{\mathrm{rot}}(\mathcal{T}) \perp_{L^2(\Omega)} \operatorname{Curl} V_{Q,1}(\mathcal{T})$$

still holds for a partition in parallelograms. However, $\nabla_{\mathrm{NC}} V_{\mathrm{NC}}^{\mathrm{rot}}(\mathcal{T}) \not\subseteq X_1^{\mathrm{rect}}(\mathcal{T})$ for general quadrilateral partitions. ♦

Proof of Theorem 3.23. Let $v_h \in V_{\mathrm{NC}}^{\mathrm{rot}}(\mathcal{T})$ and $\beta_h \in V_{Q,1}(\mathcal{T})$. A piecewise integration by parts leads to

$$(\nabla_{\mathrm{NC}} v_h, \operatorname{Curl} \beta_h)_{L^2(\Omega)} = \sum_{E \in \mathcal{E}} \int_E [v_h]_E \nabla \beta_h \cdot \tau_E \, ds.$$

Since $\mathcal{T}$ consists of parallelograms, the bilinear transformation $\psi_T : \widehat{T} \to T$ is affine and, hence, $\beta_h|_E$ is affine on each edge $E \in \mathcal{E}$. This implies that $\nabla \beta_h \cdot \tau_E$ is constant. Since the integral mean of $[v_h]_E$ vanishes, this proves the L^2 orthogonality.

Let $v_h \in V_{\mathrm{NC}}^{\mathrm{rot}}(\mathcal{T})$. A computation reveals for all $T \in \mathcal{T}$ that there exist $f_T \in \mathbb{R}$ and $g_T \in \mathbb{R}^2$ such that

$$\nabla v_h(x,y) = D(\psi_T^{-1})^\top \left(f_T \begin{pmatrix} -x \\ y \end{pmatrix} + g_T \right).$$

For $k = 1$, $X_1^{\mathrm{rect}}(\mathcal{T})$ reads

$$X_1^{\mathrm{rect}}(\mathcal{T}) = \left\{ \tau_h \in L^2(\Omega;\mathbb{R}^2) \;\middle|\; \begin{array}{l} \forall T \in \mathcal{T}\, \exists a_T \in \mathbb{R}, d_T \in \mathbb{R}^2 \text{ such that} \\ (\tau_h \circ \psi_T)|_{\widehat{T}} = \begin{pmatrix} 0 & 1 \\ -1 & 0 \end{pmatrix} (D(\psi_T^{-1})^\top \\ \qquad\qquad \circ \psi_T) \begin{pmatrix} 0 & -1 \\ 1 & 0 \end{pmatrix} \left(a_T \begin{pmatrix} -x \\ y \end{pmatrix} + d_T \right) \end{array} \right\}.$$

Since all $T \in \mathcal{T}$ are squares, $D\psi_T$ and $(0,1;-1,0)$ commute, and, hence, $\nabla v_h \in X_1^{\mathrm{rect}}(\mathcal{T})$. Thus, $\nabla_{\mathrm{NC}} V_{\mathrm{NC}}^{\mathrm{rot}}(\mathcal{T}) \oplus \operatorname{Curl} V_{Q,1}(\mathcal{T}) \subseteq X_1^{\mathrm{rect}}(\mathcal{T})$. The dimension of $\nabla_{\mathrm{NC}} V_{\mathrm{NC}}^{\mathrm{rot}}(\mathcal{T})$ equals $\operatorname{card}(\mathcal{E}(\Omega))$ and the dimension of $\operatorname{Curl} V_{Q,1}(\mathcal{T})$ equals $\operatorname{card}(\mathcal{N}) - 1$, while the dimension of $X_1^{\mathrm{rect}}(\mathcal{T})$ equals $3\operatorname{card}(\mathcal{T})$. This and Lemma 3.22 prove the assertion. ■

Remark 3.25 (arbitrary quadrilaterals)**.** The best-approximation (ii) from above proves quasi-optimal convergence even for arbitrary quadrilaterals. Standard interpolation error estimates for $V_{Q,1}(\mathcal{T})$ and for $P_0(\mathcal{T};\mathbb{R}^2) \subseteq X_1^{\mathrm{rect}}(\mathcal{T})$ [Ciarlet, 1978] lead to first-order convergence rates of h for sufficiently smooth solutions. This should be contrasted with [Rannacher and Turek, 1992], where quasi-optimal convergence is only obtained for a modification of (3.16) where $V_{\mathrm{NC}}^{\mathrm{rot}}(\mathcal{T})$ is defined in terms of local coordinates. ⧫

3.2.4. Relation to mixed Raviart-Thomas FEM

This subsection shows that the classical mixed FEM of Raviart and Thomas [1977] can be regarded as a particular choice of the ansatz spaces in the new mixed scheme.

Let $\mathcal{T}$ denote a regular triangulation of Ω in triangles. Define the space of Raviart-Thomas functions [Raviart and Thomas, 1977]

$$X_{\mathrm{RT}}(\mathcal{T}) = \{q_h \in H(\mathrm{div},\Omega) \mid \forall T \in \mathcal{T}:\ q_h|_T(x) \in P_{k-1}(T;\mathbb{R}^2) + P_{k-1}(T)\,x\}$$

and

$$Y_{\mathrm{RT}}(\mathcal{T}) := P_k(\mathcal{T}) \cap Y.$$

Then the following problem is a discretization of (3.2): Seek $(p_h,\alpha_h) \in X_{\mathrm{RT}}(\mathcal{T}) \times Y_{\mathrm{RT}}(\mathcal{T})$ with

$$\begin{aligned} (p_h,q_h)_{L^2(\Omega)} + (q_h,\mathrm{Curl}\,\alpha_h)_{L^2(\Omega)} &= (\varphi,q_h) && \text{for all } q_h \in X_{\mathrm{RT}}(\mathcal{T}),\\ (p_h,\mathrm{Curl}\,\beta_h)_{L^2(\Omega)} &= 0 && \text{for all } \beta_h \in Y_{\mathrm{RT}}(\mathcal{T}). \end{aligned} \tag{3.17}$$

Since $\mathrm{Curl}\,Y_{\mathrm{RT}}(\mathcal{T}) \subseteq P_{k-1}(\mathcal{T};\mathbb{R}^2)$ and $\mathrm{div}\,\mathrm{Curl}\,v_h = 0$ for all $v_h \in Y_{\mathrm{RT}}(\mathcal{T})$, it follows $\mathrm{Curl}\,Y_{\mathrm{RT}}(\mathcal{T}) \subseteq X_{\mathrm{RT}}(\mathcal{T})$. This and the conformity of the method guarantee as in Section 3.1 and in Subsection 3.2.3 the unique existence of solutions, a best-approximation result, and the projection property

$$\Pi_{X_{\mathrm{RT}}(\mathcal{T})}\nabla H_0^1(\Omega) \subseteq W_h(\mathcal{T}) := \{q_h \in X_{\mathrm{RT}}(\mathcal{T}) \mid \forall \beta_h \in Y_{\mathrm{RT}}(\mathcal{T}):\ (q_h,\mathrm{Curl}\,\beta_h)_{L^2(\Omega)} = 0\}.$$

The discrete Helmholtz decomposition of [Huang and Xu, 2012, Arnold et al., 1997, Brezzi et al., 1991] proves

$$X_{\mathrm{RT}}(\mathcal{T}) = \nabla_h P_{k-1}(\mathcal{T}) \oplus \mathrm{Curl}\,Y_{\mathrm{RT}}(\mathcal{T})$$

with the operator $\nabla_h : P_{k-1}(\mathcal{T}) \to X_{\mathrm{RT}}(\mathcal{T})$ defined for all $v_h \in P_{k-1}(\mathcal{T})$ by

$$(\nabla_h v_h, q_h)_{L^2(\Omega)} = -(v_h, \mathrm{div}\,q_h)_{L^2(\Omega)} \qquad \text{for all } q_h \in X_{\mathrm{RT}}(\mathcal{T}).$$

This decomposition yields the equivalence of (3.17) with the problem: Seek $(p_h,\widetilde{u}_h) \in X_{\mathrm{RT}}(\mathcal{T}) \times P_{k-1}(\mathcal{T})$ with

$$\begin{aligned} p_h &= \nabla_h \widetilde{u}_h,\\ (w_h,\mathrm{div}\,p_h)_{L^2(\Omega)} &= (\mathrm{div}\,\Pi_{X_{\mathrm{RT}}(\mathcal{T})}\varphi, w_h)_{L^2(\Omega)} \qquad \text{for all } w_h \in P_{k-1}(\mathcal{T}). \end{aligned}$$

This is the classical Raviart-Thomas discretization with f replaced by $\mathrm{div}\,\Pi_{X_{\mathrm{RT}}(\mathcal{T})}\varphi$.

3.3. Medius analysis

The medius analysis of Gudi [2010] and Carstensen, Peterseim, and Schedensack [2012] proves for the discrete solution $u_{\mathrm{CR}} \in \mathrm{CR}^1_0(\mathcal{T})$ to (3.9) the best-approximation result

$$\|\nabla_{\mathrm{NC}}(u - u_{\mathrm{CR}})\|_{L^2(\Omega)} \lesssim \min_{v_{\mathrm{CR}} \in \mathrm{CR}^1_0(\mathcal{T})} \|\nabla_{\mathrm{NC}}(u - v_{\mathrm{CR}})\|_{L^2(\Omega)} + \mathrm{osc}(f, \mathcal{T}). \tag{3.18}$$

The following theorem proves a generalization for the discretization (3.5) for the lowest order case $k = 0$.

Theorem 3.26 (best-approximation property)**.** *Let $(p, \alpha) \in X \times Y$ be the solution to (3.2) and $(p_h, \alpha_h) \in P_0(\mathcal{T}; \mathbb{R}^2) \times (P_1(\mathcal{T}) \cap Y)$ be the solution to (3.5). Then the following best-approximation result holds*

$$\begin{aligned} \|p - p_h\|_{L^2(\Omega)} \lesssim \|p - \Pi_0 p\|_{L^2(\Omega)} + \mathrm{osc}(f, \mathcal{T}) \\ + \sup_{v_{\mathrm{CR}} \in \mathrm{CR}^1_0(\mathcal{T}) \setminus \{0\}} \frac{(f, v_{\mathrm{CR}})_{L^2(\Omega)} - (\varphi, \nabla_{\mathrm{NC}} v_{\mathrm{CR}})_{L^2(\Omega)}}{\|\nabla_{\mathrm{NC}} v_{\mathrm{CR}}\|_{L^2(\Omega)}}. \end{aligned} \tag{3.19}$$

Remark 3.27. If φ is a lowest-order Raviart-Thomas function, then it allows for an integration by parts formula also with Crouzeix-Raviart functions (see Subsection 3.1.3). Therefore, the third term on the right-hand side of (3.19) vanishes. This and the equivalence with the non-conforming FEM of Crouzeix and Raviart from Subsection 3.1.3 reveal the best-approximation result (3.18). ♦

The remaining part of this section is devoted to the proof of Theorem 3.26. The following lemma from [Carstensen and Schedensack, 2014, Carstensen, Gallistl, and Schedensack, 2015] is the key ingredient of this proof. Recall the definition of $\mathrm{CR}^1_0(\mathcal{T})$ from Subsection 3.1.3.

Lemma 3.28 (companion)**.** *For any $v_{\mathrm{CR}} \in \mathrm{CR}^1_0(\mathcal{T})$ there exists $v \in H^1_0(\Omega)$ with the following properties*

(i) $\Pi_0 \nabla_{\mathrm{NC}}(v - v_{\mathrm{CR}}) = 0$,

(ii) $\Pi_0(v - v_{\mathrm{CR}}) = 0$,

(iii) $\|h_{\mathcal{T}}^{-1}(v_{\mathrm{CR}} - v)\|_{L^2(\Omega)} + \|\nabla_{\mathrm{NC}}(v_{\mathrm{CR}} - v)\|_{L^2(\Omega)} \lesssim \|\nabla_{\mathrm{NC}} v_{\mathrm{CR}}\|_{L^2(\Omega)}$. ■

Proof of Theorem 3.26. Define $q_h := \Pi_0 p - p_h \in P_0(\mathcal{T}; \mathbb{R}^2)$. The projection property of Lemma 3.11 implies that $q_h \in W_h(\mathcal{T})$ and the discrete Helmholtz decomposition (3.11) guarantees the existence of $v_{\mathrm{CR}} \in \mathrm{CR}^1_0(\mathcal{T})$ with $q_h = \nabla_{\mathrm{NC}} v_{\mathrm{CR}}$. Let $v \in H^1_0(\Omega)$ denote the companion of v_{CR} from Lemma 3.28. Then

$$\begin{aligned} (p - p_h, q_h)_{L^2(\Omega)} = (p, \nabla_{\mathrm{NC}}(v_{\mathrm{CR}} - v))_{L^2(\Omega)} + (p, \nabla v)_{L^2(\Omega)} \\ - (p_h, \nabla_{\mathrm{NC}} v_{\mathrm{CR}})_{L^2(\Omega)}. \end{aligned} \tag{3.20}$$

The properties (i) and (iii) from Lemma 3.28 yield for the first term on the right-hand side

$$\begin{aligned}(p, \nabla_{\mathrm{NC}}(v_{\mathrm{CR}} - v))_{L^2(\Omega)} &= (p - \Pi_0 p, \nabla_{\mathrm{NC}}(v_{\mathrm{CR}} - v))_{L^2(\Omega)} \\ &\lesssim \|p - \Pi_0 p\|_{L^2(\Omega)} \, \|\nabla_{\mathrm{NC}} v_{\mathrm{CR}}\|_{L^2(\Omega)}.\end{aligned} \tag{3.21}$$

The problems (3.2) and (3.5) lead for the second and third term on the right-hand side of (3.20) to

$$(p, \nabla v)_{L^2(\Omega)} - (p_h, \nabla_{\mathrm{NC}} v_{\mathrm{CR}})_{L^2(\Omega)} = (\varphi, \nabla v)_{L^2(\Omega)} - (\varphi, \nabla_{\mathrm{NC}} v_{\mathrm{CR}})_{L^2(\Omega)}.$$

Since $-\operatorname{div} \varphi = f$, it follows

$$\begin{aligned}&(\varphi, \nabla v)_{L^2(\Omega)} - (\varphi, \nabla_{\mathrm{NC}} v_{\mathrm{CR}})_{L^2(\Omega)} \\ &\qquad = (f, v - v_{\mathrm{CR}})_{L^2(\Omega)} + (f, v_{\mathrm{CR}})_{L^2(\Omega)} - (\varphi, \nabla_{\mathrm{NC}} v_{\mathrm{CR}})_{L^2(\Omega)}.\end{aligned}$$

Properties (ii) and (iii) of Lemma 3.28 prove

$$= (f, v - v_{\mathrm{CR}})_{L^2(\Omega)} \lesssim \operatorname{osc}(f, \mathcal{T}) \|\nabla_{\mathrm{NC}} v_{\mathrm{CR}}\|_{L^2(\Omega)}.$$

The combination with (3.20) and (3.21) and a Cauchy inequality yield

$$\begin{aligned}(p - p_h, q_h)_{L^2(\Omega)} \lesssim \Bigg(&\|p - \Pi_0 p\|_{L^2(\Omega)} + \operatorname{osc}(f, \mathcal{T}) \\ &+ \sup_{v_{\mathrm{CR}} \in \mathrm{CR}^1_0(\mathcal{T}) \setminus \{0\}} \frac{(f, v_{\mathrm{CR}})_{L^2(\Omega)} - (\varphi, \nabla_{\mathrm{NC}} v_{\mathrm{CR}})_{L^2(\Omega)}}{\|\nabla_{\mathrm{NC}} v_{\mathrm{CR}}\|_{L^2(\Omega)}} \Bigg) \|q_h\|_{L^2(\Omega)}.\end{aligned}$$

This and

$$\|p - p_h\|^2_{L^2(\Omega)} = \|p - \Pi_0 p\|^2_{L^2(\Omega)} + \|q_h\|^2_{L^2(\Omega)} = \|p - \Pi_0 p\|^2_{L^2(\Omega)} + (p - p_h, q_h)_{L^2(\Omega)}$$

prove the assertion. ■

Remark 3.29 (higher polynomial degrees)**.** For $k \geq 1$, Remark 3.14 implies that an analogue of Lemma 3.28 cannot be proved in the same way. ♦

3.4. A posteriori error analysis

This section proves efficiency and reliability of a residual-based error estimator and of an averaging (or gradient recovery) error estimator.

Let $(p_h, \alpha_h) \in X_h(\mathcal{T}) \times Y_h(\mathcal{T})$ solve (3.5). Define the residual-based error estimator by

$$\begin{aligned}\eta^2(T) := \|\varphi - \Pi_k \varphi\|^2_{L^2(T)} &+ \|h_{\mathcal{T}} \operatorname{curl}_{\mathrm{NC}} p_h\|^2_{L^2(T)} \\ &+ h_T \sum_{E \in \mathcal{E}(T)} \|[p_h]_E \cdot \tau_E\|^2_{L^2(E)}\end{aligned} \tag{3.22}$$

and set

$$\eta^2 := \sum_{T\in\mathcal{T}} \eta^2(T).$$

The following theorem proves efficiency and reliability of η.

Theorem 3.30 (efficiency and reliability of the residual-based error estimator)**.** *Let $(p,\alpha) \in X \times Y$ and $(p_h,\alpha_h) \in X_h(\mathcal{T}) \times Y_h(\mathcal{T})$ be the solutions to (3.2) and (3.5). There exist constants $C_{\mathrm{eff}}, C_{\mathrm{rel}} > 0$ with*

$$C_{\mathrm{eff}}^{-2}\eta^2 \le \|p-p_h\|_{L^2(\Omega)}^2 + \|\mathrm{Curl}(\alpha-\alpha_h)\|_{L^2(\Omega)}^2 \le C_{\mathrm{rel}}^2\eta^2.$$

Proof. The proof follows in 4 steps.

Step 1. Define the residuals

$$\begin{aligned} \mathrm{Res}_1(p_h,\alpha_h;q) &:= (p_h,q)_{L^2(\Omega)} + (q,\mathrm{Curl}\,\alpha_h)_{L^2(\Omega)} - (\varphi,q)_{L^2(\Omega)} && \text{for all } q\in X,\\ \mathrm{Res}_2(p_h;\beta) &:= (p_h,\mathrm{Curl}\,\beta)_{L^2(\Omega)} && \text{for all } \beta\in Y. \end{aligned}$$

The abstract theory of Carstensen [2005] proves

$$\begin{aligned} &\|p-p_h\|_{L^2(\Omega)} + \|\mathrm{Curl}(\alpha-\alpha_h)\|_{L^2(\Omega)} \\ &\qquad\approx \|\mathrm{Res}_1(p_h,\alpha_h;\bullet)\|_{X^\star} + \|\mathrm{Res}_2(p_h;\bullet)\|_{Y^\star} \end{aligned} \tag{3.23}$$

with the inf-sup constant 5 from Lemma 3.3 hidden in $\lesssim$ and continuity constant 1 of $\mathcal{B}$ from (3.3) hidden in $\gtrsim$.

Step 2 (efficiency and reliability of Res_1*).* Let $q\in X$. The discrete problem (3.5) implies $p_h + \mathrm{Curl}\,\alpha_h = \Pi_k\varphi$ and therefore

$$\mathrm{Res}_1(p_h,\alpha_h;q) = (\Pi_k\varphi-\varphi,q)_{L^2(\Omega)}.$$

This implies

$$\|\mathrm{Res}_1(p_h,\alpha_h;\bullet)\|_{X^\star} = \|\varphi-\Pi_k\varphi\|_{L^2(\Omega)}.$$

Step 3 (reliability of Res_2*).* Let $I_h : Y \to P_1(\mathcal{T})\cap Y$ denote the quasi interpolant of Clément [1975] with the approximation and stability properties

$$\|h_{\mathcal{T}}^{-1}(\beta-I_h\beta)\|_{L^2(\Omega)} + \|\mathrm{Curl}(\beta-I_h\beta)\|_{L^2(\Omega)} \lesssim \|\mathrm{Curl}\,\beta\|_{L^2(\Omega)}. \tag{3.24}$$

A piecewise integration by parts and the discrete problem (3.5) yield for the second term in (3.23) for $\beta\in Y$ with $\|\mathrm{Curl}\,\beta\|_{L^2(\Omega)} = 1$ that

$$\begin{aligned} \mathrm{Res}_2(p_h;\beta) &= (p_h,\mathrm{Curl}(\beta-I_h\beta))_{L^2(\Omega)}\\ &= -(\mathrm{curl}_{\mathrm{NC}}\,p_h,\beta-I_h\beta)_{L^2(\Omega)} + \sum_{E\in\mathcal{E}}\int_E [p_h\cdot\tau_E]_E(\beta-I_h\beta)\,ds. \end{aligned}$$

A piecewise Cauchy inequality and (3.24) imply

$$-(\operatorname{curl}_{\mathrm{NC}} p_h, \beta - I_h\beta)_{L^2(\Omega)} \lesssim \|h_{\mathcal{T}} \operatorname{curl}_{\mathrm{NC}} p_h\|_{L^2(\Omega)} \|\operatorname{Curl} \beta\|_{L^2(\Omega)}.$$

Let $E \in \mathcal{E}$ and $T \in \mathcal{T}$ with $E \in \mathcal{E}(T)$. The Cauchy and the trace inequality from Theorem 2.7 lead to

$$\begin{aligned}\int_E [p_h \cdot \tau_E]_E(\beta - I_h\beta)\, ds &\le h_T^{1/2} \|[p_h \cdot \tau_E]_E\|_{L^2(E)} h_T^{-1/2} \|\beta - I_h\beta\|_{L^2(E)} \\ &\lesssim h_T^{1/2} \|[p_h \cdot \tau_E]_E\|_{L^2(E)} \big(\|\nabla(\beta - I_h\beta)\|_{L^2(T)} + \|h_T^{-1}(\beta - I_h\beta)\|_{L^2(T)}\big).\end{aligned}$$

A Cauchy inequality and the approximation and stability properties (3.24) of I_h yield

$$\begin{aligned}&\sum_{E\in\mathcal{E}} \int_E [p_h \cdot \tau_E]_E(\beta - I_h\beta)\, ds \\ &\lesssim \big(\|\nabla(\beta - I_h\beta)\|_{L^2(\Omega)} + \|h_T^{-1}(\beta - I_h\beta)\|_{L^2(\Omega)}\big) \sqrt{\sum_{T\in\mathcal{T}} h_T^{1/2} \sum_{E\in\mathcal{E}(T)} \|[p_h \cdot \tau_E]_E\|^2_{L^2(E)}} \\ &\lesssim \|\operatorname{Curl} \beta\|_{L^2(T)} \sqrt{\sum_{T\in\mathcal{T}} h_T^{1/2} \sum_{E\in\mathcal{E}(T)} \|[p_h \cdot \tau_E]_E\|^2_{L^2(E)}}.\end{aligned}$$

The combination of the previous displayed inequalities leads to

$$\|\operatorname{Res}_2(p_h; \bullet)\|^2_{Y^\star} \lesssim \|h_{\mathcal{T}} \operatorname{curl}_{\mathrm{NC}} p_h\|^2_{L^2(\Omega)} + \sum_{T\in\mathcal{T}} h_T \sum_{E\in\mathcal{E}(T)} \|[p_h \cdot \tau_E]_E\|^2_{L^2(E)}.$$

Step 4 (efficiency of Res_2*).* The proof of the efficiency of $\|\operatorname{Res}_2(p_h; \bullet)\|_{Y^\star}$ follows with the arguments of Verfürth [1996] and is carried out for completeness. Let $E = \operatorname{conv}\{a, b\} \in \mathcal{E}$. Define the edge bubble function $\flat_E \in H^1(\Omega)$ by $\flat_E := 6\varphi_a\varphi_b$. Define $\psi_E := [Pp_h \cdot \tau_E]_E \flat_E \in P_{k+2}(\mathcal{T}) \cap H^1(\Omega)$ with the continuation operator $P : L^\infty(E) \to L^\infty(\omega_E)$ from [Verfürth, 1996]. The homogeneous boundary conditions $\flat_E|_{\partial\omega_E \setminus E} = 0$ lead to

$$\begin{aligned}\|[p_h \cdot \tau_E]_E\|^2_{L^2(E)} \lesssim \|\flat_E^{1/2} [p_h \cdot \tau_E]_E\|^2_{L^2(E)} &= \int_E [p_h \cdot \tau_E]_E \psi_E\, ds \\ &= \int_{\omega_E} p_h \cdot \operatorname{Curl} \psi_E\, dx + \int_{\omega_E} \psi_E \operatorname{curl}_{\mathrm{NC}} p_h\, dx.\end{aligned}$$

The continuous problem (3.2) and a Cauchy inequality imply

$$\int_{\omega_E} p_h \cdot \operatorname{Curl} \psi_E\, dx = \int_\Omega (p_h - p) \cdot \operatorname{Curl} \psi_E\, dx \le \|p - p_h\|_{L^2(\omega_E)} \|\operatorname{Curl} \psi_E\|_{L^2(\Omega)}.$$

This, the definition of ψ_E, and the scaling $\|\operatorname{Curl}\psi_E\|_{L^2(\Omega)} \lesssim h_E^{-1/2}\|[p_h\cdot\tau_E]_E\|_{L^2(E)}$ prove

$$\int_{\omega_E} p_h\cdot\operatorname{Curl}\psi_E\,dx \lesssim h_E^{-1/2}\|p-p_h\|_{L^2(\omega_E)}\,\|[p_h\cdot\tau_E]_E\|_{L^2(E)}.$$

The scaling $\|\psi_E\|_{L^2(\omega_E)} \lesssim h_E^{1/2}\|[p_h\cdot\tau_E]_E\|_{L^2(E)}$ and a Cauchy inequality reveal

$$\int_{\omega_E} \psi_E\operatorname{curl_{NC}} p_h\,dx \lesssim h_E^{-1/2}\|h_{\mathcal{T}}\operatorname{curl_{NC}} p_h\|_{L^2(\omega_E)}\|[p_h\cdot\tau_E]_E\|_{L^2(E)}.$$

The combination of the previously displayed inequalities leads to

$$h_E^{1/2}\|[p_h\cdot\tau_E]_E\|_{L^2(E)} \lesssim \|p-p_h\|_{L^2(\omega_E)} + \|h_{\mathcal{T}}\operatorname{curl_{NC}} p_h\|_{L^2(\omega_E)}.$$

It remains to estimate $\|h_{\mathcal{T}}\operatorname{curl_{NC}} p_h\|_{L^2(\omega_E)}$. Let $T=\operatorname{conv}\{a,b,c\}\in\mathcal{T}$. Let the volume bubble $\flat_T$ be defined by $\flat_T := 60\varphi_a\varphi_b\varphi_c$. Define $\psi_T := \flat_T\operatorname{curl_{NC}} p_h$. The homogeneous boundary conditions of ψ_T on ∂T and a piecewise integration by parts imply

$$\begin{aligned}\|\operatorname{curl_{NC}} p_h\|_{L^2(T)}^2 \lesssim \|\flat_T^{1/2}\operatorname{curl_{NC}} p_h\|_{L^2(T)}^2 &= \int_T \psi_T\operatorname{curl_{NC}} p_h\,dx\\ &= -\int_T p_h\operatorname{Curl}\psi_T\,dx.\end{aligned}$$

The continuous problem (3.2) implies

$$-\int_T p_h\operatorname{Curl}\psi_T\,dx = \int_T (p-p_h)\operatorname{Curl}\psi_T\,dx \le \|p-p_h\|_{L^2(T)}\,\|\operatorname{Curl}\psi_T\|_{L^2(T)}.$$

The scaling $\|\operatorname{Curl}\psi_T\|_{L^2(T)} \lesssim h_T^{-1}\,\|\operatorname{curl_{NC}} p_h\|_{L^2(T)}$ concludes the proof. ∎

The second part of this section is devoted to the reliability of an averaging (or gradient recovery) error estimator.

Theorem 3.31. *Let $(p,\alpha)\in X\times Y$ and $(p_h,\alpha_h)\in X_h(\mathcal{T})\times Y_h(\mathcal{T})$ be the solutions to (3.2) and (3.5). Let $\ell\in\mathbb{N}$ and $\widetilde{p}\in P_\ell(\mathcal{T};\mathbb{R}^2)$ be arbitrary. It holds*

$$\begin{aligned}&\|p-p_h\|_{L^2(\Omega)}^2 + \|\operatorname{Curl}(\alpha-\alpha_h)\|_{L^2(\Omega)}^2\\ &\qquad\lesssim \|\varphi-\Pi_k\varphi\|_{L^2(\Omega)}^2 + \|p_h-\widetilde{p}\|_{L^2(\Omega)}^2\\ &\qquad\qquad + \|h_{\mathcal{T}}\operatorname{curl_{NC}} p_h\|_{L^2(\Omega)}^2 + \sum_{E\in\mathcal{E}} h_E\|[\widetilde{p}\cdot\tau_E]_E\|_{L^2(E)}^2\end{aligned}\tag{3.25}$$

and

$$\begin{aligned}&\|p-p_h\|_{L^2(\Omega)}^2 + \|\operatorname{Curl}(\alpha-\alpha_h)\|_{L^2(\Omega)}^2\\ &\qquad\lesssim \|\varphi-\Pi_k\varphi\|_{L^2(\Omega)}^2 + \|p_h-\widetilde{p}\|_{L^2(\Omega)}^2\\ &\qquad\qquad + \|h_{\mathcal{T}}\operatorname{curl_{NC}}\widetilde{p}\|_{L^2(\Omega)}^2 + \sum_{E\in\mathcal{E}} h_E\|[\widetilde{p}\cdot\tau_E]_E\|_{L^2(E)}^2.\end{aligned}\tag{3.26}$$

The constants hidden in $\lesssim$ may depend on ℓ.

Proof. Steps 1 and 2 in the proof of Theorem 3.30 lead to

$$\begin{aligned}\|p-p_h\|_{L^2(\Omega)}^2 + \|\operatorname{Curl}(\alpha-\alpha_h)\|_{L^2(\Omega)}^2 \\ \approx \|\varphi - \Pi_k\varphi\|_{L^2(\Omega)}^2 + \|\operatorname{Res}_2(p_h;\bullet)\|_{Y^\star}^2.\end{aligned}$$

Hence, it remains to bound the residual $\|\operatorname{Res}_2(p_h;\bullet)\|_{Y^\star}$.

Let $\widetilde{p} \in P_\ell(\mathcal{T};\mathbb{R}^2)$ and $\beta \in Y$ with $\|\operatorname{Curl}\beta\|_{L^2(\Omega)} = 1$ and let $I_h : Y \to P_1(\mathcal{T}) \cap Y$ denote the quasi interpolant from Step 3 in the proof of Theorem 3.30. The orthogonality of p_h and $\operatorname{Curl} Y_h(\mathcal{T})$ implies

$$\begin{aligned}(p_h, \operatorname{Curl}\beta)_{L^2(\Omega)} = (p_h-\widetilde{p}, \operatorname{Curl}\beta)_{L^2(\Omega)} + (\widetilde{p}, \operatorname{Curl}(\beta - I_h\beta))_{L^2(\Omega)} \\ + (\widetilde{p}-p_h, \operatorname{Curl} I_h\beta)_{L^2(\Omega)}.\end{aligned} \tag{3.27}$$

A Cauchy inequality and the stability of I_h from (3.24) bound the first and the last term

$$(p_h-\widetilde{p}, \operatorname{Curl}\beta)_{L^2(\Omega)} + (\widetilde{p}-p_h, \operatorname{Curl} I_h\beta)_{L^2(\Omega)} \lesssim \|p_h-\widetilde{p}\|_{L^2(\Omega)}.$$

A piecewise integration by parts yields for the second term of (3.27)

$$(\widetilde{p}, \operatorname{Curl}(\beta - I_h\beta))_{L^2(\Omega)} = -(\operatorname{curl}_{\mathrm{NC}}\widetilde{p}, \beta - I_h\beta)_{L^2(\Omega)} + \sum_{E\in\mathcal{E}}\int_E [\widetilde{p}\cdot\tau_E]_E(\beta - I_h\beta)\,ds.$$

Two Cauchy inequalities, the trace inequality of Theorem 2.7 and the stability of I_h from (3.24) bound the second term as in Step 3 in the proof of Theorem 3.30

$$\begin{aligned}\sum_{E\in\mathcal{E}}\int_E [\widetilde{p}\cdot\tau_E]_E(\beta - I_h\beta)\,ds &\le \sqrt{\sum_{E\in\mathcal{E}} h_E\|[\widetilde{p}\cdot\tau_E]_E\|_{L^2(E)}^2}\sqrt{\sum_{E\in\mathcal{E}} h_E^{-1}\|\beta - I_h\beta\|_{L^2(E)}^2} \\ &\lesssim \sqrt{\sum_{E\in\mathcal{E}} h_E\|[\widetilde{p}\cdot\tau_E]_E\|_{L^2(E)}^2}.\end{aligned}$$

This results in

$$(\widetilde{p}, \operatorname{Curl}(\beta - I_h\beta))_{L^2(\Omega)} \lesssim |(\operatorname{curl}_{\mathrm{NC}}\widetilde{p}, \beta - I_h\beta)_{L^2(\Omega)}| + \sqrt{\sum_{E\in\mathcal{E}} h_E\|[\widetilde{p}\cdot\tau_E]_E\|_{L^2(E)}^2}.$$

A Cauchy inequality and the approximation properties (3.24) of I_h lead to

$$|(\operatorname{curl}_{\mathrm{NC}}\widetilde{p}, \beta - I_h\beta)_{L^2(\Omega)}| \lesssim \|h_{\mathcal{T}}\operatorname{curl}_{\mathrm{NC}}\widetilde{p}\|_{L^2(\Omega)},$$

which proves (3.26).

The triangle inequality yields

$$\|h_{\mathcal{T}}\operatorname{curl}_{\mathrm{NC}}\widetilde{p}\|_{L^2(\Omega)} \le \|h_{\mathcal{T}}\operatorname{curl}_{\mathrm{NC}}p_h\|_{L^2(\Omega)} + \|h_{\mathcal{T}}\operatorname{curl}_{\mathrm{NC}}(p_h-\widetilde{p})\|_{L^2(\Omega)}.$$

Since $p_h - \widetilde{p} \in P_{\max(k,\ell)}(\mathcal{T};\mathbb{R}^2)$, an inverse inequality bounds the second term on the right hand side as

$$\|h_{\mathcal{T}}\operatorname{curl}_{\mathrm{NC}}(p_h-\widetilde{p})\|_{L^2(\Omega)} \lesssim \|p_h-\widetilde{p}\|_{L^2(\Omega)}.$$

This proves (3.25). ∎

Let $k = 0$ (for higher polynomial degrees, see Remark 3.34) and define an averaging operator $A : P_0(\mathcal{T};\mathbb{R}^2) \to P_1(\mathcal{T};\mathbb{R}^2) \cap H^1(\Omega;\mathbb{R}^2)$ as follows. Given $p_h \in P_0(\mathcal{T};\mathbb{R}^2)$, let $\omega_z := \cup\{T \in \mathcal{T} \mid z \in \mathcal{N}(T)\}$ and $Ap_h \in P_1(\mathcal{T};\mathbb{R}^2) \cap H^1(\Omega;\mathbb{R}^2)$ be the piecewise affine continuation of

$$(Ap_h)(z) := \fint_{\omega_z} p_h \, dx \qquad \text{for all } z \in \mathcal{N}.$$

The following corollary proves reliability of the averaging error estimator $\|\varphi - \Pi_0\varphi\|^2_{L^2(\Omega)} + \|p_h - Ap_h\|^2_{L^2(\Omega)}$.

Corollary 3.32 (reliability of an averaging error estimator)**.** *Let $k = 0$ and $(p,\alpha) \in X \times Y$ and $(p_h,\alpha_h) \in X_h(\mathcal{T}) \times Y_h(\mathcal{T})$ be the solutions to (3.2) and (3.5). Then,*

$$\|p - p_h\|^2_{L^2(\Omega)} + \|\mathrm{Curl}(\alpha - \alpha_h)\|^2_{L^2(\Omega)} \lesssim \|\varphi - \Pi_0\varphi\|^2_{L^2(\Omega)} + \|p_h - Ap_h\|^2_{L^2(\Omega)}.$$

Proof. Theorem 3.31 proves

$$\begin{aligned}\|p - p_h\|^2_{L^2(\Omega)} &+ \|\mathrm{Curl}(\alpha - \alpha_h)\|^2_{L^2(\Omega)} \\ &\lesssim \|\varphi - \Pi_0\varphi\|^2_{L^2(\Omega)} + \|p_h - Ap_h\|^2_{L^2(\Omega)} \\ &\qquad + \|h_{\mathcal{T}} \operatorname{curl}_{\mathrm{NC}} p_h\|^2_{L^2(\Omega)} + \sum_{E\in\mathcal{E}} h_E \|[Ap_h \cdot \tau_E]_E\|^2_{L^2(E)}.\end{aligned}$$

Since $p_h \in P_0(\mathcal{T};\mathbb{R}^2)$ is piecewise constant, $\|h_{\mathcal{T}} \operatorname{curl}_{\mathrm{NC}} p_h\|_{L^2(\Omega)} = 0$ vanishes. The continuity of $Ap_h \in H^1(\Omega;\mathbb{R}^2)$ implies that also the last term on the right-hand side vanishes. ∎

Remark 3.33 (efficiency of the averaging error estimator)**.** The triangle inequality implies

$$\begin{aligned}\min_{q_h \in P_1(\mathcal{T};\mathbb{R}^2)\cap H^1(\Omega,\mathbb{R}^2)} &\|p_h - q_h\|_{L^2(\Omega)} \\ &\le \|p - p_h\|_{L^2(\Omega)} + \min_{q_h \in P_1(\mathcal{T};\mathbb{R}^2)\cap H^1(\Omega,\mathbb{R}^2)} \|p - q_h\|_{L^2(\Omega)}.\end{aligned}$$

For smooth $p \in H^1(\Omega,\mathbb{R}^2)$, the last term on the right-hand side is of higher order. This, the equivalence [Carstensen, 2004]

$$\min_{q_h \in P_1(\mathcal{T};\mathbb{R}^2)\cap H^1(\Omega,\mathbb{R}^2)} \|p_h - q_h\|_{L^2(\Omega)} \approx \|p_h - Ap_h\|_{L^2(\Omega)},$$

and the efficiency of $\|\varphi - \Pi_0\varphi\|_{L^2(\Omega)}$ from Step 2 of the proof of Theorem 3.30 prove the efficiency of $\|p_h - Ap_h\|_{L^2(\Omega)} + \|\varphi - \Pi_0\varphi\|_{L^2(\Omega)}$ for smooth p up to higher-order terms. ⧫

Remark 3.34 (averaging operator for higher polynomial degrees)**.** For $k \ge 1$, the term $\|h_{\mathcal{T}} \operatorname{curl}_{\mathrm{NC}} p_h\|_{L^2(\Omega)}$ does not vanish in general. Hence, an averaging

error estimator has to involve that term. For some operator $A : P_k(\mathcal{T};\mathbb{R}^2) \to (P_{k+1}(\mathcal{T};\mathbb{R}^2) \cap H^1(\Omega,\mathbb{R}^2))$, Theorem 3.31 proves the reliability of

$$\|\varphi - \Pi_k\varphi\|^2_{L^2(\Omega)} + \|p_h - Ap_h\|^2_{L^2(\Omega)} + \|h_{\mathcal{T}} \operatorname{curl}_{\mathrm{NC}} p_h\|^2_{L^2(\Omega)}$$

and

$$\|\varphi - \Pi_k\varphi\|^2_{L^2(\Omega)} + \|p_h - Ap_h\|^2_{L^2(\Omega)} + \|h_{\mathcal{T}} \operatorname{curl}_{\mathrm{NC}} Ap_h\|^2_{L^2(\Omega)}. \qquad \blacklozenge$$

3.5. Adaptive algorithm

This section defines an adaptive algorithm based on separate marking with the residual-based error estimator from Section 3.4 and proves its quasi-optimal convergence.

3.5.1. Adaptive algorithm and optimal convergence rates

Given a triangulation $\mathcal{T}_\ell$, define for all $T \in \mathcal{T}_\ell$ the local error estimator contributions by

$$\begin{aligned} \lambda^2(\mathcal{T}_\ell, T) &:= \|h_{\mathcal{T}} \operatorname{curl}_{\mathrm{NC}} p_h\|^2_{L^2(T)} + h_T \sum_{E\in\mathcal{E}(T)} \|[p_h]_E \cdot \tau_E\|^2_{L^2(E)}, \\ \mu^2(T) &:= \|\varphi - \Pi_k\varphi\|^2_{L^2(T)} \end{aligned} \tag{3.28}$$

and the global error estimators by

$$\begin{aligned} \lambda_\ell^2 &:= \lambda^2(\mathcal{T}_\ell, \mathcal{T}_\ell) \quad \text{with} \quad \lambda^2(\mathcal{T}_\ell, \mathcal{M}) := \sum_{T\in\mathcal{M}} \lambda^2(\mathcal{T}_\ell, T) \quad \text{for any } \mathcal{M} \subseteq \mathcal{T}_\ell, \\ \mu_\ell^2 &:= \mu^2(\mathcal{T}_\ell) \qquad \text{with} \qquad \mu^2(\mathcal{M}) := \sum_{T\in\mathcal{M}} \mu^2(T) \qquad \text{for any } \mathcal{M} \subseteq \mathcal{T}_\ell. \end{aligned} \tag{3.29}$$

The adaptive algorithm is driven by these two error estimators and runs the following loop.

Algorithm 3.35 (AFEM for the Poisson problem)**.**
Input: Initial triangulation $\mathcal{T}_0$, parameters $0 < \theta_A \le 1$, $0 < \rho_B < 1$, $0 < \kappa$.
for $\ell = 0, 1, 2, \dots$ **do**
Solve. Compute solution $(p_\ell, \alpha_\ell) \in X_h(\mathcal{T}_\ell) \times Y_h(\mathcal{T}_\ell)$ of (3.5) with respect to $\mathcal{T}_\ell$.
Estimate. Compute local contributions of the error estimators $\big(\lambda^2(\mathcal{T}_\ell, T)\big)_{T\in\mathcal{T}_\ell}$ and $\big(\mu^2(T)\big)_{T\in\mathcal{T}_\ell}$.
if $\mu_\ell^2 \le \kappa\lambda_\ell^2$ **then**
Mark. The Dörfler marking chooses a minimal subset $\mathcal{M}_\ell \subseteq \mathcal{T}_\ell$ such that $\theta_A\lambda_\ell^2 \le \lambda_\ell^2(\mathcal{T}_\ell, \mathcal{M}_\ell)$.
Refine. Generate the smallest admissible refinement $\mathcal{T}_{\ell+1}$ of $\mathcal{T}_\ell$ in which at least all triangles in $\mathcal{M}_\ell$ are refined.

else
Mark. Compute a triangulation $\mathcal{T} \in \mathbb{T}$ with $\mu^2(\mathcal{T}) \leq \rho_B \mu_\ell^2$.
Refine. Generate the overlay $\mathcal{T}_{\ell+1}$ of $\mathcal{T}_\ell$ and $\mathcal{T}$.
end if
end for
Output: Sequence of triangulations $(\mathcal{T}_\ell)_{\ell\in\mathbb{N}_0}$, discrete solutions $(p_\ell, \alpha_\ell)_{\ell\in\mathbb{N}_0}$ and error estimators $(\lambda_\ell)_{\ell\in\mathbb{N}_0}$ and $(\mu_\ell)_{\ell\in\mathbb{N}_0}$. ♦

Remark 3.36 (separate versus collective marking)**.** The residual-based error estimator from Section 3.4 involves the term $\|\varphi - \Pi_k\varphi\|_{L^2(T)}$ without a multiplicative positive power of the mesh-size. Therefore, the optimality of an adaptive algorithm based on collective marking (that is $\kappa = \infty$ and $\lambda = \eta$ from (3.22) in Algorithm 3.35) does not follow from the abstract framework from Carstensen et al. [2014a]. The reduction property (axiom (A2) from Carstensen et al. [2014a]), is not fulfilled. Algorithm 3.35 considered here is based on separate marking. In this context, the optimality of the adaptive algorithm (see Theorem 3.40) can be proved with a reduction property that only considers λ. ♦

Remark 3.37. The step *Mark* in the second case ($\mu_\ell^2 > \kappa\lambda_\ell^2$) can be realized by the algorithm `Approx` from Binev et al. [2004] and Carstensen and Rabus [2015], i.e., the thresholding second algorithm [Binev and DeVore, 2004] followed by a completion algorithm. For this algorithm, Carstensen and Rabus [2015] prove that the assumption (B1) optimal data approximation, which is assumed to hold in the following, follows from the axioms (B2) and (SA) from Subsection 3.5.5. For a discussion about other algorithms that realize *Mark* in the second case, see [Carstensen and Rabus, 2015]. ♦

Given an initial triangulation $\mathcal{T}_0$, recall the set of admissible triangulations $\mathbb{T}$ from Definition 2.4. Let $\mathbb{T}(N)$ denote the subset of all admissible triangulations with at most $\operatorname{card}(\mathcal{T}_0) + N$ triangles. For $s > 0$ and $(p, \alpha, \varphi) \in X \times Y \times H(\operatorname{div}, \Omega)$ define

$$|(p,\alpha,\varphi)|_{\mathcal{A}_s} := \sup_{N\in\mathbb{N}_0} N^s \inf_{\mathcal{T}\in\mathbb{T}(N)} \Big(\|p - \Pi_{X_h(\mathcal{T})} p\|_{L^2(\Omega)} + \inf_{\beta_\mathcal{T}\in Y_h(\mathcal{T})} \|\operatorname{Curl}(\alpha - \beta_\mathcal{T})\|_{L^2(\Omega)} + \|\varphi - \Pi_{X_h(\mathcal{T})}\varphi\|_{L^2(\Omega)} \Big).$$

Remark 3.38 (pure local approximation class)**.** Since Ω is assumed to be a Lipschitz domain, all patches in an admissible triangulation $\mathcal{T} \in \mathbb{T}$ are edge-connected, i.e., for all vertices $z \in \mathcal{N}$ and triangles $T, K \in \mathcal{T}$ with $z \in T \cap K$, there exists $m \in \mathbb{N}_0$ and $K_0, \dots, K_m \in \mathcal{T}$ with $K_0 = T$, $K_m = K$, $z \in K_0 \cap \cdots \cap K_m$ and $K_{j-1} \cap K_j \in \mathcal{E}$ for all $1 \leq j \leq m$. Under this assumption, Veeser [2014, Theorem 3.2] shows

$$\min_{v_h \in P_{k+1}(\mathcal{T}) \cap H^1(\Omega)} \|\nabla(v - v_h)\|_{L^2(\Omega)} \approx \|\nabla v - \Pi_k \nabla v\|_{L^2(\Omega)} \qquad \text{for all } v \in H^1(\Omega).$$

Hence,

$$|(p,\alpha,\varphi)|_{\mathcal{A}_s} \approx |(p,\alpha,\varphi)|_{\mathcal{A}_s'} := \sup_{N\in\mathbb{N}_0} N^s \inf_{\mathcal{T}\in\mathbb{T}(N)} \Big(\|p - \Pi_{X_h(\mathcal{T})} p\|_{L^2(\Omega)} + \big\|\operatorname{Curl}\alpha - \Pi_{X_h(\mathcal{T})} \operatorname{Curl}\alpha\big\|_{L^2(\Omega)} + \|\varphi - \Pi_{X_h(\mathcal{T})}\varphi\|_{L^2(\Omega)}\Big). \quad \blacklozenge$$

In the following, we assume that the following axiom (B1) holds for the algorithm used in the step *Mark* for $\mu_\ell^2 > \kappa\lambda_\ell^2$ (see Remark 3.37).

Assumption 3.39 ((B1) optimal data approximation)**.** Assume that $|(p,\alpha,\varphi)|_{\mathcal{A}_\sigma}$ is finite. Given a tolerance Tol, the algorithm used in *Mark* in the second case ($\mu_\ell^2 > \kappa\lambda_\ell^2$) in Algorithm 3.35 computes $\mathcal{T}_\star \in \mathbb{T}$ with

$$\operatorname{card}(\mathcal{T}_\star) - \operatorname{card}(\mathcal{T}_0) \lesssim \mathrm{Tol}^{-1/(2\sigma)} \qquad \text{and} \qquad \mu^2(\mathcal{T}_\star) \le \mathrm{Tol}. \quad \blacklozenge$$

The following theorem states optimal convergence rates of Algorithm 3.35.

Theorem 3.40 (optimal convergence rates of AFEM)**.** *For $0 < \rho_B < 1$ and sufficiently small $0 < \kappa$ and $0 < \theta < 1$, Algorithm 3.35 computes sequences of triangulations $(\mathcal{T}_\ell)_{\ell\in\mathbb{N}}$ and discrete solutions $(p_\ell,\alpha_\ell)_{\ell\in\mathbb{N}}$ for the right-hand side φ of optimal rate of convergence in the sense that*

$$(\operatorname{card}(\mathcal{T}_\ell) - \operatorname{card}(\mathcal{T}_0))^s \Big(\|p - p_\ell\|_{L^2(\Omega)} + \|\operatorname{Curl}(\alpha - \alpha_\ell)\|_{L^2(\Omega)} \Big) \lesssim |(p,\alpha,\varphi)|_{\mathcal{A}_s}.$$

The proof follows from the abstract framework of Carstensen and Rabus [2015], which employs the bounded overhead [Binev et al., 2004] of the newest-vertex bisection, under the assumptions (A1)–(A4) and (B2) and (SA) which are proved in Subsections 3.5.2–3.5.5.

3.5.2. (A1) stability and (A2) reduction

The following two theorems follow from the structure of λ.

Theorem 3.41 (stability)**.** *Let $\mathcal{T}_\star$ be an admissible refinement of $\mathcal{T}$ and $\mathcal{M} \subseteq \mathcal{T}\cap\mathcal{T}_\star$. Let $(p_{\mathcal{T}_\star},\alpha_{\mathcal{T}_\star}) \in X_h(\mathcal{T}_\star)\times Y_h(\mathcal{T}_\star)$ and $(p_{\mathcal{T}},\alpha_{\mathcal{T}}) \in X_h(\mathcal{T})\times Y_h(\mathcal{T})$ be the respective discrete solutions to* (3.5)*. Then,*

$$|\lambda(\mathcal{T}_\star,\mathcal{M}) - \lambda(\mathcal{T},\mathcal{M})| \lesssim \|p_{\mathcal{T}_\star} - p_{\mathcal{T}}\|_{L^2(\Omega)}.$$

Proof. This follows with triangle inequalities, inverse inequalities and a trace inequality, Theorem 2.7, as in Cascon et al. [2008, Proposition 3.3]. ∎

Theorem 3.42 (reduction)**.** *Let $\mathcal{T}_\star$ be an admissible refinement of $\mathcal{T}$. Then there exists $0 < \rho_2 < 1$ and $\Lambda_2 < \infty$ such that*

$$\lambda^2(\mathcal{T}_\star,\mathcal{T}_\star\setminus\mathcal{T}) \le \rho_2\lambda^2(\mathcal{T},\mathcal{T}\setminus\mathcal{T}_\star) + \Lambda_2\|p_{\mathcal{T}_\star} - p_{\mathcal{T}}\|^2_{L^2(\Omega)}.$$

Proof. This follows with a triangle inequality and the mesh-size reduction property $h^2_{\mathcal{T}_\star}|_T \le h^2_{\mathcal{T}}|_T/2$ for all $T \in \mathcal{T}_\star\setminus\mathcal{T}$ as in Cascon et al. [2008, Corollary 3.4]. ∎

3.5.3. (A4) discrete reliability

The following theorem proves discrete reliability, i.e., the difference between two discrete solutions is bounded by the error estimators on refined triangles only.

Theorem 3.43 (discrete reliability)**.** *Let $\mathcal{T}_\star$ be an admissible refinement of $\mathcal{T}$ with respective discrete solutions $(p_{\mathcal{T}_\star}, \alpha_{\mathcal{T}_\star}) \in X_h(\mathcal{T}_\star) \times Y_h(\mathcal{T}_\star)$ and $(p_{\mathcal{T}}, \alpha_{\mathcal{T}}) \in X_h(\mathcal{T}) \times Y_h(\mathcal{T})$. Then,*

$$\|p_{\mathcal{T}} - p_{\mathcal{T}_\star}\|^2_{L^2(\Omega)} + \|\mathrm{Curl}(\alpha_{\mathcal{T}} - \alpha_{\mathcal{T}_\star})\|^2_{L^2(\Omega)} \lesssim \lambda^2(\mathcal{T}, \mathcal{T} \setminus \mathcal{T}_\star) + \mu^2(\mathcal{T}, \mathcal{T} \setminus \mathcal{T}_\star).$$

Proof. Recall the definition of $W_h(\mathcal{T}_\star)$ from (3.6). Since $p_{\mathcal{T}} - p_{\mathcal{T}_\star} \in X_h(\mathcal{T}_\star)$, there exist $\sigma_{\mathcal{T}_\star} \in W_h(\mathcal{T}_\star)$ and $r_{\mathcal{T}_\star} \in Y_h(\mathcal{T}_\star)$ with $p_{\mathcal{T}} - p_{\mathcal{T}_\star} = \sigma_{\mathcal{T}_\star} + \mathrm{Curl}\, r_{\mathcal{T}_\star}$. Since $W_h(\mathcal{T}_\star) \perp_{L^2(\Omega)} \mathrm{Curl}\, Y_h(\mathcal{T}_\star)$,

$$\|\sigma_{\mathcal{T}_\star}\|^2_{L^2(\Omega)} + \|\mathrm{Curl}\, r_{\mathcal{T}_\star}\|^2_{L^2(\Omega)} = \|p_{\mathcal{T}} - p_{\mathcal{T}_\star}\|^2_{L^2(\Omega)}.$$

The orthogonality furthermore implies that the discrete error can be split as

$$\|p_{\mathcal{T}} - p_{\mathcal{T}_\star}\|^2_{L^2(\Omega)} = (p_{\mathcal{T}} - p_{\mathcal{T}_\star}, \sigma_{\mathcal{T}_\star})_{L^2(\Omega)} + (p_{\mathcal{T}} - p_{\mathcal{T}_\star}, \mathrm{Curl}\, r_{\mathcal{T}_\star})_{L^2(\Omega)}.$$

The projection property, Lemma 3.11, proves $\Pi_{X_h(\mathcal{T})}\sigma_{\mathcal{T}_\star} \in W_h(\mathcal{T})$. Hence, problem (3.5) implies that the first term of the right-hand side equals

$$(p_{\mathcal{T}} - p_{\mathcal{T}_\star}, \sigma_{\mathcal{T}_\star})_{L^2(\Omega)} = (\Pi_{X_h(\mathcal{T})}\varphi - \varphi, \sigma_{\mathcal{T}_\star})_{L^2(\Omega)} = (\Pi_{X_h(\mathcal{T})}\varphi - \Pi_{X_h(\mathcal{T}_\star)}\varphi, \sigma_{\mathcal{T}_\star})_{L^2(\Omega)}.$$

For any triangle $T \in \mathcal{T} \cap \mathcal{T}_\star$, it holds $(\Pi_{X_h(\mathcal{T})}\varphi - \Pi_{X_h(\mathcal{T}_\star)}\varphi)|_T = 0$. Therefore,

$$(\Pi_{X_h(\mathcal{T})}\varphi - \Pi_{X_h(\mathcal{T}_\star)}\varphi, \sigma_{\mathcal{T}_\star})_{L^2(\Omega)} \le \|\Pi_{X_h(\mathcal{T})}\varphi - \Pi_{X_h(\mathcal{T}_\star)}\varphi\|_{\mathcal{T}\setminus\mathcal{T}_\star}\, \|\sigma_{\mathcal{T}_\star}\|_{L^2(\Omega)}.$$

Since $\mathcal{T}_\star$ is a refinement of $\mathcal{T}$, it holds

$$\|\Pi_{X_h(\mathcal{T})}\varphi - \Pi_{X_h(\mathcal{T}_\star)}\varphi\|_{\mathcal{T}\setminus\mathcal{T}_\star} = \|\Pi_{X_h(\mathcal{T}_\star)}(\Pi_{X_h(\mathcal{T})}\varphi - \varphi)\|_{\mathcal{T}\setminus\mathcal{T}_\star} \le \|\varphi - \Pi_{X_h(\mathcal{T})}\varphi\|_{\mathcal{T}\setminus\mathcal{T}_\star}.$$

Let $r_{\mathcal{T}} \in Y_h(\mathcal{T})$ denote the quasi interpolant from Scott and Zhang [1990] of $r_{\mathcal{T}_\star}$ which satisfies the approximation and stability properties (3.24) and $(r_{\mathcal{T}})|_E = (r_{\mathcal{T}_\star})|_E$ for all edges $E \in \mathcal{E}(\mathcal{T}) \cap \mathcal{E}(\mathcal{T}_\star)$. Since $p_{\mathcal{T}} \in W_h(\mathcal{T})$ and $p_{\mathcal{T}_\star} \in W_h(\mathcal{T}_\star)$,

$$(p_{\mathcal{T}} - p_{\mathcal{T}_\star}, \mathrm{Curl}\, r_{\mathcal{T}_\star})_{L^2(\Omega)} = (p_{\mathcal{T}}, \mathrm{Curl}(r_{\mathcal{T}_\star} - r_{\mathcal{T}}))_{L^2(\Omega)}. \tag{3.30}$$

An integration by parts leads to

$$\begin{aligned}(p_{\mathcal{T}}, \mathrm{Curl}(r_{\mathcal{T}_\star} - r_{\mathcal{T}}))_{L^2(\Omega)} = -(\mathrm{curl}_{\mathrm{NC}}\, p_{\mathcal{T}}, r_{\mathcal{T}_\star} - r_{\mathcal{T}})_{L^2(\Omega)} \\ + \sum_{E \in \mathcal{E}(\mathcal{T})} \int_E [p_{\mathcal{T}} \cdot \tau_E]_E (r_{\mathcal{T}_\star} - r_{\mathcal{T}})\, ds.\end{aligned}$$

For a triangle $T \in \mathcal{T} \cap \mathcal{T}_\star$, any edge $E \in \mathcal{E}(T)$ satisfies $E \in \mathcal{E}(\mathcal{T}) \cap \mathcal{E}(\mathcal{T}_\star)$. Hence, $(r_\mathcal{T})|_T = (r_{\mathcal{T}_\star})|_T$ for all $T \in \mathcal{T} \cap \mathcal{T}_\star$. This, the Cauchy inequality and the approximation and stability properties of the quasi interpolant lead to

$$-(\operatorname{curl}_{\mathrm{NC}} p_\mathcal{T}, r_{\mathcal{T}_\star} - r_\mathcal{T})_{L^2(\Omega)} \lesssim \|h_\mathcal{T} \operatorname{curl}_{\mathrm{NC}} p_\mathcal{T}\|_{\mathcal{T} \setminus \mathcal{T}_\star} \|\operatorname{Curl} r_{\mathcal{T}_\star}\|_{L^2(\Omega)}.$$

Since $(r_\mathcal{T})|_E = (r_{\mathcal{T}_\star})|_E$ for all edges $E \in \mathcal{E}(\mathcal{T}) \cap \mathcal{E}(\mathcal{T}_\star)$, the approximation and stability properties of the quasi interpolant and the trace inequality from Theorem 2.7 lead as in the proof of Theorem 3.30 to

$$\sum_{E \in \mathcal{E}} \int_E [p_\mathcal{T} \cdot \tau_E]_E (r_{\mathcal{T}_\star} - r_\mathcal{T})\, ds \lesssim \sqrt{\sum_{E \in \mathcal{E}(\mathcal{T}) \setminus \mathcal{E}(\mathcal{T}_\star)} h_T \|[p_\mathcal{T} \cdot \tau_E]_E\|^2_{L^2(E)}}\, \|\operatorname{Curl} r_{\mathcal{T}_\star}\|_{L^2(\Omega)}.$$

The combination of the previous displayed inequalities yields

$$\|p_\mathcal{T} - p_{\mathcal{T}_\star}\|^2_{L^2(\Omega)} \lesssim \lambda^2(\mathcal{T}, \mathcal{T} \setminus \mathcal{T}_\star) + \mu^2(\mathcal{T}, \mathcal{T} \setminus \mathcal{T}_\star).$$

Since $\operatorname{Curl} \alpha_\mathcal{T} = \Pi_{X_h(\mathcal{T})} \varphi - p_\mathcal{T}$ and $\operatorname{Curl} \alpha_{\mathcal{T}_\star} = \Pi_{X_h(\mathcal{T}_\star)} \varphi - p_{\mathcal{T}_\star}$, the triangle inequality yields the assertion. ∎

3.5.4. (A3) quasi-orthogonality

The following theorem proves quasi-orthogonality of the discretization (3.5).

Theorem 3.44 (general quasi-orthogonality)**.** *Let $(\mathcal{T}_j \mid j \in \mathbb{N})$ be some sequence of triangulations with discrete solutions $(p_j, \alpha_j) \in X_h(\mathcal{T}_j) \times Y_h(\mathcal{T}_j)$ to (3.5). Let $\ell \in \mathbb{N}$. Then,*

$$\sum_{j=\ell}^{\infty} \Big(\|p_j - p_{j-1}\|^2_{L^2(\Omega)} + \|\operatorname{Curl}(\alpha_j - \alpha_{j-1})\|^2_{L^2(\Omega)} \Big) \lesssim \lambda^2_{\ell-1} + \mu^2_{\ell-1}.$$

Proof. The projection property, Lemma 3.11, proves $\Pi_{X_h(\mathcal{T}_{j-1})} p_j \in W_h(\mathcal{T}_{j-1})$ with $W_h(\mathcal{T}_{j-1})$ from (3.6). Hence, problem (3.5) leads to

$$\begin{aligned} (p_{j-1}, p_j - p_{j-1})_{L^2(\Omega)} &= (\varphi, \Pi_{X_h(\mathcal{T}_{j-1})} p_j - p_{j-1})_{L^2(\Omega)}, \\ (p_j, p_j - p_{j-1})_{L^2(\Omega)} &= (\varphi, p_j) - (\varphi, \Pi_{X_h(\mathcal{T}_{j-1})} p_j)_{L^2(\Omega)}. \end{aligned}$$

The subtraction of these two equations and an index shift leads, for any $M \in \mathbb{N}$ with $M > \ell$, to

$$\begin{aligned} \sum_{j=\ell}^{M} \|p_j - p_{j-1}\|^2_{L^2(\Omega)} &= \sum_{j=\ell}^{M} (\varphi, p_j - \Pi_{X_h(\mathcal{T}_{j-1})} p_j)_{L^2(\Omega)} \\ &\qquad - \sum_{j=\ell}^{M} (\varphi, \Pi_{X_h(\mathcal{T}_{j-1})} p_j)_{L^2(\Omega)} + \sum_{j=\ell-1}^{M-1} (\varphi, p_j)_{L^2(\Omega)} \qquad (3.31) \\ &= (\varphi, p_{\ell-1} - p_M)_{L^2(\Omega)} + 2 \sum_{j=\ell}^{M} (\varphi, p_j - \Pi_{X_h(\mathcal{T}_{j-1})} p_j)_{L^2(\Omega)}. \end{aligned}$$

Since $p_j - \Pi_{X_h(\mathcal{T}_{j-1})} p_j \in X_h(\mathcal{T}_j)$ is L^2-orthogonal to $X_h(\mathcal{T}_{j-1})$, a Cauchy and a weighted Young inequality, Lemma 2.6, imply

$$\begin{aligned}
&2\sum_{j=\ell}^{M}(\varphi, p_j - \Pi_{X_h(\mathcal{T}_{j-1})} p_j)_{L^2(\Omega)} \\
&\quad = 2\sum_{j=\ell}^{M}(\Pi_{X_h(\mathcal{T}_j)}\varphi - \Pi_{X_h(\mathcal{T}_{j-1})}\varphi, p_j - \Pi_{X_h(\mathcal{T}_{j-1})} p_j)_{L^2(\Omega)} \\
&\quad \le 2\sum_{j=\ell}^{M}\|\Pi_{X_h(\mathcal{T}_j)}\varphi - \Pi_{X_h(\mathcal{T}_{j-1})}\varphi\|^2_{L^2(\Omega)} + \frac{1}{2}\sum_{j=\ell}^{M}\|p_j - \Pi_{X_h(\mathcal{T}_{j-1})} p_j\|^2_{L^2(\Omega)}.
\end{aligned} \tag{3.32}$$

The orthogonality $\Pi_{X_h(\mathcal{T}_j)}\varphi - \Pi_{X_h(\mathcal{T}_{j-m})}\varphi \perp_{L^2(\Omega)} X_h(\mathcal{T}_{j-m})$ for all $0 \le m \le j$ proves

$$\sum_{j=\ell}^{M}\|\Pi_{X_h(\mathcal{T}_j)}\varphi - \Pi_{X_h(\mathcal{T}_{j-1})}\varphi\|^2_{L^2(\Omega)} = \|\Pi_{X_h(\mathcal{T}_M)}\varphi - \Pi_{X_h(\mathcal{T}_{\ell-1})}\varphi\|^2_{L^2(\Omega)}. \tag{3.33}$$

The definition of μ_ℓ yields

$$\begin{aligned}
\|\Pi_{X_h(\mathcal{T}_M)}\varphi - \Pi_{X_h(\mathcal{T}_{\ell-1})}\varphi\|_{L^2(\Omega)} &= \|\Pi_{X_h(\mathcal{T}_M)}(\varphi - \Pi_{X_h(\mathcal{T}_{\ell-1})}\varphi)\|_{L^2(\Omega)} \\
&\le \mu_{\ell-1}.
\end{aligned} \tag{3.34}$$

The combination of (3.31)–(3.34) and $\|p_j - \Pi_{X_h(\mathcal{T}_{j-1})} p_j\|_{L^2(\Omega)} \le \|p_j - p_{j-1}\|_{L^2(\Omega)}$ leads to

$$\frac{1}{2}\sum_{j=\ell}^{M}\|p_j - p_{j-1}\|^2_{L^2(\Omega)} \le 2\mu^2_{\ell-1} + (\varphi, p_{\ell-1} - p_M)_{L^2(\Omega)}. \tag{3.35}$$

The discrete problem (3.5), the reliability $\mathrm{Res}_2(p_{\ell-1}, \beta) \lesssim \lambda_{\ell-1}\|\mathrm{Curl}\,\beta\|_{L^2(\Omega)}$ for all $\beta \in Y$ from Theorem 3.30 and the discrete reliability $\|\mathrm{Curl}(\alpha_M - \alpha_{\ell-1})\|_{L^2(\Omega)} \lesssim \lambda_{\ell-1} + \mu_{\ell-1}$ from Theorem 3.43 lead to

$$\begin{aligned}
(p_{\ell-1} - p_M, \Pi_{X_h(\mathcal{T}_{\ell-1})}\varphi)_{L^2(\Omega)} &= (p_{\ell-1} - p_M, p_{\ell-1} + \mathrm{Curl}\,\alpha_{\ell-1})_{L^2(\Omega)} \\
&= (p_{\ell-1} - p_M, p_{\ell-1})_{L^2(\Omega)} = (\mathrm{Curl}(\alpha_M - \alpha_{\ell-1}), p_{\ell-1})_{L^2(\Omega)} \\
&= \mathrm{Res}_2(p_{\ell-1}, \alpha_M - \alpha_{\ell-1}) \lesssim \lambda_{\ell-1}\|\mathrm{Curl}(\alpha_M - \alpha_{\ell-1})\|_{L^2(\Omega)} \\
&\lesssim (\lambda_{\ell-1} + \mu_{\ell-1})^2.
\end{aligned} \tag{3.36}$$

This and a further application of Theorem 3.43 leads to

$$\begin{aligned}
&(\varphi, p_{\ell-1} - p_M)_{L^2(\Omega)} \\
&\quad = (\varphi - \Pi_{X_h(\mathcal{T}_{\ell-1})}\varphi, p_{\ell-1} - p_M)_{L^2(\Omega)} + (p_{\ell-1} - p_M, \Pi_{X_h(\mathcal{T}_{\ell-1})}\varphi)_{L^2(\Omega)} \\
&\quad \lesssim \|\varphi - \Pi_{X_h(\mathcal{T}_{\ell-1})}\varphi\|_{L^2(\Omega)}\,\|p_{\ell-1} - p_M\|_{L^2(\Omega)} + (\lambda_{\ell-1} + \mu_{\ell-1})^2_{L^2(\Omega)} \\
&\quad \lesssim (\lambda_{\ell-1} + \mu_{\ell-1})^2.
\end{aligned} \tag{3.37}$$

The combination of (3.35) with (3.37) implies

$$\sum_{j=\ell}^{M} \|p_j - p_{j-1}\|_{L^2(\Omega)}^2 \lesssim \lambda_{\ell-1}^2 + \mu_{\ell-1}^2. \tag{3.38}$$

The Young inequality from Lemma 2.6, the triangle inequality, and $\operatorname{Curl}\alpha_j = \Pi_{X_h(\mathcal{T}_j)}\varphi - p_j$ imply

$$\begin{aligned}\sum_{j=\ell}^{M} &\|\operatorname{Curl}(\alpha_j - \alpha_{j-1})\|_{L^2(\Omega)}^2 \\ &\qquad \le 2\sum_{j=\ell}^{M} \|p_j - p_{j-1}\|_{L^2(\Omega)}^2 + 2\sum_{j=\ell}^{M} \|\Pi_{X_h(\mathcal{T}_j)}\varphi - \Pi_{X_h(\mathcal{T}_{j-1})}\varphi\|_{L^2(\Omega)}^2.\end{aligned}$$

Since $M > \ell$ is arbitrary, the combination with (3.33), (3.34), and (3.38) yields the assertion. ∎

3.5.5. (B) data approximation

The following theorem together with Assumption 3.39 form the axiom (B) from Carstensen and Rabus [2015].

Theorem 3.45 ((B2) quasimonotonicity and (SA) sub-additivity)**.** *Any admissible refinement $\mathcal{T}_\star$ of $\mathcal{T}$ satisfies*

$$\mu^2(\mathcal{T}_\star) \le \mu^2(\mathcal{T})$$

and

$$\sum_{\substack{T\in\mathcal{T}_\star \\ T\subseteq K}} \mu^2(T) \le \mu^2(K) \qquad \text{for all } K \in \mathcal{T}.$$

Proof. This follows directly from the definition of μ. ∎

3.6. Extension to 3D

This section is devoted to the generalization to 3D. Subsection 3.6.1 defines the novel discretization and comments on basic properties, while Subsection 3.6.2 is devoted to optimal convergence rates for the adaptive algorithm.

3.6.1. Weak formulation and discretization

For this section, let $\Omega \subseteq \mathbb{R}^3$ be a simply connected, bounded, polygonal Lipschitz domain in $\mathbb{R}^3$. For the sake of simplicity, we also assume that $\partial\Omega$ is connected. The

Curl operator acts on a sufficiently smooth vector field $\beta : \Omega \to \mathbb{R}^3$ as

$$\operatorname{Curl} \beta = \begin{pmatrix} \partial\beta_3/\partial x_2 - \partial\beta_2/\partial x_3 \\ \partial\beta_1/\partial x_3 - \partial\beta_3/\partial x_1 \\ \partial\beta_2/\partial x_1 - \partial\beta_1/\partial x_2 \end{pmatrix}.$$

Let $H(\operatorname{Curl}, \Omega)$ denote the space of all $\beta \in L^2(\Omega; \mathbb{R}^3)$ with $\operatorname{Curl} \beta \in L^2(\Omega; \mathbb{R}^3)$ for the weak Curl, i.e.,

$$\int_\Omega v \cdot \operatorname{Curl} \beta \, dx = \int_\Omega \beta \cdot \operatorname{Curl} v \, dx \qquad \text{for all } v \in C_c^\infty(\Omega; \mathbb{R}^3).$$

In contrast to the two-dimensional case, $H(\operatorname{Curl}, \Omega) \neq H^1(\Omega; \mathbb{R}^3)$. The Helmholtz decomposition in 3D reads

$$L^2(\Omega; \mathbb{R}^3) = \nabla H_0^1(\Omega) \oplus \operatorname{Curl} H(\operatorname{Curl}, \Omega) \tag{3.39}$$

and the sum is L^2 orthogonal. It is a consequence of the identity

$$\{r \in H(\operatorname{div}, \Omega) \mid \operatorname{div} r = 0\} = \operatorname{Curl} H(\operatorname{Curl}, \Omega)$$

in the De Rham complex [Boffi et al., 2013].

Let $\varphi \in H(\operatorname{div}, \Omega)$ with $-\operatorname{div} \varphi = f$. Then the Poisson problem (3.1) is equivalent to the problem: Find $(p, \alpha) \in L^2(\Omega; \mathbb{R}^3) \times H(\operatorname{Curl}, \Omega)$ with

$$\begin{aligned} (p, q)_{L^2(\Omega)} + (q, \operatorname{Curl} \alpha)_{L^2(\Omega)} &= (\varphi, q)_{L^2(\Omega)} && \text{for all } q \in L^2(\Omega; \mathbb{R}^3), \\ (p, \operatorname{Curl} \beta)_{L^2(\Omega)} &= 0 && \text{for all } \beta \in H(\operatorname{Curl}, \Omega). \end{aligned} \tag{3.40}$$

In contrast to the two-dimensional case, the operator $\operatorname{Curl} : H(\operatorname{Curl}, \Omega) \to L^2(\Omega; \mathbb{R}^3)$ has a non-trivial kernel. Classical results [Rudin, 1976] characterize this kernel as $\nabla H^1(\Omega)$. To enforce uniqueness, we can reformulate (3.40) as follows. Seek $(p, \alpha, w) \in L^2(\Omega; \mathbb{R}^3) \times H(\operatorname{Curl}, \Omega) \times (H^1(\Omega) \cap L_0^2(\Omega))$ with

$$\begin{aligned} (p, q)_{L^2(\Omega)} + (q, \operatorname{Curl} \alpha)_{L^2(\Omega)} &= (\varphi, q)_{L^2(\Omega)} && \text{for all } q \in L^2(\Omega; \mathbb{R}^3), \\ (p, \operatorname{Curl} \beta)_{L^2(\Omega)} + (\beta, \nabla w)_{L^2(\Omega)} &= 0 && \text{for all } \beta \in H(\operatorname{Curl}, \Omega), \\ (\alpha, \nabla v)_{L^2(\Omega)} &= 0 && \text{for all } v \in (H^1(\Omega) \cap L_0^2(\Omega)). \end{aligned}$$

Note that $\{\beta \in H(\operatorname{Curl}, \Omega) \mid \operatorname{Curl} \beta = 0\} = \nabla H^1(\Omega)$ implies $w = 0$.

Standard finite element spaces to discretize $H(\operatorname{Curl}, \Omega)$ in 3D are the finite element spaces of Nédélec [1980, 1986] (also called edge elements) which are known from the context of Maxwell's equations. Let $\mathcal{T}$ be a regular triangulation of Ω in tetrahedra in the sense of [Ciarlet, 1978]. In contrast to $P_k(\mathcal{T}; \mathbb{R}^3) \cap H^1(\Omega; \mathbb{R}^3)$, the finite element spaces of Nédélec enforce only continuity between interfaces in tangential direction. This is enough to guarantee that the finite element functions are $H(\operatorname{Curl}, \Omega)$-conforming. The spaces of first kind Nédélec finite elements read

$$\begin{aligned} Y_{\mathrm{N},k}(T) &:= P_k(T; \mathbb{R}^3) + (x \wedge P_k(T; \mathbb{R}^3)), \\ Y_{\mathrm{N},k}(\mathcal{T}) &:= \{\beta_h \in H(\operatorname{Curl}, \Omega) \mid \forall T \in \mathcal{T} : \ \beta_h|_T \in Y_{\mathrm{N},k}(T)\} \end{aligned}$$

with the cross product or vector product $\wedge$. Let $X_h(\mathcal{T}) := P_k(\mathcal{T};\mathbb{R}^3)$. Since $\operatorname{Curl} Y_{\mathrm{N},k}(\mathcal{T}) \subseteq X_h(\mathcal{T})$, a generalization of (3.5) to 3D seeks $(p_h, \alpha_h) \in X_h(\mathcal{T}) \times Y_{\mathrm{N},k}(\mathcal{T})$ with

$$\begin{aligned} (p_h, q_h)_{L^2(\Omega)} + (q_h, \operatorname{Curl}\alpha_h)_{L^2(\Omega)} &= (\varphi, q_h)_{L^2(\Omega)} && \text{for all } q_h \in X_h(\mathcal{T}), \\ (p_h, \operatorname{Curl}\beta_h)_{L^2(\Omega)} &= 0 && \text{for all } \beta_h \in Y_{\mathrm{N},k}(\mathcal{T}). \end{aligned} \tag{3.41}$$

The discrete exact sequence from [Boffi et al., 2013] implies that the elements in $Y_{\mathrm{N},k}(\mathcal{T})$ with vanishing Curl are exactly the gradients of $U_h(\mathcal{T}) := P_{k+1}(\mathcal{T}) \cap H^1(\Omega) \cap L^2_0(\Omega)$ functions. Therefore, the uniqueness in (3.41) can be obtained in the following formulation. Seek $(p_h, \alpha_h, w_h) \in X_h(\mathcal{T}) \times Y_{\mathrm{N},k}(\mathcal{T}) \times U_h(\mathcal{T})$ with

$$\begin{aligned} (p_h, q_h)_{L^2(\Omega)} + (q_h, \operatorname{Curl}\alpha_h)_{L^2(\Omega)} &= (\varphi, q_h)_{L^2(\Omega)} && \text{for all } q_h \in X_h(\mathcal{T}), \\ (p_h, \operatorname{Curl}\beta_h)_{L^2(\Omega)} + (\beta_h, \nabla w_h)_{L^2(\Omega)} &= 0 && \text{for all } \beta_h \in Y_{\mathrm{N},k}(\mathcal{T}), \\ (\alpha_h, \nabla v_h)_{L^2(\Omega)} &= 0 && \text{for all } v_h \in U_h(\mathcal{T}). \end{aligned} \tag{3.42}$$

Note that $\nabla U_h(\mathcal{T})$ is the kernel of $\operatorname{Curl} : Y_{\mathrm{N},k}(\mathcal{T}) \to P_k(\mathcal{T};\mathbb{R}^3)$ and so (3.42) implies $w_h = 0$. This variable is introduced in order that (3.42) has the form of a standard mixed system. The discrete Helmholtz decomposition of Alonso Rodríguez et al. [2004, Lemma 5.4] proves that for the lowest order discretization $k = 0$, p_h is a Crouzeix-Raviart function and so (3.42) can be seen as a generalization of the non-conforming Crouzeix-Raviart FEM to higher polynomial degrees.

The inf-sup conditions follow from $\nabla U_h(\mathcal{T}) \subseteq Y_{\mathrm{N},k}(\mathcal{T})$ and $\operatorname{Curl} Y_{\mathrm{N},k}(\mathcal{T}) \subseteq X_h(\mathcal{T})$. This and the conformity of the method lead to the best-approximation result

$$\begin{aligned} &\|p - p_h\|_{L^2(\Omega)} + \|\operatorname{Curl}(\alpha - \alpha_h)\|_{L^2(\Omega)} + \|\nabla(w - w_h)\|_{L^2(\Omega)} \\ &\qquad \lesssim \Big(\min_{q_h \in X_h(\mathcal{T})} \|p - q_h\|_{L^2(\Omega)} + \min_{\beta_h \in Y_{\mathrm{N},k}(\mathcal{T})} \|\operatorname{Curl}(\alpha - \beta_h)\|_{L^2(\Omega)} \\ &\qquad\qquad + \min_{s_h \in U_h(\mathcal{T})} \|\nabla(w - s_h)\|_{L^2(\Omega)} \Big). \end{aligned}$$

Since $w = w_h = 0$, this is equivalent to

$$\begin{aligned} &\|p - p_h\|_{L^2(\Omega)} + \|\operatorname{Curl}(\alpha - \alpha_h)\|_{L^2(\Omega)} \\ &\qquad \lesssim \Big(\min_{q_h \in X_h(\mathcal{T})} \|p - q_h\|_{L^2(\Omega)} + \min_{\beta_h \in Y_{\mathrm{N},k}(\mathcal{T})} \|\operatorname{Curl}(\alpha - \beta_h)\|_{L^2(\Omega)} \Big). \end{aligned}$$

The following proposition states a projection property similar to Lemma 3.11 for the two-dimensional case. To this end, define

$$\begin{aligned} Z_h(\mathcal{T}) &:= \{\beta_h \in Y_{\mathrm{N},k}(\mathcal{T}) \mid \forall v_h \in U_h(\mathcal{T}) : \ (\beta_h, \nabla v_h)_{L^2(\Omega)} = 0)\}, \\ W_h(\mathcal{T}) &:= \{q_h \in X_h(\mathcal{T}) \mid \forall \beta_h \in Z_h(\mathcal{T}) : \ (q_h, \operatorname{Curl}\beta_h)_{L^2(\Omega)} = 0\}. \end{aligned}$$

Since $\nabla U_h(\mathcal{T})$ is the kernel of $\operatorname{Curl} : Y_{\mathrm{N},k}(\mathcal{T}) \to X_h(\mathcal{T})$, it holds

$$\operatorname{Curl} Y_{\mathrm{N},k}(\mathcal{T}) = \operatorname{Curl} Z_h(\mathcal{T}).$$

This implies

$$W_h(\mathcal{T}) = \{q_h \in X_h(\mathcal{T}) \mid \forall \beta_h \in Y_{\mathrm{N},k}(\mathcal{T}) : \ (q_h, \operatorname{Curl} \beta_h)_{L^2(\Omega)} = 0\}.$$

Lemma 3.46 (projection property). *Let $q \in L^2(\Omega;\mathbb{R}^3)$ with $(q, \operatorname{Curl}\beta)_{L^2(\Omega)} = 0$ for all $\beta \in H(\operatorname{Curl},\Omega)$ (that means that q is a gradient of a $H^1_0(\Omega)$ function). Then $\Pi_{X_h(\mathcal{T})} q \in W_h(\mathcal{T})$. If $\mathcal{T}_\star$ is an admissible refinement of $\mathcal{T}$, then $\Pi_{X_h(\mathcal{T})} W_h(\mathcal{T}_\star) \subseteq W_h(\mathcal{T})$.*

Proof. Since $\operatorname{Curl} Y_{\mathrm{N},k}(\mathcal{T}) \subseteq X_h(\mathcal{T})$ and $Y_{\mathrm{N},k}(\mathcal{T}) \subseteq H(\operatorname{Curl},\Omega)$, the assertion follows with the arguments in the proof of Lemma 3.11. ∎

3.6.2. Adaptive algorithm

This subsection outlines the proof of optimal convergence rates for Algorithm 3.35 in 3D driven by the error estimators λ and μ defined by the local contributions

$$\lambda^2(\mathcal{T}_\ell, T) := \|h_{\mathcal{T}} \operatorname{Curl}_{\mathrm{NC}} p_h\|^2_{L^2(T)} + h_T \sum_{E\in\mathcal{E}(T)} \|[p_h \wedge \nu_E]_E\|^2_{L^2(E)},$$
$$\mu^2(T) := \|\varphi - \Pi_{X_h(\mathcal{T})}\varphi\|^2_{L^2(T)}$$

and (3.29). Here, $\mathcal{E}(T)$ denotes the faces of a tetrahedron $T \in \mathcal{T}$ and $h_{\mathcal{T}} \in P_0(\mathcal{T})$ denotes the piecewise constant mesh-size function defined by $h_{\mathcal{T}}|_T := h_T := \operatorname{meas}_3(T)^{1/3}$. The refinement of triangulations in Algorithm 3.35 is done by newest-vertex bisection [Stevenson, 2008]. Let $\mathbb{T}(N)$ denote the space of admissible triangulations with at most N tetrahedra more than $\mathcal{T}_0$. As in Subsection 3.5.1, define the seminorm

$$|(p,\alpha,\varphi)|_{\mathcal{A}_s} := \sup_{N\in\mathbb{N}_0} N^s \inf_{\mathcal{T}\in\mathbb{T}(N)} \Big(\|p - \Pi_{X_h(\mathcal{T})} p\|_{L^2(\Omega)} + \inf_{\beta_{\mathcal{T}} \in Y_{\mathrm{N},k}(\mathcal{T})} \|\operatorname{Curl}(\alpha - \beta_{\mathcal{T}})\|_{L^2(\Omega)} + \|\varphi - \Pi_{X_h(\mathcal{T})}\varphi\|_{L^2(\Omega)} \Big).$$

The following theorem states optimal convergence rates for Algorithm 3.35 for 3D.

Theorem 3.47 (optimal convergence rates of AFEM for 3D). *Let $s > 0$. For $0 < \rho_B < 1$ and sufficiently small $0 < \kappa$ and $0 < \theta < 1$, Algorithm 3.35 computes sequences of triangulations $(\mathcal{T}_\ell)_{\ell\in\mathbb{N}}$ and discrete solutions $(p_\ell, \alpha_\ell)_{\ell\in\mathbb{N}}$ for the right-hand side φ of optimal rate of convergence in the sense that*

$$(\operatorname{card}(\mathcal{T}_\ell) - \operatorname{card}(\mathcal{T}_0))^s \Big(\|p - p_\ell\|_{L^2(\Omega)} + \|\operatorname{Curl}(\alpha - \alpha_\ell)\|_{L^2(\Omega)} \Big) \lesssim |(p,\alpha,\varphi)|_{\mathcal{A}_s}.$$

The proof follows as in Section 3.5 from (A1)–(A4) and (B) from Carstensen and Rabus [2015] and the efficiency of λ and μ. The proof of efficiency follows with the standard bubble-function technique of Verfürth [1996] as in Theorem 3.30. The proofs of the axioms (A1)–(A4) and (B) are outlined in the following.

The axioms (A1) stability and (A2) reduction follow as in Subsection 3.5.2 with triangle inequalities, inverse inequalities, a trace inequality similar to Theorem 2.7, and the mesh-size reduction property $h^3_{\mathcal{T}_\star}|_T \le h^3_{\mathcal{T}}|_T/2$ for all $T \in \mathcal{T}_\star \setminus \mathcal{T}$. However, for (A3) quasi-orthogonality and (A4) discrete reliability, the interpolation operator of Scott and Zhang [1990] cannot be applied directly to $r_{\mathcal{T}_\star} \in Y_{\mathrm{N},k}(\mathcal{T}_\star)$ as done in the proof of Theorem 3.43, because $Y_{\mathrm{N},k}(\mathcal{T}_\star) \not\subseteq H^1(\Omega;\mathbb{R}^3)$. This can be overcome by a quasi-interpolation based on a quasi-interpolation operator from Schöberl [2008] and a projection operator from Zhong et al. [2012]. Its properties are summarized in the following theorem.

Theorem 3.48 (quasi-interpolation)**.** *Let $\mathcal{T}_\star$ be an admissible refinement of $\mathcal{T}$ and define $\mathcal{R}(\mathcal{T},\mathcal{T}_\star) := \{T \in \mathcal{T} \mid \exists K_1 \in \mathcal{T}\setminus\mathcal{T}_\star \exists K_2 \in \mathcal{T}$ with $K_1 \cap K_2 \neq \emptyset$ and $T \cap K_2 \neq \emptyset\}$. Let $\gamma_{\mathcal{T}_\star} \in Z_h(\mathcal{T}_\star)$. Then there exists $\gamma_{\mathcal{T}} \in Y_{\mathrm{N},k}(\mathcal{T})$, $\rho \in H^1(\Omega)$, and $\Phi \in H^1(\Omega;\mathbb{R}^3)$ with*

$$\begin{aligned} \gamma_{\mathcal{T}_\star} - \gamma_{\mathcal{T}} &= \nabla\rho + \Phi, \\ (\gamma_{\mathcal{T}_\star} - \gamma_{\mathcal{T}})|_T &= 0 \text{ for all } T \in \mathcal{T} \setminus \mathcal{R}(\mathcal{T},\mathcal{T}_\star), \\ \|h_{\mathcal{T}}^{-1}\Phi\|_{L^2(\Omega)} + \|\nabla\Phi\|_{L^2(\Omega)} &\lesssim \|\operatorname{Curl}\gamma_{\mathcal{T}_\star}\|_{L^2(\Omega)}. \end{aligned}$$

Proof. The idea is already included in Zhong et al. [2012, Theorem 5.3] and sketched here for completeness. Let $I_{\mathrm{N},\mathcal{T}} : Y_{\mathrm{N},k}(\mathcal{T}_\star) \to Y_{\mathrm{N},k}(\mathcal{T})$ denote the stable and local projection operator from Zhong et al. [2012, Sections 4.3–4.4] and $P^S_{\mathcal{T}} : H(\operatorname{Curl};\Omega) \to Y_{\mathrm{N},1}(\mathcal{T})$ the quasi-interpolation from Schöberl [2008]. Note that these two operators can be naturally generalized from the Dirichlet boundary conditions imposed by Schöberl [2008], Zhong et al. [2012] to no boundary conditions. Define $\gamma_{\mathcal{T}} \in Y_{\mathrm{N},k}(\mathcal{T})$ by

$$\gamma_{\mathcal{T}} := I_{\mathrm{N},\mathcal{T}}\gamma_{\mathcal{T}_\star} + P^S_{\mathcal{T}}(\gamma_{\mathcal{T}_\star} - I_{\mathrm{N},\mathcal{T}}\gamma_{\mathcal{T}_\star}).$$

Then [Schöberl, 2008, Theorem 1] guarantees the existence of $\rho \in H^1(\Omega)$ and $\Phi \in H^1(\Omega;\mathbb{R}^3)$ with $\gamma_{\mathcal{T}_\star} - \gamma_{\mathcal{T}} = \nabla\rho + \Phi$ and

$$\begin{aligned} \|h_{\mathcal{T}}^{-1}\Phi\|_{L^2(T)} + \|\nabla\Phi\|_{L^2(T)} &\lesssim \big\|\operatorname{Curl}(\gamma_{\mathcal{T}_\star} - I_{\mathrm{N},\mathcal{T}}\gamma_{\mathcal{T}_\star})\big\|_{L^2(\Omega_T)}, \\ \|h_{\mathcal{T}}^{-1}\rho\|_{L^2(T)} + \|\nabla\rho\|_{L^2(T)} &\lesssim \big\|\gamma_{\mathcal{T}_\star} - I_{\mathrm{N},\mathcal{T}}\gamma_{\mathcal{T}_\star}\big\|_{L^2(\Omega_T)} \end{aligned}$$

with enlarged element patch $\Omega_T := \cup\{K \in \mathcal{T} \mid K \cap T \neq \emptyset\}$. Define $\widetilde{\mathcal{R}}(\mathcal{T},\mathcal{T}_\star) := \{T \in \mathcal{T} \mid \exists K \in \mathcal{T} \setminus \mathcal{T}_\star$ with $T \cap K \neq \emptyset\}$. Since Zhong et al. [2012, Theorem 4.1] prove $\gamma_{\mathcal{T}_\star}|_T = I_{\mathrm{N},\mathcal{T}}\gamma_{\mathcal{T}_\star}|_T$ for all $T \in \mathcal{T} \setminus \widetilde{\mathcal{R}}(\mathcal{T},\mathcal{T}_\star)$, the right-hand sides vanish for all $T \in \mathcal{T} \setminus \mathcal{R}(\mathcal{T},\mathcal{T}_\star)$. This proves $(\gamma_{\mathcal{T}_\star} - \gamma_{\mathcal{T}})|_T = 0$ for all $T \in \mathcal{T} \setminus \mathcal{R}(\mathcal{T},\mathcal{T}_\star)$.

The stability of $I_{\mathrm{N},\mathcal{T}}$ from Zhong et al. [2012, Sections 4.3–4.4] implies

$$\big\|\operatorname{Curl}(\gamma_{\mathcal{T}_\star} - I_{\mathrm{N},\mathcal{T}}\gamma_{\mathcal{T}_\star})\big\|_{L^2(\Omega)} \lesssim \|\operatorname{Curl}\gamma_{\mathcal{T}_\star}\|_{L^2(\Omega)} + \|\gamma_{\mathcal{T}_\star}\|_{L^2(\Omega)}.$$

Since $\gamma_{\mathcal{T}_\star} \in Z_h(\mathcal{T}_\star)$, the ellipticity on the discrete kernel from Amrouche et al. [1998, Proposition 4.6] yields

$$\|\gamma_{\mathcal{T}_\star}\|_{L^2(\Omega)} \lesssim \|\operatorname{Curl}\gamma_{\mathcal{T}_\star}\|_{L^2(\Omega)}.$$

The combination of the previous displayed inequalities concludes the proof. ∎

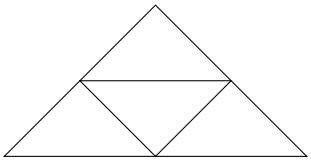

Figure 3.3.: Red-refined triangle.

The differences between the proof of (A4) discrete reliability and the proof of Theorem 3.43 are outlined in the following. Let $(p_{\mathcal{T}_\star}, \alpha_{\mathcal{T}_\star}) \in X_h(\mathcal{T}_\star) \times Z_h(\mathcal{T}_\star)$ and $(p_{\mathcal{T}}, \alpha_{\mathcal{T}}) \in X_h(\mathcal{T}) \times Z_h(\mathcal{T})$ denote the discrete solutions to (3.41). As in the proof of Theorem 3.43, let $\sigma_{\mathcal{T}_\star} \in W_h(\mathcal{T}_\star)$ and $r_{\mathcal{T}_\star} \in Z_h(\mathcal{T}_\star)$ such that $p_{\mathcal{T}} - p_{\mathcal{T}_\star} = \sigma_{\mathcal{T}_\star} + \operatorname{Curl} r_{\mathcal{T}_\star}$. The first term of the right-hand side of

$$\|p_{\mathcal{T}} - p_{\mathcal{T}_\star}\|^2 = (p_{\mathcal{T}} - p_{\mathcal{T}_\star}, \sigma_{\mathcal{T}_\star})_{L^2(\Omega)} + (p_{\mathcal{T}} - p_{\mathcal{T}_\star}, \operatorname{Curl} r_{\mathcal{T}_\star})_{L^2(\Omega)}$$

is estimated as in the proof of Theorem 3.43, while for the second term, the quasi-interpolant $r_{\mathcal{T}} \in Y_{\mathrm{N},k}(\mathcal{T})$ of $r_{\mathcal{T}_\star}$ with $r_{\mathcal{T}_\star} - r_{\mathcal{T}} = \nabla\rho + \Phi$ for $\rho \in H^1(\Omega)$ and $\Phi \in H^1(\Omega;\mathbb{R}^3)$ from Theorem 3.48 is employed. This yields

$$(p_{\mathcal{T}} - p_{\mathcal{T}_\star}, \operatorname{Curl} r_{\mathcal{T}_\star})_{L^2(\Omega)} = (p_{\mathcal{T}}, \operatorname{Curl}(r_{\mathcal{T}_\star} - r_{\mathcal{T}}))_{L^2(\Omega)} = (p_{\mathcal{T}}, \operatorname{Curl}\Phi)_{L^2(\Omega)}.$$

A piecewise integration by parts and the arguments of the proof of Theorem 3.43 conclude the proof. The crucial point is that $\Phi \in H^1(\Omega;\mathbb{R}^3)$ is smooth enough to allow for a trace inequality.

The proof of (A3) quasi-orthogonality follows as in the proof of Theorem 3.44 with the projection property of Lemma 3.46 and the following modifications in (3.36). Since (in the analogues notation as in (3.36)) $\alpha_{\ell-1} \in Z_h(\mathcal{T}_{\ell-1}) \subseteq Y_{\mathrm{N},k}(\mathcal{T}_M)$, there exists $\gamma_M \in Z_h(\mathcal{T}_M)$ with $\operatorname{Curl}\gamma_M = \operatorname{Curl}\alpha_{\ell-1}$. Theorem 3.48 guarantees the existence of $\beta_{\ell-1} \in Y_{N,k}(\mathcal{T}_{\ell-1})$, $\rho \in H^1(\Omega)$ and $\Phi \in H^1(\Omega;\mathbb{R}^3)$ with $\alpha_M - \gamma_M - \beta_{\ell-1} = \nabla\rho + \Phi$. This implies in (3.36) that

$$\begin{aligned}(\operatorname{Curl}(\alpha_M - \alpha_{\ell-1}), p_{\ell-1})_{L^2(\Omega)} &= (\operatorname{Curl}(\alpha_M - \gamma_M - \beta_{\ell-1}), p_{\ell-1})_{L^2(\Omega)} \\ &= (\operatorname{Curl}\Phi, p_{\ell-1})_{L^2(\Omega)}.\end{aligned}$$

A piecewise integration by parts and the arguments of the proof of Theorems 3.30 and 3.43 prove

$$(\operatorname{Curl}(\alpha_M - \alpha_{\ell-1}), p_{\ell-1})_{L^2(\Omega)} \lesssim (\lambda_{\ell-1} + \mu_{\ell-1}) \|\operatorname{Curl}(\alpha_M - \alpha_{\ell-1})\|_{L^2(\Omega)}.$$

This and the arguments of Theorem 3.44 eventually prove the quasi-orthogonality.

3.7. Numerical experiments

This section presents numerical experiments for the discretization (3.5) for $k = 0, 1, 2$. The implementation is based on the Matlab software package AFEM [Carstensen

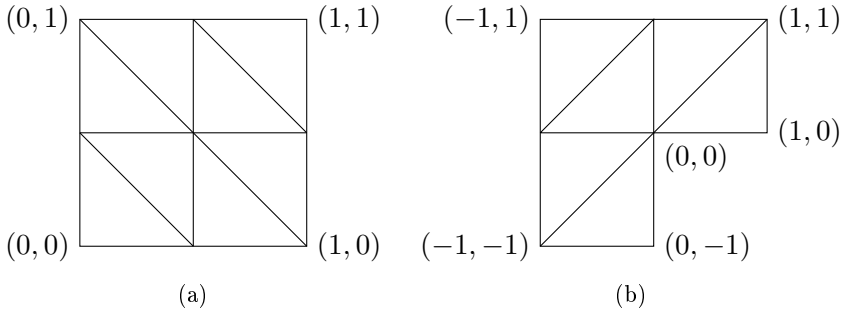

Figure 3.4.: Initial meshes for the unit square and the L-shaped domain.

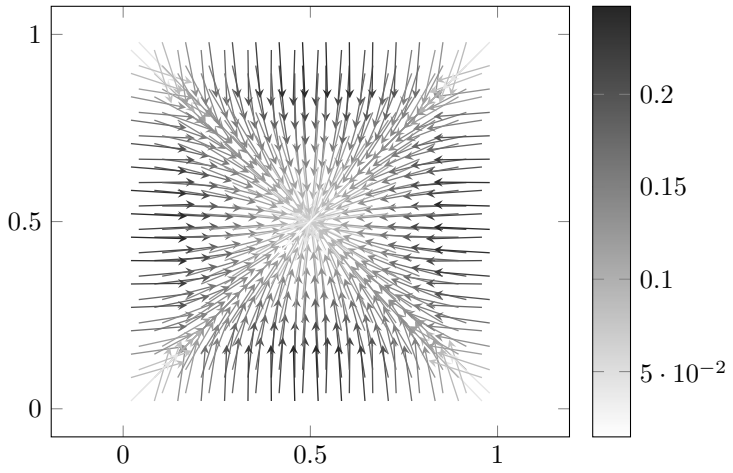

Figure 3.5.: Discrete solution for $k = 0$ for the experiment from Subsection 3.7.1 for a uniform mesh with 289 nodes.

et al., 2009] maintained at the Humboldt-Universität. The numerical computations are performed with the Matlab version 8.1.0.604 [The MathWorks, Inc., 2013]. Subsections 3.7.1–3.7.6 compute the discrete solutions on sequences of uniformly red-refined triangulations (see Figure 3.3 for a red-refined triangle) as well as on sequences of triangulations created by the adaptive algorithm 3.35 with bulk parameter $\theta = 0.1$ and $\kappa = 0.5$ and $\rho = 0.75$.

The convergence history plots are logarithmically scaled and display the error $\|p - p_h\|_{L^2(\Omega)}$ against the number of degrees of freedom of the linear system resulting from the Schur complement (see Remark 3.12).

3.7.1. Square domain with smooth solution

Given the right-hand side $f \in L^2(\Omega)$,

$$f(x,y) = 2x - 2x^2 + 2y - 2y^2,$$

on the square domain $\Omega = (0,1)^2$, the exact solution of $-\Delta u = f$ with homogeneous Dirichlet boundary conditions reads

$$u(x,y) = x(1-y)y(1-x).$$

An integration of f leads to

$$\varphi(x,y) := \begin{pmatrix} -x^2 + 2x^3/3 \\ -y^2 + 2y^3/3 \end{pmatrix}$$

with $-\operatorname{div}\varphi = f$. Figure 3.5 displays the discrete solution for $k = 0$ for a uniform triangulation with 289 nodes. The errors $\|p - p_h\|_{L^2(\Omega)}$ and the error estimator η from Section 3.4 are plotted against the degrees of freedom in Figure 3.6. The errors and error estimators show an equivalent behaviour with an overestimation of approximately 6. Since the solutions p and α are smooth, the refinement based on the adaptive algorithm as well as the uniform refinement yield optimal convergence rates, namely $\texttt{ndof}^{-1/2}$ for $k = 0$, $\texttt{ndof}^{-1}$ for $k = 1$ and $\texttt{ndof}^{-3/2}$ for $k = 2$. Figure 3.7 depicts triangulations created from the adaptive algorithm for $k = 0, 1, 2$ with approximately 1000 degrees of freedom. The smoothness of the solution causes that the meshes are quasi-uniform. The marking with respect to the data-approximation ($\mu_\ell^2 > \kappa\lambda_\ell^2$ in Algorithm 3.35) is only applied at the first three refinements for $k = 0$. All other marking steps for $k = 0, 1, 2$ used the Dörfler marking ($\mu_\ell^2 \leq \kappa\lambda_\ell^2$).

The condition numbers of the Schur complement of the system matrices of the discretization (3.5) for $k = 0$, as well as the condition numbers of the system matrices of a standard P_1 conforming FEM [Ciarlet, 1978], estimated with the Matlab routine `condest`, are displayed in Figure 3.8 on a sequence of uniformly red-refined triangulations. The condition numbers of the discretization (3.5) are approximately twice the condition numbers of the standard P_1 FEM for all triangulations. In particular, they scale in the same way.

3.7.2. L-shaped domain with Dirichlet boundary, I

Let $\Omega = (-1,1)^2 \setminus ([0,1] \times [-1,0])$ be the L-shaped domain with Dirichlet boundary $\Gamma_D = \partial\Omega$. The function u given in polar coordinates by

$$u(r,\phi) = r^{2/3}\sin((2/3)\phi)$$

solves

$$-\Delta u = 0 \quad \text{in } \Omega.$$

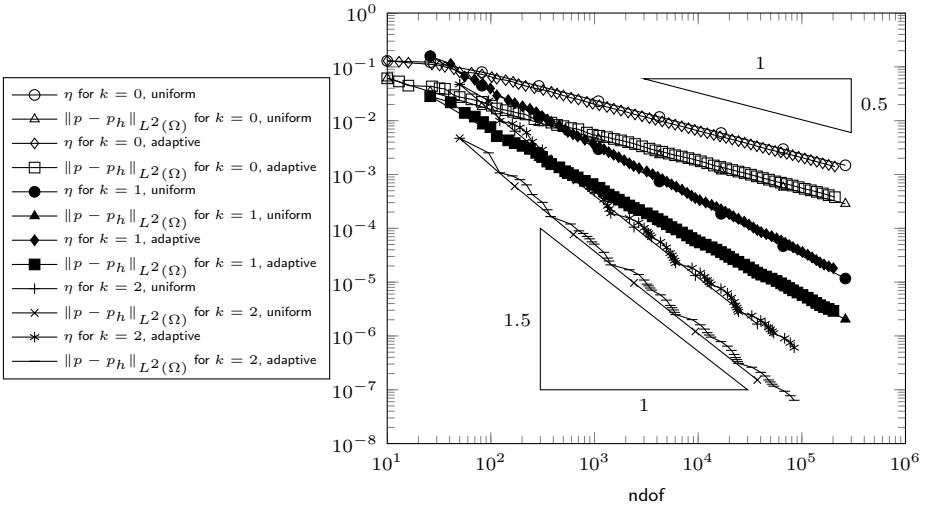

Figure 3.6.: Errors and error estimators from Subsection 3.7.1 for the square domain.

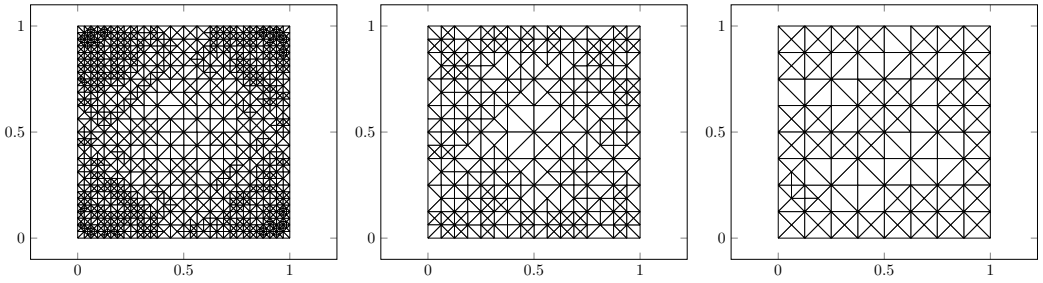

Figure 3.7.: Adaptively refined triangulations for $k = 0, 1, 2$ with 1111 nodes (1112 dofs), 292 nodes (1115 dofs), and 125 nodes (1022 dofs) for the experiment on the square domain from Subsection 3.7.1.

discretization (3.5) Square	standard P_1 FEM Square	discretization (3.5) L-shape	standard P_1 FEM L-shape
2.625000e+01	1.000000	2.899365e+01	
4.757910e+01	8.999999	6.926414e+01	2.884615
1.305197e+02	3.726470e+01	1.991659e+02	1.756275e+01
4.235010e+02	1.504169e+02	6.595024e+02	7.468677e+01
1.527148e+03	6.030519e+02	2.381177e+03	3.033437e+02
5.792301e+03	2.413598e+03	9.032306e+03	1.220281e+03
2.256465e+04	9.655787e+03	3.516437e+04	4.890763e+03
8.909059e+04	3.862454e+04	1.387472e+05	1.957543e+04
3.540600e+05	1.544995e+05	5.511823e+05	7.832252e+04
		2.197120e+06	3.133205e+05

Figure 3.8.: Condition numbers for the system matrices for the discretization (3.5) for $k = 0$ and for the standard P_1 conforming FEM for the experiments from Subsections 3.7.1–3.7.2.

For the following experiment we choose $\varphi \equiv 0$ and $u_D := g\,u$ with perturbation function $g \in H^2(\Omega)$,

$$g(x) := \begin{cases} 0 & \text{if } |x| \leq 1/2, \\ 16|x|^4 - 64|x|^3 + 88|x|^2 - 48|x| + 9 & \text{if } 1/2 \leq |x| \leq 1, \\ 1 & \text{if } |x| \geq 1, \end{cases}$$

such that $g|_\Gamma = 1$ for $\Gamma := \partial\Omega \setminus (\{0\} \times (-1,0) \cup (0,1) \times \{0\})$. Since $u|_{\partial\Omega\setminus\Gamma} = 0$, it holds $u_D|_{\partial\Omega} = u$. Let $B_{1/2}(0) := \{x \in \mathbb{R}^2 \mid |x| < 1/2\}$ denote the ball with radius $1/2$ and midpoint $(0,0)$. Since $g|_{B_{1/2}(0)} = 0$ and $u \in H^2(\Omega \setminus B_{1/2}(0))$, it holds $u_D \in H^2(\Omega)$.

For non-homogeneous Dirichlet data, the jump $[p_h]_E \cdot \tau_E$ is defined for boundary edges $E \in \mathcal{E}$, $E \subseteq \Gamma_D$ with adjacent triangle T_+ by

$$[p_h]_E \cdot \tau_E := p_h|_{T_+} \cdot \tau_E - \nabla u_D \cdot \tau_E.$$

The error estimator λ is then defined by (3.28)–(3.29). The local data error estimator contributions read

$$\mu^2(T) := \|(\varphi - \nabla u_D) - \Pi_k(\varphi - \nabla u_D)\|^2_{L^2(T)}.$$

The global error estimator μ is defined by (3.29), while $\eta = \sqrt{\mu^2 + \lambda^2}$.

The discrete solution $p_h \in P_0(\mathcal{T}; \mathbb{R}^2)$ is visualized in Figure 3.9 on a uniform triangulation with 225 nodes. The errors and error estimators for the approximation $p_h \in P_k(\mathcal{T}; \mathbb{R}^2)$ of ∇u for $k = 0, 1, 2$ are plotted in Figure 3.10 against the number of degrees of freedom. The errors and error estimators show an equivalent behaviour with an overestimation of approximately 10. Uniform refinement leads

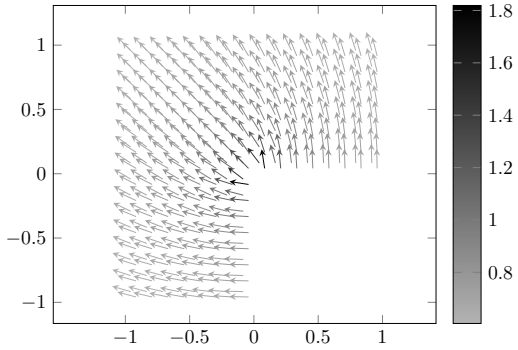

Figure 3.9.: Discrete solution for $k = 0$ for a uniform mesh with 225 nodes for the experiment from Subsection 3.7.2.

to a suboptimal convergence rate of $h^{2/3} \approx \texttt{ndof}^{-1/3}$ for $k = 0, 1, 2$. The adaptive refinement reproduces the optimal convergence rates of $\texttt{ndof}^{-(k+1)/2}$ for $k = 0, 1, 2$. Figure 3.11 depicts three meshes created by the adaptive algorithm for $k = 0$, 1, and 2 with approximately 1000 degrees of freedom. The singularity at the re-entrant corner leads to a strong refinement towards $(0, 0)$, while the refinement for $k = 0, 1$ also reflects the behaviour of the right-hand side, i.e., one also observes a moderate refinement on the circular ring $\{x \in \Omega \mid 1/2 \leq |x| \leq 1\}$. The marking with respect to the data-approximation ($\mu_\ell^2 > \kappa\lambda_\ell^2$ in Algorithm 3.35) is applied at the first 7 (resp. 5 and 10) levels for $k = 0$ (resp. $k = 1$ and $k = 2$) and then at approximately every third level.

The condition numbers of the system matrices of the discretization (3.5) for $k = 0$ and the condition numbers of the system matrices of a standard P_1 conforming FEM, estimated with the Matlab routine `condest`, are displayed in Figure 3.8 on a sequence of uniformly red-refined triangulations. On the initial triangulation of Figure 3.4b, the P_1 conforming FEM has no degree of freedom. For the other triangulations, the condition numbers of the discretization (3.5) are approximately seven times larger than the condition numbers of the standard P_1 FEM.

3.7.3. L-shaped domain with Dirichlet boundary, II

Let Ω be the L-shaped domain from Subsection 3.7.2. For $f \equiv -1$ and $u_D \equiv 0$ define $\varphi(x, y) := (1/2)(x, y)$.

Figure 3.12 depicts the discrete solution $p_h \in P_0(\mathcal{T}; \mathbb{R}^2)$ on a uniform mesh with 225 nodes. The error estimators are plotted against the degrees of freedom in Figure 3.13 for $k = 0, 1, 2$. The error estimators show for $k = 0, 1, 2$ a suboptimal convergence rate of $h^{2/3} \approx \texttt{ndof}^{-1/3}$ for uniform refinement. The adaptive algorithm 3.35 recovers the optimal convergence rate of $\texttt{ndof}^{-(k+1)/2}$. Adaptively refined meshes are depicted in Figure 3.14 for approximately 1000 degrees of freedom. The strong refinement towards the singularity at the re-entrant corner is clearly vis-

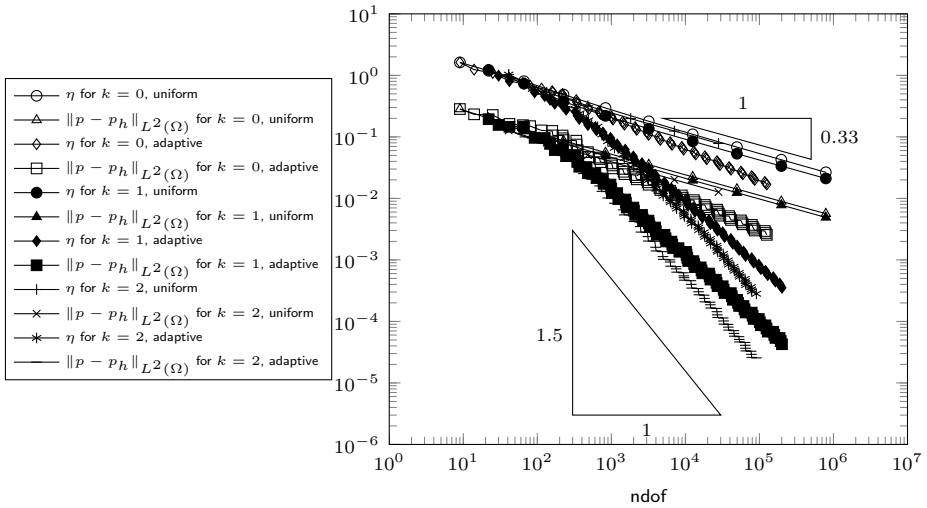

Figure 3.10.: Errors and error estimators from Subsection 3.7.2 for the L-shaped domain.

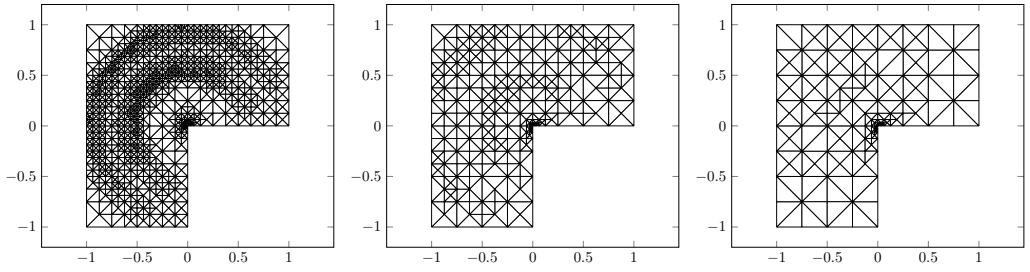

Figure 3.11.: Adaptively refined triangulations for $k = 0$ with 1006 nodes (1007 dofs), for $k = 1$ with 267 nodes (1016 dofs), and for $k = 2$ with 130 nodes (1049 dofs) for the experiment on the L-shaped domain from Subsection 3.7.2.

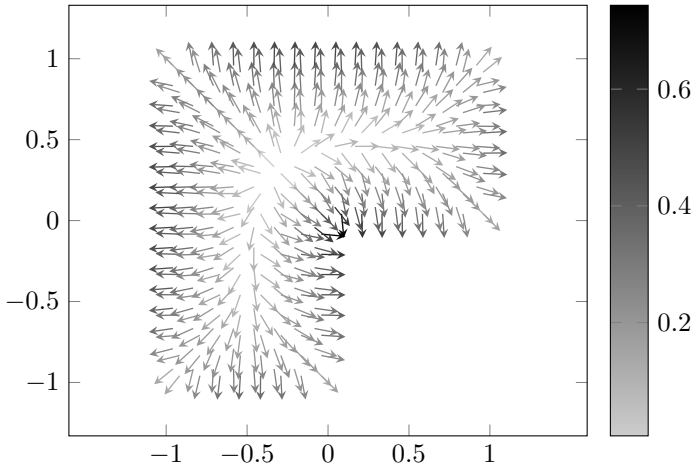

Figure 3.12.: Discrete solution for $k = 0$ for a uniform mesh with 225 nodes for the experiment from Subsection 3.7.3.

ible. The smoothness of $\varphi \in P_1(\Omega;\mathbb{R}^2)$ implies that the data-approximation error estimator μ_ℓ vanishes on all triangulations for $k = 1, 2$. For $k = 0$, μ_ℓ does not vanish, nevertheless, since $\mu_\ell^2 \leq \kappa\lambda_\ell^2$ for all ℓ, only the Dörfler marking is applied.

3.7.4. L-shaped domain with Neumann boundary, I

Consider the L-shaped domain from Subsection 3.7.2 with $\Gamma_D = (\{0\} \times [-1, 0]) \cup ([-1, 0] \times \{0\})$ illustrated in Figure 3.15a and exact solution

$$u(r,\phi) = r^{2/3}\sin(2\phi/3) \qquad \text{with} \qquad -\Delta u = 0 \text{ in } \Omega \qquad \text{and} \qquad u|_{\Gamma_D} = 0$$

from Subsection 3.7.2. Define $\chi \in P_3(\Omega;\mathbb{R}^2)$ by

$$\chi(x,y) = \begin{pmatrix} y\,(x-1)\,(x+1) \\ -x\,(y-1)\,(y+1) \end{pmatrix}.$$

Then $\chi \cdot \nu = 0$ on Γ_N and $\operatorname{div}\chi = 0$ in Ω. Let $u_D \equiv 0$ and define the right-hand side by

$$\varphi = \nabla u + \chi.$$

The discrete solution $p_h \in P_0(\mathcal{T};\mathbb{R}^2)$ for $k = 0$ is depicted in Figure 3.15b on a uniform mesh with 225 nodes.

The local error estimator contributions consider no jumps on edges on the Neumann boundary, i.e., the local error estimator contributions $\lambda^2(\mathcal{T}_\ell, T)$ are defined by

$$\lambda^2(\mathcal{T}_\ell, T) := \|h_{\mathcal{T}} \operatorname{curl}_{\mathrm{NC}} p_h\|^2_{L^2(T)} + h_T \sum_{E\in\mathcal{E}(T)\setminus\mathcal{E}(\Gamma_N)} \|[p_h]_E \cdot \tau_E\|^2_{L^2(E)}$$

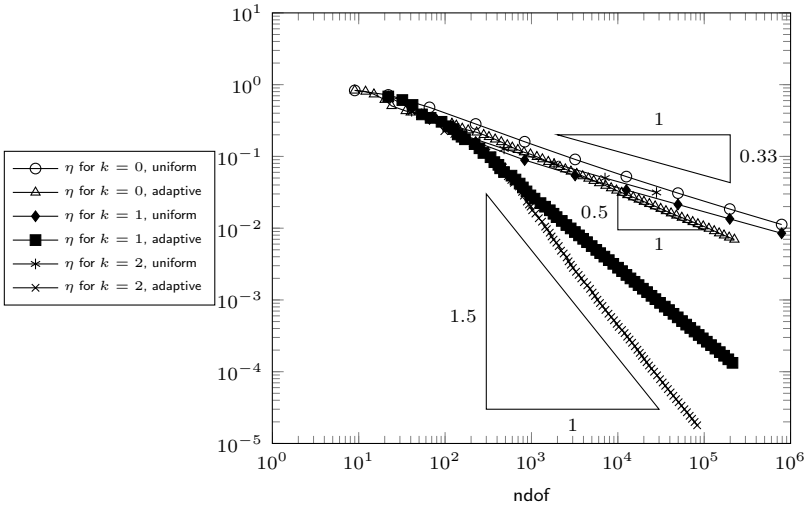

Figure 3.13.: Error estimators for the experiment on the L-shaped domain with Dirichlet boundary and unknown solution from Subsection 3.7.3.

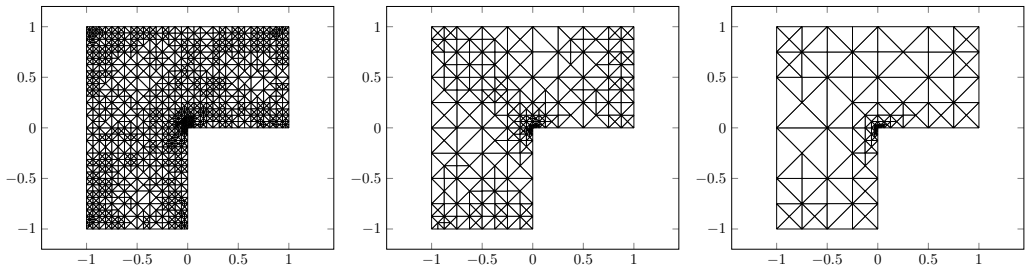

Figure 3.14.: Adaptively refined triangulations for $k = 0, 1, 2$, respectively, with 1154 nodes (1155 dofs), 287 nodes (1085 dofs), and 127 nodes (1019 dofs) for the experiment on the L-shaped domain from Subsection 3.7.3.

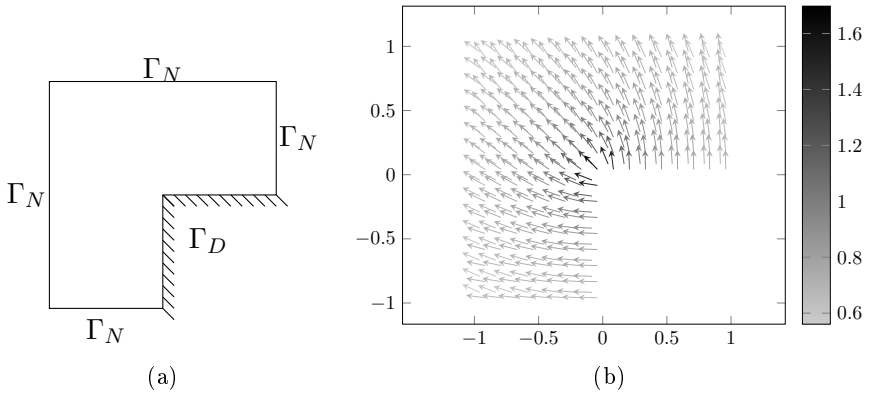

(a) (b)

Figure 3.15.: Illustration of the L-shaped domain with $\Gamma_D = (\{0\} \times [-1, 0]) \cup ([-1, 0] \times \{0\})$ and the discrete solution for $k = 0$ on a uniform mesh with 225 nodes from Subsection 3.7.4.

for $\mathcal{E}(\Gamma_N) := \{E \in \mathcal{E} \mid E \subseteq \overline{\Gamma}_N\}$.

The errors and error estimators are plotted in Figure 3.16 against the number of degrees of freedom for $k = 0, 1, 2$. The errors and error estimators show an equivalent behaviour with an overestimation approximately between 3 and 7. For uniform refinement, the errors and error estimators show a suboptimal convergence rate of $h^{2/3} \approx \texttt{ndof}^{-1/3}$. Adaptive refinement recovers the optimal convergence rates of $\texttt{ndof}^{-(k+1)/2}$. Adaptively refined meshes are depicted in Figure 3.17 for approximately 1000 degrees of freedom. The singularity at the re-entrant corner leads to a strong refinement towards this point. The marking with respect to the data-approximation ($\mu_\ell^2 > \kappa\lambda_\ell^2$ in Algorithm 3.35) is only applied at the second refinement for $k = 0$. All other marking steps for $k = 0, 1, 2$ use the Dörfler marking ($\mu_\ell^2 \leq \kappa\lambda_\ell^2$).

3.7.5. L-shaped domain with Neumann boundary, II

Let Ω be the L-shaped domain from Subsection 3.7.2 with Γ_D and Γ_N as in Subsection 3.7.4. Consider the problem

$$-\Delta u = 1 \text{ in } \Omega \qquad \text{and} \qquad u|_{\Gamma_D} = 0 \qquad \text{and} \qquad (\nabla u \cdot \nu)|_{\Gamma_N} = 0.$$

Define $\varphi \in H(\operatorname{div}, \Omega)$ by

$$\varphi(x, y) = \begin{cases} (-x - 1, 1 - y)/2 & \text{if } x \leq 0, y \geq 0, \\ (x - 1, 3 - 3y)/2 & \text{if } x \geq 0, \\ (-3 - 3x, 1 + y)/2 & \text{if } y \leq 0. \end{cases}$$

Then $-\operatorname{div} \varphi = 1$ and $(\varphi \cdot \nu)|_{\Gamma_N} = 0$.

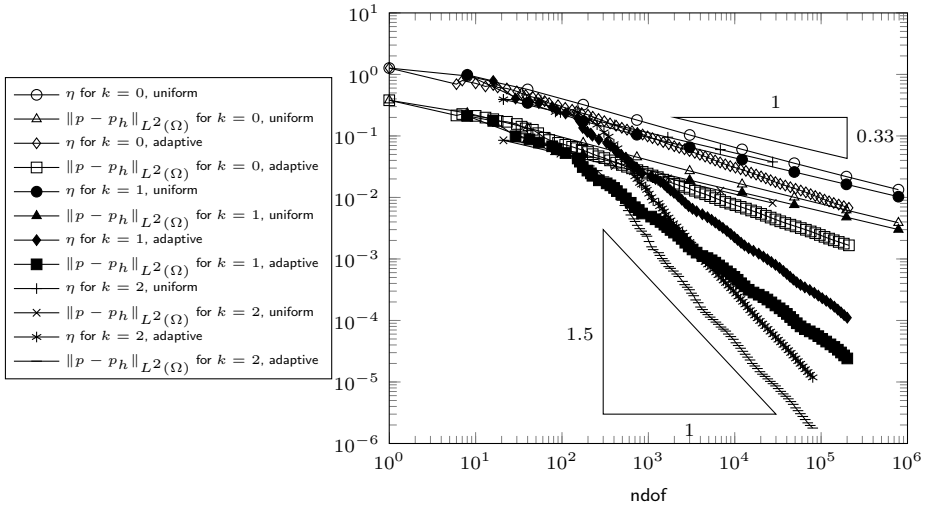

Figure 3.16.: Errors and error estimators for the experiment on the L-shaped domain with Neumann boundary with known solution from Subsection 3.7.4.

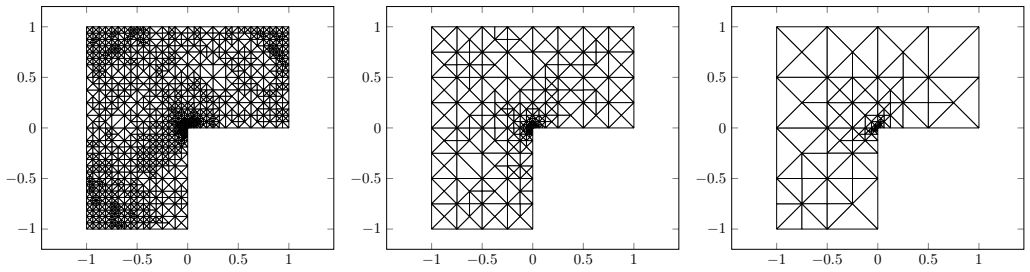

Figure 3.17.: Adaptively refined triangulations for $k = 0, 1, 2$ with 1204 nodes (1117 dofs), 296 nodes (1077 dofs), and 130 nodes (1017 dofs) for the experiment on the L-shaped domain with Neumann boundary and known solution from Subsection 3.7.4.

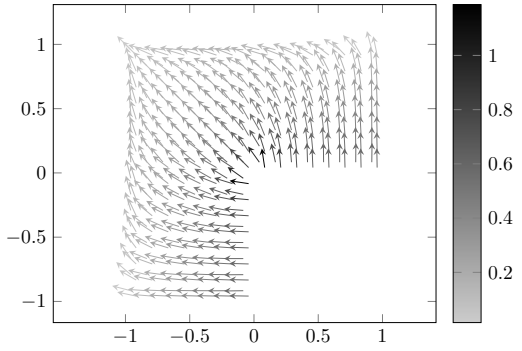

Figure 3.18.: Discrete solution for $k = 0$ for a uniform mesh with 225 nodes for the experiment from Subsection 3.7.5.

Figure 3.18 displays the discrete solution $p_h \in P_0(\mathcal{T};\mathbb{R}^2)$ for $k = 0$ on a uniform mesh with 225 nodes. In Figure 3.19 the error estimators are plotted against the number of degrees of freedom. While for uniform refinement the error estimators show a suboptimal convergence rate of $h^{2/3} \approx \texttt{ndof}^{-1/3}$, the adaptive algorithm recovers the optimal convergence rate of $\texttt{ndof}^{-(k+1)/2}$. Figure 3.20 depicts adaptively refined meshes for $k = 0, 1, 2$ with approximately 1000 degrees of freedom. The singularity leads to a strong refinement towards the re-entrant corner. The smoothness of $\varphi \in P_1(\mathcal{T};\mathbb{R}^2)$ implies that the data-approximation error estimator μ_ℓ vanishes on all triangulations for $k = 1, 2$. For $k = 0$, μ_ℓ does not vanish, nevertheless, since $\mu_\ell^2 \leq \kappa\lambda_\ell^2$ for all ℓ, only the Dörfler marking is applied.

3.7.6. Singular α

This subsection is devoted to a numerical investigation of the dependence of the error $\|p - p_h\|_{L^2(\Omega)}$ on the regularity of α. To this end, let Ω be the L-shaped domain from Subsection 3.7.2 with $\Gamma_D = \partial\Omega$. The exact smooth solution $u \in C^\infty(\Omega)$ of

$$-\Delta u = 2\sin(\pi x)\sin(\pi y) \text{ in } \Omega \qquad \text{and} \qquad u|_{\Gamma_D} = 0$$

reads

$$u(x, y) = \sin(\pi x)\sin(\pi y).$$

Define

$$\varphi = \nabla u + \operatorname{Curl}(\widetilde{\alpha})$$

with $\widetilde{\alpha} \in H^1(\Omega) \setminus H^2(\Omega)$ defined by

$$\widetilde{\alpha}(r, \phi) = r^{2/3}\sin(2\phi/3).$$

Then $\varphi \in H(\operatorname{div}, \Omega)$ with $-\operatorname{div}\varphi = f$.

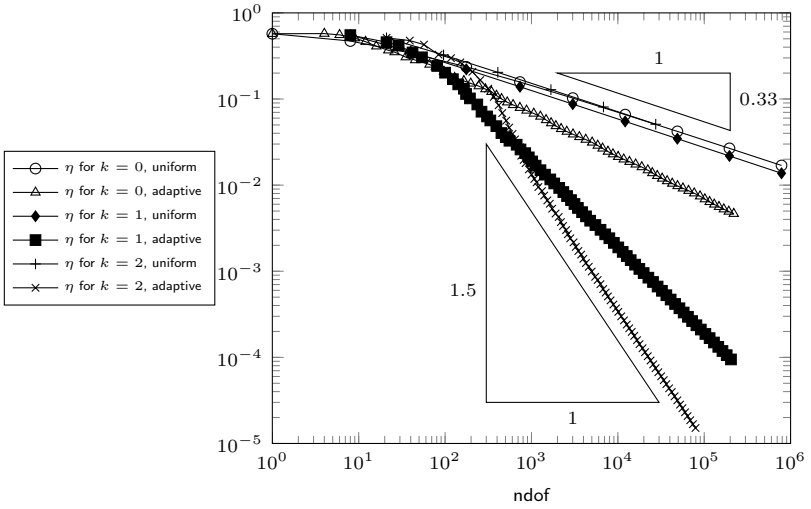

Figure 3.19.: Error estimators for the experiment on the L-shaped domain with Neumann boundary and unknown solution from Subsection 3.7.5.

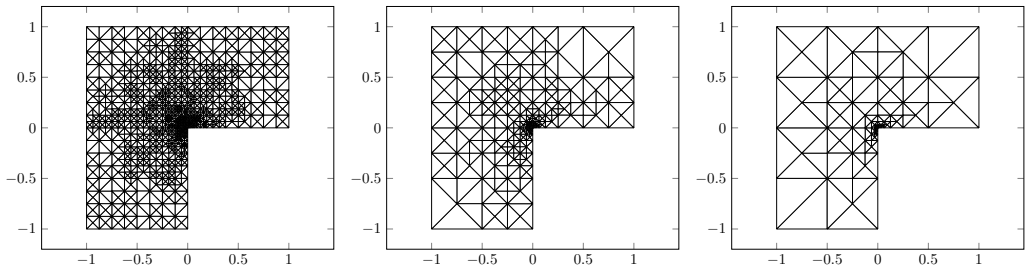

Figure 3.20.: Adaptively refined triangulations for $k = 0, 1, 2$ with 1114 nodes (1063 dofs), 277 nodes (1019 dofs), and 127 nodes (1002 dofs) for the experiment on the L-shaped domain from Subsection 3.7.5.

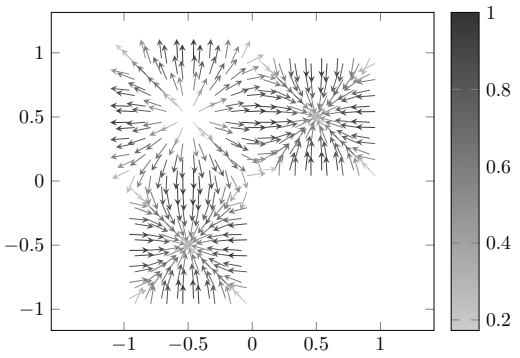

Figure 3.21.: Discrete solution for $k = 0$ for a uniform mesh with 225 nodes for the experiment from Subsection 3.7.6.

Figure 3.21 depicts the discrete solution $p_h \in P_0(\mathcal{T}; \mathbb{R}^2)$ for $k = 0$ on a uniform mesh with 225 nodes. The errors and error estimators are plotted in Figure 3.22 against the number of degrees of freedom. The convergence rate on uniform red-refined meshes for $k = 1, 2$ is $h^{2/3} \approx \texttt{ndof}^{-1/3}$ and, hence, the convergence rate seems to depend on the regularity of α. The errors and error estimators show the same convergence rate. Figure 3.23 focuses on the results for $k = 0$ and uniform mesh-refinement. The error $\|p - p_h\|_{L^2(\Omega)}$ and the error estimator η show a convergence rate between h and $h^{2/3}$, while $\|\mathrm{Curl}(\alpha - \alpha_h)\|_{L^2(\Omega)}$ converges with a rate of $h^{2/3} \approx \texttt{ndof}^{-1/3}$ due to the singularity of α. This numerical experiment suggests that the error $\|p - p_h\|_{L^2(\Omega)}$ does not depend on the regularity of α (at least in a preasymptotic regime). A triangle inequality implies $\|\mathrm{Curl}(\alpha - \alpha_h)\|_{L^2(\Omega)} \leq \|p - p_h\|_{L^2(\Omega)} + \mu$. This upper bound is also plotted in Figure 3.23.

Figure 3.24 depicts adaptively refined meshes for $k = 0, 1, 2$ with approximately 1000 degrees of freedom. The singularity of α leads to a strong refinement towards the re-entrant corner. The marking with respect to the data-approximation ($\mu_\ell^2 > \kappa\lambda_\ell^2$ in Algorithm 3.35) is only applied at levels 1–5, 7, 12, and 18 for $k = 0$. All other marking steps for $k = 0, 1, 2$ use the Dörfler marking ($\mu_\ell^2 \leq \kappa\lambda_\ell^2$).

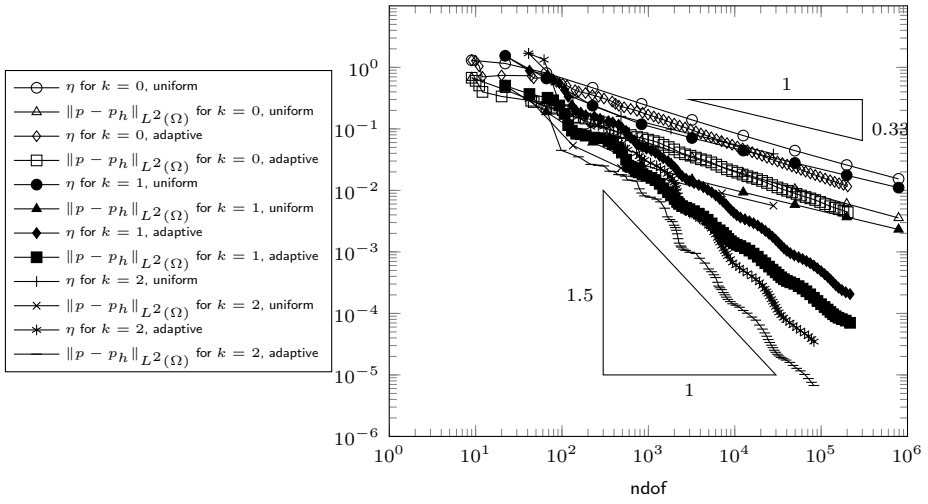

Figure 3.22.: Errors and error estimators for the experiment on the L-shaped domain with singular α from Subsection 3.7.6.

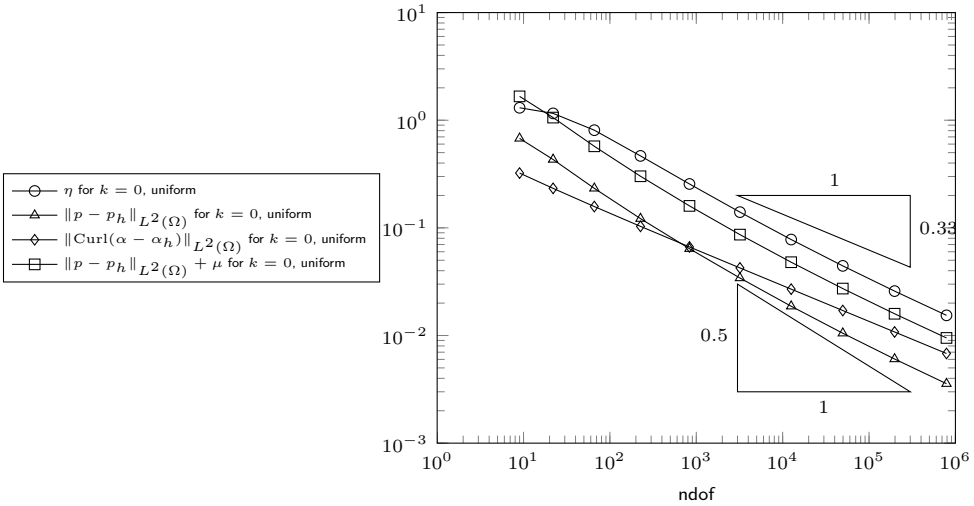

Figure 3.23.: Errors and error estimators for the experiment on the L-shaped domain with singular α from Subsection 3.7.6 and uniform refinement.

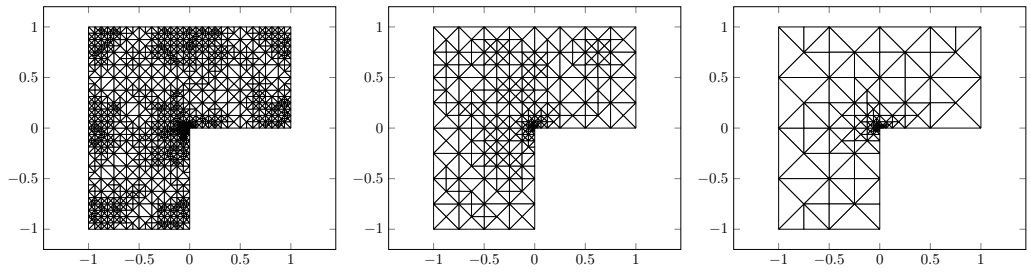

Figure 3.24.: Adaptively refined triangulations for $k = 0, 1, 2$ with 1156 nodes (1157 dofs), 284 nodes (1086 dofs), and 129 nodes (1061 dofs) for the experiment on the L-shaped domain from Subsection 3.7.6.

4. Stokes equations

This chapter considers the Stokes problem

$$-\Delta u + \nabla p = f \qquad \text{and} \qquad \operatorname{div} u = 0 \qquad \text{in } \Omega \tag{4.1}$$

with homogeneous Dirichlet boundary conditions. Standard low-order conforming methods fulfil $\operatorname{div} u = 0$ in some weak sense only. In contrast, the non-conforming method of Crouzeix and Raviart [1973] allows piecewise divergence free approximations. In Section 4.1 that method of Crouzeix and Raviart [1973] is generalized to higher polynomial degrees with deviatoric ansatz spaces for the approximation of Du. Section 4.2 defines an a posteriori error estimator and proves its efficiency and reliability, while Section 4.3 is devoted to the proof of optimal convergence rates of an adaptive algorithm. Section 4.4 concludes this chapter with numerical experiments.

Throughout this chapter $\Omega \subseteq \mathbb{R}^2$ is a simply connected, bounded, polygonal Lipschitz domain.

4.1. Weak formulation and discretization

This section introduces the new weak formulation based on the Helmholtz decomposition from Theorem 4.2 in Subsection 4.1.1 below and its discretization in Subsection 4.1.2.

4.1.1. Weak formulation

The weak form of (4.1) seeks $(u, p) \in H^1_0(\Omega;\mathbb{R}^2) \times L^2_0(\Omega)$ with

$$\begin{aligned} (Du, Dv)_{L^2(\Omega)} - (p, \operatorname{div} v)_{L^2(\Omega)} &= (f, v)_{L^2(\Omega)} && \text{for all } v \in H^1_0(\Omega;\mathbb{R}^2), \\ (q, \operatorname{div} u)_{L^2(\Omega)} &= 0 && \text{for all } q \in L^2_0(\Omega). \end{aligned} \tag{4.2}$$

Let $\mathbb{R}^{2\times 2}_{\mathrm{dev}}$ denote the 2×2 matrices with vanishing trace, i.e.,

$$\mathbb{R}^{2\times 2}_{\mathrm{dev}} := \{A \in \mathbb{R}^{2\times 2} \mid \operatorname{tr}(A) = 0\} \tag{4.3}$$

and define the operator $\operatorname{dev} : \mathbb{R}^{2\times 2} \to \mathbb{R}^{2\times 2}_{\mathrm{dev}}$ by

$$\operatorname{dev} A := A - (1/2)\operatorname{tr}(A) I_{2\times 2}.$$

Furthermore, define

$$\begin{aligned} Z &:= \{v \in H^1_0(\Omega;\mathbb{R}^2) \mid \operatorname{div} v = 0\}, \\ X &:= \left\{v \in H^1(\Omega;\mathbb{R}^2) \,\middle|\, \textstyle\int_\Omega v\,dx = 0 \text{ and } \int_\Omega \operatorname{curl} v\,dx = 0\right\}. \end{aligned} \tag{4.4}$$

The following proposition proves that $\|\operatorname{dev}\operatorname{Curl}\bullet\|_{L^2(\Omega)}$ defines a norm on X.

Proposition 4.1 (norm on X)**.** *Any $\beta \in X$ satisfies*

$$\|\operatorname{Curl}\beta\|_{L^2(\Omega)} \lesssim \|\operatorname{dev}\operatorname{Curl}\beta\|_{L^2(\Omega)}.$$

Proof. Since

$$\int_\Omega \operatorname{tr}(\operatorname{Curl}\beta)\,dx = \int_\Omega \operatorname{curl}\beta\,dx = 0 \qquad \text{for all } \beta \in X,$$

the tr-dev-div lemma, Lemma 2.9, leads to

$$\|\operatorname{tr}(\operatorname{Curl}\beta)\|_{L^2(\Omega)} \lesssim \|\operatorname{dev}\operatorname{Curl}\beta\|_{L^2(\Omega)} + \|\operatorname{div}\operatorname{Curl}\beta\|_{L^2(\Omega)}.$$

The orthogonality $\nabla H^1_0(\Omega) \perp_{L^2(\Omega)} \operatorname{Curl} H^1(\Omega)$ from Theorem 3.1 implies $\operatorname{div}\operatorname{Curl}\beta = 0$. ∎

Define

$$\Sigma := L^2(\Omega;\mathbb{R}^{2\times 2}_{\operatorname{dev}}).$$

The following Helmholtz decomposition is a continuous version of the discrete Helmholtz decomposition of Carstensen et al. [2013c].

Theorem 4.2 (Helmholtz decomposition for deviatoric functions)**.** *It holds*

$$\Sigma = DZ \oplus \operatorname{dev}\operatorname{Curl} X$$

and the sum is L^2-orthogonal.

Proof. The L^2-orthogonality follows from the L^2-orthogonality in Theorem 3.1. Proposition 4.1 implies that $(\operatorname{dev}\operatorname{Curl}\bullet, \operatorname{dev}\operatorname{Curl}\bullet)_{L^2(\Omega)}$ defines a scalar product on the complete space X. Given $\tau \in \Sigma$, this implies that there exists a unique solution $\beta \in X$ of

$$(\operatorname{dev}\operatorname{Curl}\beta, \operatorname{dev}\operatorname{Curl}\gamma)_{L^2(\Omega)} = (\tau, \operatorname{dev}\operatorname{Curl}\gamma)_{L^2(\Omega)} \qquad \text{for all } \gamma \in X.$$

Let $\widehat{\gamma} \in H^1(\Omega;\mathbb{R}^2)/\mathbb{R}^2$ be defined by

$$\widehat{\gamma}(y) := \frac{1}{2}\begin{pmatrix} -y_2 \\ y_1 \end{pmatrix} - \fint_\Omega \frac{1}{2}\begin{pmatrix} -x_2 \\ x_1 \end{pmatrix} dx.$$

Then $\operatorname{curl}\widehat{\gamma} = 1$. Given $\gamma \in H^1(\Omega;\mathbb{R}^2)$ with $\int_\Omega \gamma\,dx = 0$, define $\widetilde{\gamma} \in X$ by $\widetilde{\gamma} := \gamma - \int_\Omega \operatorname{curl}\gamma\,dx\widehat{\gamma}$. Since $\operatorname{tr}(\tau) = 0$ and $\operatorname{dev}\operatorname{Curl}\gamma = \operatorname{dev}\operatorname{Curl}\widetilde{\gamma}$, the definition of β implies

$$(\tau - \operatorname{dev}\operatorname{Curl}\beta, \operatorname{Curl}\gamma)_{L^2(\Omega)} = (\tau - \operatorname{dev}\operatorname{Curl}\beta, \operatorname{dev}\operatorname{Curl}\widetilde{\gamma})_{L^2(\Omega)} = 0.$$

Thus, the Helmholtz decomposition, Theorem 3.1, (applied row-wise) implies the existence of $u \in H^1_0(\Omega;\mathbb{R}^2)$ with $\tau - \operatorname{dev}\operatorname{Curl}\beta = Du$. Then,

$$\operatorname{div} u = \operatorname{tr}(\tau - \operatorname{dev}\operatorname{Curl}\beta) = 0$$

leads to $u \in Z$ and concludes the proof. ∎

Let $\varphi \in H(\operatorname{div},\Omega;\mathbb{R}^{2\times 2})$ with $\int_\Omega \operatorname{tr}(\varphi)\,dx = 0$ and $-\operatorname{div}\varphi = f$ and seek $(\sigma,\alpha) \in \Sigma \times X$ with

$$\begin{aligned} (\sigma,\tau)_{L^2(\Omega)} + (\tau, \operatorname{dev}\operatorname{Curl}\alpha)_{L^2(\Omega)} &= (\varphi,\tau)_{L^2(\Omega)} && \text{for all } \tau \in \Sigma, \\ (\sigma, \operatorname{dev}\operatorname{Curl}\beta)_{L^2(\Omega)} &= 0 && \text{for all } \beta \in X. \end{aligned} \tag{4.5}$$

Define the bilinear forms $a : \Sigma \times \Sigma \to \mathbb{R}$ and $b : \Sigma \times X \to \mathbb{R}$ by

$$\begin{aligned} a(\sigma,\tau) &:= (\sigma,\tau)_{L^2(\Omega)} && \text{for all } \sigma,\tau \in \Sigma, \\ b(\tau,\alpha) &:= (\tau, \operatorname{dev}\operatorname{Curl}\alpha)_{L^2(\Omega)} && \text{for all } \tau \in \Sigma, \alpha \in X. \end{aligned}$$

The following inf-sup condition is employed in the proof of the existence and uniqueness of solutions from Proposition 4.4.

Lemma 4.3 (inf-sup condition)**.** *Any $\beta \in X$ satisfies*

$$\|\operatorname{Curl}\beta\|_{L^2(\Omega)} \lesssim \sup_{\tau\in\Sigma\setminus\{0\}} \frac{b(\tau,\beta)}{\|\tau\|_{L^2(\Omega)}}.$$

Proof. The choice of $\tau := \operatorname{dev}\operatorname{Curl}\beta$ leads to

$$b(\tau,\beta) = \|\operatorname{dev}\operatorname{Curl}\beta\|^2_{L^2(\Omega)}.$$

Proposition 4.1 then yields the assertion. ∎

Proposition 4.4. *Problem (4.5) admits a unique solution $(\sigma,\alpha) \in \Sigma \times X$ and it holds $\sigma = Du$ for the solution $u \in Z$ of (4.2).*

Proof. The existence of a unique solution follows from Brezzi's splitting lemma, Theorem 2.8, and Lemma 4.3. The second equation of (4.5) and the Helmholtz decomposition of Theorem 4.2 guarantees the existence of $\widetilde{u} \in Z$ with $\sigma = D\widetilde{u}$. Then, (4.5), $-\operatorname{div}\varphi = f$ and the orthogonality $DH^1_0(\Omega;\mathbb{R}^2) \perp_{L^2(\Omega)} \operatorname{Curl} X$ imply

$$\begin{aligned} (D\widetilde{u}, Dv)_{L^2(\Omega)} &= (\varphi, Dv)_{L^2(\Omega)} - (Dv, \operatorname{dev}\operatorname{Curl}\alpha)_{L^2(\Omega)} \\ &= (f,v)_{L^2(\Omega)} - (Dv, \operatorname{Curl}\alpha) \\ &= (f,v)_{L^2(\Omega)} \end{aligned}$$

for all $v \in Z$. This yields $\widetilde{u} = u$. ∎

Remark 4.5 (pressure). Define $p := -(1/2)\mathrm{tr}(\varphi - \operatorname{Curl}\alpha) \in L^2_0(\Omega)$. Since $\operatorname{dev}(\varphi - \operatorname{Curl}\alpha) = \sigma$, it follows

$$\begin{aligned}(p, \operatorname{div} v)_{L^2(\Omega)} &= (Dv, pI_{2\times 2})_{L^2(\Omega)} \\ &= (Dv, \operatorname{dev}(\varphi - \operatorname{Curl}\alpha))_{L^2(\Omega)} - (Dv, \varphi - \operatorname{Curl}\alpha)_{L^2(\Omega)} \\ &= (\sigma, Dv)_{L^2(\Omega)} - (f, v)_{L^2(\Omega)}.\end{aligned}$$

Proposition 4.4 implies that $\sigma = Du$ for the solution $u \in Z$ of (4.2) and, hence, $(u, p) \in Z \times L^2_0(\Omega)$ fulfils (4.2). ♦

4.1.2. Discretization

For $k \geq 0$, define

$$\begin{aligned}\Sigma_h(\mathcal{T}) &:= P_k(\mathcal{T}; \mathbb{R}^{2\times 2}_{\operatorname{dev}}) \subseteq \Sigma, \\ X_h(\mathcal{T}) &:= P_{k+1}(\mathcal{T}; \mathbb{R}^2) \cap X \subseteq X.\end{aligned}$$

The discrete problem seeks $(\sigma_h, \alpha_h) \in \Sigma_h(\mathcal{T}) \times X_h(\mathcal{T})$ with

$$\begin{aligned}(\sigma_h, \tau_h)_{L^2(\Omega)} + (\tau_h, \operatorname{dev}\operatorname{Curl}\alpha_h)_{L^2(\Omega)} &= (\varphi, \tau_h)_{L^2(\Omega)} && \text{for all } \tau_h \in \Sigma_h(\mathcal{T}), \\ (\sigma_h, \operatorname{dev}\operatorname{Curl}\beta_h)_{L^2(\Omega)} &= 0 && \text{for all } \beta_h \in X_h(\mathcal{T}).\end{aligned} \tag{4.6}$$

The following lemma proves a discrete inf-sup condition.

Lemma 4.6 (discrete inf-sup condition). *Any $\beta_h \in X_h(\mathcal{T})$ satisfies*

$$\|\operatorname{Curl}\beta_h\|_{L^2(\Omega)} \lesssim \sup_{\tau_h \in \Sigma_h(\mathcal{T})\setminus\{0\}} \frac{b(\tau_h, \beta_h)}{\|\tau_h\|_{L^2(\Omega)}}.$$

Proof. As in the proof of Lemma 4.3, the choice $\tau_h := \operatorname{dev}\operatorname{Curl}\beta_h \in X_h(\mathcal{T})$ and Proposition 4.1 yield the assertion. ■

The following corollary is a consequence of Theorem 2.8, Lemma 4.6, and the standard theory of mixed FEMs [Boffi et al., 2013].

Corollary 4.7 (a priori error estimate). *The discrete problem (4.6) has a unique solution $(\sigma_h, \alpha_h) \in \Sigma_h(\mathcal{T}) \times X_h(\mathcal{T})$ and it satisfies*

$$\begin{aligned}&\|\sigma - \sigma_h\|_{L^2(\Omega)} + \|\operatorname{Curl}(\alpha - \alpha_h)\|_{L^2(\Omega)} \\ &\qquad \lesssim \min_{\tau_h \in \Sigma_h(\mathcal{T})} \|\sigma - \tau_h\|_{L^2(\Omega)} + \min_{\beta_h \in X_h(\mathcal{T})} \|\operatorname{Curl}(\alpha - \beta_h)\|_{L^2(\Omega)}.\end{aligned}$$ ■

Define

$$W_h(\mathcal{T}) := \{\tau_h \in \Sigma_h(\mathcal{T}) \mid \forall \beta_h \in X_h(\mathcal{T}) : \ (\tau_h, \operatorname{dev}\operatorname{Curl}\beta_h)_{L^2(\Omega)} = 0\}. \tag{4.7}$$

The following lemma proves a projection property for $W_h(\mathcal{T})$. This is the key argument in the a posteriori and optimality analysis in Sections 4.2 and 4.3.

Lemma 4.8 (projection property)**.** *Let $\tau \in \Sigma$ with $(\tau, \operatorname{dev}\operatorname{Curl}\beta)_{L^2(\Omega)} = 0$ for all $\beta \in X$ (that means that there exists $v \in Z$ with $\tau = Dv$). Then $\Pi_{\Sigma_h(\mathcal{T})}\tau \in W_h(\mathcal{T})$. If $\mathcal{T}_\star$ is an admissible refinement of $\mathcal{T}$ and $\tau_\star \in W_h(\mathcal{T}_\star)$, then $\Pi_{\Sigma_h(\mathcal{T})}\tau_\star \in W_h(\mathcal{T})$.*

Proof. This follows from $\operatorname{dev}\operatorname{Curl} X_h(\mathcal{T}) \subseteq \Sigma_h(\mathcal{T})$ and $X_h(\mathcal{T}) \subseteq X_h(\mathcal{T}_\star) \subseteq X$ as in the proof of Lemma 3.11. ∎

Remark 4.9. The discrete Helmholtz decomposition of Carstensen et al. [2013c] proves

$$P_0(\mathcal{T}; \mathbb{R}^{2\times 2}_{\operatorname{dev}}) = D_{\mathrm{NC}} Z_{\mathrm{CR}}(\mathcal{T}) \oplus \operatorname{dev}\operatorname{Curl}(P_1(\mathcal{T}; \mathbb{R}^2) \cap H^1(\Omega; \mathbb{R}^2))$$

for

$$Z_{\mathrm{CR}}(\mathcal{T}) := \{v_h \in \mathrm{CR}^1_0(\mathcal{T}) \times \mathrm{CR}^1_0(\mathcal{T}) \mid \operatorname{div}_{\mathrm{NC}} v_h = 0\}.$$

If $k = 0$, this proves $\sigma_h = D_{\mathrm{NC}}\widetilde{u}_{\mathrm{CR}}$ for the solution $\sigma_h \in \Sigma_h(\mathcal{T})$ of (4.6) and some $\widetilde{u}_{\mathrm{CR}} \in Z_{\mathrm{CR}}(\mathcal{T})$. If the right-hand side is a Raviart-Thomas vector field, $\varphi \in \mathrm{RT}_0(\mathcal{T}; \mathbb{R}^2) := \mathrm{RT}_0(\mathcal{T}) \times \mathrm{RT}_0(\mathcal{T})$ with $\mathrm{RT}_0(\mathcal{T})$ from (3.10), a piecewise integration by parts proves, for all $v_{\mathrm{CR}} \in Z_{\mathrm{CR}}(\mathcal{T})$,

$$(D_{\mathrm{NC}}\widetilde{u}_{\mathrm{CR}}, D_{\mathrm{NC}}v_{\mathrm{CR}})_{L^2(\Omega)} = (\varphi, D_{\mathrm{NC}}v_{\mathrm{CR}})_{L^2(\Omega)} = (f, v_{\mathrm{CR}})_{L^2(\Omega)}$$

and hence $\widetilde{u}_{\mathrm{CR}}$ is the solution of the P_1 non-conforming FEM of Crouzeix and Raviart [1973].

Let $\mathcal{E}(\Omega)$ (resp. $\mathcal{N}(\Omega)$) denote the interior edges (resp. nodes) of $\mathcal{T}$. A computation reveals

$$\begin{aligned} &\dim(W_h(\mathcal{T})) = 3\operatorname{card}(\mathcal{E}(\Omega)) + \operatorname{card}(\mathcal{N}(\Omega)) && \text{for } k = 1,\\ &\dim(W_h(\mathcal{T})) = 6\operatorname{card}(\mathcal{E}(\Omega)) + 1 && \text{for } k = 2, \end{aligned}$$

while the non-conforming piecewise quadratic finite element space with vanishing divergence of Fortin and Soulie [1983] has dimension $3\operatorname{card}(\mathcal{N}(\Omega)) + \operatorname{card}(\mathcal{E}(\Omega))$ and the non-conforming piecewise cubic finite element space with vanishing divergence of Crouzeix and Falk [1989] has dimension $\operatorname{card}(\mathcal{N}) + 7\operatorname{card}(\mathcal{E}(\Omega)) + 1$. Therefore, these non-conforming FEMs are different from the discretization (4.6). ⧫

Remark 4.10 (Extension to 3D)**.** Recall the notation from Section 3.6 for a three-dimensional simply connected, bounded, polygonal Lipschitz domain $\Omega \subseteq \mathbb{R}^3$. For a matrix-valued function $\beta : \Omega \to \mathbb{R}^{3\times 3}$ define the Curl by the row-wise application, i.e.,

$$\operatorname{Curl}\beta = \begin{pmatrix} (\operatorname{Curl}\beta_{1\bullet})^\top \\ (\operatorname{Curl}\beta_{2\bullet})^\top \\ (\operatorname{Curl}\beta_{3\bullet})^\top \end{pmatrix}$$

and let $H(\operatorname{Curl},\Omega;\mathbb{R}^{3\times3})$ denote the space of all $\beta\in L^2(\Omega,\mathbb{R}^{3\times3})$ with $\operatorname{Curl}\beta\in L^2(\Omega;\mathbb{R}^{3\times3})$ for the weak Curl, i.e.,

$$\int_\Omega v\cdot\operatorname{Curl}\beta\,dx=\int_\Omega\beta\cdot\operatorname{Curl}v\,dx\qquad\text{for all } v\in C_c^\infty(\Omega;\mathbb{R}^{3\times3}).$$

The arguments of Theorem 4.2 together with the Helmholtz decomposition (3.39) lead to

$$L^2(\Omega;\mathbb{R}^{3\times3}_{\operatorname{dev}})=DZ\oplus\operatorname{dev}\operatorname{Curl}X.$$

Let $\varphi\in H(\operatorname{div},\Omega;\mathbb{R}^{3\times3})$ with $-\operatorname{div}\varphi=f$ and $\int_\Omega\operatorname{tr}(\varphi)\,dx=0$ and define $Y(\Omega;\mathbb{R}^{3\times3}):=H(\operatorname{Curl},\Omega;\mathbb{R}^{3\times3})$ and $U:=H^1(\Omega;\mathbb{R}^3)\cap L^2_0(\Omega;\mathbb{R}^3)$. The Stokes problem (4.1) is then equivalent to the following problem. Seek $(\sigma,\alpha,w)\in L^2\Omega;\mathbb{R}^{3\times3}_{\operatorname{dev}})\times Y(\Omega;\mathbb{R}^{3\times3})\times U$ with

$$\begin{aligned}(\sigma,\tau)_{L^2(\Omega)}+(\tau,\operatorname{dev}\operatorname{Curl}\alpha)_{L^2(\Omega)}&=(\varphi,\tau)_{L^2(\Omega)}&&\text{for all }\tau\in L^2(\Omega;\mathbb{R}^{3\times3}_{\operatorname{dev}}),\\(\sigma,\operatorname{dev}\operatorname{Curl}\beta)_{L^2(\Omega)}+(\beta,Dw)_{L^2(\Omega)}&=0&&\text{for all }\beta\in Y(\Omega;\mathbb{R}^{3\times3}),\\(\alpha,Dv)_{L^2(\Omega)}&=0&&\text{for all }v\in U.\end{aligned}\tag{4.8}$$

Define $\Sigma_h(\mathcal{T};\mathbb{R}^{3\times3}_{\operatorname{dev}}):=P_k(\mathcal{T};\mathbb{R}^{3\times3}_{\operatorname{dev}})$, $Y_{\mathrm{N},k}(\mathcal{T};\mathbb{R}^{3\times3}):=\{\beta\in L^2(\Omega;\mathbb{R}^{3\times3})\mid\beta_{k\bullet}^\top\in Y_{\mathrm{N},k}(\mathcal{T})\}$, and $U_h(\mathcal{T};\mathbb{R}^3):=P_{k+1}(\mathcal{T};\mathbb{R}^3)\cap U$. Then, the discretization of (4.8) seeks $(\sigma_h,\alpha_h,w_h)\in\Sigma_h(\mathcal{T};\mathbb{R}^{3\times3}_{\operatorname{dev}})\times Y_{\mathrm{N},k}(\mathcal{T};\mathbb{R}^{3\times3})\times U_h(\mathcal{T};\mathbb{R}^3)$ with

$$\begin{aligned}(\sigma_h,\tau_h)_{L^2(\Omega)}+(\tau_h,\operatorname{dev}\operatorname{Curl}\alpha_h)_{L^2(\Omega)}&=(\varphi,\tau_h)_{L^2(\Omega)}&&\text{for all }\tau_h\in\Sigma_h(\mathcal{T};\mathbb{R}^{3\times3}_{\operatorname{dev}}),\\(\sigma_h,\operatorname{dev}\operatorname{Curl}\beta_h)_{L^2(\Omega)}+(\beta_h,Dw_h)_{L^2(\Omega)}&=0&&\text{for all }\beta_h\in Y_{\mathrm{N},k}(\mathcal{T};\mathbb{R}^{3\times3}),\\(\alpha_h,Dv_h)_{L^2(\Omega)}&=0&&\text{for all }v_h\in U_h(\mathcal{T};\mathbb{R}^3).\end{aligned}$$

The proof of Proposition 4.1 also applies to the three-dimensional situation. This and the arguments of Sections 3.6 and 4.1 above lead to the unique existence of solutions, a best-approximation property, and the projection property. ♦

4.2. A posteriori error analysis

Define for any $T\in\mathcal{T}$ the error estimator

$$\begin{aligned}\eta^2(T):=\|\operatorname{dev}(\varphi-\Pi_{\Sigma_h(\mathcal{T})}\varphi)\|^2_{L^2(T)}+\|h_{\mathcal{T}}\operatorname{curl}_{\mathrm{NC}}\sigma_h\|^2_{L^2(T)}\\+h_T\sum_{E\in\mathcal{E}(T)}\|[\sigma_h\tau_E]_E\|^2_{L^2(E)}\end{aligned}\tag{4.9}$$

and

$$\eta^2:=\sum_{T\in\mathcal{T}}\eta^2(T).\tag{4.10}$$

The following theorem proves efficiency and reliability of η.

Theorem 4.11 (efficiency, reliability). *There exist constants* $C_{\mathrm{eff}}, C_{\mathrm{rel}} > 0$ *with*

$$C_{\mathrm{eff}}^{-2}\eta^2 \le \|\sigma - \sigma_h\|_{L^2(\Omega)}^2 + \|\mathrm{Curl}(\alpha - \alpha_h)\|_{L^2(\Omega)}^2 \le C_{\mathrm{rel}}^2\eta^2$$

Proof. The proof is similar to that of Theorem 3.30.

Define, for all $\tau \in \Sigma$ and all $\beta \in X$, the residuals

$$\begin{aligned}\mathrm{Res}_1(\sigma_h, \alpha_h; \tau) &:= (\sigma_h, \tau)_{L^2(\Omega)} + (\tau, \operatorname{dev}\operatorname{Curl}\alpha_h)_{L^2(\Omega)} - (\varphi, \tau)_{L^2(\Omega)},\\ \mathrm{Res}_2(\sigma_h; \beta) &:= (\sigma_h, \operatorname{dev}\operatorname{Curl}\beta)_{L^2(\Omega)}.\end{aligned}$$

The abstract theory of Carstensen [2005] proves

$$\begin{aligned}&\|\sigma - \sigma_h\|_{L^2(\Omega)}^2 + \|\mathrm{Curl}(\alpha - \alpha_h)\|_{L^2(\Omega)}^2\\ &\quad\approx \|\mathrm{Res}_1(\sigma_h, \alpha_h; \bullet)\|_{\Sigma^\star}^2 + \|\mathrm{Res}_2(\sigma_h; \bullet)\|_{X^\star}^2.\end{aligned} \tag{4.11}$$

Step 2 of the proof of Theorem 3.30 leads to

$$\|\mathrm{Res}_1(\sigma_h, \alpha_h; \bullet)\|_{\Sigma^\star} = \|\operatorname{dev}(\varphi - \Pi_{\Sigma_h(\mathcal{T})}\varphi)\|_{L^2(\Omega)}.$$

Since $\operatorname{tr}(\sigma) = \operatorname{tr}(\sigma_h) = 0$,

$$\mathrm{Res}_2(\sigma_h; \beta) = (\sigma_h, \operatorname{Curl}\beta)_{L^2(\Omega)}$$

for all $\beta \in X$. This enables the arguments of Steps 3 and 4 of the proof of Theorem 3.30 and yields

$$\|\mathrm{Res}_2(\sigma_h; \bullet)\|_{X^\star}^2 \approx \|h_{\mathcal{T}}\operatorname{curl}_{\mathrm{NC}}\sigma_h\|_{L^2(\Omega)}^2 + h_T\sum_{E\in\mathcal{E}}\|[\sigma_h\tau_E]_E\|_{L^2(E)}^2.$$

The efficiency follows with the well-known bubble function technique as in the proof of Theorem 3.30. ∎

4.3. Adaptive algorithm

This section defines an adaptive algorithm in Subsection 4.3.1 and proves its optimal convergence rates in Subsections 4.3.2–4.3.5.

4.3.1. Adaptive algorithm and optimal convergence rates

Given a triangulation $\mathcal{T}_\ell$, define for all $T \in \mathcal{T}_\ell$ the local error estimator contributions by

$$\begin{aligned}\lambda^2(\mathcal{T}_\ell, T) &:= \|h_{\mathcal{T}}\operatorname{curl}_{\mathrm{NC}}\sigma_h\|_{L^2(T)}^2 + h_T\sum_{E\in\mathcal{E}(T)}\|[\sigma_h\tau_E]_E\|_{L^2(E)}^2,\\ \mu^2(T) &:= \|\operatorname{dev}(\varphi - \Pi_{\Sigma_h(\mathcal{T})}\varphi)\|_{L^2(T)}^2\end{aligned} \tag{4.12}$$

and the global error estimator by

$$\begin{aligned} \lambda_\ell^2 &:= \lambda^2(\mathcal{T}_\ell, \mathcal{T}_\ell) \quad \text{with} \quad \lambda^2(\mathcal{T}_\ell, \mathcal{M}) := \sum_{T\in\mathcal{M}} \lambda^2(\mathcal{T}_\ell, T) \qquad \text{for any } \mathcal{M} \subseteq \mathcal{T}_\ell, \\ \mu_\ell^2 &:= \mu^2(\mathcal{T}_\ell) \qquad \text{with} \quad \mu^2(\mathcal{M}) := \sum_{T\in\mathcal{M}} \mu^2(T) \qquad \text{for any } \mathcal{M} \subseteq \mathcal{T}_\ell. \end{aligned} \tag{4.13}$$

The adaptive algorithm is driven by these two error estimators and runs the following loop.

Algorithm 4.12 (AFEM for the Stokes problem)**.**
Input: Initial triangulation $\mathcal{T}_0$, parameters $0 < \theta_A \leq 1$, $0 < \rho_B < 1$, $0 < \kappa$.
for $\ell = 0, 1, 2, \dots$ **do**
Solve. Compute solution $(\sigma_\ell, \alpha_\ell) \in \Sigma_h(\mathcal{T}_\ell) \times X_h(\mathcal{T}_\ell)$ of (4.6) with respect to $\mathcal{T}_\ell$.
Estimate. Compute local contributions of the error estimators $\big(\lambda^2(\mathcal{T}_\ell, T)\big)_{T\in\mathcal{T}_\ell}$ and $\big(\mu^2(T)\big)_{T\in\mathcal{T}_\ell}$.
if $\mu_\ell^2 \leq \kappa\lambda_\ell^2$ **then**
Mark. The Dörfler marking chooses a minimal subset $\mathcal{M}_\ell \subseteq \mathcal{T}_\ell$ such that $\theta_A\lambda_\ell^2 \leq \lambda_\ell^2(\mathcal{T}_\ell, \mathcal{M}_\ell)$.
Refine. Generate the smallest admissible refinement $\mathcal{T}_{\ell+1}$ of $\mathcal{T}_\ell$ in which at least all triangles in $\mathcal{M}_\ell$ are refined.
else
Mark. Compute a triangulation $\mathcal{T} \in \mathbb{T}$ with $\mu^2(\mathcal{T}) \leq \rho_B\mu_\ell^2$.
Refine. Generate the overlay $\mathcal{T}_{\ell+1}$ of $\mathcal{T}_\ell$ and $\mathcal{T}$.
end if
end for
Output: Sequences of triangulations $(\mathcal{T}_\ell)_{\ell\in\mathbb{N}_0}$, discrete solutions $(\sigma_\ell, \alpha_\ell)_{\ell\in\mathbb{N}_0}$ and error estimators $(\lambda_\ell)_{\ell\in\mathbb{N}_0}$ and $(\mu_\ell)_{\ell\in\mathbb{N}_0}$. ⧫

Given an initial triangulation $\mathcal{T}_0$, recall the set of admissible triangulations $\mathbb{T}$ from Definition 2.4. Let $\mathbb{T}(N)$ denote the subset of all admissible triangulations with at most $\operatorname{card}(\mathcal{T}_0) + N$ triangles. For $s > 0$ and $(\sigma, \alpha, \varphi) \in \Sigma \times X \times H(\operatorname{div}, \Omega; \mathbb{R}^{2\times 2})$ define the seminorm

$$\begin{aligned} |(\sigma, \alpha, \varphi)|_{\mathcal{A}_s} := \sup_{N\in\mathbb{N}_0} N^s \inf_{\mathcal{T}\in\mathbb{T}(N)} \Big(&\|\sigma - \Pi_{\Sigma_h(\mathcal{T})}\sigma\|_{L^2(\Omega)} \\ &+ \inf_{\beta_\mathcal{T}\in X_h(\mathcal{T})} \|\operatorname{Curl}(\alpha - \beta_\mathcal{T})\|_{L^2(\Omega)} + \|\operatorname{dev}(\varphi - \Pi_{\Sigma_h(\mathcal{T})}\varphi)\|_{L^2(\Omega)}\Big). \end{aligned}$$

Remark 4.13 (pure local approximation class)**.** Since Ω is assumed to be a Lipschitz domain, all patches in an admissible triangulation $\mathcal{T} \in \mathbb{T}$ are edge-connected (see also Remark 3.38). Under this assumption, Veeser [2014, Theorem 3.2] proves

$$\min_{v_h\in P_{k+1}(\mathcal{T})\cap H^1(\Omega)} \|\nabla(v - v_h)\|_{L^2(\Omega)} \approx \|\nabla v - \Pi_{P_k(\mathcal{T};\mathbb{R}^2)}\nabla v\|_{L^2(\Omega)} \quad \text{for all } v \in H^1(\Omega).$$

Hence,

$$\begin{aligned}|(\sigma,\alpha,\varphi)|_{\mathcal{A}_s} &\approx |(\sigma,\alpha,\varphi)|_{\mathcal{A}_s'}\\ &:= \sup_{N\in\mathbb{N}} N^s \inf_{\mathcal{T}\in\mathbb{T}(N)} \Big(\|\sigma-\Pi_{\Sigma_h(\mathcal{T})}\sigma\|_{L^2(\Omega)}\\ &\qquad + \big\|\operatorname{Curl}\alpha-\Pi_{\Sigma_h(\mathcal{T})}\operatorname{Curl}\alpha\big\|_{L^2(\Omega)} + \|\operatorname{dev}(\varphi-\Pi_{\Sigma_h(\mathcal{T})}\varphi)\|_{L^2(\Omega)}\Big). \quad \blacklozenge\end{aligned}$$

We assume that the algorithm used in the marking step for $\mu_\ell^2 > \kappa\lambda_\ell^2$ fulfils the following axiom (B1). This assumption follows for the algorithm `Approx` from Carstensen and Rabus [2015] if the axioms (B2) and (SA) from Subsection 4.3.5 below are fulfilled (cf. Remark 3.37).

Assumption 4.14 ((B1) optimal data approximation)**.** Assume that $|(\sigma,\alpha,\varphi)|_{\mathcal{A}_s}$ is finite. Given a tolerance Tol, the algorithm used in *Mark* in the second case ($\mu_\ell^2 > \kappa\lambda_\ell^2$) in Algorithm 4.12 computes $\mathcal{T}_\star \in \mathbb{T}$ with

$$\operatorname{card}(\mathcal{T}_\star) - \operatorname{card}(\mathcal{T}_0) \lesssim \mathrm{Tol}^{-1/(2s)} \qquad \text{and} \qquad \mu^2(\mathcal{T}_\star) \le \mathrm{Tol}. \quad \blacklozenge$$

The following theorem proves optimal convergence rates of Algorithm 4.12.

Theorem 4.15 (optimal convergence rates of AFEM)**.** *Let $s > 0$. For $0 < \rho_B < 1$ and sufficiently small $0 < \kappa$ and $0 < \theta < 1$, Algorithm 4.12 computes sequences of triangulations $(\mathcal{T}_\ell)_{\ell\in\mathbb{N}}$ and discrete solutions $(\sigma_\ell,\alpha_\ell)_{\ell\in\mathbb{N}}$ for the right-hand side φ of optimal rate of convergence in the sense that*

$$(\operatorname{card}(\mathcal{T}_\ell) - \operatorname{card}(\mathcal{T}_0))^s \Big(\|\sigma-\sigma_\ell\|_{L^2(\Omega)} + \|\operatorname{Curl}(\alpha-\alpha_\ell)\|_{L^2(\Omega)}\Big) \lesssim |(\sigma,\alpha,\varphi)|_{\mathcal{A}_s}.$$

The proof follows from the abstract framework of Carstensen and Rabus [2015] under the assumptions (A1)–(A4) and (B2) and (SA) which are proved in Subsections 4.3.2–4.3.5, and the efficiency of Theorem 4.11.

Remark 4.16 (optimal convergence rates for the 3D Stokes problem)**.** The combination of the techniques of Section 3.6 with the techniques of the following subsections prove optimal convergence rates for an adaptive algorithm for 3D driven by the local error estimator contributions

$$\begin{aligned}\lambda^2(\mathcal{T}_\ell,T) &:= \|h_{\mathcal{T}}\operatorname{Curl}_{\mathrm{NC}}\sigma_h\|_{L^2(T)}^2 + h_T\sum_{E\in\mathcal{E}(T)}\|[\sigma_h\wedge\nu_E]_E\|_{L^2(E)}^2,\\ \mu^2(T) &:= \|\operatorname{dev}(\varphi-\Pi_{\Sigma_h(\mathcal{T})}\varphi)\|_{L^2(T)}^2,\end{aligned}$$

where $A\wedge b\in\mathbb{R}^{3\times3}$ is defined, for all $A\in\mathbb{R}^{3\times3}$ and $b\in\mathbb{R}^3$, by

$$A\wedge b := \begin{pmatrix}(A_{1\bullet}\wedge b)^\top\\ (A_{2\bullet}\wedge b)^\top\\ (A_{3\bullet}\wedge b)^\top\end{pmatrix}. \quad \blacklozenge$$

4.3.2. (A1) stability and (A2) reduction

The following two theorems follow from the structure of λ.

Theorem 4.17 (stability)**.** *Let $\mathcal{T}_\star$ be an admissible refinement of $\mathcal{T}$ and $\mathcal{M} \subseteq \mathcal{T} \cap \mathcal{T}_\star$. Let $(\sigma_{\mathcal{T}_\star}, \alpha_{\mathcal{T}_\star}) \in \Sigma_h(\mathcal{T}_\star) \times X_h(\mathcal{T}_\star)$ and $(\sigma_{\mathcal{T}}, \alpha_{\mathcal{T}}) \in \Sigma_h(\mathcal{T}) \times X_h(\mathcal{T})$ be the respective discrete solutions to (4.6). Then,*

$$|\lambda(\mathcal{T}_\star, \mathcal{M}) - \lambda(\mathcal{T}, \mathcal{M})| \lesssim \|\sigma_{\mathcal{T}_\star} - \sigma_{\mathcal{T}}\|_{L^2(\Omega)}.$$

Proof. This follows with triangle inequalities, inverse inequalities and a trace inequality as in Cascon et al. [2008, Proposition 3.3]. ∎

Theorem 4.18. *Let $\mathcal{T}_\star$ be an admissible refinement of $\mathcal{T}$. Then there exists $0 < \rho_2 < 1$ and $\Lambda_2 < \infty$ such that*

$$\lambda^2(\mathcal{T}_\star, \mathcal{T}_\star \setminus \mathcal{T}) \le \rho_2 \lambda^2(\mathcal{T}, \mathcal{T} \setminus \mathcal{T}_\star) + \Lambda_2 \|\sigma_{\mathcal{T}_\star} - \sigma_{\mathcal{T}}\|^2_{L^2(\Omega)}.$$

Proof. This follows with a triangle inequality and the mesh-size reduction property $h^2_{\mathcal{T}_\star}|_T \le h^2_{\mathcal{T}}|_T/2$ for all $T \in \mathcal{T}_\star \setminus \mathcal{T}$ as in Cascon et al. [2008, Corollary 3.4]. ∎

4.3.3. (A4) discrete reliability

Theorem 4.19 (discrete reliability)**.** *Let $\mathcal{T}_\star$ be an admissible refinement of $\mathcal{T}$ with respective discrete solutions $(\sigma_{\mathcal{T}_\star}, \alpha_{\mathcal{T}_\star}) \in X_h(\mathcal{T}_\star) \times Y_h(\mathcal{T}_\star)$ and $(\sigma_{\mathcal{T}}, \alpha_{\mathcal{T}}) \in X_h(\mathcal{T}) \times Y_h(\mathcal{T})$. Then it holds that*

$$\|\sigma_{\mathcal{T}} - \sigma_{\mathcal{T}_\star}\|^2_{L^2(\Omega)} + \|\operatorname{Curl}(\alpha_{\mathcal{T}} - \alpha_{\mathcal{T}_\star})\|^2_{L^2(\Omega)} \lesssim \lambda^2(\mathcal{T}, \mathcal{T} \setminus \mathcal{T}_\star) + \mu^2(\mathcal{T}, \mathcal{T} \setminus \mathcal{T}_\star).$$

Proof. Recall the definition of $W_h(\mathcal{T}_\star)$ from (4.7). There exists a solution $(\Phi_{\mathcal{T}_\star}, r_{\mathcal{T}_\star}) \in W_h(\mathcal{T}_\star) \times X_h(\mathcal{T}_\star)$ of (4.6) with right-hand side $\sigma_{\mathcal{T}} - \sigma_{\mathcal{T}_\star}$. Since $\sigma_{\mathcal{T}} - \sigma_{\mathcal{T}_\star} \in \Sigma_h(\mathcal{T}_\star)$, it holds $\sigma_{\mathcal{T}} - \sigma_{\mathcal{T}_\star} = \Phi_{\mathcal{T}_\star} + \operatorname{dev}\operatorname{Curl} r_{\mathcal{T}_\star}$. The discrete error can be split as

$$\|\sigma_{\mathcal{T}} - \sigma_{\mathcal{T}_\star}\|^2_{L^2(\Omega)} = (\sigma_{\mathcal{T}} - \sigma_{\mathcal{T}_\star}, \Phi_{\mathcal{T}_\star})_{L^2(\Omega)} + (\sigma_{\mathcal{T}} - \sigma_{\mathcal{T}_\star}, \operatorname{dev}\operatorname{Curl} r_{\mathcal{T}_\star})_{L^2(\Omega)}.$$

As in the proof of Theorem 3.43, the projection property, Lemma 4.8, proves

$$(\sigma_{\mathcal{T}} - \sigma_{\mathcal{T}_\star}, \Phi_{\mathcal{T}_\star})_{L^2(\Omega)} \lesssim \big\|\operatorname{dev}(\varphi - \Pi_{\Sigma_h(\mathcal{T})}\varphi)\big\|_{\mathcal{T}\setminus\mathcal{T}_\star} \|\sigma_{\mathcal{T}} - \sigma_{\mathcal{T}_\star}\|_{L^2(\Omega)}.$$

Since the trace of $\sigma_{\mathcal{T}} - \sigma_{\mathcal{T}_\star}$ vanishes,

$$(\sigma_{\mathcal{T}} - \sigma_{\mathcal{T}_\star}, \operatorname{dev}\operatorname{Curl} r_{\mathcal{T}_\star})_{L^2(\Omega)} = (\sigma_{\mathcal{T}} - \sigma_{\mathcal{T}_\star}, \operatorname{Curl} r_{\mathcal{T}_\star})_{L^2(\Omega)}$$

and the arguments of the proof of Theorem 3.43 yield

$$\begin{aligned}
&(\sigma_{\mathcal{T}} - \sigma_{\mathcal{T}_\star}, \operatorname{dev}\operatorname{Curl} r_{\mathcal{T}_\star})_{L^2(\Omega)} \\
&\quad\lesssim \Bigg(\|h_{\mathcal{T}} \operatorname{curl}_{\mathrm{NC}} \sigma_{\mathcal{T}}\|_{\mathcal{T}\setminus\mathcal{T}_\star} \\
&\qquad\qquad + \sqrt{\sum_{E \in \mathcal{E}(\mathcal{T})\setminus\mathcal{E}(\mathcal{T}_\star)} h_E \|[\sigma_{\mathcal{T}} \tau_E]_E\|^2_{L^2(E)}} \Bigg) \|\sigma_{\mathcal{T}} - \sigma_{\mathcal{T}_\star}\|_{L^2(\Omega)}.
\end{aligned}$$ ∎

4.3.4. (A3) quasi-orthogonality

Theorem 4.20 (general quasi-orthogonality). *Let $\mathcal{T}_j$ be some sequence of triangulations with discrete solutions $(\sigma_j, \alpha_j) \in \Sigma_h(\mathcal{T}_j) \times X_h(\mathcal{T}_j)$ of (4.6) and let $\ell \in \mathbb{N}$. Then,*

$$\sum_{j=\ell}^{\infty} \Big(\|\sigma_j - \sigma_{j-1}\|^2 + \|\mathrm{Curl}(\alpha_j - \alpha_{j-1})\|^2 \Big) \lesssim \lambda_{\ell-1}^2 + \mu_{\ell-1}^2.$$

Proof. As in the proof of Theorem 3.44, the projection property, Lemma 4.8, yields for $M \in \mathbb{N}$, $M \geq \ell$,

$$\sum_{j=\ell}^{M} \|\sigma_j - \sigma_{j-1}\|_{L^2(\Omega)}^2 = (\varphi, \sigma_{\ell-1} - \sigma_M)_{L^2(\Omega)} + 2 \sum_{j=\ell}^{M} (\varphi, \sigma_j - \Pi_{\Sigma_h(\mathcal{T}_{j-1})} \sigma_j)_{L^2(\Omega)}.$$

The orthogonality of $\sigma_j - \Pi_{\Sigma_h(\mathcal{T}_{j-1})}\sigma_j$ and $\Sigma_h(\mathcal{T}_{j-1})$ proves as in (3.32)–(3.34)

$$2 \sum_{j=\ell}^{M} (\varphi, \sigma_j - \Pi_{\Sigma_h(\mathcal{T}_{j-1})} \sigma_j)_{L^2(\Omega)} \leq 2\mu_{\ell-1}^2 + \frac{1}{2} \sum_{j=\ell}^{M} \|\sigma_j - \sigma_{j-1}\|_{L^2(\Omega)}^2.$$

The discrete reliability from Theorem 4.19 leads as in (3.36)–(3.37) to

$$(\varphi, \sigma_{\ell-1} - \sigma_M)_{L^2(\Omega)} \lesssim \lambda_{\ell-1}^2 + \mu_{\ell-1}^2.$$

This and a triangle inequality for

$$\mathrm{Curl}(\alpha_j - \alpha_{j-1}) = \Pi_{\Sigma_h(\mathcal{T}_j)} \varphi - \Pi_{\Sigma_h(\mathcal{T}_{j-1})} \varphi - \sigma_j + \sigma_{j-1}$$

eventually yield the assertion. ∎

4.3.5. (B2) data approximation

The following theorem proves quasimonotonicity and sub-additivity of the error estimator μ.

Theorem 4.21 ((B2) quasimonotonicity and (SA) sub-additivity). *Any admissible refinement $\mathcal{T}_\star$ of $\mathcal{T}$ satisfies*

$$\mu^2(\mathcal{T}_\star) \leq \mu^2(\mathcal{T})$$

and

$$\sum_{\substack{T \in \mathcal{T}_\star \\ T \subseteq K}} \mu^2(T) \leq \mu^2(K) \qquad \text{for all } K \in \mathcal{T}.$$

Proof. This follows directly from the definition of μ. ∎

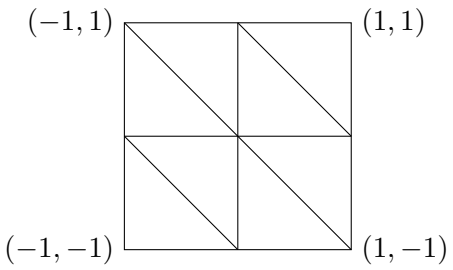

Figure 4.1.: Initial mesh for the square from Subsection 4.4.1.

4.4. Numerical experiments

This section is devoted to three numerical experiments for the Stokes equations. The discretization (4.6) is realized for $k = 0, 1$. As in Section 3.7, the implementation is based on the software package AFEM [Carstensen et al., 2009] maintained at the Humboldt-Universität. The three experiments compare the errors and error estimators on a sequence of uniformly red-refined triangulations (see Figure 3.3 for a red-refined triangle) with the errors and error estimators on a sequence of triangulations created by Algorithm 4.12 with bulk parameter $\theta = 0.1$ and $\kappa = 0.5$ and $\rho = 0.75$.

The convergence history plots are logarithmically scaled and display the error $\|\sigma - \sigma_h\|_{L^2(\Omega)}$ against the number of degrees of freedom of the resulting linear system resulting from the Schur complement (see Remark 3.12).

4.4.1. Colliding flow

Let $\Omega = (-1, 1)^2$. Then

$$u(x, y) = \begin{pmatrix} 20xy^4 - 4x^5 \\ 20x^4y - 4y^5 \end{pmatrix}$$

is the solution to the Stokes problem with right-hand side $f = 0$ and corresponding inhomogeneous Dirichlet boundary conditions. Define

$$u_D(x, y) = \big(1 - (x - 1)(x + 1)(y - 1)(y + 1)\big)\, u(x, y)$$

and $\varphi = 0$. Then $u_D|_{\partial\Omega} = u|_{\partial\Omega}$ and $-\operatorname{div}\varphi = 0$. For non-homogeneous boundary data, the corresponding modification of the weak formulation (4.5) seeks $\sigma \in \Sigma$ and $\alpha \in X$ with

$$\begin{aligned} (\sigma, \tau)_{L^2(\Omega)} + (\tau, \operatorname{Curl}\alpha)_{L^2(\Omega)} &= (\varphi, \tau)_{L^2(\Omega)} && \text{for all } \tau \in \Sigma, \\ (\sigma, \operatorname{Curl}\beta)_{L^2(\Omega)} &= (Du_D, \operatorname{Curl}\beta)_{L^2(\Omega)} && \text{for all } \beta \in X. \end{aligned}$$

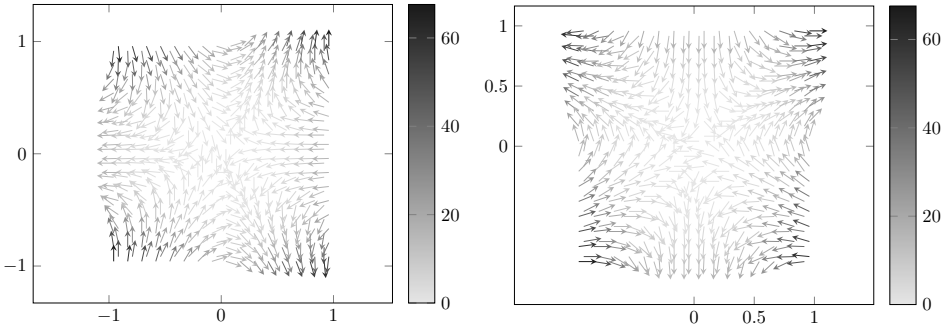

Figure 4.2.: Discrete solution σ_h for $k = 0$ for a uniform mesh with 289 nodes for the experiment from Subsection 4.4.1.

The corresponding discretization seeks $\sigma_h \in \Sigma_h(\mathcal{T})$ and $\alpha_h \in X_h(\mathcal{T})$ with

$$\begin{aligned}(\sigma_h, \tau_h)_{L^2(\Omega)} + (\tau_h, \operatorname{Curl} \alpha_h)_{L^2(\Omega)} &= (\varphi, \tau_h)_{L^2(\Omega)} && \text{for all } \tau_h \in \Sigma_h(\mathcal{T}),\\ (\sigma_h, \operatorname{Curl} \beta_h)_{L^2(\Omega)} &= (Du_D, \operatorname{Curl} \beta_h)_{L^2(\Omega)} && \text{for all } \beta_h \in X_h(\mathcal{T}).\end{aligned}$$

As in Subsection 3.7.2, the jump $[\sigma_h \tau_E]_E$ is defined for boundary edges $E \in \mathcal{E}$, $E \subseteq \partial\Omega$, with adjacent triangle T_+ by

$$[\sigma_h \tau_E]_E := \sigma_h|_{T_+} \tau_E - Du_D \tau_E$$

and λ is then defined by (4.12)–(4.13). The local data error estimator contributions read

$$\mu^2(T) := \|\operatorname{dev}((\varphi - Du_D) - \Pi_{\Sigma_h(\mathcal{T})}(\varphi - Du_D))\|^2_{L^2(T)}.$$

The global error estimator μ is defined by (4.13), while $\eta = \sqrt{\mu^2 + \lambda^2}$.

The initial triangulation $\mathcal{T}_0$ for the adaptive algorithm 4.12 is depicted in Figure 4.1. The discrete solution $\sigma_h \in P_0(\mathcal{T}; \mathbb{R}^{2\times 2})$ is displayed in Figure 4.2. The error $\|\sigma - \sigma_h\|_{L^2(\Omega)}$, the pressure error $\|p - p_h\|_{L^2(\Omega)}$ with

$$p_h := -(1/2)\operatorname{tr}(\Pi_{\Sigma_h(\mathcal{T})}\varphi - \operatorname{Curl} \alpha_h)$$

and p defined as in Remark 4.5, and the error estimator η are plotted in Figure 4.3 against the number of degrees of freedom. They show a convergence rate of $\texttt{ndof}^{1/2}$ and $\texttt{ndof}$ for $k = 0$ and $k = 1$, respectively, for adaptive as well as for uniform mesh-refinement. Since the solution is smooth, this is what Corollary 4.7 predicts. Figure 4.4 depicts triangulations with approximately 1500 degrees of freedom created by the adaptive algorithm for $k = 0, 1$. The refinement is almost uniform. The adaptive algorithm only applied the marking with respect to λ ($\mu_\ell^2 \leq \kappa \lambda_\ell^2$).

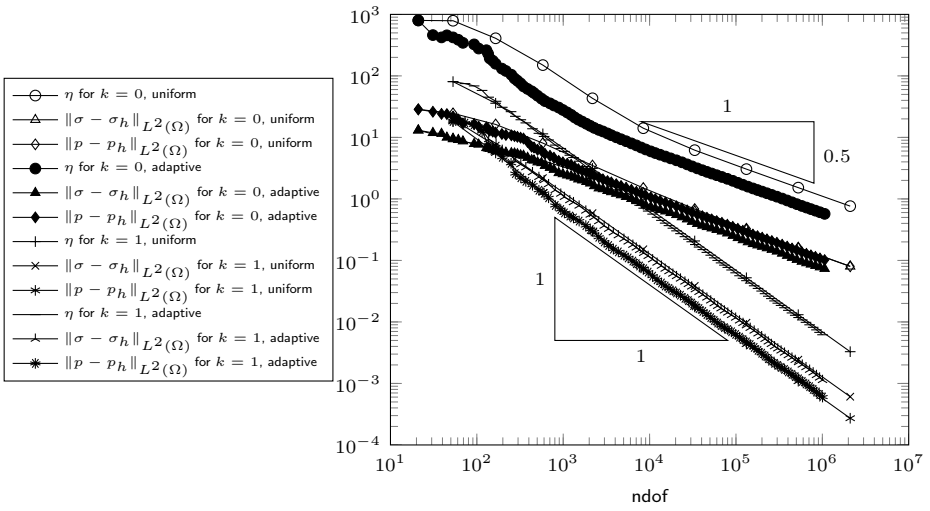

Figure 4.3.: Errors and error estimators for the colliding flow experiment from Subsection 4.4.1.

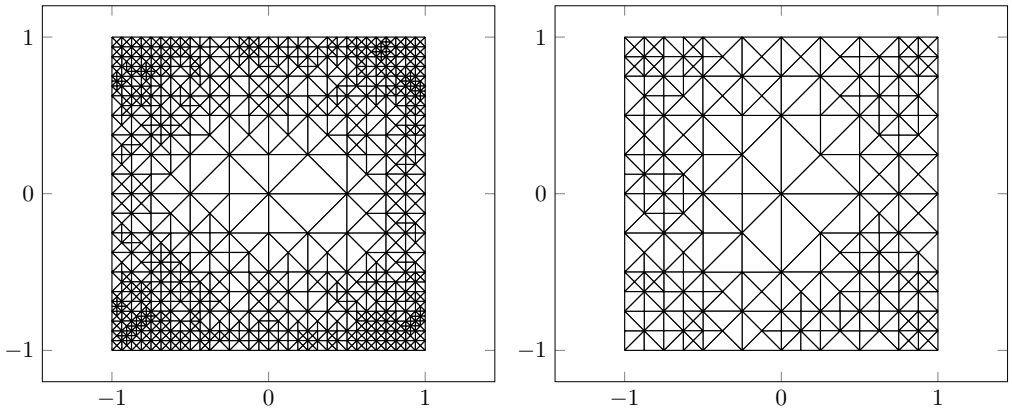

Figure 4.4.: Adaptively refined triangulations for $k = 0$ with 829 nodes (1661 dofs) and for $k = 1$ with 203 nodes (1529 dofs) for the colliding flow experiment from Subsection 4.4.1.

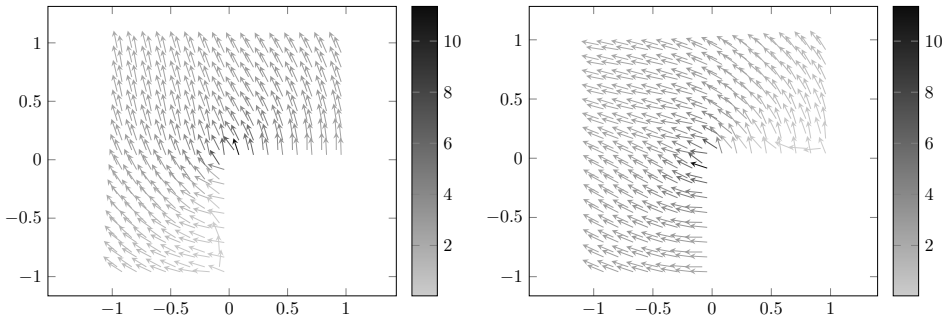

Figure 4.5.: Discrete solution σ_h for $k = 0$ for a uniform mesh with 225 nodes for the experiment from Subsection 4.4.2.

4.4.2. L-shaped domain

On the L-shaped domain $\Omega = ((-1,1) \times (-1,1)) \setminus ([0,1] \times [-1,0])$ with initial triangulation $\mathcal{T}_0$ from Figure 3.4b, the exact solution for the right-hand side $f = 0$ and corresponding Dirichlet boundary conditions reads

$$u(r,\vartheta) = \begin{pmatrix} r^\alpha((1+\alpha)\sin(\vartheta)w(\vartheta) + \cos(\vartheta)w_\vartheta(\vartheta)) \\ r^\alpha(-(1+\alpha)\cos(\vartheta)w(\vartheta) + \sin(\vartheta)w_\vartheta(\vartheta)) \end{pmatrix}$$

in polar coordinates with $\alpha = 0.54448373$ and

$$\begin{aligned} w(\vartheta) =& (\sin((1+\alpha)\vartheta)\cos(\alpha\omega))/(1+\alpha) - \cos((1+\alpha)\vartheta) \\ & - (\sin((1-\alpha)\vartheta)\cos(\alpha\omega))/(1-\alpha) + \cos((1-\alpha)\vartheta). \end{aligned}$$

Define

$$u_D(x,y) = \big(1 - x(x-1)(x+1)y(y-1)(y+1)\big)\, u(x,y)$$

and $\varphi = 0$. Then $u_D|_{\partial\Omega} = u|_{\partial\Omega}$.

The discrete solution $\sigma_h \in P_0(\mathcal{T};\mathbb{R}^{2\times 2})$ is depicted in Figure 4.5. The errors and error estimators for $k = 0, 1$ are plotted in Figure 4.6 against the number of degrees of freedom. For uniform refinement, the errors and error estimators show a convergence rate of $h^{1/2} \approx \texttt{ndof}^{1/4}$. The error $\|\sigma - \sigma_h\|_{L^2(\Omega)}$ for $k = 1$ lies even above the error $\|\sigma - \sigma_h\|_{L^2(\Omega)}$ for $k = 0$. Note that the saddle-point structure implies that this does not contradict the conformity of the method. The adaptive refinement leads to an optimal convergence rate of $\texttt{ndof}^{(k+1)/2}$. Figure 4.7 depicts triangulations with approximately 1500 degrees of freedom created by the adaptive algorithm for $k = 0, 1$. The singularity of u leads to a strong refinement towards the re-entrant corner. The marking with respect to the data-approximation ($\mu_\ell^2 > \kappa\lambda_\ell^2$ in Algorithm 4.12) is only applied at the first three refinements for $k = 0$. All other marking steps for $k = 0, 1$ used the Dörfler marking ($\mu_\ell^2 \leq \kappa\lambda_\ell^2$).

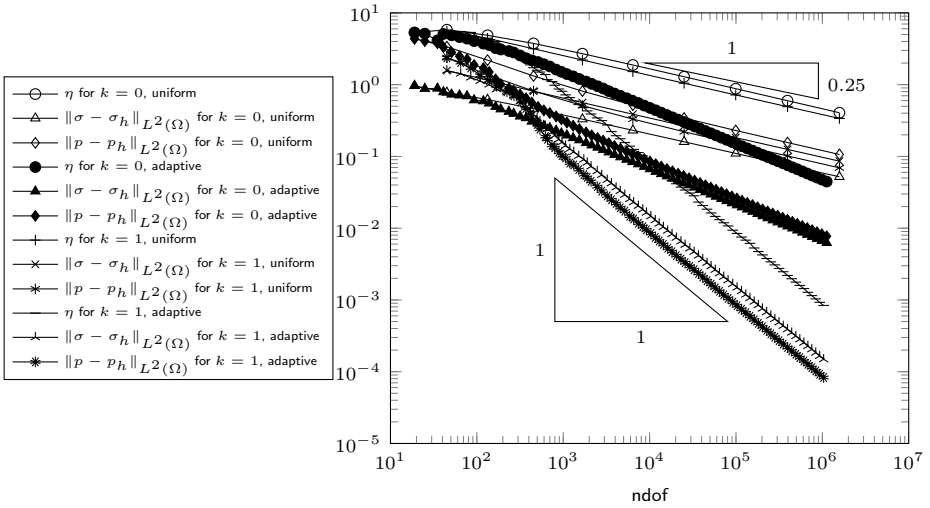

Figure 4.6.: Errors and error estimators for the experiment on the L-shaped domain from Subsection 4.4.2.

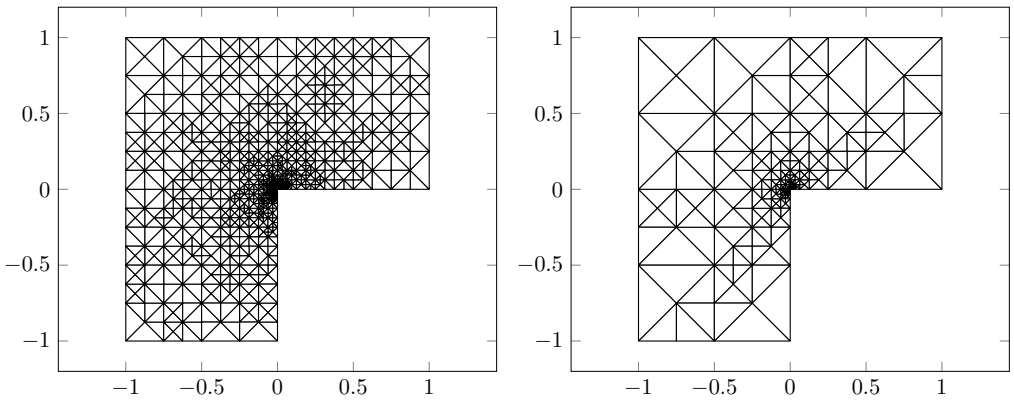

Figure 4.7.: Adaptively refined triangulations for $k = 0$ with 767 nodes (1537 dofs) and for $k = 1$ with 199 nodes (1513 dofs) for the numerical experiment on the L-shaped domain from Subsection 4.4.2.

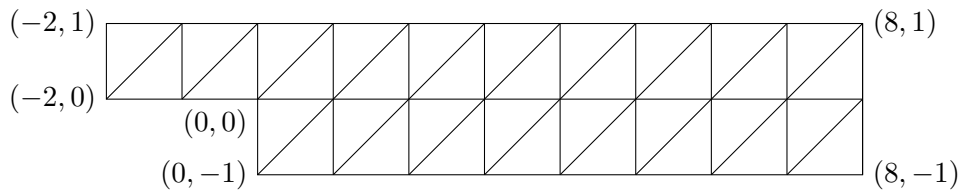

Figure 4.8.: Initial mesh of the backward-facing step from Subsection 4.4.3.

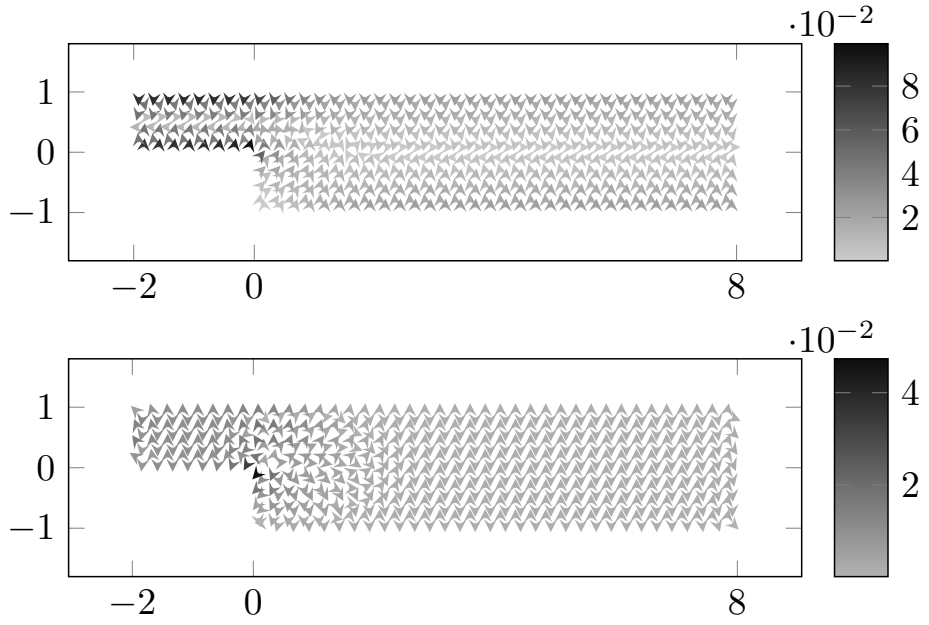

Figure 4.9.: Discrete solution σ_h for $k = 0$ for a uniform mesh with 337 nodes for the experiment from Subsection 4.4.3.

4.4.3. Backward-facing step

This benchmark example considers the domain $\Omega = ((-2, 8) \times (-1, 1)) \setminus ([-2, 0] \times [-1, 0])$ with initial mesh from Figure 4.8 with volume force $f = 0$ and Dirichlet data u_D defined by

$$u_D|_{\partial\Omega}(x, y) = \begin{cases} (0, 0) & \text{if } -2 < x < 8, \\ (-y(y-1)/10, 0) & \text{if } x = -2, \\ (-(y+1)(y-1)/80, 0) & \text{if } x = 8. \end{cases}$$

The extension

$$u_D(x, y) = \begin{cases} (-x^2 y(y-1)/40, 0) & \text{if } x < 0, \\ (-x^2(y+1)(y-1)/5120, 0) & \text{if } x > 0 \end{cases}$$

of u_D to Ω and $\varphi = 0$ are chosen for the numerical computations.

The solution $\sigma_h \in P_0(\mathcal{T}; \mathbb{R}^{2\times 2})$ is depicted in Figure 4.9. The error estimators for $k = 0, 1$ are plotted in Figure 4.10 against the number of degrees of freedom. For uniform refinement and $k = 0$, the error estimator η shows a convergence rate of $h^{4/5} \approx \texttt{ndof}^{2/5}$. The error estimator for $k = 1$ shows a convergence rate of $h^{2/3} \approx \texttt{ndof}^{1/3}$ for uniform refinements. Since this is the expected convergence rate for the interior angle of $3\pi/2$ at the re-entrant corner for $k = 0, 1$, the better convergence

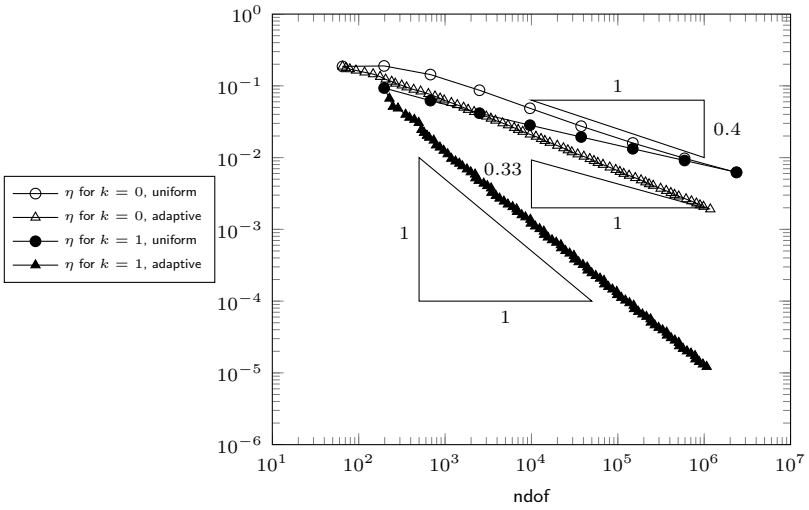

Figure 4.10.: Error estimators for the backward facing step experiment from Subsection 4.4.3.

rate for $k = 0$ is possibly a preasymptotic effect. This convergence rate for a first-order method was also observed for a pseudostress approach in [Carstensen, Gallistl, and Schedensack, 2013a]. The adaptive refinement leads to optimal convergence rates of $\texttt{ndof}^{(k+1)/2}$. Figure 4.11 depicts triangulations with approximately 1500 degrees of freedom created by the adaptive algorithm for $k = 0, 1$. The singularity of u leads to a strong refinement towards the re-entrant corner. The marking with respect to the data-approximation ($\mu_\ell^2 > \kappa\lambda_\ell^2$ in Algorithm 4.12) is applied at the levels 25, 31, 37, 41, 47, 52, 58, 64, 69, 75, 80, and 85 for $k = 1$. All other marking steps for $k = 0, 1$ used the Dörfler marking ($\mu_\ell^2 \leq \kappa\lambda_\ell^2$).

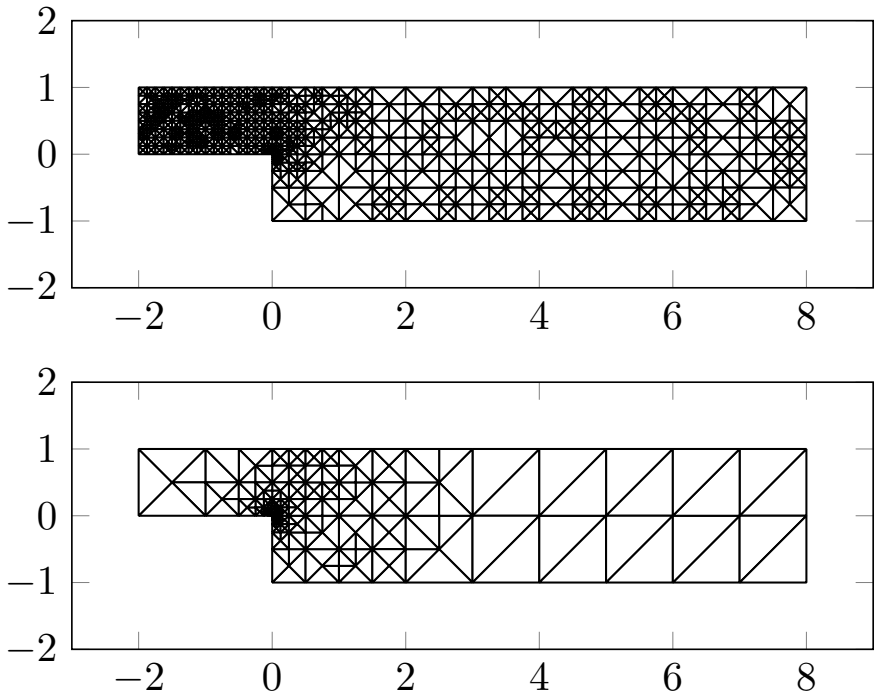

Figure 4.11.: Adaptively refined triangulations for $k = 0$ with 818 nodes (1639 dofs) and for $k = 1$ with 211 nodes (1585 dofs) for the numerical experiment for the backward-facing step from Subsection 4.4.3.

5. Linear elasticity and Stokes equations with symmetric gradient

This chapter considers the Navier-Lamé equations of linear elasticity and the Stokes equations with the symmetric part of the gradient. After some preliminary remarks in Section 5.1, Sections 5.2 and 5.3 introduce the novel weak formulation for the Navier-Lamé equations based on a Helmholtz decomposition from Carstensen and Dolzmann [1998] and its discretizations. Section 5.4 is devoted to the a posteriori error analysis of the discretizations. Section 5.5 discusses the approximation of the symmetric part of the gradient in the Stokes problem with Neumann boundary conditions. Section 5.6 concludes this chapter with numerical experiments for linear elasticity.

Throughout this chapter $\Omega \subseteq \mathbb{R}^2$ is a simply connected, bounded, polygonal Lipschitz domain. The analysis in this chapter also considers almost incompressible materials; the constants hidden in $\lesssim, \gtrsim, \approx$ are independent of the Lamé parameter λ.

5.1. Preliminary remark

This section recursively applies Brezzi's splitting lemma, Theorem 2.8, to prove existence of solutions of problems of the form (5.1) defined below. Given some Hilbert spaces $(\Sigma, \|\bullet\|_\Sigma)$, $(X, \|\bullet\|_X)$, $(Y, \|\bullet\|_Y)$, bilinear forms

$$a : \Sigma \times \Sigma \to \mathbb{R}, \qquad b : \Sigma \times X \to \mathbb{R}, \qquad c : X \times Y \to \mathbb{R},$$

and $F \in \Sigma^\star$, $G \in X^\star$, $H \in Y^\star$, seek $(\sigma, \alpha, \chi) \in \Sigma \times X \times Y$ with

$$\begin{aligned} a(\sigma,\tau) + b(\tau,\alpha) &= F(\tau) && \text{for all } \tau \in \Sigma, \\ b(\sigma,\beta) + c(\beta,\chi) &= G(\beta) && \text{for all } \beta \in X, \\ c(\alpha,\xi) &= H(\xi) && \text{for all } \xi \in Y. \end{aligned} \tag{5.1}$$

Proposition 5.1 (existence of solutions)**.** *If a, b, c are continuous, a is elliptic and b and c fulfil the inf-sup conditions*

$$\|\beta\|_X \lesssim \sup_{\tau \in \Sigma\setminus\{0\}} \frac{b(\tau,\beta)}{\|\tau\|_\Sigma} \qquad \textit{for all } \beta \in X,$$

$$\|\xi\|_Y \lesssim \sup_{\beta \in X\setminus\{0\}} \frac{c(\beta,\xi)}{\|\beta\|_X} \qquad \textit{for all } \xi \in Y,$$

then (5.1) *has a unique solution. Furthermore, the mapping* $(F, G, H) \mapsto (\sigma, \alpha, \chi)$ *is an isomorphism and*

$$\|\sigma\|_\Sigma + \|\alpha\|_X + \|\chi\|_Y \lesssim \|F\|_{\Sigma^\star} + \|G\|_{X^\star} + \|H\|_{Y^\star}.$$

Proof. The continuity of a and b, the ellipticity of a, and the inf-sup condition of b together with Theorem 2.8 imply that $\mathcal{B}_1 : (\Sigma \times X) \times (\Sigma \times X) \to \mathbb{R}$, defined by

$$\mathcal{B}_1((\sigma, \alpha), (\tau, \beta)) := a(\sigma, \tau) + b(\tau, \alpha) + b(\sigma, \beta) \qquad \text{for all } (\sigma, \alpha), (\tau, \beta) \in \Sigma \times X,$$

fulfils the inf-sup conditions

$$(\|\sigma\|_\Sigma + \|\alpha\|_X) \lesssim \sup_{(\tau,\beta)\in(\Sigma\times X)\setminus\{0\}} \frac{\mathcal{B}_1((\sigma, \alpha), (\tau, \beta))}{(\|\tau\|_\Sigma + \|\beta\|_X)} \qquad \text{for all } \sigma \in \Sigma, \alpha \in X,$$

$$(\|\tau\|_\Sigma + \|\beta\|_X) \lesssim \sup_{(\sigma,\alpha)\in(\Sigma\times X)\setminus\{0\}} \frac{\mathcal{B}_1((\sigma, \alpha), (\tau, \beta))}{(\|\sigma\|_\Sigma + \|\alpha\|_X)} \qquad \text{for all } \tau \in \Sigma, \beta \in X.$$

Define $\widetilde{c} : (\Sigma \times X) \times Y \to \mathbb{R}$ and $\widetilde{F} \in (\Sigma \times X)^\star$ by

$$\begin{aligned} \widetilde{c}((\tau, \beta), \xi) &:= c(\beta, \xi) && \text{for all } \tau \in \Sigma, \beta \in X, \xi \in Y, \\ \widetilde{F}(\tau, \beta) &:= F(\tau) + G(\beta) && \text{for all } \tau \in \Sigma, \beta \in X. \end{aligned}$$

The inf-sup condition of c yields the inf-sup condition

$$\|\xi\|_Y \lesssim \sup_{(\tau,\beta)\in(\Sigma\times X)\setminus\{0\}} \frac{\widetilde{c}((\tau, \beta), \xi)}{\|\tau\|_\Sigma + \|\beta\|_X}$$

for $\widetilde{c}$. The repeated application of Theorem 2.8 implies that the system

$$\begin{aligned} \mathcal{B}_1((\sigma, \alpha), (\tau, \beta)) + \widetilde{c}((\tau, \beta), \chi) &= \widetilde{F}(\tau, \beta) && \text{for all } \tau \in \Sigma, \beta \in X \\ \widetilde{c}((\sigma, \alpha), \xi) &= H(\xi) && \text{for all } \xi \in Y \end{aligned}$$

has a unique solution and $(\widetilde{F}, H) \mapsto (\sigma, \alpha, \chi)$ is an isomorphism. Since this system equals (5.1), this concludes the proof. ∎

5.2. Weak formulation

Given the simply connected, bounded, polygonal Lipschitz domain $\Omega \subseteq \mathbb{R}^2$ and the volume force $f \in L^2(\Omega; \mathbb{R}^2)$, the linear elasticity problem seeks the displacement $u \in H^1_0(\Omega; \mathbb{R}^2)$ and the stress $\sigma \in H(\operatorname{div}, \Omega; \mathbb{R}^{2\times 2})$ with

$$\begin{aligned} -\operatorname{div} \sigma &= f && \text{in } \Omega, \\ \sigma &= \mathbb{C}\varepsilon(u) && \text{in } \Omega, \\ u &= 0 && \text{on } \partial\Omega. \end{aligned} \tag{5.2}$$

The linear Green strain is defined by $\varepsilon(u) := (Du + Du^\top)/2$ and the fourth-order elasticity tensor acts as $\mathbb{C}A = 2\mu A + \lambda \mathrm{tr}(A) I_{2\times 2}$ for Lamé parameters $\mu > 0$ and $\lambda > 0$. Define the spaces

$$\begin{aligned} \Sigma &:= L^2(\Omega;\mathbb{R}^{2\times 2}), \\ X &:= \left\{ v \in H^1(\Omega;\mathbb{R}^2) \,\middle|\, \int_\Omega v\,dx = 0 \text{ and } \int_\Omega \operatorname{curl} v\,dx = 0 \right\}, \\ Z &:= \{v \in X \mid \operatorname{Curl} v \in L^2(\Omega;\mathbb{S})\} = \{v \in X \mid \operatorname{div} v = 0\}, \\ L^2(\Omega;\mathbb{S})/\mathbb{R} &:= \left\{ \tau \in L^2(\Omega;\mathbb{S}) \,\middle|\, \int_\Omega \operatorname{tr}(\tau)\,dx = 0 \right\} \end{aligned} \tag{5.3}$$

and the scalar product $(\sigma,\tau)_{\mathbb{C}^{-1/2}} := (\sigma, \mathbb{C}^{-1}\tau)_{L^2(\Omega)}$ for $\sigma,\tau \in \Sigma$. Note that $\operatorname{Curl} v$ is symmetric if and only if $\operatorname{div} v = 0$.

The following theorem states a Helmholtz decomposition for symmetric vector fields and is already proved by Carstensen and Dolzmann [1998]. Recall that $\Omega \subseteq \mathbb{R}^2$ is a simply connected, bounded, polygonal Lipschitz domain.

Theorem 5.2 (Helmholtz decomposition for symmetric vector fields)**.** *It holds that*

$$L^2(\Omega;\mathbb{S})/\mathbb{R} = \varepsilon(H^1_0(\Omega;\mathbb{R}^2)) \oplus \operatorname{Curl} Z \tag{5.4}$$

and the sum is orthogonal with respect to the L^2 scalar product, or, equivalently,

$$L^2(\Omega;\mathbb{S})/\mathbb{R} = \mathbb{C}\varepsilon(H^1_0(\Omega;\mathbb{R}^2)) \oplus \operatorname{Curl} Z$$

and the sum is orthogonal with respect to $(\bullet,\bullet)_{\mathbb{C}^{-1/2}}$. ∎

Let $\varphi \in H(\operatorname{div},\Omega;\mathbb{S})$ with $\int_\Omega \operatorname{tr}\varphi\,dx = 0$ and $-\operatorname{div}\varphi = f$. Define the bilinear forms

$$\begin{aligned} a(\tau,\sigma) &:= (\mathbb{C}^{-1}\tau,\sigma)_{L^2(\Omega)} && \text{for all } \tau,\sigma \in \Sigma, \\ b(\tau,\beta) &:= (\mathbb{C}^{-1}\tau, \operatorname{Curl}\beta)_{L^2(\Omega)} && \text{for all } \tau \in \Sigma, \beta \in X \end{aligned} \tag{5.5}$$

and the norm $\| \bullet \|_{\mathbb{C}^{-1/2}} := \sqrt{a(\bullet,\bullet)}$. Consider the problem: Seek $(\sigma,\alpha) \in \Sigma \times Z$ with

$$\begin{aligned} a(\tau,\sigma) + b(\tau,\alpha) &= (\varphi, \mathbb{C}^{-1}\tau)_{L^2(\Omega)} && \text{for all } \tau \in \Sigma, \\ b(\sigma,\beta) &= 0 && \text{for all } \beta \in Z. \end{aligned} \tag{5.6}$$

The following lemma proves the inf-sup condition for b.

Lemma 5.3 (inf-sup condition for b)**.** *Any $\beta \in X$ satisfies*

$$\|\operatorname{Curl}\beta\|_{L^2(\Omega)} \lesssim \sup_{\tau\in\Sigma\setminus\{0\}} \frac{b(\tau,\beta)}{\|\tau\|_{\mathbb{C}^{-1/2}}}.$$

Proof. The crucial point in this inf-sup condition is that the constant hidden in $\lesssim$ is independent of the Lamé parameter λ. Let $\beta \in X$. Proposition 4.1 proves

$$\|\operatorname{Curl}\beta\|_{L^2(\Omega)} \lesssim \|\operatorname{dev}(\operatorname{Curl}\beta)\|_{L^2(\Omega)}.$$

A computation reveals

$$\mathbb{C}^{-1}A = \frac{1}{2\mu}\mathrm{dev}(A) + \frac{1}{4(\lambda+\mu)}\mathrm{tr}(A)I_{2\times 2}. \tag{5.7}$$

This implies

$$\|\mathrm{Curl}\,\beta\|_{L^2(\Omega)} \lesssim \|\mathrm{Curl}\,\beta\|_{\mathbb{C}^{-1/2}}\,. \tag{5.8}$$

With the choice $\tau := \mathrm{Curl}\,\beta$, this proves the inf-sup condition of b. ∎

Proposition 5.4 (solutions to (5.6)). *There exists a unique solution $(\sigma,\alpha)\in\Sigma\times Z$ to (5.6) and it satisfies $\sigma = \mathbb{C}\varepsilon(u)$ for the solution $u\in H^1_0(\Omega;\mathbb{R}^2)$ to (5.2).*

Proof. Since a is elliptic with respect to $\|\bullet\|_{\mathbb{C}^{-1/2}}$ and b fulfils the inf-sup condition of Lemma 5.3, Theorem 2.8 implies the unique existence of a solution $(\sigma,\alpha)\in\Sigma\times Z$ of (5.6). The Helmholtz decomposition of Theorem 5.2 guarantees the existence of $\widetilde{u}\in H^1_0(\Omega;\mathbb{R}^2)$ with $\sigma = \mathbb{C}\varepsilon(\widetilde{u})$. Problem (5.6) and the symmetry of φ and $\mathrm{Curl}\,\alpha$ imply, for all $v\in H^1_0(\Omega;\mathbb{R}^2)$, that

$$\begin{aligned}(\mathbb{C}\varepsilon(\widetilde{u}),\varepsilon(v))_{L^2(\Omega)} &= (\varphi,\varepsilon(v))_{L^2(\Omega)} - (\varepsilon(v),\mathrm{Curl}\,\alpha)_{L^2(\Omega)}\\ &= (\varphi,Dv)_{L^2(\Omega)} - (Dv,\mathrm{Curl}\,\alpha)_{L^2(\Omega)}\\ &= (\varphi,Dv)_{L^2(\Omega)} = (f,v)_{L^2(\Omega)}.\end{aligned}$$

Hence, $\widetilde{u}$ solves (5.2). ∎

A conforming discretization of Z with piecewise smooth functions would involve the restriction $\mathrm{div}\,\bullet = 0$ pointwise. This leads to complicated finite element methods as in [Scott and Vogelius, 1985, Guzmán and Neilan, 2014]. Therefore, it seems useful to include the divergence-free constraint in the mixed formulation. To this end, define the space

$$Y := L^2_0(\Omega)$$

and the bilinear form

$$c(\xi,\beta) := (\xi,\mathrm{div}\,\beta)_{L^2(\Omega)} \qquad \text{for all } \xi\in Y,\beta\in X. \tag{5.9}$$

Consider the problem: Seek $(\sigma,\alpha,\chi)\in\Sigma\times X\times Y$ with

$$\begin{aligned} a(\tau,\sigma)+b(\tau,\alpha) &= (\varphi,\mathbb{C}^{-1}\tau) && \text{for all } \tau\in\Sigma,\\ b(\sigma,\beta)+c(\chi,\beta) &= 0 && \text{for all } \beta\in X,\\ c(\xi,\alpha) &= 0 && \text{for all } \xi\in Y.\end{aligned} \tag{5.10}$$

Since $\|\mathrm{Curl}\,\beta\|_{L^2(\Omega)} = \|D\beta\|_{L^2(\Omega)}$, the inf-sup condition for c,

$$\|\xi\|_{L^2(\Omega)} \lesssim \sup_{\beta\in X\setminus\{0\}} \frac{c(\xi,\beta)}{\|\mathrm{Curl}\,\beta\|_{L^2(\Omega)}} \qquad \text{for all } \xi\in Y$$

is the standard inf-sup condition for the Stokes equations [Girault and Raviart, 1986].

The following theorem proves the equivalence of (5.6) and (5.10). It is a consequence of the theory of Lagrange multipliers [Zeidler, 1985] and, together with Proposition 5.4, implies the existence of a unique solution $(\sigma, \alpha, \chi) \in \Sigma \times X \times Y$ to (5.10).

Theorem 5.5. *Problems* (5.6) *and* (5.10) *are equivalent in the sense that* $(\sigma, \alpha) \in \Sigma \times X$ *is a solution to* (5.6) *if and only if there exists* $\chi \in Y$ *such that* $(\sigma, \alpha, \chi) \in \Sigma \times X \times Y$ *is a solution to* (5.10).

Proof. If (σ, α, χ) is a solution to (5.10), then it is clear that (σ, α) solves (5.6).

For the converse direction, let (σ, α) be a solution of (5.6). Since $\alpha \in Z$, it remains to show the existence of $\chi \in Y$ such that the second equation of (5.10) is fulfilled. Define $A : X \to Y$, $A\beta := \Pi_Y \operatorname{div} \beta$ and $B : X \to \mathbb{R}$, $B\beta := (\mathbb{C}^{-1}\sigma, \operatorname{Curl} \beta)$. If $\beta \in X$ with $A\beta = 0$, then $(q, \operatorname{div} \beta) = (q, \Pi_Y \operatorname{div} \beta) = 0$ for all $q \in Y$ and, since $\int_\Omega \operatorname{div} \beta \, dx = 0$, it follows $\operatorname{div} \beta = 0$ and therefore $\beta \in Z$. The problem (5.6) implies $B\beta = 0$. Hence, [Zeidler, 1985, Proposition 43.1] implies the existence of $\chi \in Y^\star \equiv Y$ such that, for all $\gamma \in X$,

$$\begin{aligned} 0 = B\gamma + \chi(A\gamma) &\equiv (\mathbb{C}^{-1}\sigma, \operatorname{Curl} \gamma) + (\chi, \Pi_Y \operatorname{div} \gamma) \\ &= (\mathbb{C}^{-1}\sigma, \operatorname{Curl} \gamma) + (\chi, \operatorname{div} \gamma). \end{aligned}$$

∎

Remark 5.6. The meaning of the variable χ is that $\chi = \operatorname{curl} u/2$ for the solution $u \in H^1_0(\Omega; \mathbb{R}^2)$ to (5.2): Since $\operatorname{div} \beta$ determines the antisymmetric part of $\operatorname{Curl} \beta$, the second equality of (5.10) reads

$$\left(\mathbb{C}^{-1}\sigma + \chi \begin{pmatrix} 0 & 1 \\ -1 & 0 \end{pmatrix}, \operatorname{Curl} \beta \right) = 0 \qquad \text{for all } \beta \in X,$$

which is equivalent to the fact that $\mathbb{C}^{-1}\sigma + \chi(0, 1; -1, 0)$ is a derivative and χ determines its antisymmetric part. ♦

Remark 5.7 (more general boundary conditions)**.** Let $\partial\Omega = \Gamma_D \cup \Gamma_N$ with closed Dirichlet boundary $\Gamma_D \neq \emptyset$ and Neumann boundary $\Gamma_N = \partial\Omega \setminus \Gamma_D \neq \emptyset$. The linear elasticity problem with mixed boundary conditions reads

$$\begin{aligned} -\operatorname{div} \sigma &= f && \text{in } \Omega, \\ \sigma &= \mathbb{C}\varepsilon(u) && \text{in } \Omega, \\ \sigma\nu &= g && \text{on } \Gamma_N, \\ u &= u_D && \text{on } \Gamma_D. \end{aligned}$$

The procedure of Section 3.2.1 leads to the modified spaces

$$\begin{aligned} X_{\Gamma_N} &:= \{v \in H^1(\Omega; \mathbb{R}^2) \mid v \text{ is constant on each connectivity component of } \Gamma_N\}, \\ Z_{\Gamma_N} &:= \{v \in X_{\Gamma_N} \mid \operatorname{div} v = 0\}. \end{aligned}$$

Let $\varphi \in H(\operatorname{div}, \Omega; \mathbb{S})$ with $-\operatorname{div}\varphi = f$ additionally fulfil $(\varphi\nu)|_{\Gamma_N} = g$. Then the solution of the linear elasticity problem with mixed boundary conditions is equivalent to

$$\begin{aligned} a(\tau,\sigma) + b(\tau,\alpha) &= (\varphi, \mathbb{C}^{-1}\tau)_{L^2(\Omega)} && \text{for all } \tau \in \Sigma, \\ b(\sigma,\beta) &= (Du_D, \operatorname{Curl}\beta)_{L^2(\Omega)} && \text{for all } \beta \in Z_{\Gamma_N}, \end{aligned}$$

or equivalently

$$\begin{aligned} a(\tau,\sigma) + b(\tau,\alpha) &= (\varphi, \mathbb{C}^{-1}\tau)_{L^2(\Omega)} && \text{for all } \tau \in \Sigma, \\ b(\sigma,\beta) + c(\chi,\beta) &= (Du_D, \operatorname{Curl}\beta)_{L^2(\Omega)} && \text{for all } \beta \in X_{\Gamma_N}, \\ c(\xi,\alpha) &= 0 && \text{for all } \xi \in Y. \end{aligned}$$

The unique existence of solutions remains true for these boundary conditions. ♦

5.3. Discretizations

This section introduces robust discretizations of (5.10). Since the discrete inf-sup condition for the bilinear form c of (5.9) is the same as for a standard Stokes discretization, the following discretizations of X and Y employ well-known Stokes finite elements [Boffi et al., 2013], namely the Mini FEM in Subsection 5.3.2, the Taylor-Hood FEM in Subsection 5.3.3, and the $P_2\,P_0$ FEM in Subsection 5.3.4. Subsection 5.3.5 discusses the non-conforming FEM of Kouhia and Stenberg [1995] in this context.

5.3.1. Abstract discretizations

Recall the bilinear forms a, b, c from (5.5) and (5.9). Let $\Sigma_h(\mathcal{T}) \subseteq \Sigma$, $X_h(\mathcal{T}) \subseteq X$, and $Y_h(\mathcal{T}) \subseteq Y$ be some (finite dimensional) closed subspaces of Σ, X, Y. Then the discretization of (5.10) seeks $(\sigma_h, \alpha_h, \xi_h) \in \Sigma_h(\mathcal{T}) \times X_h(\mathcal{T}) \times Y_h(\mathcal{T})$ such that

$$\begin{aligned} a(\tau_h,\sigma_h) + b(\tau_h,\alpha_h) &= (\varphi, \mathbb{C}^{-1}\tau_h)_{L^2(\Omega)} && \text{for all } \tau_h \in \Sigma_h(\mathcal{T}), \\ b(\sigma_h,\beta_h) + c(\chi_h,\beta_h) &= 0 && \text{for all } \beta_h \in X_h(\mathcal{T}), \\ c(\xi_h,\alpha_h) &= 0 && \text{for all } \xi_h \in Y_h(\mathcal{T}). \end{aligned} \tag{5.11}$$

Assume now that $\operatorname{Curl} X_h(\mathcal{T}) \subseteq \Sigma_h(\mathcal{T})$ and that $X_h(\mathcal{T})$ and $Y_h(\mathcal{T})$ fulfil the discrete inf-sup condition

$$\|\xi_h\|_{L^2(\Omega)} \lesssim \sup_{\beta_h \in X_h(\mathcal{T})\setminus\{0\}} \frac{c(\xi_h,\beta_h)}{\|\operatorname{Curl}\beta_h\|_{L^2(\Omega)}} \qquad \text{for all } \xi_h \in Y_h(\mathcal{T}). \tag{5.12}$$

Theorem 5.8 (a priori error estimate)**.** *Problem* (5.11) *has a unique solution* $(\sigma_h, \alpha_h, \xi_h) \in \Sigma_h(\mathcal{T}) \times X_h(\mathcal{T}) \times Y_h(\mathcal{T})$ *and it satisfies*

$$\begin{aligned}\|\sigma - \sigma_h\|_{\mathbb{C}^{-1/2}} + \|\mathrm{Curl}(\alpha - \alpha_h)\|_{L^2(\Omega)} + \|\chi - \chi_h\|_{L^2(\Omega)} \\ \lesssim \inf_{\substack{\tau_h \in \Sigma_h(\mathcal{T}),\\ \beta_h \in X_h(\mathcal{T}),\\ \xi_h \in Y_h(\mathcal{T})}} \Big(\|\sigma - \tau_h\|_{\mathbb{C}^{-1/2}} + \|\mathrm{Curl}(\alpha - \beta_h)\|_{L^2(\Omega)} + \|\chi - \xi_h\|_{L^2(\Omega)} \Big).\end{aligned}$$

Proof. The bilinear form a is continuous and elliptic with respect to $\|\bullet\|_{\mathbb{C}^{-1/2}}$. The Cauchy inequality yields for $\tau_h \in \Sigma_h(\mathcal{T})$ and $\beta_h \in X_h(\mathcal{T})$

$$\begin{aligned} b(\tau_h, \beta_h) &= (\mathbb{C}^{-1}\tau_h, \mathrm{Curl}\,\beta_h)_{L^2(\Omega)} \\ &\le \|\tau_h\|_{\mathbb{C}^{-1/2}} \|\mathrm{Curl}\,\beta_h\|_{\mathbb{C}^{-1/2}} \\ &\lesssim \|\tau_h\|_{\mathbb{C}^{-1/2}} \|\mathrm{Curl}\,\beta_h\|_{L^2(\Omega)}, \end{aligned}$$

where the last inequality follows from $A : \mathbb{C}^{-1}A \lesssim A : A$ for all $A \in \mathbb{R}^{2\times 2}$ (cf. (5.7)). This proves the continuity of b with respect to $\|\bullet\|_{\mathbb{C}^{-1/2}}$ and $\|\mathrm{Curl}\,\bullet\|_{L^2(\Omega)}$. For given $\beta_h \in X_h(\mathcal{T}) \setminus \{0\}$, define $\tau_h := \mathrm{Curl}\,\beta_h$. Since $\mathrm{Curl}\, X_h(\mathcal{T}) \subseteq \Sigma_h(\mathcal{T})$, this defines an element in $\Sigma_h(\mathcal{T})$ and

$$\frac{b(\tau_h, \beta_h)}{\|\tau_h\|_{\mathbb{C}^{-1/2}}} = \|\mathrm{Curl}\,\beta_h\|_{\mathbb{C}^{-1/2}}.$$

Proposition 4.1 and $A : \mathrm{dev} A \lesssim A : \mathbb{C}^{-1}A$ for all $A \in \mathbb{R}^{2\times 2}$ prove

$$\|\mathrm{Curl}\,\beta_h\|_{L^2(\Omega)} \lesssim \|\mathrm{dev}\,\mathrm{Curl}\,\beta_h\|_{L^2(\Omega)} \lesssim \|\mathrm{Curl}\,\beta_h\|_{\mathbb{C}^{-1/2}}.$$

This proves the discrete inf-sup condition for b with a constant independent of λ. The Cauchy inequality reveals the continuity of the bilinear form c. This, the inf-sup condition (5.12), and Proposition 5.1 yield the unique existence of a solution of (5.11). The stability of Proposition 5.1 and standard arguments for conforming mixed FEMs lead to the a priori error estimate. ∎

5.3.2. Mini or stabilized discretization

Define the space of (cubic) bubble functions

$$\mathcal{B}(\mathcal{T}; \mathbb{R}^2) := \left\{ \psi \in P_3(\mathcal{T}; \mathbb{R}^2) \cap H^1_0(\Omega; \mathbb{R}^2) \;\middle|\; \begin{array}{l} \forall T = \mathrm{conv}\{a, b, c\} \in \mathcal{T} \\ \exists \alpha_T \in \mathbb{R}^2 : \psi|_T = \varphi_a \varphi_b \varphi_c \alpha_T \end{array} \right\}$$

and

$$\begin{aligned} \Sigma_h(\mathcal{T}) &:= P_0(\mathcal{T}; \mathbb{R}^{2\times 2}) + \mathrm{Curl}(\mathcal{B}(\mathcal{T}; \mathbb{R}^2)), \\ X_h(\mathcal{T}) &:= V_{\mathrm{Mini}}(\mathcal{T}) := (P_1(\mathcal{T}; \mathbb{R}^2) + \mathcal{B}(\mathcal{T}; \mathbb{R}^2)) \cap X, \\ Y_h(\mathcal{T}) &:= P_1(\mathcal{T}) \cap H^1(\Omega) \cap L^2_0(\Omega). \end{aligned}$$

The Mini finite element discretization of (5.10) seeks $(\sigma_h, \alpha_h, \chi_h) \in \Sigma_h(\mathcal{T}) \times X_h(\mathcal{T}) \times Y_h(\mathcal{T})$ with (5.11). The inf-sup condition (5.12) for the bilinear form c from (5.9) is the same as the inf-sup condition for the Stokes equations and is proved by Arnold et al. [1984]. Since $\operatorname{Curl} X_h(\mathcal{T}) \subseteq \Sigma_h(\mathcal{T})$ by definition, the following corollary is a consequence of Theorem 5.8.

Corollary 5.9 (a priori error estimate for the Mini discretization)**.** *With the above choice of spaces, there exists a unique solution* $(\sigma_h, \alpha_h, \xi_h) \in \Sigma_h(\mathcal{T}) \times X_h(\mathcal{T}) \times Y_h(\mathcal{T})$ *to* (5.11)*, which satisfies*

$$\begin{aligned}&\|\sigma - \sigma_h\|_{\mathbb{C}^{-1/2}} + \|\operatorname{Curl}(\alpha - \alpha_h)\|_{L^2(\Omega)} + \|\chi - \chi_h\|_{L^2(\Omega)} \\ &\qquad \lesssim \inf_{\substack{\tau_h \in \Sigma_h(\mathcal{T}),\\ \beta_h \in X_h(\mathcal{T}),\\ \xi_h \in Y_h(\mathcal{T})}} \Big(\|\sigma - \tau_h\|_{\mathbb{C}^{-1/2}} + \|\operatorname{Curl}(\alpha - \beta_h)\|_{L^2(\Omega)} + \|\chi - \xi_h\|_{L^2(\Omega)} \Big). \qquad \blacksquare\end{aligned}$$

5.3.3. Taylor-Hood discretization

The Taylor-Hood discretization of (5.10) employs the discrete spaces

$$\begin{aligned}\Sigma_h(\mathcal{T}) &:= P_k(\mathcal{T}; \mathbb{R}^{2\times 2}),\\ X_h(\mathcal{T}) &:= P_{k+1}(\mathcal{T}; \mathbb{R}^2) \cap X,\\ Y_h(\mathcal{T}) &:= P_k(\mathcal{T}) \cap H^1(\Omega) \cap L^2_0(\Omega)\end{aligned}$$

and seeks $(\sigma_h, \alpha_h, \chi_h) \in \Sigma_h(\mathcal{T}) \times X_h(\mathcal{T}) \times Y_h(\mathcal{T})$ with (5.11). The inf-sup condition (5.12) for the bilinear form c from (5.9) is the same as the inf-sup condition for the Stokes equations and is proved in [Boffi et al., 2013]. Since $\operatorname{Curl} X_h(\mathcal{T}) \subseteq \Sigma_h(\mathcal{T})$, Theorem 5.8 yields the following corollary.

Corollary 5.10 (a priori error estimate for the Taylor-Hood discretization)**.** *For the above choice of spaces, there exists a unique solution* $(\sigma_h, \alpha_h, \xi_h) \in \Sigma_h(\mathcal{T}) \times X_h(\mathcal{T}) \times Y_h(\mathcal{T})$ *to* (5.11)*, which satisfies*

$$\begin{aligned}&\|\sigma - \sigma_h\|_{\mathbb{C}^{-1/2}} + \|\operatorname{Curl}(\alpha - \alpha_h)\|_{L^2(\Omega)} + \|\chi - \chi_h\|_{L^2(\Omega)} \\ &\qquad \lesssim \inf_{\substack{\tau_h \in \Sigma_h(\mathcal{T}),\\ \beta_h \in X_h(\mathcal{T}),\\ \xi_h \in Y_h(\mathcal{T})}} \Big(\|\sigma - \tau_h\|_{\mathbb{C}^{-1/2}} + \|\operatorname{Curl}(\alpha - \beta_h)\|_{L^2(\Omega)} + \|\chi - \xi_h\|_{L^2(\Omega)} \Big). \qquad \blacksquare\end{aligned}$$

5.3.4. $P_2\,P_0$ method

The $P_2\,P_0$ discretization of (5.10) considers the discrete spaces

$$\begin{aligned}\Sigma_h(\mathcal{T}) &:= P_1(\mathcal{T}; \mathbb{R}^{2\times 2}),\\ X_h(\mathcal{T}) &:= P_2(\mathcal{T}; \mathbb{R}^2) \cap X,\\ Y_h(\mathcal{T}) &:= P_0(\mathcal{T}) \cap L^2_0(\Omega)\end{aligned}$$

and seeks $(\sigma_h, \alpha_h, \chi_h) \in \Sigma_h(\mathcal{T}) \times X_h(\mathcal{T}) \times Y_h(\mathcal{T})$ with (5.11). The inf-sup condition (5.12) for the bilinear form c from (5.9) is the same as the inf-sup condition for the Stokes equations and is proved in [Boffi et al., 2013]. Since $\operatorname{Curl} X_h(\mathcal{T}) \subseteq \Sigma_h(\mathcal{T})$, Theorem 5.8 proves the following corollary.

Corollary 5.11 (a priori error estimate for the $P_2 P_0$ discretization)**.** *For the above choice of spaces, there exists a unique solution* $(\sigma_h, \alpha_h, \xi_h) \in \Sigma_h(\mathcal{T}) \times X_h(\mathcal{T}) \times Y_h(\mathcal{T})$ *to* (5.11)*, which satisfies*

$$\begin{aligned}&\|\sigma - \sigma_h\|_{\mathbb{C}^{-1/2}} + \|\operatorname{Curl}(\alpha - \alpha_h)\|_{L^2(\Omega)} + \|\chi - \chi_h\|_{L^2(\Omega)} \\ &\quad\lesssim \inf_{\substack{\tau_h \in \Sigma_h(\mathcal{T}),\\ \beta_h \in X_h(\mathcal{T}),\\ \xi_h \in Y_h(\mathcal{T})}} \Big(\|\sigma - \tau_h\|_{\mathbb{C}^{-1/2}} + \|\operatorname{Curl}(\alpha - \beta_h)\|_{L^2(\Omega)} + \|\chi - \xi_h\|_{L^2(\Omega)} \Big).\end{aligned}$$ ■

5.3.5. The non-conforming FEM of Kouhia and Stenberg

The non-conforming finite element space of Kouhia and Stenberg [1995] reads

$$V_{\mathrm{KS}}(\mathcal{T}) := (P_1(\mathcal{T}) \cap H^1_0(\mathcal{T})) \times \mathrm{CR}^1_0(\mathcal{T})$$

with $\mathrm{CR}^1_0(\mathcal{T})$ from Subsection 3.1.3. Let $\varepsilon_{\mathrm{NC}}$ and $\operatorname{Curl}_{\mathrm{NC}}$ denote the piecewise versions of ε and Curl. The finite element method of Kouhia and Stenberg seeks $u_{\mathrm{KS}} \in V_{\mathrm{KS}}(\mathcal{T})$ such that

$$(\varepsilon_{\mathrm{NC}}(v_{\mathrm{KS}}), \mathbb{C}\varepsilon_{\mathrm{NC}}(u_{\mathrm{KS}}))_{L^2(\Omega)} = (f, v_{\mathrm{KS}})_{L^2(\Omega)} \qquad \text{for all } v_{\mathrm{KS}} \in V_{\mathrm{KS}}(\mathcal{T}). \tag{5.13}$$

Define

$$\begin{aligned}\mathrm{CR}^1(\mathcal{T}) &:= \{v_h \in P_1(\mathcal{T}) \mid v_h \text{ is continuous at midpoints of interior edges}\},\\ \widetilde{V}_{\mathrm{KS}}(\mathcal{T}) &:= (\mathrm{CR}^1(\mathcal{T}) \cap L^2_0(\Omega)) \times (P_1(\mathcal{T}) \cap H^1(\Omega) \cap L^2_0(\Omega)),\\ Z_{\mathrm{KS}}(\mathcal{T}) &:= \{v_{\mathrm{KS}} \in \widetilde{V}_{\mathrm{KS}}(\mathcal{T}) \mid \operatorname{Curl}_{\mathrm{NC}} v_{\mathrm{KS}} \in P_0(\mathcal{T}; \mathbb{S})\}.\end{aligned}$$

Then, Carstensen and Schedensack [2014] prove the discrete Helmholtz decomposition

$$P_0(\mathcal{T}; \mathbb{S}) = \mathbb{C}\varepsilon_{\mathrm{NC}}(V_{\mathrm{KS}}(\mathcal{T})) \oplus \operatorname{Curl}_{\mathrm{NC}}(Z_{\mathrm{KS}}(\mathcal{T}))$$

and the sum is orthogonal with respect to $(\bullet, \bullet)_{\mathbb{C}^{-1/2}}$. If $\varphi \in H(\operatorname{div}, \Omega; \mathbb{R}^{2\times 2})$ additionally allows for an integration by parts with Kouhia-Stenberg functions, i.e.,

$$(\varphi, D_{\mathrm{NC}} v_{\mathrm{KS}})_{L^2(\Omega)} = (f, v_{\mathrm{KS}})_{L^2(\Omega)} \qquad \text{for all } v_{\mathrm{KS}} \in V_{\mathrm{KS}}(\mathcal{T})$$

(e.g., φ is a lowest-order Raviart-Thomas function [Raviart and Thomas, 1977] as in Subsection 3.1.3), then this implies that (5.13) is equivalent to the problem: Seek $(\sigma_h, \alpha_h) \in P_0(\mathcal{T}; \mathbb{S}) \times Z_{\mathrm{KS}}(\mathcal{T})$ such that, for all $\tau_h \in P_0(\mathcal{T}; \mathbb{S})$ and all $\beta_h \in Z_{\mathrm{KS}}(\mathcal{T})$

$$\begin{aligned}(\mathbb{C}^{-1}\tau_h, \sigma_h)_{L^2(\Omega)} + (\mathbb{C}^{-1}\tau_h, \operatorname{Curl}_{\mathrm{NC}} \alpha_h)_{L^2(\Omega)} &= (\varphi, \mathbb{C}^{-1}\tau_h)_{L^2(\Omega)},\\ (\mathbb{C}^{-1}\sigma_h, \operatorname{Curl}_{\mathrm{NC}} \beta_h)_{L^2(\Omega)} &= 0.\end{aligned}$$

Compare also with Subsection 3.1.3. In contrast to the discretizations of Subsections 5.3.2–5.3.4, this is a direct discretization of (5.6) and the symmetry of σ_h is fulfilled pointwise. However, since $Z_{\mathrm{KS}}(\mathcal{T}) \not\subseteq X$, the approximation is non-conforming and Theorem 5.8 is not applicable; the a priori analysis requires techniques in the spirit of the Strang-Fix lemma [Braess, 2007] and is not further discussed here. A priori analysis for the standard FEM of Kouhia and Stenberg [1995] can be found in [Kouhia and Stenberg, 1995, Carstensen and Schedensack, 2014].

5.4. A posteriori error analysis

This section introduces an error estimator and proves its efficiency and reliability in Subsection 5.4.1 and discusses optimal convergence rates of an adaptive algorithm in Subsection 5.4.2. The results apply to all of the discretizations from Subsections 5.3.2–5.3.4.

5.4.1. An a posteriori error estimator

Given $T \in \mathcal{T}$, let $\| \bullet \|_{\mathbb{C}^{-1/2},T} := \sqrt{(\bullet, \mathbb{C}^{-1}\bullet)_{L^2(T)}}$ denote the $\mathbb{C}^{-1/2}$-norm on T. Define the local error estimator contribution

$$\begin{aligned}\eta^2(T) := \|\varphi - \Pi_{\Sigma_h(\mathcal{T})}\varphi\|^2_{\mathbb{C}^{-1/2},T} + \|\operatorname{div}\alpha_h\|^2_{L^2(T)} \\ + h_T^2 \left\|\operatorname{curl}_{\mathrm{NC}} \mathbb{C}^{-1}\sigma_h + \nabla_{\mathrm{NC}}\chi_h\right\|^2_{L^2(T)} \\ + h_T \sum_{E\in\mathcal{E}(T)} \left\| \left[\mathbb{C}^{-1}\sigma_h + \chi_h \begin{pmatrix} 0 & 1 \\ -1 & 0 \end{pmatrix}\right]_E \tau_E \right\|^2_{L^2(E)}\end{aligned} \tag{5.14}$$

and the global error estimator by

$$\eta^2 := \sum_{T\in\mathcal{T}} \eta^2(T). \tag{5.15}$$

Theorem 5.12 (efficiency and reliability)**.** *The estimator η is reliable and efficient in the sense that*

$$\eta \approx \|\sigma - \sigma_h\|_{\mathbb{C}^{-1/2}} + \|\mathrm{Curl}(\alpha - \alpha_h)\|_{L^2(\Omega)} + \|\chi - \chi_h\|_{L^2(\Omega)}.$$

Proof. The proof is similar to the proof of Theorem 3.30 and is split into four steps.

Step 1 (equivalence to residuals). Define for all $\tau \in \Sigma$, $\beta \in X$, and $\xi \in Y$ the residuals

$$\begin{aligned}\mathrm{Res}_1(\sigma_h, \alpha_h; \tau) &:= a(\tau, \sigma_h) + b(\tau, \alpha_h) - (\varphi, \mathbb{C}^{-1}\tau)_{L^2(\Omega)}, \\ \mathrm{Res}_2(\sigma_h, \chi_h; \beta) &:= b(\sigma_h, \beta) + c(\chi_h, \beta), \\ \mathrm{Res}_3(\alpha_h; \xi) &:= c(\xi, \alpha_h).\end{aligned}$$

The abstract theory of Carstensen [2005] proves the equivalence

$$\begin{aligned}\|\sigma-\sigma_h\|_{\mathbb{C}^{-1/2}}+\|\mathrm{Curl}(\alpha-\alpha_h)\|_{L^2(\Omega)}+\|\chi-\chi_h\|_{L^2(\Omega)}\\ \approx \|\mathrm{Res}_1(\sigma_h,\alpha_h;\bullet)\|_{\Sigma^\star}+\|\mathrm{Res}_2(\sigma_h,\chi_h;\bullet)\|_{X^\star}+\|\mathrm{Res}_3(\alpha_h;\bullet)\|_{Y^\star},\end{aligned}$$

where $\|\bullet\|_{\Sigma^\star}$ denotes the dual norm with respect to $\|\bullet\|_{\mathbb{C}^{-1/2}}$, i.e.,

$$\|\mathrm{Res}_1(\sigma_h,\alpha_h;\bullet)\|_{\Sigma^\star}:=\sup_{\tau\in\Sigma\setminus\{0\}}\frac{\mathrm{Res}_1(\sigma_h,\alpha_h;\tau)}{\|\tau\|_{\mathbb{C}^{-1/2}}}.$$

Step 2 (efficiency and reliability of Res_1*).* Since

$$\mathrm{Res}_1(\sigma_h,\alpha_h;\tau)=(\Pi_{\Sigma_h(\mathcal{T})}\varphi-\varphi,\mathbb{C}^{-1}\tau)_{L^2(\Omega)}\qquad\text{for all }\tau\in\Sigma,$$

it follows

$$\|\mathrm{Res}_1(\sigma_h,\alpha_h;\bullet)\|_{\Sigma^\star}=\|\varphi-\Pi_{\Sigma_h(\mathcal{T})}\varphi\|_{\mathbb{C}^{-1/2}}.$$

Step 3 (efficiency and reliability of Res_2*).* Let I_h denote the (component-wise) quasi interpolant from Section 3.4. Since $P_1(\mathcal{T};\mathbb{R}^2)\cap H^1(\Omega;\mathbb{R}^2)\subseteq X_h(\mathcal{T})$ for all discretizations from Subsection 5.3.2–5.3.4, the discrete problem (5.11) and a piecewise integration by parts lead for all $\beta\in X$ to

$$\begin{aligned}\mathrm{Res}_2(\sigma_h,\chi_h;\beta)&=(\mathbb{C}^{-1}\sigma_h,\mathrm{Curl}(\beta-I_h\beta))_{L^2(\Omega)}+(\chi_h,\mathrm{div}(\beta-I_h\beta))_{L^2(\Omega)}\\&=(\mathrm{curl}_{\mathrm{NC}}\,\mathbb{C}^{-1}\sigma_h+\nabla_{\mathrm{NC}}\chi_h,\beta-I_h\beta)_{L^2(\Omega)}\\&\quad+\sum_{E\in\mathcal{E}}\int_E(\beta-I_h\beta)\cdot\left(\left[\mathbb{C}^{-1}\sigma_h+\chi_h\begin{pmatrix}0&1\\-1&0\end{pmatrix}\right]_E\tau_E\right)ds.\end{aligned}$$

A Cauchy and a trace inequality and the approximation properties of the quasi-interpolation (3.24) yield as in Section 3.4

$$\begin{aligned}\mathrm{Res}_2(\sigma_h,\chi_h;\beta)\lesssim\Bigg(&\|h_{\mathcal{T}}(\mathrm{curl}_{\mathrm{NC}}\,\mathbb{C}^{-1}\sigma_h+\nabla_{\mathrm{NC}}\chi_h)\|_{L^2(\Omega)}\\&+\sqrt{\sum_{E\in\mathcal{E}}h_T\left\|\left[\mathbb{C}^{-1}\sigma_h+\chi_h\begin{pmatrix}0&1\\-1&0\end{pmatrix}\right]_E\tau_E\right\|^2_{L^2(E)}}\Bigg)\|\mathrm{Curl}\,\beta\|_{L^2(\Omega)}.\end{aligned}$$

The efficiency follows with the standard bubble function technique of Verfürth [1996].

Step 4 (efficiency and reliability of Res_3*).* The Cauchy inequality implies

$$\mathrm{Res}_3(\alpha_h,\xi)=(\xi,\mathrm{div}\,\alpha_h)_{L^2(\Omega)}\le\|\xi\|_{L^2(\Omega)}\ \|\mathrm{div}\,\alpha_h\|_{L^2(\Omega)}.$$

This and $\mathrm{div}\,X_h(\mathcal{T})\subseteq Y$ yield

$$\|\mathrm{Res}_3(\alpha_h,\xi)\|_{Y^\star}=\|\mathrm{div}\,\alpha_h\|_{L^2(\Omega)}.$$ ∎

5.4.2. Remark on optimal convergence rates for an adaptive algorithm

Let $\mathcal{E}(\partial\Omega) := \{E \in \mathcal{E} \mid E \subseteq \partial\Omega\}$ and define the error estimators μ and λ by

$$\begin{aligned}\mu^2(T) &:= \|\varphi - \Pi_{\Sigma_h(\mathcal{T})}\varphi\|^2_{\mathbb{C}^{-1/2},T}\,,\\ \lambda^2(T) &:= h_T^2 \left\|\operatorname{curl}_{\mathrm{NC}} \mathbb{C}^{-1}\sigma_h + \nabla_{\mathrm{NC}}\chi_h\right\|^2_{L^2(T)}\\ &\qquad + h_T \sum_{E\in\mathcal{E}(T)} \left\| \left[\mathbb{C}^{-1}\sigma_h + \chi_h \begin{pmatrix} 0 & 1\\ -1 & 0\end{pmatrix}\right]_E \tau_E \right\|^2_{L^2(E)}\\ &\qquad + h_T \sum_{E\in\mathcal{E}(T)\setminus\mathcal{E}(\partial\Omega)} \|[\nabla\alpha_h]\cdot\nu_E\|^2_{L^2(E)}\end{aligned} \tag{5.16}$$

and

$$\mu^2 := \sum_{T\in\mathcal{T}} \mu^2(T) \qquad \text{and} \qquad \lambda^2 := \sum_{T\in\mathcal{T}} \lambda^2(T).$$

Then, the axiom (A1) stability can be proved with triangle, inverse and trace inequalities, and since all error estimator contributions in λ involve the local mesh-size, (A2) reduction follows as in Subsection 3.5.2. The axiom (A4) discrete reliability can be proved for η from (5.14)–(5.15) as in Section 3.5. A local version of the interpolation estimate of Bänsch et al. [2002, Proposition 5.4] reads

$$\|g\|^2_{L^2(T)} \lesssim h_T \sum_{E\in\mathcal{E}(\Omega_T)\setminus\mathcal{E}(\partial\Omega)} \|[g]_E\|^2_{L^2(E)} \tag{5.17}$$

for all $g \in P_k(\mathcal{T})$ with $g \perp_{L^2(\Omega)} P_k(\mathcal{T}) \cap H^1(\Omega)$, with $\Omega_T := \cup\{K \in \mathcal{T} \mid K \cap T \neq \emptyset\}$ and $\mathcal{E}(\Omega_T) := \{E \in \mathcal{E} \mid E \cap T \neq \emptyset\}$ for $T \in \mathcal{T}$. An application to $\operatorname{div}\alpha_h$ yields discrete reliability for μ and λ for the Taylor-Hood scheme from Subsection 5.3.3. Efficiency of λ can be proved for the additional regularity assumption $\varphi - \sigma \in H(\operatorname{curl},\Omega)$ with oscillations of $\operatorname{curl}\operatorname{Curl}\alpha$.

However, since the spaces

$$Z_h(\mathcal{T}) := \{\beta_h \in X_h(\mathcal{T}) \mid \forall \xi_h \in Y_h(\mathcal{T}) :\ (\xi_h, \operatorname{div}\beta_h)_{L^2(\Omega)} = 0\}$$

are not nested for nested triangulations, the discretizations of Section 5.3 lack a projection property. This disables the proof of (A3) quasi-orthogonality and, thus, the proof of optimal convergence rates of an adaptive algorithm. The same difficulties also arise for the approximation of the Stokes equations with Taylor-Hood FEMs: The work [Gantumur, 2014] states the quasi-orthogonality as an assumption without proof.

5.5. Stokes equations with symmetric gradient

The Stokes equations already discussed in Chapter 4 can be interpreted as the incompressible limit $\lambda \to \infty$ of (5.2). The symmetric formulation is favourable for the

discretization of Neumann boundary conditions (cf. [Boffi et al., 2013, Remark 8.1.3] and Remark 5.13 below). Let $\Omega \subseteq \mathbb{R}^2$ with closed Dirichlet boundary $\emptyset \neq \Gamma_D \subseteq \partial\Omega$ and Neumann boundary $\Gamma_N = \partial\Omega \setminus \Gamma_D \neq \emptyset$. The Stokes problem with Neumann boundary conditions then seeks $(u,p) \in H^1_{\Gamma_D}(\Omega;\mathbb{R}^2) \times L^2(\Omega)$ with

$$\left.\begin{aligned} -\operatorname{div}\varepsilon(u) + \nabla p &= f \\ \operatorname{div} u &= 0 \end{aligned}\right\} \text{ in } \Omega \quad \text{and} \quad (\varepsilon(u) + pI_{2\times 2})|_{\Gamma_N}\nu = 0. \tag{5.18}$$

In the presence of these boundary conditions, a weak formulation has to involve the symmetric part of the gradient $\varepsilon(u)$ (see Remark 5.13 below). This excludes the discretization of Chapter 4.

5.5.1. Weak formulation

The classical weak formulation of (5.18) seeks $(u,p) \in H^1_{\Gamma_D}(\Omega;\mathbb{R}^2) \times L^2(\Omega)$ such that, for all $v \in H^1_{\Gamma_D}(\Omega;\mathbb{R}^2)$ and for all $q \in L^2(\Omega)$,

$$\begin{aligned} (\varepsilon(v),\varepsilon(u))_{L^2(\Omega)} - (p,\operatorname{div} v)_{L^2(\Omega)} &= (f,v)_{L^2(\Omega)}, \\ (q,\operatorname{div} u)_{L^2(\Omega)} &= 0. \end{aligned} \tag{5.19}$$

Remark 5.13 (symmetric vs. non-symmetric approximation)**.** For the pure Dirichlet problem, an integration by parts proves for all $u,v \in \{w \in H^1_0(\Omega;\mathbb{R}^2) \mid \operatorname{div} w = 0\}$ that

$$2(\varepsilon(u),\varepsilon(v))_{L^2(\Omega)} = (Du,Dv)_{L^2(\Omega)} + (\operatorname{div} u,\operatorname{div} v)_{L^2(\Omega)} = (Du,Dv)_{L^2(\Omega)}.$$

This shows equivalence of (4.2) and (5.19). However, this equivalence does no longer hold if $\Gamma_D \neq \partial\Omega$. Problem (5.19) covers also the Neumann boundary condition $(\varepsilon(u) + pI_{2\times 2})|_{\Gamma_N}\nu = 0$. ♦

Define $\mathbb{R}^{2\times 2}_{\mathrm{dev,sym}} := \mathbb{R}^{2\times 2}_{\mathrm{dev}} \cap \mathbb{S}$ with $\mathbb{R}^{2\times 2}_{\mathrm{dev}}$ from (4.3) and

$$\begin{aligned} \Sigma^N &:= L^2(\Omega;\mathbb{R}^{2\times 2}_{\mathrm{dev}}), \\ Z^{\mathfrak{s}} &:= \{v \in H^1_{\Gamma_D}(\Omega;\mathbb{R}^2) \mid \operatorname{div} v = 0\}, \\ X^N &:= \left\{\beta \in H^1(\Omega;\mathbb{R}^2) \,|\beta \text{ is constant on each connectivity component of } \Gamma_N\right\}, \\ X^{\mathfrak{s}} &:= \left\{\beta \in X^N \,\middle|\, \operatorname{Curl}\beta \in L^2(\Omega;\mathbb{S})\right\}. \end{aligned}$$

A computation reveals for $\Omega \subseteq \mathbb{R}^2$

$$X^{\mathfrak{s}} = \left\{\beta \in X^N \mid \operatorname{div}\beta = 0\right\}.$$

Theorem 5.14 (Helmholtz decomposition for deviatoric and symmetric functions)**.** *It holds*

$$L^2(\Omega;\mathbb{R}^{2\times 2}_{\mathrm{dev,sym}}) = \varepsilon(Z^{\mathfrak{s}}) \oplus \operatorname{dev}(\operatorname{Curl} X^{\mathfrak{s}})$$

and the sum is L^2 orthogonal.

Proof. Let $\phi \in L^2(\Omega;\mathbb{R}^{2\times 2}_{\mathrm{dev,sym}})$. Korn's inequality, Theorem 2.10, the inf-sup condition for the bilinear form $(\bullet, \operatorname{div}\bullet)_{L^2(\Omega)}$ on $L^2(\Omega)\times H^1_{\Gamma_D}(\Omega;\mathbb{R}^2)$ [Girault and Raviart, 1986], and Brezzi's splitting lemma, Theorem 2.8, guarantee the existence of a solution $(u,p) \in H^1_{\Gamma_D}(\Omega;\mathbb{R}^2) \times L^2(\Omega)$ of

$$\begin{aligned} (\varepsilon(v),\varepsilon(u))_{L^2(\Omega)} - (p, \operatorname{div} v)_{L^2(\Omega)} &= (\phi, \varepsilon(v))_{L^2(\Omega)} && \text{for all } v \in H^1_{\Gamma_D}(\Omega;\mathbb{R}^2), \\ (q, \operatorname{div} u)_{L^2(\Omega)} &= 0 && \text{for all } q \in L^2(\Omega). \end{aligned}$$

This implies $u \in Z^{\mathfrak{s}}$ and $(\phi - \varepsilon(u) - pI_{2\times 2}) \perp_{L^2(\Omega)} \nabla H^1_{\Gamma_D}(\Omega;\mathbb{R}^2)$. The Helmholtz decomposition of Theorem 3.15 (applied row-wise) yields the existence of $\alpha \in X^N$ with $\phi - \varepsilon(u) - pI_{2\times 2} = \operatorname{Curl}\alpha$. Since $u \in Z^{\mathfrak{s}}$, this implies

$$\operatorname{dev}\operatorname{Curl}\alpha = \operatorname{dev}(\phi - \varepsilon(u) - pI_{2\times 2}) = \phi - \varepsilon(u).$$

Any $A \in \mathbb{R}^{2\times 2}$ is symmetric if and only if $\operatorname{dev} A$ is symmetric. Since $\phi - \varepsilon(u) \in L^2(\Omega;\mathbb{S})$ is symmetric, it follows $\alpha \in X^{\mathfrak{s}}$. ∎

Let $\varphi \in H(\operatorname{div},\Omega;\mathbb{S})$ with $-\operatorname{div}\varphi = f$ and $\varphi|_{\Gamma_N}\nu = 0$. Consider the problem: Seek $(\sigma,\alpha) \in \Sigma^N \times X^{\mathfrak{s}}$ with

$$\begin{aligned} (\sigma,\tau)_{L^2(\Omega)} + (\tau, \operatorname{dev}\operatorname{Curl}\alpha)_{L^2(\Omega)} &= (\varphi,\tau)_{L^2(\Omega)} && \text{for all } \tau \in \Sigma^N, \\ (\sigma, \operatorname{dev}\operatorname{Curl}\beta)_{L^2(\Omega)} &= 0 && \text{for all } \beta \in X^{\mathfrak{s}}. \end{aligned} \tag{5.20}$$

As in Section 5.2 for linear elasticity, it appears useful to include the divergence-free constraint in the mixed formulation. For

$$Y^N := L^2(\Omega),$$

this leads to the problem: Find $(\sigma,\alpha,\chi) \in \Sigma^N \times X^N \times Y^N$ such that, for all $(\tau,\beta,\xi) \in \Sigma^N \times X^N \times Y^N$,

$$\begin{aligned} (\sigma,\tau)_{L^2(\Omega)} + (\tau, \operatorname{dev}\operatorname{Curl}\alpha)_{L^2(\Omega)} &= (\varphi,\tau)_{L^2(\Omega)}, \\ (\sigma, \operatorname{dev}\operatorname{Curl}\beta)_{L^2(\Omega)} + (\chi, \operatorname{div}\beta)_{L^2(\Omega)} &= 0, \\ (\xi, \operatorname{div}\alpha)_{L^2(\Omega)} &= 0. \end{aligned} \tag{5.21}$$

The following theorem proves the equivalence of (5.20) and (5.21). As Theorem 5.5, it is a consequence of the theory of Lagrange multipliers.

Theorem 5.15. *Problems* (5.20) *and* (5.21) *are equivalent, in the sense that* $(\sigma,\alpha) \in \Sigma^N \times X^{\mathfrak{s}}$ *solves* (5.20) *if and only if there exists* $\chi \in Y^N$ *such that* $(\sigma,\alpha,\chi) \in \Sigma^N \times X^{\mathfrak{s}} \times Y^N$ *solves* (5.21).

Proof. If (σ,α,χ) is a solution to (5.21), then it is clear that (σ,α) solves (5.20).

For the converse direction, let (σ,α) be a solution to (5.20). Since $\operatorname{div}\alpha = 0$ by definition, it remains to show the existence of $\chi \in Y$, such that the second equation of (5.21) is fulfilled. To this end, define $A : X^N \to Y^N$, $A\beta := \Pi_{Y^N}\operatorname{div}\beta$ and

$B : X^N \to \mathbb{R}$, $B\beta = (\sigma, \operatorname{dev}\operatorname{Curl}\beta)$. If $\beta \in X^N$ with $A\beta = 0$, then $(q, \operatorname{div}\beta) = (q, \Pi_{Y^N}\operatorname{div}\beta) = 0$ for all $q \in Y^N$ and, hence, $\beta \in X^{\mathfrak{s}}$. Problem (5.20) implies $B\beta = 0$. Hence, [Zeidler, 1985, Proposition 43.1] implies the existence of $\chi \in (Y^N)^\star \equiv Y^N$ with

$$\begin{aligned} 0 = B\beta + \chi(A\beta) &\equiv (\sigma, \operatorname{dev}\operatorname{Curl}\beta) + (\chi, \Pi_{Y^N}\operatorname{div}\beta) \\ &= (\sigma, \operatorname{dev}\operatorname{Curl}\beta) + (\chi, \operatorname{div}\beta). \end{aligned}$$

■

Define the bilinear forms $a : \Sigma^N \times \Sigma^N \to \mathbb{R}$ and $b : \Sigma^N \times X^N \to \mathbb{R}$ by

$$\begin{aligned} a(\sigma,\tau) &:= (\sigma,\tau)_{L^2(\Omega)} && \text{for all } \sigma,\tau \in \Sigma^N, \\ b(\tau,\alpha) &:= (\tau, \operatorname{dev}\operatorname{Curl}\alpha)_{L^2(\Omega)} && \text{for all } \tau \in \Sigma^N, \alpha \in X^N. \end{aligned} \tag{5.22}$$

Lemma 5.16 (inf-sup condition)**.** *Any $\beta \in X^N$ satisfies*

$$\|\operatorname{Curl}\beta\|_{L^2(\Omega)} \lesssim \sup_{\tau\in\Sigma\setminus\{0\}} \frac{b(\tau,\beta)}{\|\tau\|_{L^2(\Omega)}}.$$

Proof. Given $\beta \in X^N$, the choice of $\tau := \operatorname{dev}\operatorname{Curl}\beta$ leads to

$$b(\tau,\beta) = \|\operatorname{dev}\operatorname{Curl}\beta\|^2_{L^2(\Omega)}.$$

The boundary conditions for X^N lead to $(\operatorname{Curl}\beta)|_{\Gamma_N}\nu = 0$. Since $\operatorname{div}\operatorname{Curl}\beta = 0$, this and Lemma 2.9 prove

$$\|\operatorname{Curl}\beta\|_{L^2(\Omega)} \lesssim \|\operatorname{dev}\operatorname{Curl}\beta\|_{L^2(\Omega)}. \tag{5.23}$$

This yields the assertion. ■

Proposition 5.17. *Problem* (5.20) *(and therefore* (5.21)*) has a unique solution $(\sigma,\alpha) \in \Sigma \times X^{\mathfrak{s}}$. The solution $u \in Z^{\mathfrak{s}}$ to* (5.19) *satisfies $\sigma = \varepsilon(u)$.*

Proof. The existence of a unique solution follows from Theorem 2.8 and Lemma 5.16. The second equation of (5.20) and the Helmholtz decomposition of Theorem 5.14 guarantee the existence of $\widetilde{u} \in Z^{\mathfrak{s}}$ with $\sigma = \varepsilon(\widetilde{u})$. Let $v \in Z^{\mathfrak{s}}$. Then, (5.20) and an integration by parts imply

$$(D\widetilde{u}, Dv)_{L^2(\Omega)} = (\varphi, Dv)_{L^2(\Omega)} - (Dv, \operatorname{dev}\operatorname{Curl}\alpha)_{L^2(\Omega)} = (f,v)_{L^2(\Omega)}.$$

This yields $\widetilde{u} = u$. ■

Remark 5.18 (pressure)**.** As in Remark 4.5, define $p := -\operatorname{tr}(\varphi - \operatorname{Curl}\alpha)/2$. Since $\sigma + \operatorname{dev}\operatorname{Curl}\alpha = \operatorname{dev}\varphi$ and $\operatorname{Curl}\alpha \perp_{L^2(\Omega)} D\big(H^1_{\Gamma_D}(\Omega;\mathbb{R}^2)\big)$, the function p satisfies for all $v \in H^1_{\Gamma_D}(\Omega;\mathbb{R}^2)$ that

$$(p, \operatorname{div} v)_{L^2(\Omega)} = (pI_{2\times 2}, Dv)_{L^2(\Omega)} = (\sigma, \varepsilon(v))_{L^2(\Omega)} - (\varphi, Dv)_{L^2(\Omega)}.$$

This, an integration by parts and $\varphi|_{\Gamma_N}\nu = 0$ lead to

$$\begin{aligned} -(p, \operatorname{div} v)_{L^2(\Omega)} &= (f,v)_{L^2(\Omega)} + \int_{\Gamma_N} \varphi\nu \cdot v \, ds - (\sigma, \varepsilon(v))_{L^2(\Omega)} \\ &= (f,v)_{L^2(\Omega)} - (\sigma, \varepsilon(v))_{L^2(\Omega)}. \end{aligned}$$

This implies that p is the pressure from (5.19). ♦

5.5.2. Discretization

Let $\Sigma_h^N(\mathcal{T})$, $X_h^N(\mathcal{T}) \cap X^N \subseteq X^N$, and $Y_h^N(\mathcal{T}) \subseteq Y^N$ be one of the choices of discrete spaces from Subsections 5.3.2–5.3.4 without the respective conditions $\int_\Omega \operatorname{tr}(\tau_h)\,dx = 0$, $\int_\Omega \beta_h\,dx = 0$, $\int_\Omega \operatorname{curl}\beta_h\,dx = 0$ and $\int_\Omega \xi_h\,dx = 0$, and define

$$\Sigma_h^{\mathrm{dev}}(\mathcal{T}) := \operatorname{dev}\Sigma_h^N(\mathcal{T}) \subseteq \Sigma^N.$$

Recall the bilinear forms a, b from (5.22) and define $c : Y^N \times X^N \to \mathbb{R}$ by

$$c(\xi,\beta) := (\xi, \operatorname{div}\beta)_{L^2(\Omega)} \qquad \text{for all } \xi \in Y^N, \beta \in X^N.$$

Then the discretization of (5.21) seeks $(\sigma_h, \alpha_h, \xi_h) \in \Sigma_h^{\mathrm{dev}}(\mathcal{T}) \times X_h^N(\mathcal{T}) \times Y_h^N(\mathcal{T})$ such that

$$\begin{aligned} a(\tau_h,\sigma_h) + b(\tau_h,\alpha_h) &= (\varphi,\tau_h)_{L^2(\Omega)} && \text{for all } \tau_h \in \Sigma_h^{\mathrm{dev}}(\mathcal{T}),\\ b(\sigma_h,\beta_h) + c(\chi_h,\beta_h) &= 0 && \text{for all } \beta_h \in X_h^N(\mathcal{T}),\\ c(\xi_h,\alpha_h) &= 0 && \text{for all } \xi_h \in Y_h^N(\mathcal{T}). \end{aligned} \tag{5.24}$$

The following theorem proves an a priori error estimate similar to Theorem 5.8.

Theorem 5.19 (best-approximation)**.** *The discrete problem* (5.24) *has a unique solution* $(\sigma_h, \alpha_h, \chi_h) \in \Sigma_h^{\mathrm{dev}}(\mathcal{T}) \times X_h^N(\mathcal{T}) \times Y_h^N(\mathcal{T})$*, which satisfies*

$$\begin{aligned} &\|\sigma-\sigma_h\|_{L^2(\Omega)} + \|\operatorname{Curl}(\alpha-\alpha_h)\|_{L^2(\Omega)} + \|\chi-\chi_h\|_{L^2(\Omega)}\\ &\quad\lesssim \inf_{\substack{\tau_h\in\Sigma_h^{\mathrm{dev}}(\mathcal{T})\\ \beta_h\in X_h^N(\mathcal{T})\\ \xi_h\in Y_h^N(\mathcal{T})}} \Big(\|\sigma-\tau_h\|_{L^2(\Omega)} + \|\operatorname{Curl}(\alpha-\beta_h)\|_{L^2(\Omega)} + \|\chi-\xi_h\|_{L^2(\Omega)}\Big). \end{aligned}$$

Proof. The bilinear form a is continuous and elliptic with respect to $\|\bullet\|_{L^2(\Omega)}$. A Cauchy inequality implies that the bilinear forms b and c are continuous with respect to $\|\bullet\|_{L^2(\Omega)}$ and $\|\operatorname{Curl}\bullet\|_{L^2(\Omega)}$. The inf-sup condition

$$\|\operatorname{Curl}\beta_h\|_{L^2(\Omega)} \lesssim \sup_{\tau_h\in\Sigma_h^{\mathrm{dev}}(\mathcal{T})\setminus\{0\}} \frac{b(\tau_h,\beta_h)}{\|\tau_h\|_{L^2(\Omega)}} \qquad \text{for all } \beta_h \in X_h^N(\mathcal{T})$$

follows from $\operatorname{dev}\operatorname{Curl} X_h^N(\mathcal{T}) \subseteq \Sigma_h^{\mathrm{dev}}(\mathcal{T})$ and (5.23). The discrete inf-sup conditions for c for the choices of $X_h^N(\mathcal{T})$ and $Y_h^N(\mathcal{T})$ from above are proved in [Arnold et al., 1984, Boffi et al., 2013]. Proposition 5.1 and standard arguments for conforming mixed FEMs lead to the assertion. ∎

Remark 5.20 (non-conforming approximation)**.** Since $(\varepsilon_{\mathrm{NC}}\bullet, \varepsilon_{\mathrm{NC}}\bullet)$ for the piecewise symmetric gradient $\varepsilon_{\mathrm{NC}}$ is not positive definite on $\mathrm{CR}_0^1(\mathcal{T})$, there is no obvious non-conforming approximation of the Stokes problem (5.19) and so no non-conforming approximation for the Neumann problem of the form (5.18). The indef-

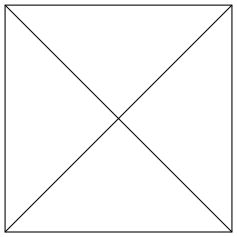

Figure 5.1.: Criss-cross triangulation.

initeness of $(\varepsilon_{\mathrm{NC}}\bullet, \varepsilon_{\mathrm{NC}}\bullet)$ is illustrated in the following example. Consider the triangulation from Figure 5.1 of the unit square $\Omega = (0,1)^2$. Define $v_{\mathrm{CR}} \in \mathrm{CR}^1_0(\mathcal{T};\mathbb{R}^2)$ for $s > 0$ by

$$\begin{aligned} v_{\mathrm{CR}}(0.25,0.25) &= (s,s) & \qquad v_{\mathrm{CR}}(0.75,0.25) &= (s,-s) \\ v_{\mathrm{CR}}(0.25,0.75) &= (-s,s) & \qquad v_{\mathrm{CR}}(0.75,0.75) &= (-s,-s). \end{aligned}$$

Then $v_{\mathrm{CR}} \not\equiv 0$, but $\varepsilon(v_{\mathrm{CR}}) = 0$. ♦

5.5.3. A posteriori error analysis

Let $\mathcal{E}(\Gamma_N) := \{E \in \mathcal{E} \mid E \subseteq \overline{\Gamma}_N\}$ denote the edges on the Neumann boundary. Define

$$\begin{aligned} \eta_1^2(T) := \|\mathrm{dev}(\varphi - \Pi_{\Sigma_h^{\mathrm{dev}}(\mathcal{T})}\varphi)\|^2_{L^2(T)} + \|h_{\mathcal{T}}(\mathrm{curl}_{\mathrm{NC}}\,\sigma_h + \nabla_{\mathrm{NC}}\chi_h)\|^2_{L^2(T)} \\ + \|\mathrm{div}\,\alpha_h\|^2_{L^2(T)} + h_T \sum_{E\in\mathcal{E}(T)\setminus\mathcal{E}(\Gamma_N)} \left\| \left[\sigma_h + \chi_h \begin{pmatrix} 0 & 1 \\ -1 & 0 \end{pmatrix}\right]_E \tau_E \right\|^2_{L^2(E)} \end{aligned}$$

and $\eta_1^2 := \sum_{T\in\mathcal{T}} \eta_1^2(T)$. The following theorem states efficiency and reliability of η_1. The proof is similar to the proof of Theorem 5.12 and therefore omitted.

Theorem 5.21 (efficiency, reliability)**.** *The error estimator η_1 is reliable and efficient in the sense that*

$$\eta_1^2 \approx \|\sigma - \sigma_h\|^2_{L^2(\Omega)} + \|\mathrm{Curl}(\alpha - \alpha_h)\|^2_{L^2(\Omega)} + \|\chi - \chi_h\|^2_{L^2(\Omega)}.$$ ■

Remark 5.22 (optimal convergence rates of an adaptive algorithm)**.** As for linear elasticity, the axioms (A1) stability, (A2) reduction, and (A4) discrete reliability can be proved for a modified error estimator with $\|\mathrm{div}\,\alpha_h\|^2_{L^2(T)}$ replaced by

$$h_T \sum_{E\in\mathcal{E}(T)\setminus\mathcal{E}(\Gamma_N)} \|[\nabla\alpha_h]_E \cdot \nu_E\|^2_{L^2(E)}.$$

However, as discussed in Subsection 5.4.2, (A3) quasi-orthogonality cannot be proved because of the missing projection property. ♦

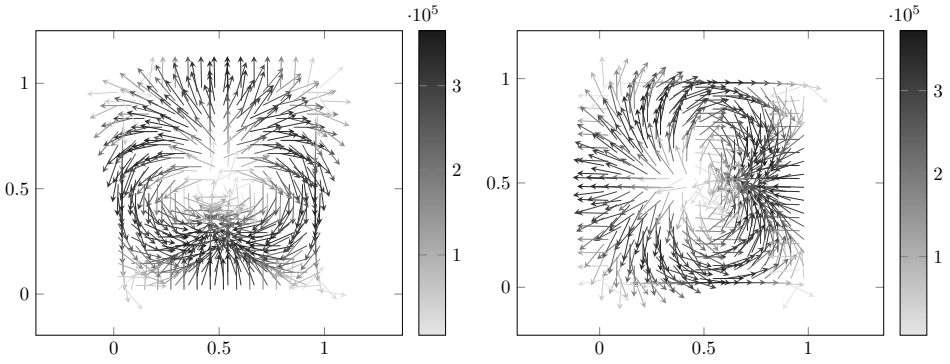

Figure 5.2.: Discrete solution on a uniform mesh with 289 nodes for the experiment from Subsection 5.6.1.

5.6. Numerical experiments

This section is devoted to numerical experiments for the Taylor-Hood discretization from Subsection 5.3.3 for $k = 1$ for linear elasticity. As in Sections 3.7 and 4.4, the implementation is based on the software package AFEM [Carstensen et al., 2009] maintained at the Humboldt-Universität. The experiments compare the errors and error estimators on a sequence of uniformly red-refined triangulations (see Figure 3.3 for a red-refined triangle) with the errors and error estimators on a sequence of triangulations created by an adaptive algorithm defined in Subsection 5.6.1 below. Furthermore, the robustness of the method with respect to $\lambda \to \infty$ is compared with the conforming P_1 FEM defined in Subsection 5.6.1 below.

The convergence history plots are logarithmically scaled and display the error $\|\sigma - \sigma_h\|_{L^2(\Omega)}$ against the number of degrees of freedom of the resulting linear system for the Schur complement (see Remark 3.12).

5.6.1. Academic example on the square

Let $\Omega = (0,1)^2$ with initial triangulation $\mathcal{T}_0$ from Figure 3.4a and Dirichlet boundary $\Gamma_D := \partial\Omega$. The exact solution of (5.2) for the pure Dirichlet problem with homogeneous boundary conditions and volume force

$$f(x,y) = \begin{pmatrix} -2\,\mu\,\pi^3\,\cos(\pi y)\,\sin(\pi y)\,(2\,\cos(2\pi x) - 1) \\ 2\,\mu\,\pi^3\,\cos(\pi x)\,\sin(\pi x)\,(2\,\cos(2\pi y) - 1) \end{pmatrix}$$

reads

$$u(x,y) = \begin{pmatrix} \pi\cos(\pi y)\,\sin^2(\pi x)\,\sin(\pi y) \\ -\pi\cos(\pi x)\,\sin^2(\pi y)\sin(\pi x) \end{pmatrix}.$$

Define the right-hand side $\varphi = (\varphi_{11}, \varphi_{12}; \varphi_{21}, \varphi_{22}) \in H(\mathrm{div}, \Omega; \mathbb{S})$ with $-\mathrm{div}\,\varphi = f$ by

$$\begin{aligned}\varphi_{11}(x,y) &:= 2\mu\pi^3 \cos(\pi y)\sin(\pi y)((1/\pi)\sin(2\pi x) - x),\\ \varphi_{12} &:= \varphi_{21} := 0,\\ \varphi_{22}(x,y) &:= -2\mu\pi^3 \cos(\pi x)\sin(\pi x)((1/\pi)\sin(2\pi y) - y).\end{aligned}$$

Let E denote Young's modulus and ν the Poisson ratio, i.e.,

$$\lambda = \frac{E\nu}{(1+\nu)(1-2\nu)} \qquad \text{and} \qquad \mu = \frac{E}{2(1+\nu)}$$

with $\lambda \to \infty$ if $\nu \to 1/2$. Figure 5.2 depicts the discrete solution from Subsection 5.3.3 on a uniform triangulation with 289 nodes for Young's modulus $E = 10^5$ and Poisson ratio $\nu = 0.4$. The discrete problems are solved on a sequence of red-refined triangulations and on a sequence of triangulations generated by the following adaptive algorithm. Define for $T \in \mathcal{T}$ the local error estimator contributions

$$\begin{aligned}\mathfrak{y}^2(\mathcal{T}, T) := h_T^2 \left\|\mathrm{curl}_{\mathrm{NC}}\, \mathbb{C}^{-1}\sigma_h + \nabla_{\mathrm{NC}}\chi_h\right\|^2_{L^2(T)} + \|\mathrm{div}\,\alpha_h\|^2_{L^2(T)}\\ + h_T \sum_{E\in\mathcal{E}(T)} \left\| \left[\mathbb{C}^{-1}\sigma_h + \chi_h \begin{pmatrix} 0 & 1\\ -1 & 0\end{pmatrix}\right]_E \tau_E \right\|^2_{L^2(E)}\end{aligned} \tag{5.25}$$

and let $\mu^2(T)$ be defined by (5.16). Furthermore, define

$$\begin{aligned}&\mathfrak{y}_\ell^2 := \mathfrak{y}^2(\mathcal{T}_\ell, \mathcal{T}_\ell) \quad \text{with} \quad \mathfrak{y}^2(\mathcal{T}_\ell, \mathcal{M}) := \sum_{T\in\mathcal{M}} \mathfrak{y}^2(\mathcal{T}_\ell, T) \quad \text{for any } \mathcal{M} \subseteq \mathcal{T}_\ell,\\ &\mu_\ell^2 := \mu^2(\mathcal{T}_\ell) \quad \text{with} \quad \mu^2(\mathcal{M}) := \sum_{T\in\mathcal{M}} \mu^2(T) \quad \text{for any } \mathcal{M} \subseteq \mathcal{T}_\ell.\end{aligned} \tag{5.26}$$

The adaptive algorithms then reads as follows.

Algorithm 5.23 (AFEM for linear elasticity)**.**
Input: Initial triangulation $\mathcal{T}_0$, parameters $0 < \theta_A \le 1$, $0 < \rho_B < 1$, $0 < \kappa$.
for $\ell = 0, 1, 2, \ldots$ **do**
Solve. Compute solution $(\sigma_\ell, \alpha_\ell, \chi_\ell) \in \Sigma_h(\mathcal{T}) \times X_h(\mathcal{T}_\ell) \times Y_h(\mathcal{T}_\ell)$ of (5.11) with respect to $\mathcal{T}_\ell$.
Estimate. Compute local contributions of the error estimators $\big(\mathfrak{y}^2(\mathcal{T}_\ell, T)\big)_{T\in\mathcal{T}_\ell}$ and $\big(\mu^2(T)\big)_{T\in\mathcal{T}_\ell}$.
if $\mu_\ell^2 \le \kappa\mathfrak{y}_\ell^2$ **then**
Mark. The Dörfler marking chooses a minimal subset $\mathcal{M}_\ell \subseteq \mathcal{T}_\ell$ such that $\theta_A\mathfrak{y}_\ell^2 \le \mathfrak{y}_\ell^2(\mathcal{T}_\ell, \mathcal{M}_\ell)$.
Refine. Generate the smallest admissible refinement $\mathcal{T}_{\ell+1}$ of $\mathcal{T}_\ell$ in which at least all triangles in $\mathcal{M}_\ell$ are refined.
else

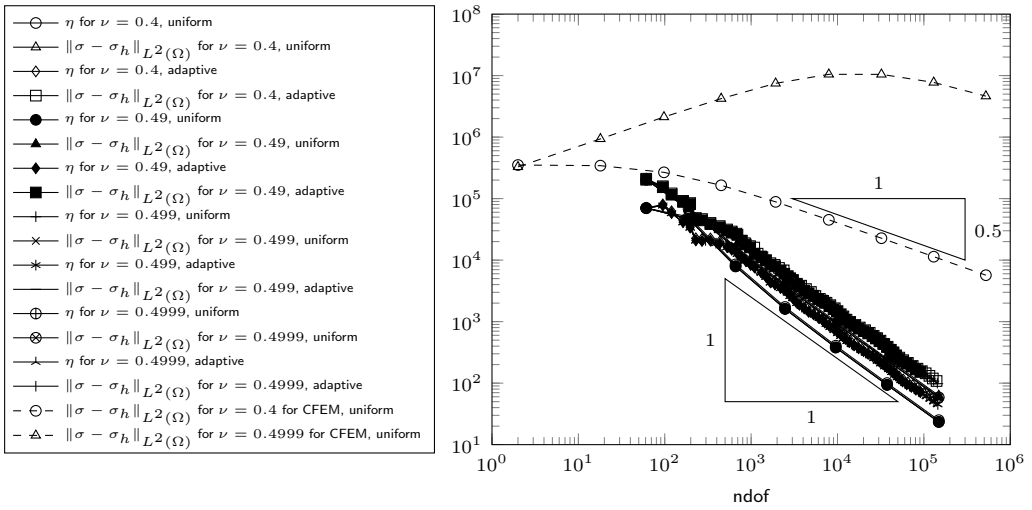

Figure 5.3.: Errors and error estimators for the experiment on the square domain from Subsection 5.6.1.

Mark. Compute a triangulation $\mathcal{T} \in \mathbb{T}$ with $\mu^2(\mathcal{T}) \leq \rho_B \mu_\ell^2$.
Refine. Generate the overlay $\mathcal{T}_{\ell+1}$ of $\mathcal{T}_\ell$ and $\mathcal{T}$.
end if
end for
Output: Sequences of triangulations $(\mathcal{T}_\ell)_{\ell\in\mathbb{N}_0}$, discrete solutions $(\sigma_\ell, \alpha_\ell, \chi_\ell)_{\ell\in\mathbb{N}_0}$ and error estimators $(\mathfrak{y}_\ell)_{\ell\in\mathbb{N}_0}$ and $(\mu_\ell)_{\ell\in\mathbb{N}_0}$. ♦

The stress errors $\|\sigma - \sigma_h\|_{L^2(\Omega)}$ and error estimators η from (5.14)–(5.15) are plotted against the number of degrees of freedom in Figure 5.3 for Young's modulus $E = 10^5$ and Poisson ratios $\nu = 0.4$, 0.49, 0.499, and 0.4999. In contrast to standard conforming low-order FEMs, the discretization (5.11), as predicted by Corollary 5.10, does not show a locking behaviour for $\lambda \to \infty$. To illustrate this, the errors $\|\sigma - \mathbb{C}\varepsilon(u_C)\|_{L^2(\Omega)}$ for the solution u_C of the conforming P_1 FEM are included in Figure 5.3 for comparison for Poisson ratios $\nu = 0.4$ and $\nu = 0.4999$ on a sequence of uniformly red-refined triangulations. The P_1 conforming FEM seeks $u_C \in P_1(\mathcal{T};\mathbb{R}^2) \cap H^1_{\Gamma_D}(\Omega;\mathbb{R}^2)$ with

$$\int_\Omega \varepsilon(v_C) : \mathbb{C}\varepsilon(u_C)\, dx = \int_\Omega f \cdot v_C\, dx \quad \text{for all } v_C \in P_1(\mathcal{T};\mathbb{R}^2) \cap H^1_{\Gamma_D}(\Omega;\mathbb{R}^2). \quad (5.27)$$

While the size of the error of the conforming P_1 FEM has an almost linear dependence on λ, the errors of the discretization (5.11) are of the same size for all considered Poisson ratios. Both uniform and adaptive refinement yield the optimal convergence rates of $\texttt{ndof}^{-1}$. Figure 5.4 depicts triangulations created by Algorithm 5.23 for Poisson ratios $\nu = 0.4$ and $\nu = 0.4999$ with approximately 1500

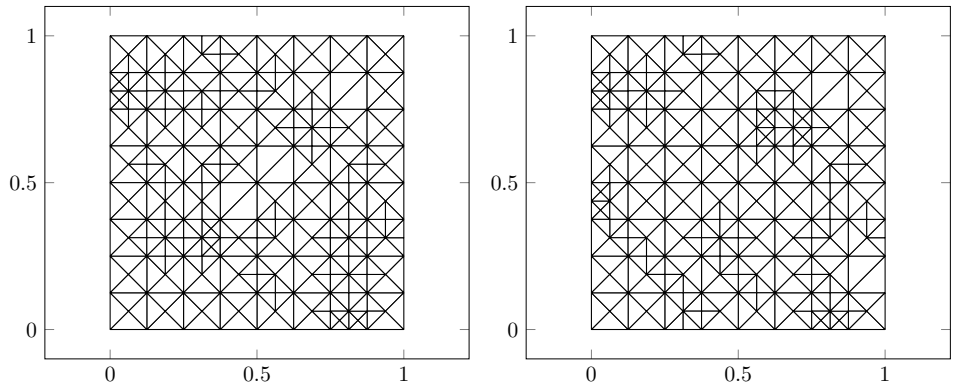

Figure 5.4.: Adaptively refined triangulations for $\nu = 0.4$ with 194 nodes (1670 dofs) and for $\nu = 0.4999$ with 195 nodes (1675 dofs) for the experiment on the square from Subsection 5.6.1.

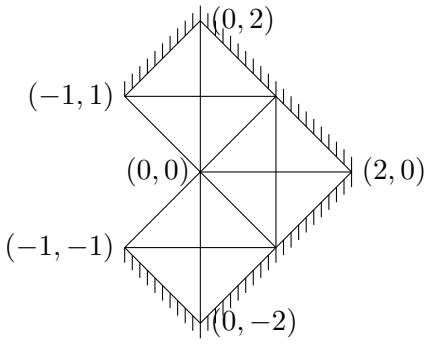

Figure 5.5.: Initial triangulation of the L-shaped domain from Subsection 5.6.2.

degrees of freedom. Since the exact solution is smooth, the refinement is almost uniform. All marking steps in Algorithm 5.23 used the Dörfler marking ($\mu_\ell^2 \leq \kappa \eta_\ell^2$).

5.6.2. Rotated L-shaped domain

Let $\Omega := \operatorname{conv}\{(-1,-1),(0,-2),(2,0),(1,1)\} \cup \operatorname{conv}\{(0,2),(-1,1),(0,0),(1,1)\}$ be the rotated L-shaped domain from Figure 5.5. The considered exact solution in radial components for the right-hand side $f = 0$ reads

$$u_r(r,\varphi) = \frac{r^\alpha}{2\mu}(-(\alpha+1)\,\cos((\alpha+1)\,\varphi) + (C_2 - \alpha - 1)\,C_1\,\cos((\alpha-1)\varphi)),$$
$$u_\varphi(r,\varphi) = \frac{r^\alpha}{2\mu}((\alpha+1)\,\sin((\alpha+1)\,\varphi) + (C_2 + \alpha - 1)\,C_1\,\sin((\alpha-1)\varphi))$$

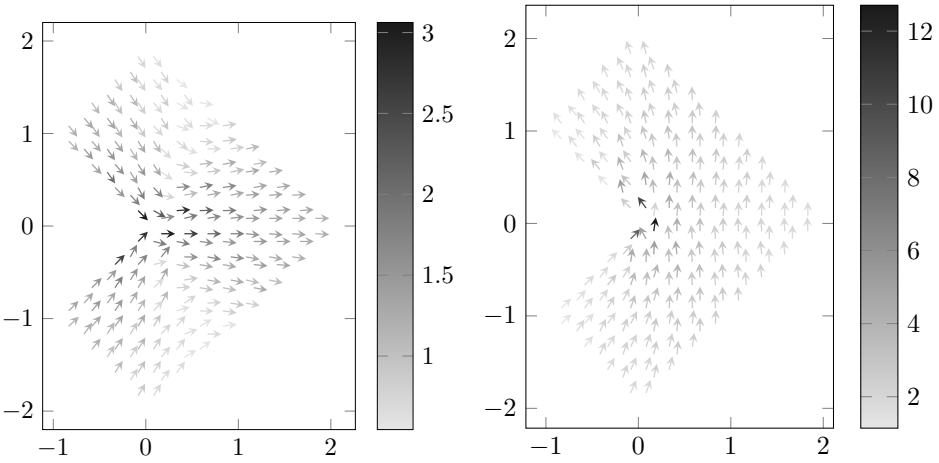

Figure 5.6.: Discrete solution on a uniform mesh with 113 nodes for the experiment from Subsection 5.6.2.

with

$$C_1 := \frac{-\cos((\alpha+1)\,\omega)}{\cos((\alpha-1)\,\omega)}, \quad C_2 := \frac{2\,(\lambda+2\mu)}{\lambda+\mu},$$

and the positive solution $\alpha \approx 0.544483736782$ to

$$\alpha \sin(2\omega) + \sin(2\omega\alpha) = 0 \qquad \text{with} \qquad \omega = \frac{3\pi}{4}.$$

Dirichlet boundary conditions are applied on

$$\Gamma_D := \operatorname{conv}\{(-1,-1),(0,-2)\} \cup \operatorname{conv}\{(0,-2),(2,0)\} \\ \cup \operatorname{conv}\{(2,0),(0,2)\} \cup \operatorname{conv}\{(0,2),(-1,1)\},$$

while $(\sigma\nu)|_{\Gamma_N} = g := 0$ on the Neumann boundary $\Gamma_N := \partial\Omega \setminus \Gamma_D$ (see Remark 5.7 for mixed boundary conditions). Let $\varphi := 0 \in H(\operatorname{div}, \Omega; \mathbb{S})$ and define $u_D := qu$ with

$$q(r,\theta) := \begin{cases} 0 & \text{if } r \le 1/2, \\ 16r^4 - 64r^3 + 88r^2 - 48r + 9 & \text{if } 1/2 \le r \le 1, \\ 1 & \text{if } r \ge 1. \end{cases}$$

Then $u_D \in H^2(\Omega;\mathbb{R}^2)$ and $u_D|_{\Gamma_D} = u|_{\Gamma_D}$.

The discrete solution on a uniform triangulation with 113 nodes is depicted in Figure 5.6 for Young's modulus $E = 10^5$ and Poisson ratio $\nu = 0.4$. The error estimator μ defined by (5.16) and (5.26) for non-homogeneous Dirichlet data is modified as

$$\mu^2(T) := \left\| (\varphi - \mathbb{C}Du_D) - \Pi_{\Sigma_h(\mathcal{T})}(\varphi - \mathbb{C}Du_D) \right\|^2_{\mathbb{C}^{-1/2},T}.$$

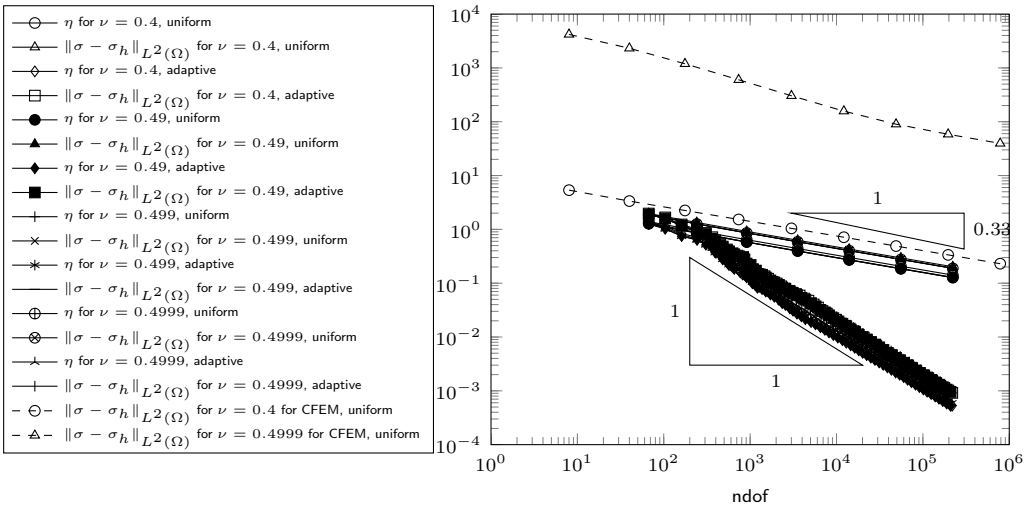

Figure 5.7.: Errors and error estimators for the experiment on the rotated L-shaped domain from Subsection 5.6.2.

For edges on the Dirichlet boundary $E \in \mathcal{E}$, $E \subseteq \Gamma_D$, with the one adjacent triangle T_+, the jump reads

$$\left[\mathbb{C}^{-1}\sigma_h + \chi_h \begin{pmatrix} 0 & 1 \\ -1 & 0 \end{pmatrix}\right]_E := \left(\mathbb{C}^{-1}\sigma_h + \chi_h \begin{pmatrix} 0 & 1 \\ -1 & 0 \end{pmatrix}\right)\Big|_{T_+} - Du_D.$$

The sum in the definition of the error estimator $\mathfrak{y}$ in (5.25) runs only over edges that do not lie on the Neumann boundary $\overline{\Gamma}_N$. The stress errors $\|\sigma - \sigma_h\|_{L^2(\Omega)}$ and the error estimators $\eta := \sqrt{\mu^2 + \mathfrak{y}^2}$ are computed on a sequence of uniformly red-refined triangulations and on a sequence of triangulations created by Algorithm 5.23 for Young's modulus $E = 10^5$ and Poisson ratios $\nu = 0.4$, 0.49, 0.499, and 0.4999. They are plotted against the number of degrees of freedom in Figure 5.7. For uniformly refined meshes, the convergence rates of $h^{2/3} \approx \texttt{ndof}^{-1/3}$ are suboptimal, while Algorithm 5.23 reveals the optimal convergence rate of $\texttt{ndof}^{-1}$. In contrast to the P_1 conforming FEM of (5.27), the size of the errors and error estimators is almost the same for all Poisson ratios $\nu = 0.4$, 0.49, 0.499, and 0.4999, i.e., the discretization from Subsection 5.3.3 does not show a locking behaviour. Figure 5.8 depicts triangulations created by Algorithm 5.23 for Poisson ratios $\nu = 0.4$ and $\nu = 0.4999$ with approximately 1500 degrees of freedom. The singularity at $(0, 0)$ leads to a strong refinement towards the re-entrant corner. For $\nu = 0.4$ and $\nu = 0.49$ all marking steps in Algorithm 5.23 used the Dörfler marking ($\mu_\ell^2 \leq \kappa\mathfrak{y}_\ell^2$), while for $\nu = 0.499$ the marking with respect to the data-approximation ($\mu_\ell^2 > \kappa\mathfrak{y}_\ell^2$ in Algorithm 5.23) was applied at level 54 (55696 dofs) and level 62 (118732 dofs) and for $\nu = 0.4999$ from level 11 onwards at approximately every third refinement.

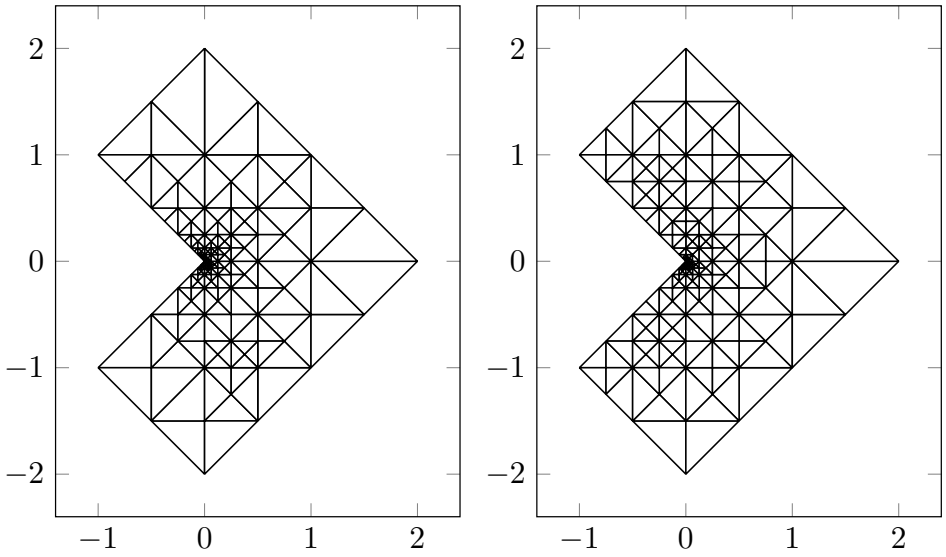

Figure 5.8.: Adaptively refined triangulations for $\nu = 0.4$ with 202 nodes (1612 dofs) and for $\nu = 0.4999$ with 188 nodes (1512 dofs) for the experiment on the rotated L-shaped domain from Subsection 5.6.2.

5.6.3. L-shaped domain with piecewise constant f, I

This example considers the L-shaped domain $\Omega = (-1,1)^2 \setminus ([0,1] \times [-1,0])$ from Figure 3.4b with pure Dirichlet boundary $\Gamma_D := \partial\Omega$. Define the piecewise constant volume force $f \in L^2(\Omega;\mathbb{R}^2)$ by

$$f(x,y) := \begin{cases} (0,0) & \text{if } x \le 0 \text{ and } y \ge 0, \\ (0,1) & \text{if } x, y \ge 0, \\ (1,0) & \text{if } x, y \le 0. \end{cases}$$

Define $\varphi = (\varphi_{11}, \varphi_{12}; \varphi_{21}, \varphi_{22}) \in H(\operatorname{div}, \Omega; \mathbb{S})$ with $-\operatorname{div}\varphi = f$ by

$$\begin{aligned} \varphi_{11} &:= \begin{cases} -x & \text{if } y \le 0, \\ 0 & \text{else}, \end{cases} \\ \varphi_{12} &:= \varphi_{21} := 0, \\ \varphi_{22} &:= \begin{cases} -y & \text{if } x \ge 0, \\ 0 & \text{else} \end{cases} \end{aligned}$$

and let $u_D = 0$.

Figure 5.9 depicts the discrete solution for Young's modulus $E = 10^5$ and Poisson ratio $\nu = 0.4$ on a uniform triangulation with 225 nodes. The error estimators $\eta := \sqrt{\mu^2 + \mathfrak{y}^2}$ are plotted in Figure 5.10 on a sequence of uniformly red-refined

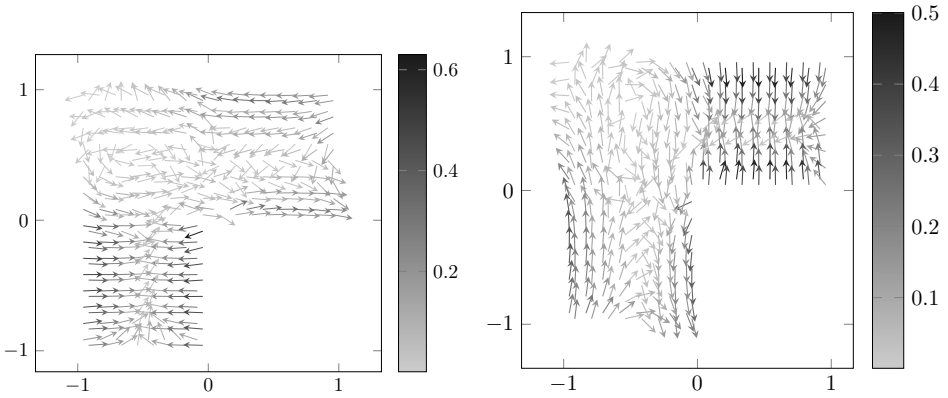

Figure 5.9.: Discrete solution on a uniform mesh with 225 nodes for the experiment on the L-shaped domain from Subsection 5.6.3.

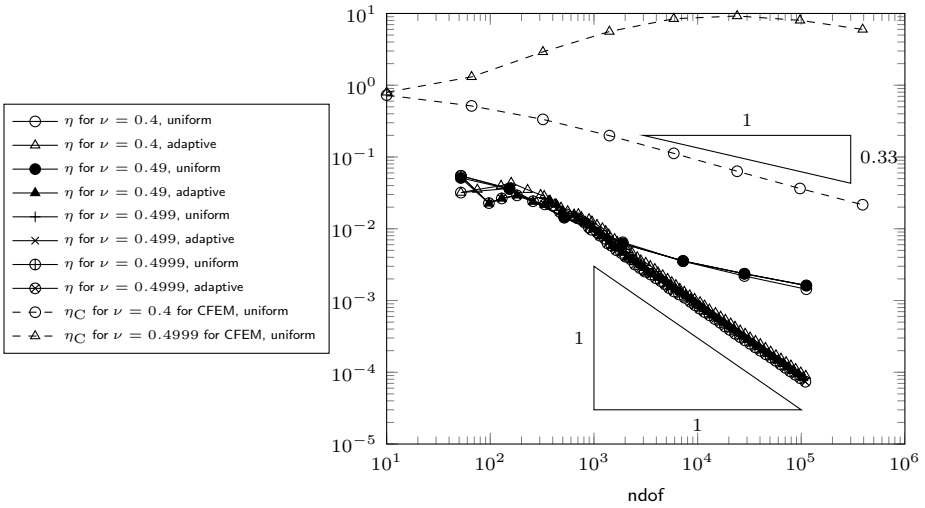

Figure 5.10.: Error estimators for the experiment on the L-shaped domain from Subsection 5.6.3.

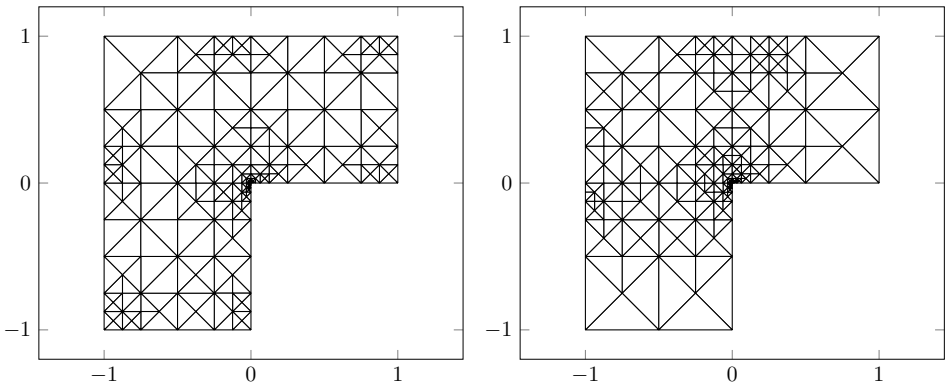

Figure 5.11.: Adaptively refined triangulations for $\nu = 0.4$ with 180 nodes (1516 dofs) and for $\nu = 0.4999$ with 189 nodes (1615 dofs) for the experiment on the L-shaped domain from Subsection 5.6.3.

triangulations and on a sequence of triangulations created by Algorithm 5.23 for Young's modulus $E = 10^5$ and Poisson ratios $\nu = 0.4$, 0.49, 0.499, and 0.4999. Uniform refinement yields a suboptimal convergence rate of $h^{2/3} \approx \mathtt{ndof}^{-1/3}$, while Algorithm 5.23 recovers the optimal convergence rates of $\mathtt{ndof}^{-1}$. For a comparison, the P_1 conforming FEM from (5.27) is computed. Since the exact solution is not known for this example, the efficient and reliable error estimator $\eta_{\mathrm{C}} = \eta_{\mathrm{C}}(\mathcal{T})$ (with efficiency and reliability constants that are independent of the Lamé parameter λ [Carstensen, 2005]), defined by

$$\eta_{\mathrm{C}}^2(\mathcal{T}, T) := \|h_{\mathcal{T}} f\|_{L^2(T)}^2 + h_T \sum_{E \in \mathcal{E}(T) \setminus \mathcal{E}(\Gamma_D)} \|[\mathbb{C}\varepsilon(u_{\mathrm{C}})]_E \nu_E\|_{L^2(E)}^2 \qquad \text{for all } T \in \mathcal{T},$$

$$\eta_{\mathrm{C}}(\mathcal{T}) := \sqrt{\sum_{T \in \mathcal{T}} \eta_{\mathrm{C}}^2(\mathcal{T}, T)}$$

for $\mathcal{E}(\Gamma_D) := \{E \in \mathcal{E} \mid E \subseteq \Gamma_D\}$ the set of edges that lie on the Dirichlet boundary, is plotted in Figure 5.10. These error estimators are approximately 250 times larger for the Poisson ratio $\nu = 0.4999$ in comparison with the Poisson ratio $\nu = 0.4$ on a triangulation with 391170 dofs. The error estimators for the discretization from Subsection 5.3.3 are almost of the same size for all considered Poisson ratios. Figure 5.11 depicts triangulations created by Algorithm 5.23 with approximately 1500 degrees of freedom for Poisson ratios $\nu = 0.4$ and $\nu = 0.4999$. The strong refinement towards the singularity at the re-entrant corner is clearly visible. Since φ is piecewise affine, the error estimator μ with respect to the data approximation vanishes and only the Dörfler marking ($\mu_\ell^2 \leq \kappa \mathfrak{y}_\ell^2$) was applied in Algorithm 5.23.

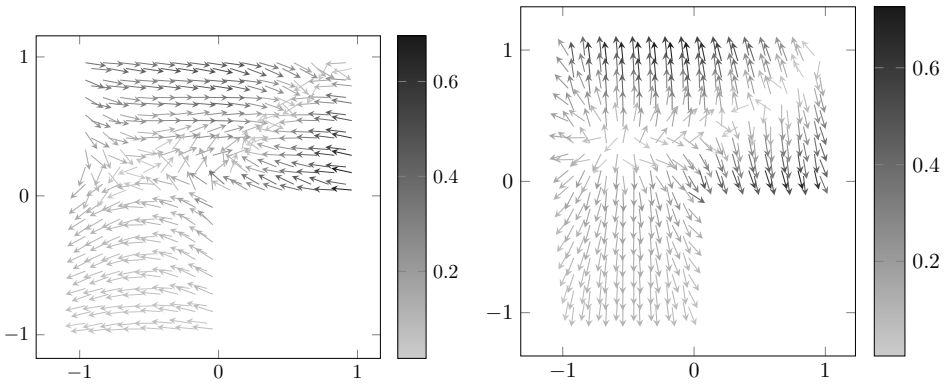

Figure 5.12.: Discrete solution on a uniform mesh with 225 nodes for the experiment on the L-shaped domain from Subsection 5.6.4.

5.6.4. L-shaped domain with piecewise constant f, II

This section considers the L-shaped domain $\Omega = (-1,1)^2 \setminus ([0,1] \times [-1,0])$ from Figure 3.4b with Dirichlet boundary $\Gamma_D := \partial\Omega$. Define the piecewise constant volume force $f \in L^2(\Omega;\mathbb{R}^2)$ by

$$f(x,y) := \begin{cases} (0,-1) & \text{if } x \le 0 \text{ and } y \ge 0, \\ (1,-1) & \text{if } x, y \ge 0, \\ (0,0) & \text{if } x, y \le 0. \end{cases}$$

Define $\varphi = (\varphi_{11}, \varphi_{12}; \varphi_{21}, \varphi_{22}) \in H(\operatorname{div}, \Omega; \mathbb{S})$ with $-\operatorname{div}\varphi = f$ by

$$\varphi_{11} := \begin{cases} y & \text{if } y \ge 0, \\ 0 & \text{else,} \end{cases}$$
$$\varphi_{12} := \varphi_{21} := 0,$$
$$\varphi_{22} := \begin{cases} -x & \text{if } x \ge 0, \\ 0 & \text{else} \end{cases}$$

and let $u_D = 0$.

Figure 5.12 depicts the discrete solution on a uniform triangulation with 225 nodes for Young's modulus $E = 10^5$ and Poisson ratio $\nu = 0.4$. The error estimators $\eta := \sqrt{\mu^2 + \mathfrak{y}^2}$ are plotted in Figure 5.13 on a sequence of uniformly red-refined triangulations and on a sequence of triangulations created by Algorithm 5.23 for Young's modulus $E = 10^5$ and Poisson ratios $\nu = 0.4$, 0.49, 0.499, and 0.4999. Uniform refinement yields a suboptimal convergence rate of $h^{2/3} \approx \texttt{ndof}^{-1/3}$, while Algorithm 5.23 recovers the optimal convergence rates of $\texttt{ndof}^{-1}$. In this example, $\operatorname{curl} f = 0$ in the sense of distributions and, hence, the solution of the Stokes problem (which is formally the limit problem for $\lambda \to \infty$), vanishes. The P_1 conforming

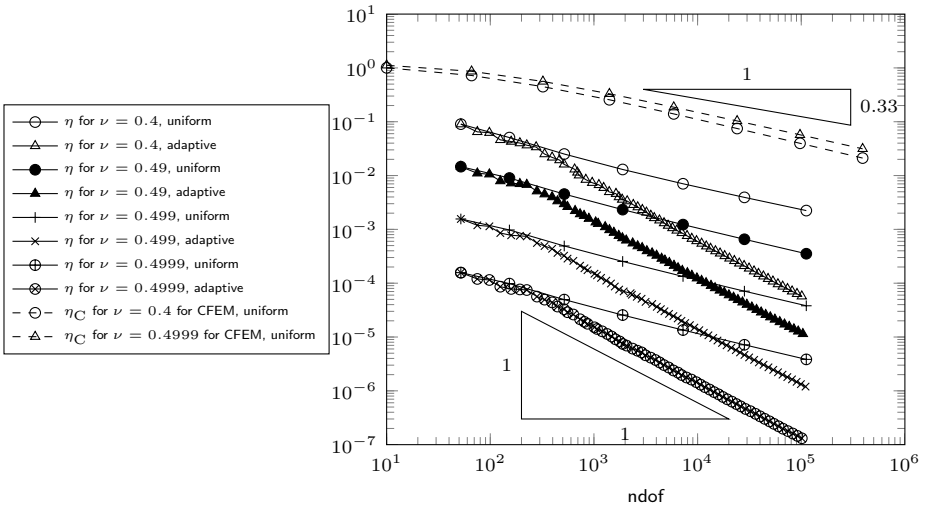

Figure 5.13.: Errors and error estimators for the experiment on the L-shaped domain from Subsection 5.6.4.

FEM shows no locking behaviour in this example. The error estimators for the discretization from Subsection 5.3.3 are even of smaller size for $\nu \to 1/2$. Figure 5.14 depicts triangulations created by Algorithm 5.23 with approximately 1500 degrees of freedom for Poisson ratios $\nu = 0.4$ and $\nu = 0.4999$. Since φ is piecewise affine, the error estimator μ with respect to the data approximation vanishes and only the Dörfler marking ($\mu_\ell^2 \leq \kappa \mathfrak{y}_\ell^2$) was applied in Algorithm 5.23.

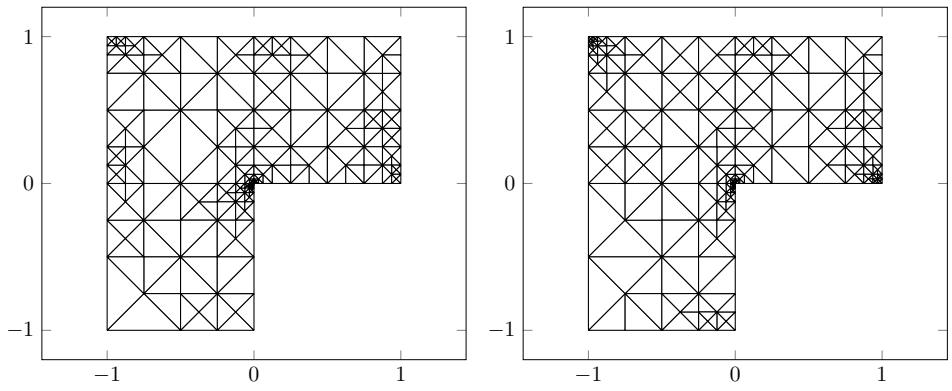

Figure 5.14.: Adaptively refined triangulations for $\nu = 0.4$ with 194 nodes (1632 dofs) and for $\nu = 0.4999$ with 192 nodes (1612 dofs) for the experiment on the L-shaped domain from Subsection 5.6.4.

6. Higher-order problems

This chapter considers mth-Laplace equations for any $m \in \mathbb{N}$: Seek $u \in H_0^m(\Omega)$ with

$$(-1)^m \Delta^m u = f \quad \text{in } \Omega. \tag{6.1}$$

Section 6.1 introduces some notation for mth-order tensors while some preliminary results are proved in Section 6.2. The proposed discretization of (6.1) in Section 6.4 is based on a novel Helmholtz decomposition for higher derivatives which is stated and proved in Section 6.3 and also allows for lowest-order ansatz spaces (even first-order polynomials for arbitrary m). Section 6.5 is devoted to the a posteriori analysis of the discretization and Section 6.6 introduces an adaptive algorithm and proves its optimal convergence rates. Section 6.7 concludes this chapter with some numerical experiments on fourth- and sixth-order problems ($m = 2$ and $m = 3$).

Throughout this chapter $\Omega \subseteq \mathbb{R}^2$ is a simply connected, bounded, polygonal Lipschitz domain.

6.1. Notation for higher-order tensors

This section is devoted to notation for higher-order tensors and tensor-valued functions. Definitions 6.1–6.4 introduce basic notation on tensors, while Definitions 6.5–6.6 specify notation related to differential operators for tensors.

Definition 6.1. Define the set of ℓ-tensors over $\mathbb{R}^2$ by

$$\mathbb{X}(\ell) := \begin{cases} \mathbb{R} & \text{for } \ell = 0, \\ \prod_{j=1}^{\ell} \mathbb{R}^2 = \mathbb{R}^2 \times \cdots \times \mathbb{R}^2 \cong \mathbb{R}^{2^\ell} & \text{for } \ell \geq 1. \end{cases}$$ ♦

Definition 6.2 (symmetric group, permutation)**.** Define the symmetric group $\mathfrak{S}_\ell := \{\sigma : \{1, \dots, \ell\} \to \{1, \dots, \ell\} \mid \sigma \text{ is bijective}\}$, i.e., the set of all permutations of $(1, \dots, \ell)$. ♦

Definition 6.3 (symmetric tensors, symmetric part of tensors)**.** Define the set of symmetric tensors $\mathbb{S}(\ell) \subseteq \mathbb{X}(\ell)$ by

$$\mathbb{S}(\ell) := \{A \in \mathbb{X}(\ell) \mid \forall (j_1, \dots, j_\ell) \in \{1,2\}^\ell \, \forall \sigma \in \mathfrak{S}_\ell : \; A_{j_1,\dots,j_\ell} = A_{j_{\sigma(1)},\dots,j_{\sigma(\ell)}}\}.$$

The symmetric part $\operatorname{sym} A \in \mathbb{S}(m)$ of a tensor $A \in \mathbb{X}(\ell)$ is defined by

$$(\operatorname{sym} A)_{j_1,\dots,j_\ell} := (\operatorname{card}(\mathfrak{S}_\ell))^{-1} \sum_{\sigma \in \mathfrak{S}_\ell} A_{j_{\sigma(1)},\dots,j_{\sigma(\ell)}}$$

for all $(j_1, \dots, j_\ell) \in \{1,2\}^\ell$. ♦

For $m = 2$, the set $\mathbb{S}(2)$ coincides with the set of symmetric 2×2 matrices, while for $m = 3$, the tensors $A \in \mathbb{S}(3)$ consist of the four different components A_{111}, $A_{112} = A_{121} = A_{211}$, $A_{122} = A_{212} = A_{221}$, and A_{222}.

The following definition generalizes the scalar product : and the matrix-vector product, in this context denoted as $\cdot$, from matrices to tensors of arbitrary order.

Definition 6.4 (scalar and dot product of tensors)**.** Let $A, B \in \mathbb{X}(\ell)$ be tensors and $q \in \mathbb{R}^2$ a vector. Define the scalar product $A : B \in \mathbb{R}$ and the dot product $A \cdot q \in \mathbb{X}(\ell - 1)$ by

$$\begin{aligned} A : B &:= \sum_{(j_1,\dots,j_\ell)\in\{1,2\}^\ell} A_{j_1,\dots,j_\ell} B_{j_1,\dots,j_\ell}, \\ (A \cdot q)_{j_1,\dots,j_{\ell-1}} &:= A_{j_1,\dots,j_{\ell-1},1}\, q_1 + A_{j_1,\dots,j_{\ell-1},2}\, q_2 \end{aligned}$$

for all $(j_1, \dots, j_{\ell-1}) \in \{1, 2\}^{\ell-1}$. ⧫

The following definition specifies some differential operators.

Definition 6.5 (differential operators)**.** Let $v \in H^\ell_0(\Omega)$ and $\sigma \in H^1(\Omega; \mathbb{X}(\ell))$ and define $\mathfrak{p} : \{1, 2\} \to \{1, 2\}$ by $\mathfrak{p}(1) = 2$ and $\mathfrak{p}(2) = 1$. Define the ℓth derivative $D^\ell v \in L^2(\Omega; \mathbb{X}(\ell))$ of v, the derivative $D\sigma \in L^2(\Omega; \mathbb{X}(\ell+1))$, the divergence $\operatorname{div}\sigma \in L^2(\Omega; \mathbb{X}(\ell-1))$, the Curl, $\operatorname{Curl}\sigma \in L^2(\Omega; \mathbb{X}(\ell+1))$, and the curl, $\operatorname{curl}\sigma \in L^2(\Omega; \mathbb{X}(\ell-1))$ by

$$\begin{aligned} (D^\ell v)_{j_1,\dots,j_\ell} &:= \frac{\partial^\ell}{\partial x_{j_1} \dots \partial x_{j_\ell}} v, \\ (D\sigma)_{j_1,\dots,j_{\ell+1}} &:= \frac{\partial}{\partial x_{j_{\ell+1}}} \sigma_{j_1,\dots,j_\ell}, \\ (\operatorname{div}\sigma)_{j_1,\dots,j_{\ell-1}} &:= \frac{\partial}{\partial x_1} \sigma_{j_1,\dots,j_{\ell-1},1} + \frac{\partial}{\partial x_2} \sigma_{j_1,\dots,j_{\ell-1},2} \\ (\operatorname{Curl}\sigma)_{j_1,\dots,j_{\ell+1}} &:= (-1)^{j_{\ell+1}} \frac{\partial}{\partial x_{\mathfrak{p}(j_{\ell+1})}} \sigma_{j_1,\dots,j_\ell} \\ (\operatorname{curl}\sigma)_{j_1,\dots,j_{\ell-1}} &:= -\frac{\partial}{\partial x_2} \sigma_{j_1,\dots,j_{\ell-1},1} + \frac{\partial}{\partial x_1} \sigma_{j_1,\dots,j_{\ell-1},2} \end{aligned}$$

for $(j_1, \dots, j_{\ell+1}) \in \{1, 2\}^{\ell+1}$. ⧫

For $m = 2$, these definitions coincide with the row-wise application of D, div, Curl, and curl.

The L^2 scalar product $(\bullet, \bullet)_{L^2(\Omega)}$ of tensor-valued functions $f, g : \Omega \to \mathbb{X}(\ell)$ is defined by

$$(f, g)_{L^2(\Omega)} := \int_\Omega f : g \, dx.$$

Lemma 6.11 below proves the L^2-orthogonality of Curl and D^ℓ for tensors.

Definition 6.6. Let $\psi \in L^2(\Omega;\mathbb{X}(\ell))$. If there exists $g \in L^2(\Omega)$ such that

$$(\psi, D^\ell v)_{L^2(\Omega)} = (-1)^\ell (g, v)_{L^2(\Omega)} \qquad \text{for all } v \in H_0^\ell(\Omega),$$

then g is called the ℓth weak divergence of ψ, written $\operatorname{div}^\ell \psi := g$. The space $H(\operatorname{div}^\ell, \Omega) \subseteq L^2(\Omega;\mathbb{X}(\ell))$ is defined by

$$H(\operatorname{div}^\ell, \Omega) := \{\psi \in L^2(\Omega;\mathbb{X}(\ell)) \mid \exists \operatorname{div}^\ell \psi \text{ and } \operatorname{div}^\ell \psi \in L^2(\Omega)\}.$$

Define furthermore for $k \geq \ell$

$$H(\operatorname{div}^\ell, \Omega;\mathbb{X}(k)) := \left\{ \psi \in L^2(\Omega;\mathbb{X}(k)) \;\middle|\; \begin{array}{l} \forall (j_1,\dots,j_{k-\ell}) \in \{1,2\}^{k-\ell} : \\ \psi_{j_1,\dots,j_{k-\ell},\bullet} \in H(\operatorname{div}^\ell, \Omega) \end{array} \right\}. \qquad \blacklozenge$$

Remark 6.7. Note that the existence of the ℓth weak divergence does not imply the existence of any kth divergence for $1 \leq k < \ell$, e.g., $H(\operatorname{div}, \Omega;\mathbb{X}(\ell)) \not\subseteq H(\operatorname{div}^\ell, \Omega)$ for $\ell > 1$. $\blacklozenge$

6.2. Results for tensor-valued functions

The main result of this section is Theorem 6.9, which proves that $\|\operatorname{sym}\operatorname{Curl}\bullet\|_{L^2(\Omega)}$ defines a norm on the space Y defined in (6.6) below and can, thus, be viewed as a generalized Korn inequality. Lemma 6.11 shows orthogonality of $\operatorname{sym}\operatorname{Curl}$ and D^m. The following theorem is used in the proof of Theorem 6.9. Recall the definition of the Curl and the symmetric part of a tensor from Definitions 6.5 and 6.3.

Theorem 6.8. *Any $\gamma \in H^1(\Omega;\mathbb{S}(m-1))$ satisfies*

$$\|\operatorname{Curl}\gamma\|_{L^2(\Omega)} \lesssim \|\operatorname{sym}\operatorname{Curl}\gamma\|_{L^2(\Omega)} + \|\gamma\|_{L^2(\Omega)}.$$

Proof. The proof is subdivided in three steps.

Step 1. Let $0 \leq k \leq m$ and $\mathbf{j}(k) = (j_1,\dots,j_m) \in \{1,2\}^m$ with $j_\ell = 1$ for all $\ell \in \{1,\dots,k\}$ and $j_\ell = 2$ for all $\ell \in \{k+1,\dots,m\}$, i.e.,

$$\mathbf{j}(k) = (\underbrace{1,\dots,1}_{k},\underbrace{2,\dots,2}_{m-k}).$$

The combination of the definitions of sym and Curl reads

$$(\operatorname{sym}\operatorname{Curl}\gamma)_{\mathbf{j}(k)} = \operatorname{card}(\mathfrak{S}_m)^{-1} \sum_{\sigma\in\mathfrak{S}_m} (-1)^{j_{\sigma(m)}} \frac{\partial}{\partial x_{\mathfrak{p}(j_{\sigma(m)})}} \gamma_{j_{\sigma(1)},\dots,j_{\sigma(m-1)}}. \tag{6.2}$$

Let $\bar{\mathbf{j}}(k) := (j_1,\dots,j_{m-1}) \in \{1,2\}^{m-1}$ the multi-index with the same number of ones and the number of twos reduced by one and $\underline{\mathbf{j}}(k) := (j_2,\dots,j_m) \in \{1,2\}^{m-1}$

the multi-index with the same number of twos and the number of ones reduced by one, i.e.,

$$\bar{\mathbf{j}}(k) = (\underbrace{1,\dots,1}_{k},\underbrace{2,\dots,2}_{m-k-1}) \qquad \text{and} \qquad \underline{\mathbf{j}}(k) = (\underbrace{1,\dots,1}_{k-1},\underbrace{2,\dots,2}_{m-k}).$$

The symmetry of γ implies that

$$\gamma_{j_{\sigma(1)},\dots,j_{\sigma(m-1)}} = \begin{cases} \gamma_{\underline{\mathbf{j}}(k)} & \text{if } j_{\sigma(m)} = 1, \\ \gamma_{\bar{\mathbf{j}}(k)} & \text{if } j_{\sigma(m)} = 2. \end{cases}$$

Since the number of permutations $\sigma \in \mathfrak{S}_m$ such that $j_{\sigma(m)} = 1$ is $k\,\mathrm{card}(\mathfrak{S}_{m-1})$ and the number of permutations $\sigma \in \mathfrak{S}_m$ such that $j_{\sigma(m)} = 2$ is $(m-k)\,\mathrm{card}(\mathfrak{S}_{m-1})$, this implies that the expression in (6.2) equals

$$(\operatorname{sym}\operatorname{Curl}\gamma)_{\mathbf{j}(k)} = \mathrm{card}(\mathfrak{S}_m)^{-1}\mathrm{card}(\mathfrak{S}_{m-1})\left((m-k)\frac{\partial}{\partial x}\gamma_{\bar{\mathbf{j}}(k)} - k\frac{\partial}{\partial y}\gamma_{\underline{\mathbf{j}}(k)}\right).$$

Since $\mathrm{card}(\mathfrak{S}_m) = m!$ and $\mathrm{card}(\mathfrak{S}_{m-1}) = (m-1)!$, this simplifies to

$$(\operatorname{sym}\operatorname{Curl}\gamma)_{\mathbf{j}(k)} = \frac{m-k}{m}\,\frac{\partial}{\partial x}\gamma_{\bar{\mathbf{j}}(k)} - \frac{k}{m}\,\frac{\partial}{\partial y}\gamma_{\underline{\mathbf{j}}(k)}. \tag{6.3}$$

Step 2. This step applies Theorem 2.11 to operators N_k defined below. Step 3 then proves a relation between these operators and the sym Curl.

Define for $k \in \{1,\dots,m+1\}$, $s \in \{1,\dots,m\}$, and a multi-index $\kappa \in \{(1,0),(0,1)\}$

$$a_{k,s,\kappa} := \begin{cases} -(k-1)/m & \text{if } s = k-1 \text{ and } \kappa = (0,1), \\ (m-k+1)/m & \text{if } s = k \text{ and } \kappa = (1,0), \\ 0 & \text{else.} \end{cases}$$

Furthermore, define for $\xi \in \mathbb{R}^2$

$$\mathfrak{N}_{ks}\xi := \sum_{\kappa=(1,0),(0,1)} a_{k,s,\kappa}\xi^\kappa = \begin{cases} -(k-1)\xi_2/m & \text{if } s = k-1, \\ (m-k+1)\xi_1/m & \text{if } s = k, \\ 0 & \text{else} \end{cases}$$

with the multi-index notation $\xi^\kappa = \xi_1^{\kappa_1}\xi_2^{\kappa_2}$. Then the matrix $(\mathfrak{N}_{ks}\xi)_{\substack{1\le k\le(m+1)\\ 1\le s\le m}}$ reads

$$\frac{1}{m}\begin{pmatrix} m\xi_1 & 0 & 0 & 0 & \dots & 0 \\ -\xi_2 & (m-1)\xi_1 & 0 & 0 & \dots & 0 \\ 0 & -2\xi_2 & (m-2)\xi_1 & 0 & \dots & 0 \\ \vdots & & & & & \vdots \\ \vdots & & \ddots & \ddots & & \vdots \\ \vdots & & & & & \vdots \\ 0 & \dots & 0 & -(m-2)\xi_2 & 2\xi_1 & 0 \\ 0 & \dots & & 0 & -(m-1)\xi_2 & \xi_1 \\ 0 & \dots & & & 0 & -m\xi_2 \end{pmatrix} \in \mathbb{R}^{(m+1)\times m}.$$

If $\xi \neq 0$, the columns of this matrix are linearly independent. Define the operators $(N_k)_{k=1,\dots,m+1}$, $N_k : H^1(\Omega;\mathbb{R}^m) \to L^2(\Omega)$, for all $v = (v_1,\dots,v_m) \in H^1(\Omega;\mathbb{R}^m)$ by

$$N_k v := \sum_{s=1}^{m} \sum_{\kappa=(1,0),(0,1)} a_{k,s,\kappa} D^\kappa v_s.$$

Theorem 2.11 then proves

$$\sum_{s=1}^{m} \|v_s\|^2_{H^1(\Omega)} \lesssim \sum_{k=1}^{m+1} \|N_k v\|^2_{L^2(\Omega)} + \sum_{s=1}^{m} \|v_s\|^2_{L^2(\Omega)}. \tag{6.4}$$

Step 3. This step proves a relation between $(N_k)_{k=1,\dots,m+1}$ and sym Curl for a proper choice of $v = (v_1,\dots,v_m)$.

Define $v = (v_1,\dots,v_m) \in H^1(\Omega;\mathbb{R}^m)$ by setting for each $s \in \{1,\dots,m\}$ the function $v_s := \gamma_{\ell_1,\dots,\ell_{m-1}}$ with $\ell_1 = \cdots = \ell_{s-1} = 1$ and $\ell_s = \cdots = \ell_{m-1} = 2$ (with $(\ell_1,\dots,\ell_{m-1}) = (2,\dots,2)$ for $s = 1$ and $(\ell_1,\dots,\ell_{m-1}) = (1,\dots,1)$ for $s = m$). The symmetry of γ proves

$$\begin{aligned} \|\operatorname{Curl}\gamma\|^2_{L^2(\Omega)} &\lesssim \sum_{s=1}^{m} \|v_s\|^2_{H^1(\Omega)}, \\ \sum_{s=1}^{m} \|v_s\|^2_{L^2(\Omega)} &\approx \|\gamma\|^2_{L^2(\Omega)}. \end{aligned} \tag{6.5}$$

With the notation from Step 1 it holds that $v_s = \gamma_{\overline{\mathbf{j}}(s-1)} = \gamma_{\underline{\mathbf{j}}(s)}$ and the definition of N_k from Step 2 and (6.3) reveal

$$N_{k+1} v = \frac{m-k}{m} \frac{\partial}{\partial x} v_{k+1} - \frac{k}{m} \frac{\partial}{\partial y} v_k = (\operatorname{sym}\operatorname{Curl}\gamma)_{\mathbf{j}(k)}.$$

This leads to

$$\sum_{k=1}^{m+1} \|N_k v\|^2_{L^2(\Omega)} \leq \|\operatorname{sym}\operatorname{Curl}\gamma\|^2_{L^2(\Omega)}.$$

This, (6.5), and an application of (6.4) imply the assertion. ∎

Define, for $m \geq 1$, the spaces

$$\begin{aligned} \mathfrak{H}(\Omega, m-1) &:= \left\{ v \in H^1(\Omega;\mathbb{S}(m-1)) \,\middle|\, \textstyle\int_\Omega v\,dx = 0 \right\}, \\ Z &:= \{ \beta \in \mathfrak{H}(\Omega, m-1) \mid \operatorname{sym}\operatorname{Curl}\beta = 0 \}, \\ Y &:= \left\{ \gamma \in \mathfrak{H}(\Omega, m-1) \,\middle|\, \forall \beta \in Z:\ (\operatorname{Curl}\beta, \operatorname{Curl}\gamma)_{L^2(\Omega)} = 0 \right\}. \end{aligned} \tag{6.6}$$

A computation reveals for $m = 2$, that the spaces Z and Y read

$$\begin{aligned} Z &= \{ \gamma \in \mathfrak{H}(\Omega, 1) \mid \exists c_1 \in \mathbb{R}, c_2 \in \mathbb{R}^2 \text{ with } \gamma(x) = c_1 x + c_2 \}, \\ Y &= \left\{ \gamma \in H^1(\Omega;\mathbb{R}^2) \,\middle|\, \int_\Omega \gamma\,dx = 0 \text{ and } \int_\Omega \operatorname{div}\gamma\,dx = 0 \right\} \end{aligned} \tag{6.7}$$

and for $m = 3$ the space Z reads

$$Z = \left\{ \gamma \in \mathfrak{H}(\Omega, 2) \;\middle|\; \begin{array}{l} \exists c_1, c_2, c_3 \in \mathbb{R}, c_4 \in \mathbb{R}^{2\times 2} \text{ with} \\ \gamma(x,y) = \begin{pmatrix} c_1 x^2 + 2c_2 x & c_1 xy + c_2 y + c_3 x \\ c_1 xy + c_2 y + c_3 x & c_1 y^2 + 2c_3 y \end{pmatrix} + c_4 \end{array} \right\}.$$

The following theorem generalizes [Carstensen et al., 2014b, Lemma 3.3] from $m = 2$ to higher-order tensors $m > 2$ and states that $\|\operatorname{sym}\operatorname{Curl}\bullet\|_{L^2(\Omega)}$ defines a norm on Y. Note, that $\|\operatorname{Curl}\bullet\|_{L^2(\Omega)} = \|D\bullet\|_{L^2(\Omega)}$.

Theorem 6.9. *Any $\gamma \in Y$ satisfies*

$$\|\operatorname{Curl}\gamma\|_{L^2(\Omega)} \lesssim \|\operatorname{sym}\operatorname{Curl}\gamma\|_{L^2(\Omega)}.$$

Proof. Assume for contradiction that the statement does not hold. Then there exists a sequence $(\gamma_n)_{n\in\mathbb{N}} \in Y^{\mathbb{N}}$ with

$$n\,\|\operatorname{sym}\operatorname{Curl}\gamma_n\|_{L^2(\Omega)} \le \|\operatorname{Curl}\gamma_n\|_{L^2(\Omega)} = 1.$$

Since $Y \subseteq \mathfrak{H}(\Omega, m-1)$, Poincaré's inequality implies that all components of γ_n are bounded in $H^1(\Omega)$. Since $H^1(\Omega;\mathbb{X}(m-1))$ is reflexive and compactly embedded in $L^2(\Omega;\mathbb{X}(m-1))$, there exists a subsequence (not relabelled) with a limit $\gamma \in L^2(\Omega;\mathbb{X}(m-1))$, $\gamma_n \to \gamma$ in $L^2(\Omega;\mathbb{X}(m-1))$. This and Theorem 6.8 imply

$$\begin{aligned} \|\operatorname{Curl}(\gamma_n - \gamma_\ell)\|_{L^2(\Omega)} &\lesssim \|\operatorname{sym}\operatorname{Curl}(\gamma_n - \gamma_\ell)\|_{L^2(\Omega)} + \|\gamma_n - \gamma_\ell\|_{L^2(\Omega)} \\ &\le \frac{1}{n} + \frac{1}{\ell} + \|\gamma_n - \gamma_\ell\|_{L^2(\Omega)} \to 0 \qquad \text{as } n, \ell \to \infty. \end{aligned}$$

The Poincaré inequality and the completeness of $H^1(\Omega;\mathbb{X}(m-1))$ imply the existence of $\widetilde{\gamma} \in H^1(\Omega;\mathbb{X}(m-1))$ with $\gamma_n \to \widetilde{\gamma}$ in $H^1(\Omega;\mathbb{X}(m-1))$ and thus $\gamma = \widetilde{\gamma}$. It holds that $\|\operatorname{sym}\operatorname{Curl}\bullet\|_{L^2(\Omega)} \le \|\operatorname{Curl}\bullet\|_{L^2(\Omega)}$ and, therefore, $\|\operatorname{sym}\operatorname{Curl}\bullet\|_{L^2(\Omega)}$ defines a bounded functional on $H^1(\Omega;\mathbb{X}(m-1))$. Hence,

$$\|\operatorname{sym}\operatorname{Curl}\gamma\|_{L^2(\Omega)} = \lim_{n\to\infty} \|\operatorname{sym}\operatorname{Curl}\gamma_n\|_{L^2(\Omega)} = 0. \tag{6.8}$$

Let $\beta \in Z$. Since $\gamma_n \in Y$, the Cauchy inequality reveals

$$\begin{aligned} (\operatorname{Curl}\beta, \operatorname{Curl}\gamma)_{L^2(\Omega)} &= (\operatorname{Curl}\beta, \operatorname{Curl}(\gamma - \gamma_n))_{L^2(\Omega)} \\ &\le \|\operatorname{Curl}\beta\|_{L^2(\Omega)}\ \|\operatorname{Curl}(\gamma - \gamma_n)\|_{L^2(\Omega)} \to 0 \qquad \text{as } n \to \infty. \end{aligned}$$

This and (6.8) lead to $\gamma \in Z \cap Y$ and therefore $\gamma = 0$. This contradicts $\|\operatorname{Curl}\gamma\|_{L^2(\Omega)} = \lim_{n\to\infty} \|\operatorname{Curl}\gamma_n\|_{L^2(\Omega)} = 1$ and, hence, implies the assertion. ∎

Remark 6.10 (dependence on the domain)**.** The proof by contradiction from Theorem 6.9 does not provide information about the dependence on the domain. A scaling argument reveals that it does not depend on the size of the domain, but it may depend on its shape. ♦

The following lemma proves the L^2 orthogonality of Curl and D^m for tensors.

Lemma 6.11 (L^2 orthogonality of Curl and D^m)**.** *Any* $\beta \in H^1(\Omega; \mathbb{X}(m-1))$ *and* $v \in H^m_0(\Omega)$ *satisfy*

$$(\operatorname{Curl}\beta, D^m v)_{L^2(\Omega)} = 0 \qquad \text{and} \qquad (\operatorname{sym}\operatorname{Curl}\beta, D^m v)_{L^2(\Omega)} = 0.$$

Proof. Since the Curl of a tensor-valued function is the row-wise application of the standard Curl, the assertion basically follows from $D^m v = D(D^{m-1}v)$ and the standard L^2 orthogonality of Curl and ∇. Indeed, let $\beta \in C^\infty(\Omega; \mathbb{X}(m-1))$, $v \in C^\infty_c(\Omega)$, and $\alpha = (j_1, \dots, j_m) \in \{1,2\}^m$. An integration by parts reveals

$$\begin{aligned}\int_\Omega \sum_{j_m=1}^{2} (\operatorname{Curl}\beta)_{j_1,\dots,j_m} (D^m v)_{j_1,\dots,j_m}\, dx &= \int_\Omega \sum_{j_m=1}^{2} (-1)^{j_m} \frac{\partial}{\partial x_{\mathfrak{p}(j_m)}} \beta_{j_1,\dots,j_{m-1}} D^\alpha v\, dx \\ &= \int_\Omega \sum_{j_m=1}^{2} (-1)^{j_m+1} \beta_{j_1,\dots,j_{m-1}} \frac{\partial}{\partial x_{\mathfrak{p}(j_m)}} D^\alpha v\, dx.\end{aligned}$$

Since the partial derivatives of v commute, this equals

$$\int_\Omega \beta_{j_1,\dots,j_{m-1}} \left(\frac{\partial^2}{\partial x_2 \partial x_1} D^{(j_1,\dots,j_{m-1})} v - \frac{\partial^2}{\partial x_1 \partial x_2} D^{(j_1,\dots,j_{m-1})} v \right) dx = 0.$$

This proves the first assertion. The symmetry of $D^m v$ implies

$$(\operatorname{sym}\operatorname{Curl}\beta, D^m v)_{L^2(\Omega)} = (\operatorname{Curl}\beta, D^m v)_{L^2(\Omega)} = 0.$$

The statement of the lemma then follows by density arguments. ∎

6.3. Helmholtz decomposition for higher orders

This section proves a Helmholtz decomposition of L^2 tensors into mth derivatives and the symmetric part of a Curl in Theorem 6.15. This is a generalization of the Helmholtz decomposition of Beirão da Veiga et al. [2007] for fourth-order problems ($m = 2$). The proof is based on Theorem 6.12 below, which characterizes mth-divergence-free smooth functions as symmetric parts of Curls.

Theorem 6.12. *Let* $m \geq 1$ *and* $\tau \in C^\infty(\Omega; \mathbb{S}(m))$ *with* $\operatorname{div}^m \tau = 0$. *Then there exists* $\gamma \in C^\infty(\Omega; \mathbb{X}(m-1))$ *with*

$$\tau = \operatorname{sym}\operatorname{Curl}\gamma.$$

Proof. The proof is based on mathematical induction.

Base case. For $m = 1$, the statement is a classical result [Rudin, 1976].

Induction hypothesis. Assume that the statement holds for $(m-1)$, i.e., for all $\widetilde{\tau} \in C^\infty(\Omega; \mathbb{S}(m-1))$ with $\operatorname{div}^{m-1}\widetilde{\tau} = 0$ there exists $\gamma \in C^\infty(\Omega; \mathbb{X}(m-2))$ with $\widetilde{\tau} = \operatorname{sym}\operatorname{Curl}\gamma$.

Inductive step. The inductive step is split in five steps. Suppose that $\tau \in C^\infty(\Omega;\mathbb{S}(m))$ with $\operatorname{div}^m \tau = 0$.

Step 1. Then $\operatorname{div}\tau \in C^\infty(\Omega;\mathbb{X}(m-1))$ and $\operatorname{div}^{m-1}\operatorname{div}\tau = 0$. Let $(j_1,\dots,j_{m-1}) \in \{1,2\}^{m-1}$ and $\sigma \in \mathfrak{S}_{m-1}$. Recall the definition of the divergence from Definition 6.5. The symmetry of τ implies

$$\begin{aligned}(\operatorname{div}\tau)_{j_1,\dots,j_{m-1}} &= \frac{\partial}{\partial x_1}\tau_{j_1,\dots,j_{m-1},1} + \frac{\partial}{\partial x_2}\tau_{j_1,\dots,j_{m-1},2}\\ &= \frac{\partial}{\partial x_1}\tau_{j_{\sigma(1)},\dots,j_{\sigma(m-1)},1} + \frac{\partial}{\partial x_2}\tau_{j_{\sigma(1)},\dots,j_{\sigma(m-1)},2}\\ &= (\operatorname{div}\tau)_{j_{\sigma(1)},\dots,j_{\sigma(m-1)}}.\end{aligned}$$

Hence, $\operatorname{div}\tau \in C^\infty(\Omega;\mathbb{S}(m-1))$. The induction hypothesis guarantees the existence of $\beta \in C^\infty(\Omega;\mathbb{X}(m-2))$ with $\operatorname{div}\tau = \operatorname{sym}\operatorname{Curl}\beta$.

Step 2. This step defines some $\widehat{\beta} \in C^\infty(\Omega;\mathbb{X}(m))$ with $\operatorname{div}\widehat{\beta} = \operatorname{div}\tau$.

Definitions 6.3 and 6.5 of sym and Curl for tensors combine to

$$\begin{aligned}&(\operatorname{sym}\operatorname{Curl}\beta)_{j_1,\dots,j_{m-1}}\\ &\quad= (\operatorname{card}(\mathfrak{S}_{m-1}))^{-1}\sum_{\sigma\in\mathfrak{S}_{m-1}}(-1)^{j_{\sigma(m-1)}}\frac{\partial}{\partial x_{\mathfrak{p}(j_{\sigma(m-1)})}}\beta_{j_{\sigma(1)},\dots,j_{\sigma(m-2)}}.\end{aligned}\tag{6.9}$$

Define $\widehat{\beta} \in C^\infty(\Omega;\mathbb{X}(m))$ by

$$\widehat{\beta}_{j_1,\dots,j_m} := (-1)^{\mathfrak{p}(j_m)}(\operatorname{card}(\mathfrak{S}_{m-1}))^{-1}\sum_{\substack{\sigma\in\mathfrak{S}_{m-1}\\ j_{\sigma(m-1)}=\mathfrak{p}(j_m)}}\beta_{j_{\sigma(1)},\dots,j_{\sigma(m-2)}}.\tag{6.10}$$

The definition of $\widehat{\beta}$ implies

$$(\operatorname{div}\widehat{\beta})_{j_1,\dots,j_{m-1}} = (\operatorname{card}(\mathfrak{S}_{m-1}))^{-1}\sum_{k=1}^{2}(-1)^{\mathfrak{p}(k)}\frac{\partial}{\partial x_k}\sum_{\substack{\sigma\in\mathfrak{S}_{m-1}\\ j_{\sigma(m-1)}=\mathfrak{p}(k)}}\beta_{j_{\sigma(1)},\dots,j_{\sigma(m-2)}}.$$

Since $j_{\sigma(m-1)} = \mathfrak{p}(k)$ if and only if $\mathfrak{p}(j_{\sigma(m-1)}) = k$, this equals

$$\begin{aligned}&(\operatorname{card}(\mathfrak{S}_{m-1}))^{-1}\sum_{k=1}^{2}\sum_{\substack{\sigma\in\mathfrak{S}_{m-1}\\ \mathfrak{p}(j_{\sigma(m-1)})=k}}(-1)^{j_{\sigma(m-1)}}\frac{\partial}{\partial x_{\mathfrak{p}(j_{\sigma(m-1)})}}\beta_{j_{\sigma(1)},\dots,j_{\sigma(m-2)}}\\ &\quad= (\operatorname{card}(\mathfrak{S}_{m-1}))^{-1}\sum_{\sigma\in\mathfrak{S}_{m-1}}(-1)^{j_{\sigma(m-1)}}\frac{\partial}{\partial x_{\mathfrak{p}(j_{\sigma(m-1)})}}\beta_{j_{\sigma(1)},\dots,j_{\sigma(m-2)}}\end{aligned}$$

and, hence, the combination of the foregoing two displayed formulae with (6.9) leads to $\operatorname{div}\widehat{\beta} = \operatorname{sym}\operatorname{Curl}\beta$. The combination with Step 1 proves

$$\operatorname{div}\widehat{\beta} = \operatorname{div}\tau.$$

Step 3. Since $\operatorname{div}(\tau - \widehat{\beta}) = 0$, the base case (applied "row-wise" to $(\tau - \widehat{\beta})_{j_1,\dots,j_{m-1},\bullet}$) guarantees the existence of $\gamma \in C^\infty(\Omega; \mathbb{X}(m-1))$ with $\tau - \widehat{\beta} = \operatorname{Curl}\gamma$.

Step 4. This step shows $\operatorname{sym}(\widehat{\beta}) = 0$.

Let $(j_1, \dots, j_m) \in \{1,2\}^m$ be fixed and let $N_1 := \operatorname{card}(\{k \in \{1,\dots,m\} \mid j_k = 1\})$ and $N_2 := \operatorname{card}(\{k \in \{1,\dots,m\} \mid j_k = 2\})$ be the number of ones and twos. Then

$$M_1(j_m) := N_1 - (2 - j_m) \quad \text{and} \quad M_2(j_m) := N_2 - (j_m - 1) \tag{6.11}$$

are the numbers of ones and twos in $(j_1, \dots, j_{m-1})$. Define the index set

$$\mathfrak{T} := \left\{ (k_1, \dots, k_{m-2}) \in \{1,2\}^{m-2} \;\middle|\; \sum_{\ell=1}^{m-2} k_\ell = (N_1 - 1) + 2(N_2 - 1) \right\}.$$

This set $\mathfrak{T}$ contains exactly all indices $(k_1, \dots, k_{m-2})$ with $(N_1 - 1)$ ones and $(N_2 - 1)$ twos. Note that $j_{\sigma(m-1)} = \mathfrak{p}(j_m)$ implies that $\{j_{\sigma(m-1)}, j_m\} = \{1,2\}$ and the elements of $\mathfrak{T}$ are the only indices which appear as indices of β in the sum in (6.10). For $\mathbf{j} \in \mathfrak{T}$, each $\beta_{\mathbf{j}}$ appears $M_1(j_m)!M_2(j_m)!$ times in that sum. This and (6.10) yield

$$\widehat{\beta}_{j_1,\dots,j_m} = (-1)^{\mathfrak{p}(j_m)} (\operatorname{card}(\mathfrak{S}_{m-1}))^{-1} M_1(j_m)!\, M_2(j_m)! \sum_{\mathbf{j} \in \mathfrak{T}} \beta_{\mathbf{j}}.$$

This reveals

$$\begin{aligned}
(\operatorname{sym}\widehat{\beta})_{j_1,\dots,j_m} &= (\operatorname{card}(\mathfrak{S}_m))^{-1} \sum_{\sigma \in \mathfrak{S}_m} \widehat{\beta}_{j_{\sigma(1)},\dots,j_{\sigma(m)}} \\
&= (\operatorname{card}(\mathfrak{S}_m))^{-1} (\operatorname{card}(\mathfrak{S}_{m-1}))^{-1} \\
&\qquad \times \left(\sum_{\mathbf{j} \in \mathfrak{T}} \beta_{\mathbf{j}} \right) \sum_{\sigma \in \mathfrak{S}_m} (-1)^{\mathfrak{p}(j_{\sigma(m)})} M_1(j_{\sigma(m)})!\, M_2(j_{\sigma(m)})!.
\end{aligned}$$

A reordering of the summands and the definition of M_1 and M_2 in (6.11) leads to

$$\begin{aligned}
&\sum_{\sigma \in \mathfrak{S}_m} (-1)^{\mathfrak{p}(j_{\sigma(m)})} M_1(j_{\sigma(m)})!\, M_2(j_{\sigma(m)})! \\
&\qquad = \left(M_1(1)!\, M_2(1)! \sum_{\substack{\sigma \in \mathfrak{S}_m \\ j_{\sigma(m)} = 1}} 1 \right) - \left(M_1(2)!\, M_2(2)! \sum_{\substack{\sigma \in \mathfrak{S}_m \\ j_{\sigma(m)} = 2}} 1 \right) \\
&\qquad = (N_1 - 1)!\, N_2! \operatorname{card}(\{\sigma \in \mathfrak{S}_m \mid j_{\sigma(m)} = 1\}) \\
&\qquad\qquad - N_1!\, (N_2 - 1)! \operatorname{card}(\{\sigma \in \mathfrak{S}_m \mid j_{\sigma(m)} = 2\}).
\end{aligned}$$

Since $\operatorname{card}(\{\sigma \in \mathfrak{S}_m \mid j_{\sigma(m)} = 1\}) = N_1 \operatorname{card}(\mathfrak{S}_{m-1})$ and $\operatorname{card}(\{\sigma \in \mathfrak{S}_m \mid j_{\sigma(m)} = 2\}) = N_2 \operatorname{card}(\mathfrak{S}_{m-1})$, this vanishes. This proves $\operatorname{sym}\widehat{\beta} = 0$.

Step 5. Step 4 and $\tau \in C^\infty(\Omega;\mathbb{S}(m))$ leads to

$$\tau = \operatorname{sym}(\tau) = \operatorname{sym}(\tau - \widehat{\beta}).$$

Step 3 then yields

$$\tau = \operatorname{sym}\operatorname{Curl}\gamma$$

and concludes the proof. ∎

The following theorem states a Helmholtz decomposition into mth derivatives and symmetric parts of Curls. The proof uses Theorem 6.12 and a density argument. The following assumption assumes that the constant in Theorem 6.9 does continuously depend on the domain. To this end, define

$$\Omega_\varepsilon := \{x \in \Omega \mid \operatorname{dist}(x, \partial\Omega) > \varepsilon\}. \tag{6.12}$$

Assumption 6.13. There exist sequences $(\varepsilon_n)_{n\in\mathbb{N}} \in \mathbb{R}^{\mathbb{N}}$, $(\delta_n)_{n\in\mathbb{N}} \in \mathbb{R}^{\mathbb{N}}$, and $(\Omega^{(n)})_{n\in\mathbb{N}}$ with $\Omega_{\delta_n} \subseteq \Omega^{(n)} \subseteq \Omega_{\varepsilon_n} \subseteq \Omega$ and $\varepsilon_n \to 0$ and $\delta_n \to 0$ as $n \to \infty$, such that the constants C_n from Theorem 6.9 with respect to $\Omega^{(n)}$ are uniformly bounded,

$$\sup_{n\in\mathbb{N}} C_n \lesssim 1.$$ ♦

Remark 6.14. Remark 6.10 implies that Assumption 6.13 is fulfilled on star-shaped domains. ♦

Recall the definition of Y from (6.6).

Theorem 6.15 (Helmholtz decomposition for higher-order derivatives)**.** *If Assumption 6.13 is satisfied, then it holds that*

$$L^2(\Omega;\mathbb{S}(m)) = D^m(H_0^m(\Omega)) \oplus \operatorname{sym}\operatorname{Curl} Y$$

and the decomposition is orthogonal in $L^2(\Omega;\mathbb{S}(m))$. For any $\tau \in L^2(\Omega;\mathbb{S}(m))$, $u \in H_0^m(\Omega)$, and $\alpha \in Y$ with $\tau = D^m u + \operatorname{sym}\operatorname{Curl}\alpha$, the function $u \in H_0^m(\Omega)$ solves

$$(D^m u, D^m v) = (\tau, D^m v) \qquad \text{for all } v \in H_0^m(\Omega). \tag{6.13}$$

Proof. Given $\tau \in L^2(\Omega;\mathbb{S}(m))$, let $u \in H_0^m(\Omega)$ be the solution to (6.13). Define $r := \tau - D^m u \in L^2(\Omega;\mathbb{S}(m))$ with $\operatorname{div}^m r = 0$ according to Definition 6.6.

Let $(\varepsilon_n)_{n\in\mathbb{N}}$, $(\delta_n)_{n\in\mathbb{N}}$, and $(\Omega^{(n)})_{n\in\mathbb{N}}$ denote the sequences from Assumption 6.13 and let $\eta_n \in C_c^\infty(\mathbb{R}^2)$ denote the standard mollifier [Evans, 2010] with $\operatorname{supp}(\eta_n) \subseteq B_{\varepsilon_n}(0)$ and define the regularized function $r_n := r * \eta_n \in C^\infty(\Omega;\mathbb{S}(m))$ with convolution $*$. Then $r_n \to r$ in $L^2(\Omega;\mathbb{S}(m))$ as $n \to \infty$. Recall the definition of Ω_{ε_n} from (6.12). Since $\operatorname{supp}(\eta_n) \subseteq B_{\varepsilon_n}(0)$ and $\operatorname{div}^m r = 0$, it follows

$(\operatorname{div}^m r_n)|_{\Omega_{\varepsilon_n}} = (r * D^m \eta_n)|_{\Omega_{\varepsilon_n}} = 0$. Since $\Omega^{(n)} \subseteq \Omega_{\varepsilon_n}$, Theorem 6.12 guarantees the existence of $\gamma_n \in C^\infty(\Omega^{(n)}; \mathbb{X}(m-1))$ with $r_n|_{\Omega^{(n)}} = \operatorname{sym}\operatorname{Curl}\gamma_n$. Recall the definition of $\mathfrak{H}(\Omega, m-1)$ from (6.6) and define

$$\begin{aligned} Z_n &:= \{\beta_n \in \mathfrak{H}(\Omega^{(n)}, m-1) \mid \operatorname{sym}\operatorname{Curl}\beta_n = 0\}, \\ Y_n &:= \{\zeta_n \in \mathfrak{H}(\Omega^{(n)}, m-1) \mid \forall \beta_n \in Z_n : \ (\operatorname{Curl}\beta_n, \operatorname{Curl}\zeta_n)_{L^2(\Omega)} = 0\}. \end{aligned}$$

Let $\widetilde{\gamma}_n \in Y_n$ be the orthogonal projection (with respect to $(\operatorname{Curl}\bullet, \operatorname{Curl}\bullet)_{L^2(\Omega)}$) of γ_n to Y_n. Then $\gamma_n - \widetilde{\gamma}_n \in Z_n$ and, hence, $\operatorname{sym}\operatorname{Curl}\widetilde{\gamma}_n = \operatorname{sym}\operatorname{Curl}\gamma_n = r_n|_{\Omega^{(n)}}$. Lions and Magenes [1972, Theorem 8.1] prove the existence of an extension $\rho_n \in H^1(\Omega; \mathbb{X}(m-1))$ of $\widetilde{\gamma}_n$ to Ω with $\|\rho_n\|_{H^1(\Omega)} \lesssim \|\widetilde{\gamma}_n\|_{H^1(\Omega^{(n)})}$. This, a Poincaré inequality, and Theorem 6.9 together with Assumption 6.13 imply

$$\|\rho_n\|_{H^1(\Omega)} \lesssim \|\operatorname{Curl}\widetilde{\gamma}_n\|_{L^2(\Omega^{(n)})} \lesssim \|\operatorname{sym}\operatorname{Curl}\widetilde{\gamma}_n\|_{L^2(\Omega^{(n)})} = \|r_n\|_{L^2(\Omega^{(n)})} \lesssim 1.$$

Since $H^1(\Omega; \mathbb{X}(m-1))$ is reflexive, there exists a subsequence of $(\rho_n)_{n\in\mathbb{N}}$ (again denoted by ρ_n) and $\gamma \in H^1(\Omega; \mathbb{X}(m-1))$ with $\rho_n \rightharpoonup \gamma$ in $H^1(\Omega; \mathbb{X}(m-1))$. Let $\varphi \in L^2(\Omega; \mathbb{X}(m))$ with $\operatorname{supp}(\varphi) \subseteq \Omega_{\delta_n}$. Since $\Omega_{\delta_n} \subseteq \Omega^{(n)}$ and therefore $\operatorname{sym}\operatorname{Curl}\rho_n|_{\Omega_{\delta_n}} = \operatorname{sym}\operatorname{Curl}\widetilde{\gamma}_n|_{\Omega_{\delta_n}} = r_n$, it follows

$$(\varphi, \operatorname{sym}\operatorname{Curl}\gamma)_{L^2(\Omega)} = (\varphi, r)_{L^2(\Omega)} + (\varphi, \operatorname{sym}\operatorname{Curl}(\gamma - \rho_n))_{L^2(\Omega)} + (\varphi, r_n - r)_{L^2(\Omega)}.$$

Since $\rho_n \rightharpoonup \gamma$ in $H^1(\Omega; \mathbb{X}(m-1))$ and $r_n \to r$ in $L^2(\Omega; \mathbb{S}(m))$ and $\delta_n \to 0$, this leads to $\operatorname{sym}\operatorname{Curl}\gamma = r$. Let $\rho \in Y$ be the orthogonal projection of γ to Y (with respect to $(\operatorname{Curl}\bullet, \operatorname{Curl}\bullet)_{L^2(\Omega)}$). Then $\rho - \gamma \in Z$ and, hence, $\operatorname{sym}\operatorname{Curl}\rho = \operatorname{sym}\operatorname{Curl}\gamma = r$. This proves the decomposition.

The L^2-orthogonality follows from Lemma 6.11. ∎

6.4. Weak formulation and discretization

Subsection 6.4.1 introduces the weak formulation of problem (6.1) based on the Helmholtz decomposition from Section 6.3 and its discretization follows in Subsection 6.4.2.

6.4.1. Weak formulation

Recall the definition of the divergence from Definition 6.6 and the definition of Y from (6.6). Let $\varphi \in H(\operatorname{div}^m, \Omega)$ with $(-1)^m \operatorname{div}^m \varphi = f$ and consider the problem: Seek $(\sigma, \alpha) \in L^2(\Omega; \mathbb{S}(m)) \times Y$ with

$$\begin{aligned} (\sigma, \tau)_{L^2(\Omega)} + (\tau, \operatorname{sym}\operatorname{Curl}\alpha)_{L^2(\Omega)} &= (\varphi, \tau)_{L^2(\Omega)} \quad && \text{for all } \tau \in L^2(\Omega; \mathbb{S}(m)), \\ (\sigma, \operatorname{sym}\operatorname{Curl}\beta)_{L^2(\Omega)} &= 0 && \text{for all } \beta \in Y. \end{aligned} \tag{6.14}$$

The following theorem states the equivalence of this problem with (6.1).

Theorem 6.16 (existence of solutions)**.** *There exists a unique solution* $(\sigma,\alpha)\in L^2(\Omega;\mathbb{S}(m))\times Y$ *to* (6.14) *with*

$$\|\sigma\|^2_{L^2(\Omega)}+\|\operatorname{Curl}\alpha\|^2_{L^2(\Omega)}\lesssim\|\sigma\|^2_{L^2(\Omega)}+\|\operatorname{sym}\operatorname{Curl}\alpha\|^2_{L^2(\Omega)}=\|\operatorname{sym}\varphi\|^2_{L^2(\Omega)}\,. \quad (6.15)$$

If Assumption 6.13 is satisfied, then (σ,α) *satisfies* $\sigma=D^m u$ *for the solution* $u\in H^m_0(\Omega)$ *to* (6.1).

Proof. The inf-sup condition

$$\|\operatorname{Curl}\beta\|_{L^2(\Omega)}\lesssim\sup_{\tau\in L^2(\Omega;\mathbb{S}(m))\setminus\{0\}}\frac{(\tau,\operatorname{sym}\operatorname{Curl}\beta)_{L^2(\Omega)}}{\|\tau\|_{L^2(\Omega)}}$$

follows from Theorem 6.9. This and Theorem 2.8 proves the unique existence of a solution to (6.14). Since

$$\sigma+\operatorname{sym}\operatorname{Curl}\alpha=\operatorname{sym}(\varphi),$$

Theorem 6.9 leads to the stability (6.15).

If Assumption 6.13 is fulfilled, then the Helmholtz decomposition of Theorem 6.15 holds and the L^2 orthogonality of σ to $\operatorname{sym}\operatorname{Curl}Y$ yields the existence of $\widetilde{u}\in H^m_0(\Omega)$ with $\sigma=D^m\widetilde{u}$. The orthogonality of Lemma 6.11, $(-1)^m\operatorname{div}^m\varphi=f$, and the symmetry of the mth derivative imply for all $v\in H^m_0(\Omega)$ that

$$(D^m\widetilde{u},D^m v)_{L^2(\Omega)}=(\varphi,D^m v)_{L^2(\Omega)}-(D^m v,\operatorname{sym}\operatorname{Curl}\alpha)_{L^2(\Omega)}=(f,v).$$

Hence, $\widetilde{u}$ solves (6.1). ∎

6.4.2. Discretization

The discretization of (6.14) employs the discrete spaces

$$\begin{aligned}X_h(\mathcal{T})&:=P_k(\mathcal{T};\mathbb{S}(m)),\\ Y_h(\mathcal{T})&:=P_{k+1}(\mathcal{T};\mathbb{X}(m-1))\cap Y\end{aligned}$$

and seeks $\sigma_h\in X_h(\mathcal{T})$ and $\alpha_h\in Y_h(\mathcal{T})$ with

$$\begin{aligned}(\sigma_h,\tau_h)_{L^2(\Omega)}+(\tau_h,\operatorname{sym}\operatorname{Curl}\alpha_h)_{L^2(\Omega)}&=(\varphi,\tau_h)_{L^2(\Omega)}\quad&&\text{for all }\tau_h\in X_h(\mathcal{T}),\\ (\sigma_h,\operatorname{sym}\operatorname{Curl}\beta_h)_{L^2(\Omega)}&=0&&\text{for all }\beta_h\in Y_h(\mathcal{T}).\end{aligned}\quad (6.16)$$

Remark 6.17. Note that there is no constraint on the polynomial degree $k\geq 0$. A discretization with the lowest polynomial degree involves only piecewise constant and piecewise affine functions for any $m\geq 1$. This should be contrasted to a standard conforming FEM where the $H^m_0(\Omega)$ conformity causes that the lowest possible polynomial degree is very high (cf. the Argyris FEM with piecewise P_5 functions and 21 local degrees of freedom for $m=2$ or the conforming FEMs of Ženíšek [1970] for arbitrary m with piecewise $P_{4(m-1)+1}$ functions). Discontinuous Galerkin FEMs such as C^0 interior penalty methods [Engel et al., 2002, Brenner, 2012] need at least piecewise P_2 functions for $m=2$ and piecewise P_3 functions for $m=3$ [Gudi and Neilan, 2011]. ♦

Remark 6.18. Since the finite element spaces $X_h(\mathcal{T})$ and $Y_h(\mathcal{T})$ differ only in the number of components and the bilinear forms of (6.16) are similar for all m, an implementation in a single program which runs for all m is possible as illustrated in Figure 1.2 of the introduction. In particular, the system matrices are obtained by integration of standard FEM basis functions. ♦

Theorem 6.19 (best-approximation result)**.** *There exists a unique solution* $(\sigma_h, \alpha_h) \in X_h(\mathcal{T}) \times Y_h(\mathcal{T})$ *to* (6.16)*, which satisfies*

$$\begin{aligned} &\|\sigma - \sigma_h\|_{L^2(\Omega)} + \|\operatorname{sym}\operatorname{Curl}(\alpha - \alpha_h)\|_{L^2(\Omega)} \\ &\quad \lesssim \min_{\tau_h \in X_h(\mathcal{T})} \|\sigma - \tau_h\|_{L^2(\Omega)} + \min_{\beta_h \in Y_h(\mathcal{T})} \|\operatorname{sym}\operatorname{Curl}(\alpha - \beta_h)\|_{L^2(\Omega)}\,. \end{aligned} \tag{6.17}$$

Proof. Since $\operatorname{sym}\operatorname{Curl} Y_h(\mathcal{T}) \subseteq X_h(\mathcal{T})$, the inf-sup condition

$$\|\operatorname{sym}\operatorname{Curl}\beta_h\|_{L^2(\Omega)} \leq \sup_{\tau_h \in X_h(\mathcal{T})\setminus\{0\}} \frac{(\tau_h, \operatorname{sym}\operatorname{Curl}\beta_h)_{L^2(\Omega)}}{\|\tau_h\|_{L^2(\Omega)}} \qquad \text{for all } \beta_h \in Y_h(\mathcal{T})$$

is fulfilled with constant 1. Theorem 2.8 therefore leads to the unique existence of a solution of problem (6.16). This, the conformity of the discretization, and standard arguments for mixed FEMs [Boffi et al., 2013] lead to the best-approximation result (6.17). ■

Define the space

$$W_h(\mathcal{T}) := \{\tau_h \in X_h(\mathcal{T}) \mid \forall \beta_h \in Y_h(\mathcal{T}) :\ (\tau_h, \operatorname{sym}\operatorname{Curl}\beta_h)_{L^2(\Omega)} = 0\}. \tag{6.18}$$

The following lemma proves a projection property similar to Lemma 3.11.

Lemma 6.20 (projection property)**.** *Let* $\tau \in L^2(\Omega; \mathbb{S}(m))$ *with*

$$(\tau, \operatorname{sym}\operatorname{Curl}\beta)_{L^2(\Omega)} = 0 \qquad \textit{for all } \beta \in Y.$$

Then $\Pi_{X_h(\mathcal{T})}\tau \in W_h(\mathcal{T})$*. If* $\mathcal{T}_\star$ *is an admissible refinement of* $\mathcal{T}$ *and* $\tau_\star \in W_h(\mathcal{T}_\star)$*, then* $\Pi_{X_h(\mathcal{T})}\tau_\star \in W_h(\mathcal{T})$*.*

Proof. Let $\beta_h \in Y_h(\mathcal{T})$. Since $\operatorname{sym}\operatorname{Curl}\beta_h \in X_h(\mathcal{T})$, the conformity $Y_h(\mathcal{T}) \subseteq Y$ implies

$$(\Pi_{X_h(\mathcal{T})}\tau, \operatorname{sym}\operatorname{Curl}\beta_h) = (\tau, \operatorname{sym}\operatorname{Curl}\beta_h) = 0.$$

The same arguments apply to $\tau_\star \in W_h(\mathcal{T}_\star)$. ■

6.4.3. Application to Kirchhoff plates

For $m = 2$, the problem (6.1) becomes the biharmonic problem: Find $u \in H^2_0(\Omega)$ with

$$\Delta^2 u = f \qquad \text{in } \Omega. \tag{6.19}$$

This problem arises in the theory of Kirchhoff plates with clamped boundary. In this situation, the Helmholtz decomposition of Theorem 6.15 is already proved by Beirão da Veiga et al. [2007]. Let $\varphi \in H(\operatorname{div}^2, \Omega)$ with $\operatorname{div}^2 \varphi = f$. Since the plate bending problem is the most prominent instance of (6.1), the weak form (6.14) and its discretization (6.16) are discussed in more detail.

Recall Y from (6.7). The weak formulation of (6.19) based on the Helmholtz decomposition seeks $\sigma \in L^2(\Omega; \mathbb{S}(2))$ and $\alpha \in Y$ with

$$\begin{aligned} (\sigma, \tau)_{L^2(\Omega)} + (\tau, \operatorname{sym} \operatorname{Curl} \alpha)_{L^2(\Omega)} &= (\varphi, \tau)_{L^2(\Omega)} && \text{for all } \tau \in L^2(\Omega, \mathbb{S}(2)), \\ (\sigma, \operatorname{sym} \operatorname{Curl} \beta)_{L^2(\Omega)} &= 0 && \text{for all } \beta \in Y. \end{aligned}$$

The discrete spaces read $X_h(\mathcal{T}) = P_k(\mathcal{T}; \mathbb{S}(2))$ and $Y_h(\mathcal{T}) = P_{k+1}(\mathcal{T}; \mathbb{R}^2) \cap Y$. The discretization (6.16) seeks $\sigma_h \in X_h(\mathcal{T})$ and $\alpha_h \in Y_h(\mathcal{T})$ with

$$\begin{aligned} (\sigma_h, \tau_h)_{L^2(\Omega)} + (\tau_h, \operatorname{sym} \operatorname{Curl} \alpha_h)_{L^2(\Omega)} &= (\varphi, \tau_h)_{L^2(\Omega)} && \text{for all } \tau_h \in X_h(\mathcal{T}), \\ (\sigma_h, \operatorname{sym} \operatorname{Curl} \beta_h)_{L^2(\Omega)} &= 0 && \text{for all } \beta_h \in Y_h(\mathcal{T}). \end{aligned}$$

The best-approximation result in this context reads

$$\begin{aligned} &\|\sigma - \sigma_h\|_{L^2(\Omega)} + \|\operatorname{Curl}(\alpha - \alpha_h)\|_{L^2(\Omega)} \\ &\quad \lesssim \Big(\min_{\tau_h \in X_h(\mathcal{T})} \|\sigma - \tau_h\|_{L^2(\Omega)} + \min_{\beta_h \in Y_h(\mathcal{T})} \|\operatorname{Curl}(\alpha - \beta_h)\|_{L^2(\Omega)} \Big). \end{aligned}$$

If the solution is sufficiently smooth, say $\sigma \in H^{k+1}(\Omega; \mathbb{S}(2))$ and $\alpha \in H^{k+2}(\Omega; \mathbb{R}^2)$, this yields a convergence rate of $\mathcal{O}(h^{k+1})$.

For plate bending problems, Morley [1968] introduced a P_2 non-conforming finite element method with non-conforming finite element space

$$V_M(\mathcal{T}) := \left\{ v_h \in P_2(\mathcal{T}) \;\middle|\; \begin{array}{l} v_h \text{ is continuous at the interior nodes and vanishes at} \\ \text{boundary nodes; } \nabla_{\mathrm{NC}} v_h \text{ is continuous at the interior} \\ \text{edges' midpoints and vanishes at the midpoints of} \\ \text{boundary edges} \end{array} \right\}.$$

Carstensen et al. [2014b] prove the discrete Helmholtz decomposition

$$P_0(\mathcal{T}; \mathbb{S}(2)) = D^2_{\mathrm{NC}} V_M(\mathcal{T}) \oplus \operatorname{sym} \operatorname{Curl} \big(P_1(\mathcal{T}; \mathbb{R}^2) \cap Y \big).$$

This shows the relation

$$D^2_{\mathrm{NC}} V_M(\mathcal{T}) = W_h(\mathcal{T})$$

with $W_h(\mathcal{T})$ from (6.18). This means that in the lowest-order case, the solution is the discrete Hessian of a Morley finite element function. In this sense, the proposed new discretization (6.16) generalizes the Morley FEM to higher polynomial degrees.

6.5. A posteriori error analysis

Recall Definitions 6.4 and 6.5 for the dot product $\cdot$ and the curl operator for tensors. Define the local error estimator contributions

$$\eta^2(T) := \|\operatorname{sym}(\varphi) - \Pi_k \operatorname{sym}(\varphi)\|^2_{L^2(T)} + \|h_{\mathcal{T}} \operatorname{curl}_{\mathrm{NC}} \sigma_h\|^2_{L^2(T)} + h_T \sum_{E\in\mathcal{E}(T)} \|[\sigma_h]_E \cdot \tau_E\|^2_{L^2(E)}$$

and the global error estimator

$$\eta^2 := \sum_{T\in\mathcal{T}} \eta^2(T).$$

The following theorem proves efficiency and reliability of η.

Theorem 6.21 (efficiency and reliability)**.** *There exist constants $C_{\mathrm{eff}}, C_{\mathrm{rel}} > 0$ with*

$$C_{\mathrm{eff}}^{-2}\eta_\ell^2 \le \|\sigma - \sigma_h\|^2_{L^2(\Omega)} + \|\operatorname{sym}\operatorname{Curl}(\alpha - \alpha_h)\|^2_{L^2(\Omega)} \le C_{\mathrm{rel}}^2\eta_\ell^2$$

Proof. The proof is similar to that of Theorem 3.30 and is therefore only sketched. Let $X := L^2(\Omega;\mathbb{S}(m))$ and define the residuals

$$\begin{aligned} \operatorname{Res}_1(\sigma_h,\alpha_h;q) &:= (\sigma_h,\tau) + (\tau,\operatorname{sym}\operatorname{Curl}\alpha_h) - (\varphi,\tau) && \text{for all } \tau\in X,\\ \operatorname{Res}_2(\sigma_h;\beta) &:= (\sigma_h,\operatorname{sym}\operatorname{Curl}\beta) && \text{for all } \beta\in Y. \end{aligned}$$

The abstract theory of Carstensen [2005] proves

$$\|\sigma - \sigma_h\|^2_{L^2(\Omega)} + \|\operatorname{sym}\operatorname{Curl}(\alpha-\alpha_h)\|^2_{L^2(\Omega)} \approx \|\operatorname{Res}_1(\sigma_h,\alpha_h;\bullet)\|^2_{X^\star} + \|\operatorname{Res}_2(\sigma_h;\bullet)\|^2_{Y^\star}.$$

Since $\sigma_h + \operatorname{sym}\operatorname{Curl}\alpha_h = \Pi_k\operatorname{sym}(\varphi)$,

$$\|\operatorname{Res}_1(\sigma_h,\alpha_h;\bullet)\|_{X^\star} = \|\operatorname{sym}(\varphi) - \Pi_k\operatorname{sym}(\varphi)\|_{L^2(\Omega)}.$$

Since σ and σ_h are symmetric,

$$\operatorname{Res}_2(\sigma_h;\beta) = (\sigma_h,\operatorname{Curl}\beta) \qquad \text{for all } \beta\in Y.$$

This enables the arguments of Steps 3 and 4 in the proof of Theorem 3.30 and yields

$$\|\operatorname{Res}_2(\sigma_h;\bullet)\|^2_{X^\star} \approx \|h_{\mathcal{T}}\operatorname{curl}_{\mathrm{NC}}\sigma_h\|^2_{L^2(\Omega)} + \sum_{T\in\mathcal{T}} h_T \sum_{E\in\mathcal{E}(T)} \|[\sigma_h\cdot\tau_E]_E\|^2_{L^2(E)}. \qquad \blacksquare$$

6.6. Adaptive algorithm

This section defines the adaptive algorithm and proves its quasi-optimal convergence.

6.6.1. Adaptive algorithm and optimal convergence rates

As for the Poisson problem in Section 3.5, the adaptive algorithm is based on separate marking. Given a triangulation $\mathcal{T}_\ell$, define for all $T \in \mathcal{T}_\ell$ the local error estimator contributions by

$$\lambda^2(\mathcal{T}_\ell, T) := \|h_{\mathcal{T}} \operatorname{curl}_{\mathrm{NC}} \sigma_h\|^2_{L^2(T)} + h_T \sum_{E \in \mathcal{E}(T)} \|[\sigma_h]_E \cdot \tau_E\|^2_{L^2(E)},$$
$$\mu^2(T) := \|\operatorname{sym}(\varphi) - \Pi_k \operatorname{sym}(\varphi)\|^2_{L^2(T)}$$

and the global error estimators by

$$\lambda_\ell^2 := \lambda^2(\mathcal{T}_\ell, \mathcal{T}_\ell) \quad \text{with} \quad \lambda^2(\mathcal{T}_\ell, \mathcal{M}) := \sum_{T \in \mathcal{M}} \lambda^2(\mathcal{T}_\ell, T) \quad \text{for all } \mathcal{M} \subseteq \mathcal{T}_\ell,$$
$$\mu_\ell^2 := \mu^2(\mathcal{T}_\ell) \quad \text{with} \quad \mu^2(\mathcal{M}) := \sum_{T \in \mathcal{M}} \mu^2(T) \quad \text{for all } \mathcal{M} \subseteq \mathcal{T}_\ell.$$

The adaptive algorithm is driven by these two error estimators and runs the following loop.

Algorithm 6.22 (AFEM for higher-order problems)**.**
Input: Initial triangulation $\mathcal{T}_0$, parameters $0 < \theta_A \leq 1$, $0 < \rho_B < 1$, $0 < \kappa$.
for $\ell = 0, 1, 2, \dots$ **do**
Solve. Compute solution $(\sigma_\ell, \alpha_\ell) \in X_h(\mathcal{T}_\ell) \times Y_h(\mathcal{T}_\ell)$ of (6.16) with respect to $\mathcal{T}_\ell$.
Estimate. Compute local contributions of the error estimators $\big(\lambda^2(\mathcal{T}_\ell, T)\big)_{T \in \mathcal{T}_\ell}$ and $\big(\mu^2(T)\big)_{T \in \mathcal{T}_\ell}$.
if $\mu_\ell^2 \leq \kappa \lambda_\ell^2$ **then**
Mark. The Dörfler marking chooses a minimal subset $\mathcal{M}_\ell \subseteq \mathcal{T}_\ell$ such that $\theta_A \lambda_\ell^2 \leq \lambda_\ell^2(\mathcal{T}_\ell, \mathcal{M}_\ell)$.
Refine. Generate the smallest admissible refinement $\mathcal{T}_{\ell+1}$ of $\mathcal{T}_\ell$ in which at least all triangles in $\mathcal{M}_\ell$ are refined.
else
Mark. Compute a triangulation $\mathcal{T} \in \mathbb{T}$ with $\mu_{\mathcal{T}}^2 \leq \rho_B \mu_\ell^2$.
Refine. Generate the overlay $\mathcal{T}_{\ell+1}$ of $\mathcal{T}_\ell$ and $\mathcal{T}$.
end if
end for
Output: Sequence of triangulations $(\mathcal{T}_\ell)_{\ell \in \mathbb{N}_0}$, discrete solutions $(\sigma_\ell, \alpha_\ell)_{\ell \in \mathbb{N}_0}$ and error estimators $(\lambda_\ell)_{\ell \in \mathbb{N}_0}$ and $(\mu_\ell)_{\ell \in \mathbb{N}_0}$. ♦

Given an initial triangulation $\mathcal{T}_0$, recall the set of admissible triangulations $\mathbb{T}$ from Definition 2.4. Let $\mathbb{T}(N)$ denote the subset of all admissible triangulations with at most $\operatorname{card}(\mathcal{T}_0)+N$ triangles. For $s > 0$ and $(\sigma, \alpha, \varphi) \in L^2(\Omega; \mathbb{S}(m)) \times Y \times H(\operatorname{div}^m, \Omega)$,

define

$$|(\sigma,\alpha,\varphi)|_{\mathcal{A}_s} := \sup_{N\in\mathbb{N}_0} N^s \inf_{\mathcal{T}\in\mathbb{T}(N)} \Big(\big\|\sigma - \Pi_{X_h(\mathcal{T})}\sigma\big\|_{L^2(\Omega)} + \inf_{\beta_{\mathcal{T}}\in Y_h(\mathcal{T})} \|\operatorname{sym}\operatorname{Curl}(\alpha-\beta_{\mathcal{T}})\|_{L^2(\Omega)} + \|\varphi - \Pi_{X_h(\mathcal{T})}\varphi\|_{L^2(\Omega)}\Big).$$

Remark 6.23 (pure local approximation class)**.** A "row-wise" application of [Veeser, 2014, Theorem 3.2] proves as in Remark 3.38

$$|(\sigma,\alpha,\varphi)|_{\mathcal{A}_s} \approx |(\sigma,\alpha,\varphi)|_{\mathcal{A}'_s} := \sup_{N\in\mathbb{N}} N^s \inf_{\mathcal{T}\in\mathbb{T}(N)} \Big(\|\sigma - \Pi_{X_h(\mathcal{T})}\sigma\|_{L^2(\Omega)} + \big\|\operatorname{sym}(\operatorname{Curl}\alpha) - \Pi_{X_h(\mathcal{T})}\operatorname{sym}(\operatorname{Curl}\alpha)\big\|_{L^2(\Omega)} + \big\|\operatorname{sym}(\varphi) - \Pi_{X_h(\mathcal{T})}\operatorname{sym}(\varphi)\big\|_{L^2(\Omega)}\Big). \qquad \blacklozenge$$

In the following, we assume that the following axiom (B1) holds for the algorithm used in the step *Mark* for $\mu_\ell^2 > \kappa\lambda_\ell^2$ (see Remark 3.37). For the algorithm `Approx`, this assumption is a consequence of Axioms (B2) and (SA) from Subsection 6.6.5 [Carstensen and Rabus, 2015] (see Remark 3.37).

Assumption 6.24 ((B1) optimal data approximation)**.** Assume that $|(\sigma,\alpha,\varphi)|_{\mathcal{A}_s}$ is finite. Given a tolerance Tol, the algorithm used in *Mark* in the second case ($\mu_\ell^2 > \kappa\lambda_\ell^2$) in Algorithm 6.22 computes $\mathcal{T}_\star \in \mathbb{T}$ with

$$\operatorname{card}(\mathcal{T}_\star) - \operatorname{card}(\mathcal{T}_0) \lesssim \mathrm{Tol}^{-1/(2s)} \qquad \text{and} \qquad \mu^2(\mathcal{T}_\star) \le \mathrm{Tol}. \qquad \blacklozenge$$

The following theorem states optimal convergence rates of Algorithm 6.22.

Theorem 6.25 (optimal convergence rates of AFEM)**.** *Let $s > 0$. For $0 < \rho_B < 1$ and sufficiently small $0 < \kappa$ and $0 < \theta < 1$, Algorithm 6.22 computes sequences of triangulations $(\mathcal{T}_\ell)_{\ell\in\mathbb{N}}$ and discrete solutions $(\sigma_\ell,\alpha_\ell)_{\ell\in\mathbb{N}}$ for the right-hand side φ of optimal rate of convergence in the sense that*

$$(\operatorname{card}(\mathcal{T}_\ell) - \operatorname{card}(\mathcal{T}_0))^s \Big(\|\sigma-\sigma_\ell\|_{L^2(\Omega)} + \|\operatorname{sym}\operatorname{Curl}(\alpha-\alpha_\ell)\|_{L^2(\Omega)}\Big) \lesssim |(\sigma,\alpha,\varphi)|_{\mathcal{A}_s}.$$

The proof follows as for the Poisson problem in Section 3.5 from the abstract framework of Carstensen and Rabus [2015], under the assumptions (A1)–(A4) and (B2) and (SA) which are proved in Subsections 6.6.2–6.6.5, and the efficiency of Theorem 6.21.

6.6.2. (A1) stability and (A2) reduction

The following two theorems follow from the structure of the error estimator λ.

Theorem 6.26 (stability)**.** *Let $\mathcal{T}_\star$ be an admissible refinement of $\mathcal{T}$ and $\mathcal{M} \subseteq \mathcal{T}\cap\mathcal{T}_\star$. Let $(\sigma_{\mathcal{T}_\star},\alpha_{\mathcal{T}_\star}) \in X_h(\mathcal{T}_\star)\times Y_h(\mathcal{T}_\star)$ and $(\sigma_{\mathcal{T}},\alpha_{\mathcal{T}}) \in X_h(\mathcal{T})\times Y_h(\mathcal{T})$ be the respective discrete solutions to* (6.16)*. Then,*

$$|\lambda(\mathcal{T}_\star,\mathcal{M}) - \lambda(\mathcal{T},\mathcal{M})| \lesssim \|\sigma_{\mathcal{T}_\star} - \sigma_{\mathcal{T}}\|_{L^2(\Omega)}.$$

Proof. This follows with triangle inequalities, inverse inequalities and the trace inequality from Theorem 2.7 as in Cascon et al. [2008, Proposition 3.3]. ■

Theorem 6.27 (reduction). *Let $\mathcal{T}_\star$ be an admissible refinement of $\mathcal{T}$. Then there exists $0 < \rho_2 < 1$ and $\Lambda_2 < \infty$ such that*

$$\lambda^2(\mathcal{T}_\star, \mathcal{T}_\star \setminus \mathcal{T}) \le \rho_2 \lambda^2(\mathcal{T}, \mathcal{T} \setminus \mathcal{T}_\star) + \Lambda_2 \|\sigma_{\mathcal{T}_\star} - \sigma_{\mathcal{T}}\|^2.$$

Proof. This follows with a triangle inequality and the mesh-size reduction property $h^2_{\mathcal{T}_\star}|_T \le h^2_{\mathcal{T}}|_T/2$ for all $T \in \mathcal{T}_\star \setminus \mathcal{T}$ as in Cascon et al. [2008, Corollary 3.4]. ■

6.6.3. (A4) discrete reliability

Theorem 6.28 (discrete reliability). *Let $\mathcal{T}_\star$ be an admissible refinement of $\mathcal{T}$ with respective discrete solutions $(\sigma_{\mathcal{T}_\star}, \alpha_{\mathcal{T}_\star}) \in X_h(\mathcal{T}_\star) \times Y_h(\mathcal{T}_\star)$ and $(\sigma_{\mathcal{T}}, \alpha_{\mathcal{T}}) \in X_h(\mathcal{T}) \times Y_h(\mathcal{T})$ of (6.16). Then,*

$$\|\sigma_{\mathcal{T}} - \sigma_{\mathcal{T}_\star}\|^2 + \|\operatorname{sym}\operatorname{Curl}(\alpha_{\mathcal{T}} - \alpha_{\mathcal{T}_\star})\|_{L^2(\Omega)} \lesssim \lambda^2(\mathcal{T}, \mathcal{T} \setminus \mathcal{T}_\star) + \mu^2(\mathcal{T}, \mathcal{T} \setminus \mathcal{T}_\star).$$

Proof. The proof is similar to the proof of Theorem 3.43 and therefore only sketched.

Recall the definition of $W_h(\mathcal{T}_\star)$ from (6.18). Since $\sigma_{\mathcal{T}} - \sigma_{\mathcal{T}_\star} \in X_h(\mathcal{T}_\star)$, there exist $p_{\mathcal{T}_\star} \in W_h(\mathcal{T}_\star)$ and $r_{\mathcal{T}_\star} \in Y_h(\mathcal{T}_\star)$ with $\sigma_{\mathcal{T}} - \sigma_{\mathcal{T}_\star} = p_{\mathcal{T}_\star} + \operatorname{sym}\operatorname{Curl} r_{\mathcal{T}_\star}$. The discrete error can be split as

$$\|\sigma_{\mathcal{T}} - \sigma_{\mathcal{T}_\star}\|^2_{L^2(\Omega)} = (\sigma_{\mathcal{T}} - \sigma_{\mathcal{T}_\star}, p_{\mathcal{T}_\star})_{L^2(\Omega)} + (\sigma_{\mathcal{T}} - \sigma_{\mathcal{T}_\star}, \operatorname{sym}\operatorname{Curl} r_{\mathcal{T}_\star})_{L^2(\Omega)}. \tag{6.20}$$

The arguments of the proof of Theorem 3.43 prove for the first term on the right-hand side that

$$(\sigma_{\mathcal{T}} - \sigma_{\mathcal{T}_\star}, p_{\mathcal{T}_\star})_{L^2(\Omega)} \lesssim \mu(\mathcal{T}, \mathcal{T} \setminus \mathcal{T}_\star) \|p_{\mathcal{T}_\star}\|_{L^2(\Omega)}.$$

Since $\sigma_{\mathcal{T}} - \sigma_{\mathcal{T}_\star}$ is symmetric, the second term of the right-hand side of (6.20) equals

$$(\sigma_{\mathcal{T}} - \sigma_{\mathcal{T}_\star}, \operatorname{sym}\operatorname{Curl} r_{\mathcal{T}_\star})_{L^2(\Omega)} = (\sigma_{\mathcal{T}} - \sigma_{\mathcal{T}_\star}, \operatorname{Curl} r_{\mathcal{T}_\star})_{L^2(\Omega)}.$$

This enables the arguments from the proof of Theorem 3.43 and proves

$$(\sigma_{\mathcal{T}} - \sigma_{\mathcal{T}_\star}, \operatorname{sym}\operatorname{Curl} r_{\mathcal{T}_\star})_{L^2(\Omega)} \lesssim \lambda(\mathcal{T}, \mathcal{T} \setminus \mathcal{T}_\star) \|\operatorname{Curl} r_{\mathcal{T}_\star}\|_{L^2(\Omega)}.$$

Theorem 6.9 and $\|p_{\mathcal{T}_\star}\|^2_{L^2(\Omega)} + \|\operatorname{sym}\operatorname{Curl} r_{\mathcal{T}_\star}\|^2_{L^2(\Omega)} = \|\sigma_{\mathcal{T}} - \sigma_{\mathcal{T}_\star}\|^2_{L^2(\Omega)}$ yield the assertion. ■

6.6.4. (A3) quasi-orthogonality

Theorem 6.29 (general quasi-orthogonality). *Let $(\mathcal{T}_j \mid j \in \mathbb{N})$ be some sequence of triangulations with discrete solutions $(\sigma_j, \alpha_j) \in X_h(\mathcal{T}_j) \times Y_h(\mathcal{T}_j)$ to (6.16) and let $\ell \in \mathbb{N}$. Then,*

$$\sum_{j=\ell}^{\infty} \Big(\|\sigma_j - \sigma_{j-1}\|^2 + \|\operatorname{sym}\operatorname{Curl}(\alpha_j - \alpha_{j-1})\|^2 \Big) \lesssim \lambda^2_{\ell-1} + \mu^2_{\ell-1}.$$

Proof. The proof follows as in Theorem 3.44 with the projection property from Lemma 6.20, the discrete reliability from Theorem 6.28, and

$$\|\operatorname{Curl}\beta\|_{L^2(\Omega)} \lesssim \|\operatorname{sym}\operatorname{Curl}\beta\|_{L^2(\Omega)}$$

from Theorem 6.9. ∎

6.6.5. (B) data approximation

The following theorem states quasi-monotonicity and sub-additivity for the data-approximation error estimator μ. Carstensen and Rabus [2015] prove that this implies Assumption 6.24 if the algorithm `Approx` from Binev and DeVore [2004], Binev et al. [2004], Carstensen and Rabus [2015] is used in the second marking step ($\mu_\ell^2 \geq \kappa\lambda_\ell^2$) in Algorithm 6.22.

Theorem 6.30 ((B2) quasi-monotonicity and (SA) sub-additivity)**.** *Any admissible refinement $\mathcal{T}_\star$ of $\mathcal{T}$ satisfies*

$$\mu^2(\mathcal{T}_\star) \leq \mu^2(\mathcal{T}) \qquad \text{and} \qquad \sum_{\substack{T\in\mathcal{T}_\star\\ T\subseteq K}} \mu^2(T) \leq \mu^2(K) \quad \text{for all } K \in \mathcal{T}.$$

Proof. This follows directly from the definition of μ. ∎

6.7. Numerical experiments

This section is devoted to numerical experiments for the plate problem $\Delta^2 u = f$ and the sixth-order problem $-\Delta^3 u = f$. The discretization (6.16) is realized for $k = 0, 1$ for the plate problem and for $k = 0, 1, 2$ for the sixth-order problem. As in the foregoing chapters, the implementation is based on the software package AFEM [Carstensen et al., 2009] maintained at the Humboldt-Universität. The experiments compare the errors and error estimators on a sequence of uniformly red-refined triangulations (see Figure 3.3 for a red-refined triangle) with the errors and error estimators on a sequence of triangulations created by Algorithm 6.22 with bulk parameter $\theta = 0.1$ and $\kappa = 0.5$ and $\rho = 0.75$.

The convergence history plots are logarithmically scaled and display the error $\|\sigma - \sigma_h\|_{L^2(\Omega)}$ against the number of degrees of freedom of the linear system resulting from the Schur complement (see Remark 3.12).

6.7.1. Square with known solution for $m = 2$

The exact solution to

$$\begin{aligned}\Delta^2 u(x,y) = f(x,y) :=& 24(x^2 - 2x^3 + x^4 + y^2 - 2y^3 + y^4)\\ &+ 2(2 - 12x + 12x^2)(2 - 12y + 12y^2)\end{aligned}$$

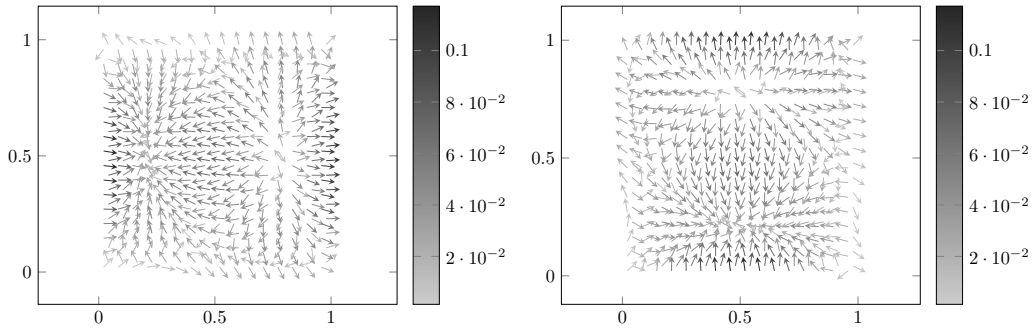

Figure 6.1.: Discrete solution for $k = 0$ for a uniform mesh with 289 nodes for the experiment from Subsection 6.7.1. The first plot shows the components $((\sigma_h)_{11}, (\sigma_h)_{12})$ and the second plot contains $((\sigma_h)_{21}, (\sigma_h)_{22})$.

with clamped boundary conditions $u|_{\partial\Omega} = (\partial u/\partial\nu)|_{\partial\Omega} = 0$ reads

$$u(x, y) = x^2(1 - x)^2y^2(1 - y)^2.$$

Define $\varphi = (\varphi_{jk})_{1\leq j,k\leq 2} \in H(\operatorname{div}^2, \Omega)$ by

$$\begin{aligned}
\varphi_{11} &:= 24(x^4/12 - x^5/10 + x^6/30) + (x^2 - 2x^3 + x^4)(2 - 12y + 12y^2),\\
\varphi_{22} &:= 24(y^4/12 - y^5/10 + y^6/30) + (y^2 - 2y^3 + y^4)(2 - 12x + 12x^2),\\
\varphi_{12} &:= \varphi_{21} := 0.
\end{aligned}$$

Then $\operatorname{div}^2 \varphi = f$ and φ is an admissible right-hand side for (6.16).

The discrete solution σ_h for $k = 0$ is depicted in Figure 6.1 on a uniform mesh with 289 nodes. The errors $\|\sigma - \sigma_h\|_{L^2(\Omega)}$ and error estimators η from Section 6.5 are plotted in Figure 6.2 versus the numbers of degrees of freedom. The errors and error estimators show an equivalent behaviour with an overestimation factor of approximately 10. The errors and error estimators show a convergence rate of $\texttt{ndof}^{-1/2}$ for $k = 0$ and of $\texttt{ndof}^{-1}$ for $k = 1$ on the sequence of uniformly red-refined triangulations as well as on the sequence of triangulations generated by Algorithm 6.22. Figure 6.3 displays triangulations with approximately 1500 degrees of freedom generated by Algorithm 6.22 for $k = 0$ and $k = 1$. The smoothness of the solution leads to almost uniform refinement. All marking steps in Algorithm 6.22 for $k = 0, 1$ applied the Dörfler marking ($\mu_\ell^2 \leq \kappa\lambda_\ell^2$).

6.7.2. L-shaped domain with unknown solution for $m = 2$

This subsection considers the problem

$$\Delta^2 u = 1$$

on the L-shaped domain $\Omega := (-1, 1)^2 \setminus ([0, 1] \times [-1, 0])$ from Figure 3.4b with clamped boundary conditions $u|_{\partial\Omega} = (\partial u/\partial\nu)|_{\partial\Omega} = 0$ and unknown solution. Define

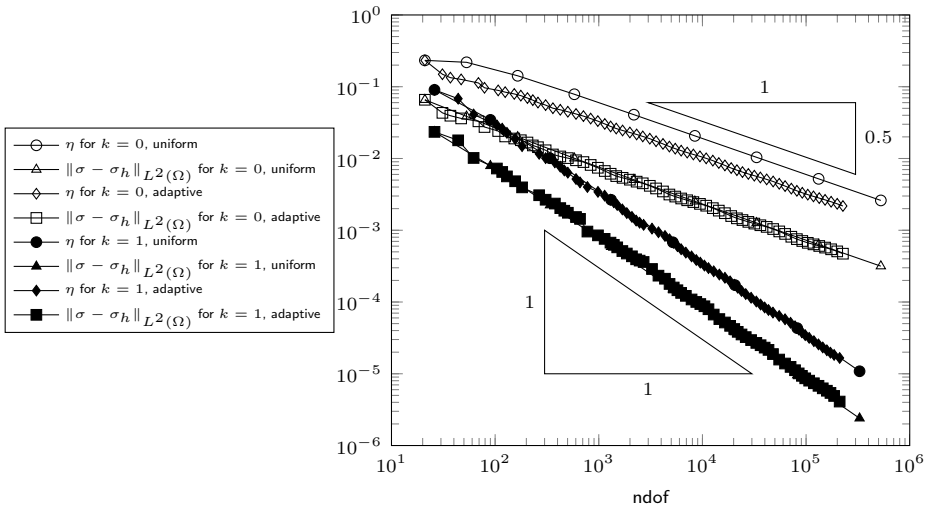

Figure 6.2.: Errors and error estimators for the experiment on the square from Subsection 6.7.1.

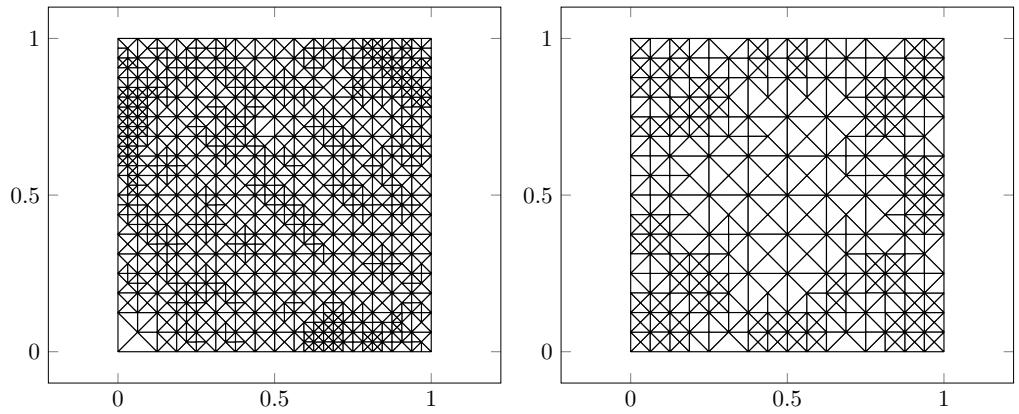

Figure 6.3.: Adaptively refined triangulations for $k = 0$ with 847 nodes (1697 dofs) and for $k = 1$ with 325 nodes (1506 dofs) for the experiment on the square from Subsection 6.7.1.

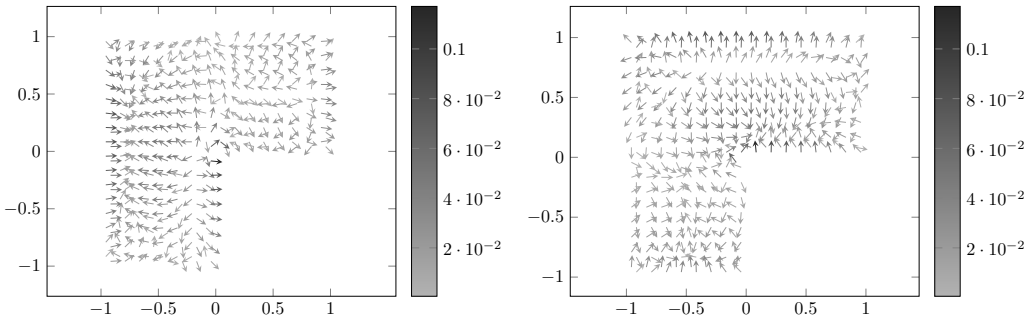

Figure 6.4.: Discrete solution for $k = 0$ for a uniform mesh with 225 nodes for the experiment from Subsection 6.7.2. The first plot shows the components $((\sigma_h)_{11}, (\sigma_h)_{12})$ and the second plot contains $((\sigma_h)_{21}, (\sigma_h)_{22})$.

the right-hand side $\varphi \in H(\operatorname{div}^2, \Omega)$ with $\operatorname{div}^2 \varphi = 1$ by

$$\varphi(x, y) := \begin{pmatrix} x^2/4 & 0 \\ 0 & y^2/4 \end{pmatrix}.$$

The discrete solution σ_h for $k = 0$ is depicted in Figure 6.4 on a uniform mesh with 225 nodes. The error estimators η from Section 6.5 are plotted in Figure 6.5 versus the degrees of freedom. For uniform mesh-refinement the convergence rate of the error estimator for $k = 1$ is $\texttt{ndof}^{-1/3}$. The convergence rate for $k = 0$ is slightly larger, but the size of the error estimator is larger as for $k = 1$. This suggests that the observed larger convergence rate is a preasymptotic effect. On the sequences of triangulations generated by Algorithm 6.22, the error estimators show the optimal convergence rates of $\texttt{ndof}^{-1/2}$ and $\texttt{ndof}^{-1}$ for $k = 0$ and $k = 1$, respectively. Figure 6.6 displays triangulations with approximately 1500 degrees of freedom generated by Algorithm 6.22 for $k = 0$ and $k = 1$. A stronger refinement towards the re-entrant corner is clearly visible. The marking with respect to the data-approximation ($\mu_\ell^2 > \kappa\lambda_\ell^2$ in Algorithm 6.22) is only applied at the first two levels for $k = 0$. All other marking steps for $k = 0, 1$ employed the Dörfler marking ($\mu_\ell^2 \leq \kappa\lambda_\ell^2$).

6.7.3. Square for $m = 3$

In this subsection, let $\Omega = (0, 1)^2$ be the unit square and $u \in H_0^3(\Omega)$ be defined by

$$u(x, y) = x^3(1 - x)^3 y^3(1 - y)^3$$

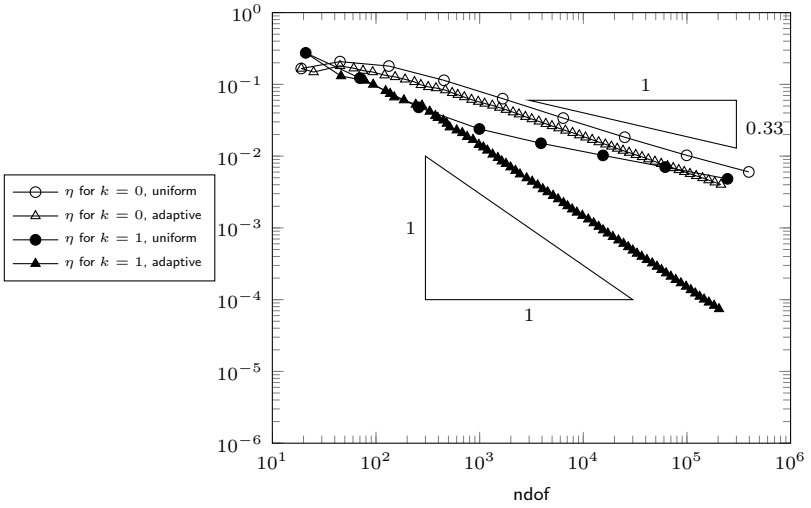

Figure 6.5.: Error estimators for the experiment on the L-shaped domain from Subsection 6.7.2.

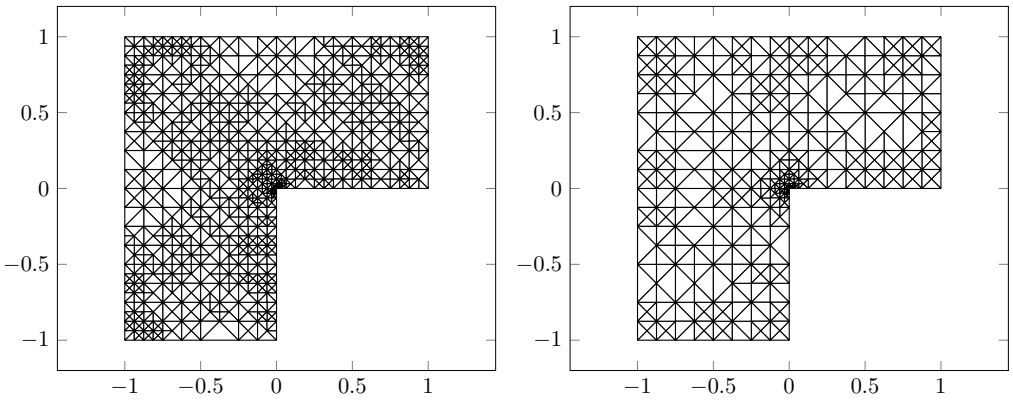

Figure 6.6.: Adaptively refined triangulations for $k = 0$ with 772 nodes (1547 dofs) and for $k = 1$ with 356 nodes (1635 dofs) for the experiment on the L-shaped domain from Subsection 6.7.2.

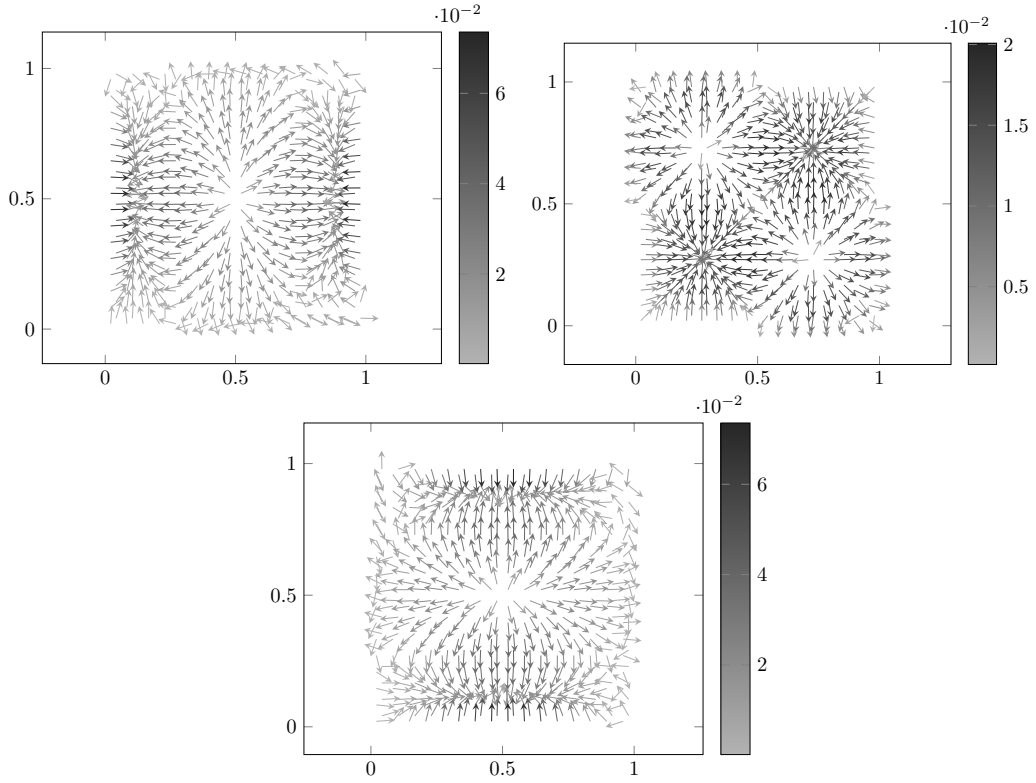

Figure 6.7.: Discrete solution for $k = 2$ for a uniform mesh with 289 nodes for the experiment from Subsection 6.7.3. The first plot shows the components $((\sigma_h)_{111}, (\sigma_h)_{112})$, the second plot contains $((\sigma_h)_{121}, (\sigma_h)_{122}) = ((\sigma_h)_{211}, (\sigma_h)_{212})$, and the third plot contains $((\sigma_h)_{221}, (\sigma_h)_{222})$.

with corresponding right-hand side $f := -\Delta^3 u$. Let $\varphi = (\varphi_{jk\ell})_{1\leq j,k,\ell\leq 2} \in H(\operatorname{div}^3, \Omega)$ be defined by

$$\varphi_{111}(x,y) := -\frac{1}{2}\int_0^x \int_0^s \int_0^t f(\xi, y)\, d\xi\, dt\, ds,$$
$$\varphi_{222}(x,y) := -\frac{1}{2}\int_0^y \int_0^s \int_0^t f(x, \xi)\, d\xi\, dt\, ds,$$
$$\varphi_{112} := \varphi_{121} := \varphi_{122} := \varphi_{211} := \varphi_{212} := \varphi_{221} := 0.$$

The functions φ_{111} and φ_{222} were computed with the computer algebra system Mathematica [Wolfram Research, Inc., 2012]. Then $-\operatorname{div}^3 \varphi = f$ and φ is an admissible right-hand side for (6.16).

The discrete solution σ_h for $k = 2$ is depicted in Figure 6.7 on a uniform mesh with 289 nodes. The errors $\|\sigma - \sigma_h\|_{L^2(\Omega)}$ and error estimators η from Section 6.5 are plotted in Figure 6.8 and (a different image section) in Figure 6.9 versus the number of degrees of freedom. The errors show the optimal convergence rates of

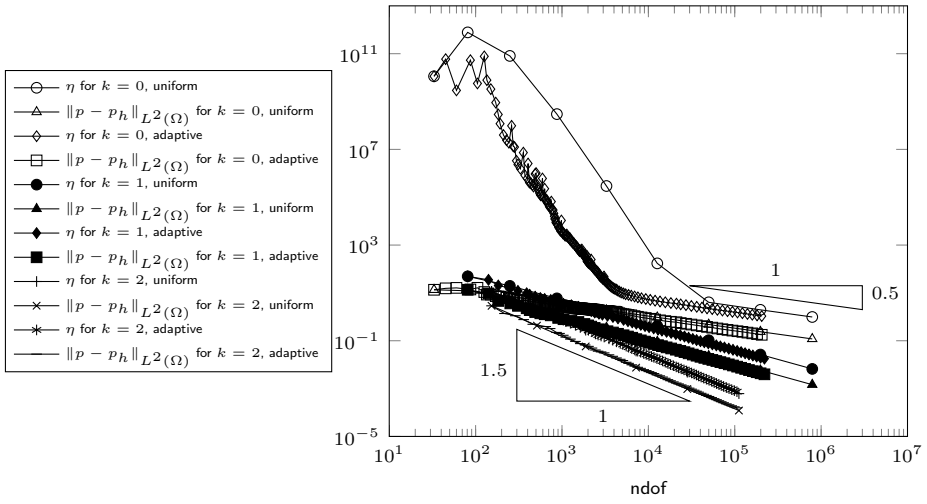

Figure 6.8.: Errors and error estimators for the experiment on the square for $m = 3$ from Subsection 6.7.3.

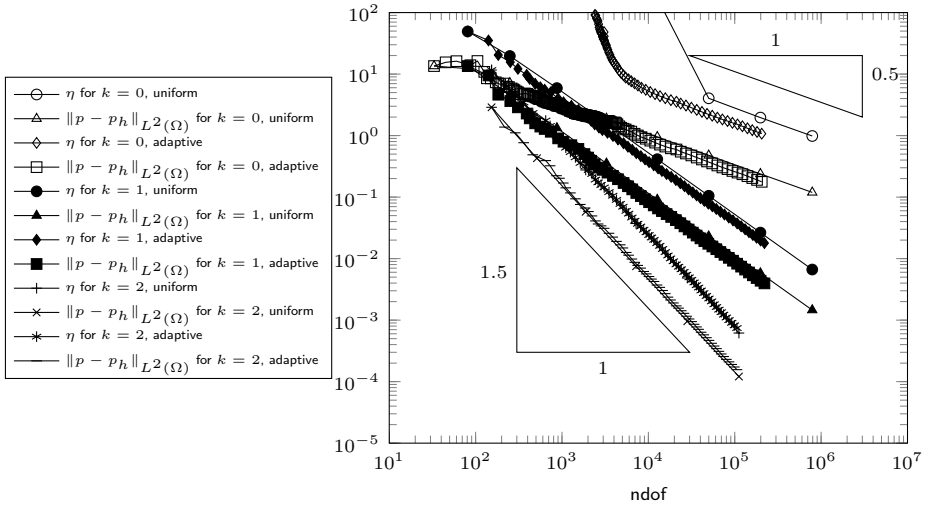

Figure 6.9.: Errors and error estimators for the experiment on the square for $m = 3$ from Subsection 6.7.3, zoom of Figure 6.8.

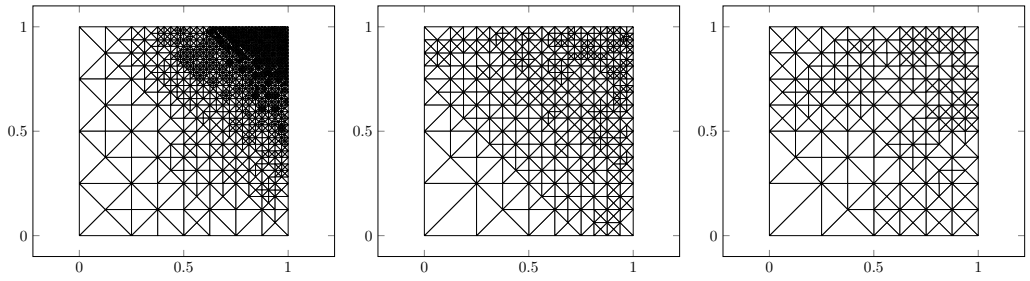

Figure 6.10.: Adaptively refined triangulations for $k = 0$ with 1716 nodes (5154 dofs), for $k = 1$ with 444 nodes (5163 dofs), and for $k = 2$ with 200 nodes (5067 dofs) for the experiment on the square from Subsection 6.7.3.

$\texttt{ndof}^{-1/2}$, $\texttt{ndof}^{-1}$, and $\texttt{ndof}^{-3/2}$ for $k = 0, 1, 2$ for uniform refinement as well as for the sequence of triangulations generated by Algorithm 6.22. The error estimators for $k = 1, 2$ show an equivalent behaviour as the respective errors with an overestimation of approximately 5. The error estimator for $k = 0$, however, shows a strong overestimation between approximately 10 and 10^{11} in the range up to 5×10^4 degrees of freedom.

Although the convergence rates are optimal, one has to consider that the H^3-seminorm of the exact solution $\|\sigma\|_{L^2(\Omega)}$ is approximately 2×10^{-2}. That means that the relative errors for $k = 1$ (resp. $k = 2$) are larger than 100% up to 10^5 (resp. 10^4) degrees of freedom and for $k = 0$, they do not even reach this threshold. While the L^2 norm of the function σ of interest is approximately 10^{-2}, the L^2 norm of φ (and thus $\|\operatorname{Curl} \alpha\|_{L^2(\Omega)}$) is approximately 80. The best-approximation result (6.17) therefore seems to suffer from the large term

$$\inf_{\beta_h \in Y_h(\mathcal{T})} \|\operatorname{Curl}(\alpha - \beta_h)\|_{L^2(\Omega)}$$

on the right-hand side.

Figure 6.10 displays triangulations with approximately 5000 degrees of freedom generated by Algorithm 6.22 for $k = 0, 1, 2$. Although the solution is smooth, a strong refinement towards the corner $(1, 1)$ can be observed. Since the relative errors for $k = 0, 1, 2$ are still over 100% for 5000 degrees of freedom, the discrete solution probably does not reflect the behaviour of the exact smooth solution.

All marking steps in Algorithm 6.22 for $k = 0, 1, 2$ used the Dörfler marking ($\mu_\ell^2 \leq \kappa \lambda_\ell^2$).

6.7.4. Singular solution on the square for $m = 3$

This example from Gudi and Neilan [2011] considers the unit square $\Omega = (0, 1)^2$ with exact solution $u \in H_0^3(\Omega)$ given by

$$u(x, y) = (x^2 + y^2)^{7.1/4} x^3 (1 - x)^3 y^3 (1 - y)^3.$$

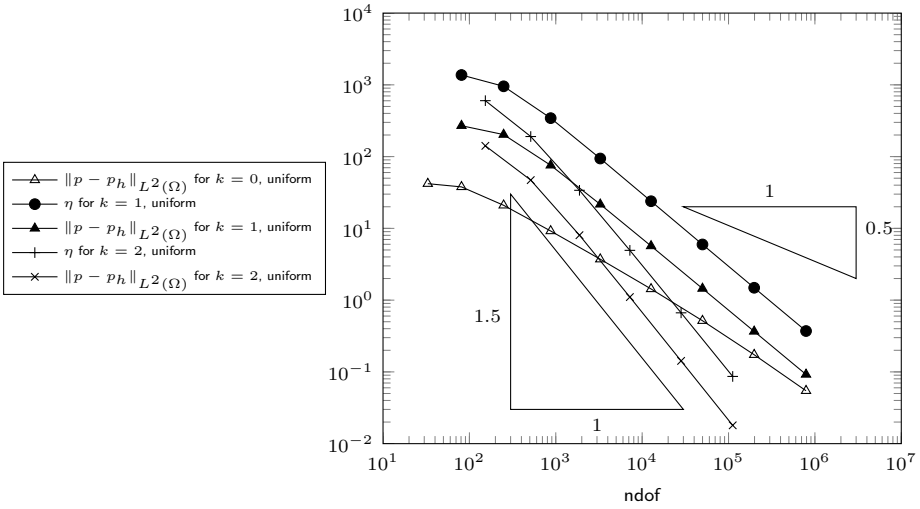

Figure 6.11.: Errors and error estimators for the experiment on the square for $m = 3$ from Subsection 6.7.4 for uniform refinement.

Let $f := -\Delta^3 u$ denote the right-hand side and define $\varphi = (\varphi_{jk\ell})_{1\le j,k,\ell\le 2} \in H(\operatorname{div}^3, \Omega)$ by

$$\varphi_{111}(x,y) := -\int_0^x \int_0^s \int_0^t f(\xi, y)\, d\xi\, dt\, ds,$$
$$\varphi_{222} := \varphi_{112} := \varphi_{121} := \varphi_{122} := \varphi_{211} := \varphi_{212} := \varphi_{221} := 0$$

The function φ_{111} was computed with the computer algebra system Mathematica [Wolfram Research, Inc., 2012]. Then $-\operatorname{div}^3 \varphi = f$ and φ is an admissible right-hand side for (6.16).

The errors $\|\sigma - \sigma_h\|_{L^2(\Omega)}$ for $k = 0, 1, 2$ and error estimators η for $k = 1, 2$ from Section 6.5 on a sequence of uniformly red-refined triangulations are plotted in Figure 6.11 versus the number of degrees of freedom. The observed convergence rates are $\texttt{ndof}^{-1/2}$ for $k = 0$, $\texttt{ndof}^{-1}$ for $k = 1$, and $\texttt{ndof}^{-3/2}$ for $k = 2$. Although the convergence rate for $k = 0$ is smaller than for $k = 1$, the size of the error is less in the whole computational range. The errors and error estimators for $k = 1, 2$ show an equivalent behaviour with an overestimation of approximately 5. The errors and error estimators for $k = 0$ are displayed in Figure 6.12 on a sequence of uniformly red-refined triangulations and on a sequence of triangulations generated by Algorithm 6.22. The error estimator overestimates the error by a factor between 10^2 and 10^{22}. The behaviour of the error and error estimator for the adaptive mesh-refinement at approximately $10^{4.1}$ degrees of freedom is displayed in Figure 6.13 in more detail. While the error estimator shows a strong peak, the error decreases more steeply. The errors and error estimators are plotted in Figures 6.14–6.16 for uniformly and adaptively refined triangulations for $k = 0, 1, 2$ (the error estimator

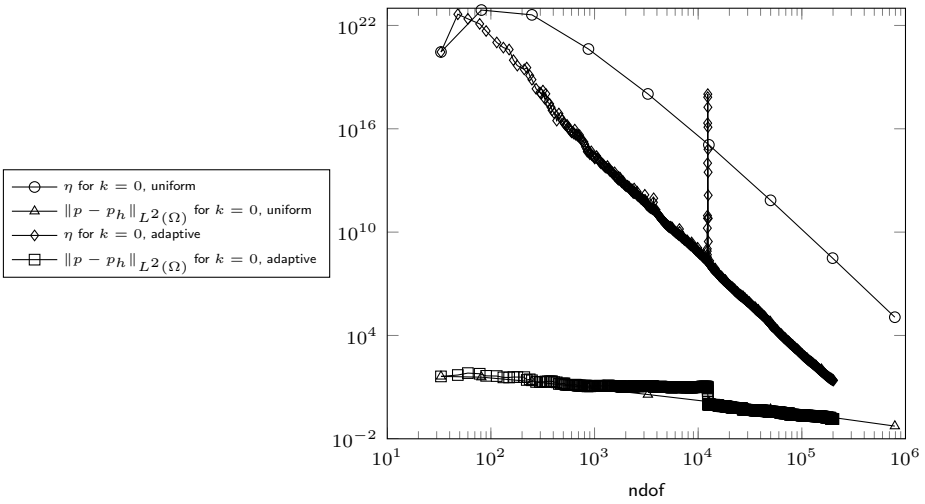

Figure 6.12.: Errors and error estimators for $k = 0$ for the experiment on the square for $m = 3$ from Subsection 6.7.4.

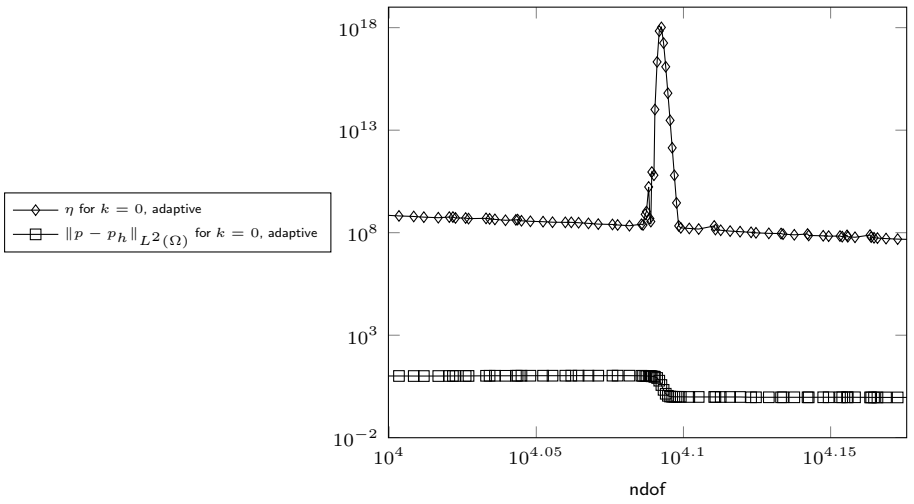

Figure 6.13.: Errors and error estimators for $k = 0$ for adaptive mesh-refinement for the experiment on the square for $m = 3$ from Subsection 6.7.4.

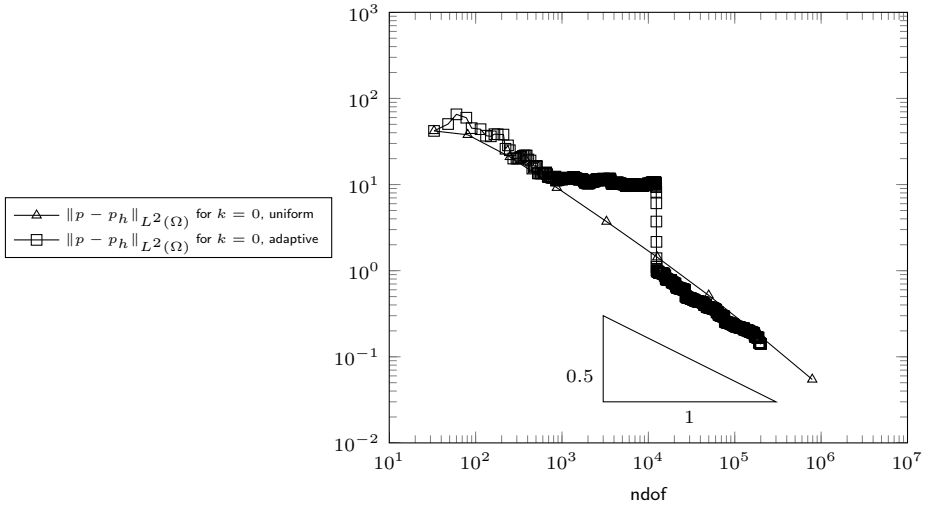

Figure 6.14.: Errors for $k = 0$ for the experiment on the square for $m = 3$ from Subsection 6.7.4.

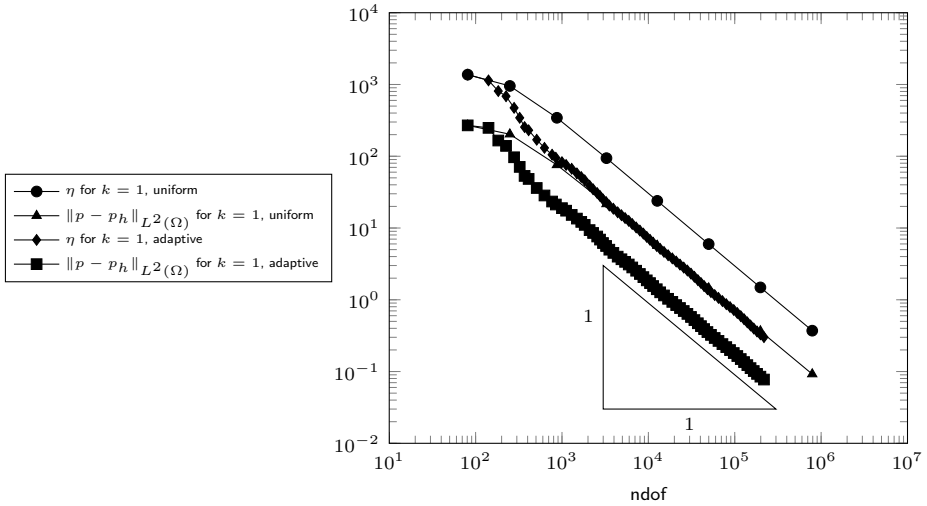

Figure 6.15.: Errors and error estimators for $k = 1$ for the experiment on the square for $m = 3$ from Subsection 6.7.4.

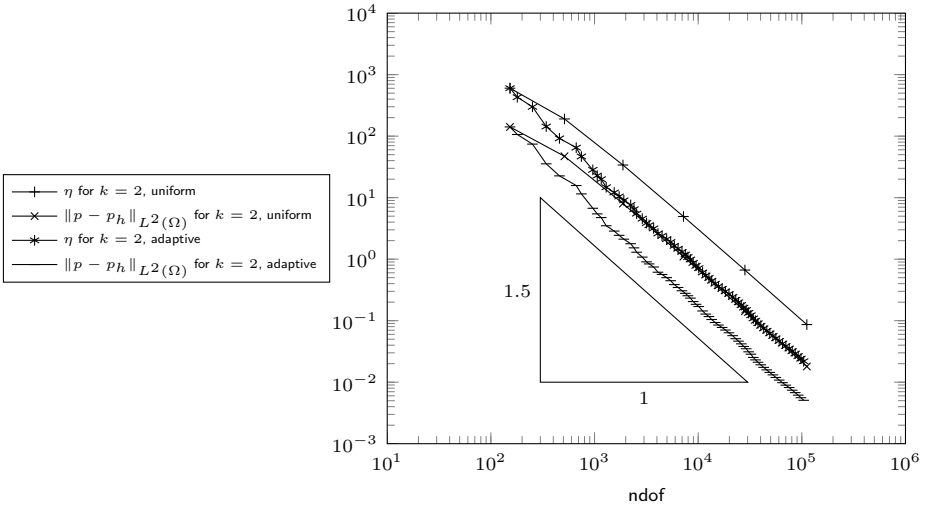

Figure 6.16.: Errors and error estimators for $k = 2$ for the experiment on the square for $m = 3$ from Subsection 6.7.4.

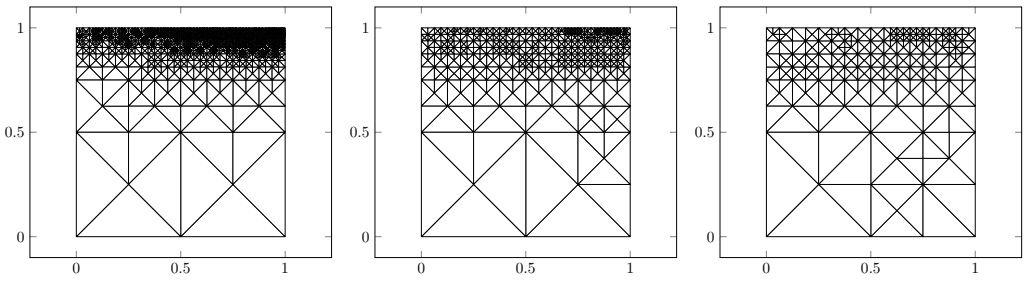

Figure 6.17.: Adaptively refined triangulations for $k = 0$ with 1676 nodes (5034 dofs), for $k = 1$ with 465 nodes (5376 dofs), and for $k = 2$ with 216 nodes (5427 dofs) for the experiment on the square from Subsection 6.7.4.

for $k = 0$ is again dropped in order to not overload the convergence graph). The errors and error estimators show the same convergence rates for uniform and adaptive mesh-refinement, but are of slightly smaller size on the sequence of triangulations generated by Algorithm 6.22. Although the convergence rates are optimal, one has to consider that the H^3 seminorm of the exact solution $\|\sigma\|_{L^2(\Omega)}$ is approximately 2×10^{-2}. That means that the relative error for $k = 2$ reaches the threshold 100% only from 35 000 degrees of freedom onwards on adaptively refined triangulations.

Figure 6.17 displays triangulations with approximately 5000 degrees of freedom generated by Algorithm 6.22 for $k = 0, 1, 2$. As in the previous example in Subsection 6.7.3, the refinement does not reflect the regularity of u (which has a singularity only at $(0, 0)$), but a strong refinement at $[0, 1] \times \{1\}$ is visible. The marking with respect to the data-approximation ($\mu_\ell^2 > \kappa\lambda_\ell^2$ in Algorithm 6.22) is only applied at levels 1 and 7 for $k = 2$. All other marking steps for $k = 0, 1, 2$ employed the Dörfler marking ($\mu_\ell^2 \leq \kappa\lambda_\ell^2$).

6.7.5. L-shaped domain for $m = 3$

This section considers the problem: Find $u \in H_0^3(\Omega)$ with

$$-\Delta^3 u = 1$$

and homogeneous Dirichlet boundary conditions on the L-shaped domain $\Omega := (-1, 1)^2 \setminus ([0, 1] \times [-1, 0])$ from Figure 3.4b. Let $\varphi = (\varphi_{jk\ell})_{1\leq j,k,\ell\leq 2} \in H(\mathrm{div}^3, \Omega)$ be defined by

$$\begin{aligned}\varphi_{111}(x, y) &:= -x^3/12,\\ \varphi_{222} &:= -y^3/12,\\ \varphi_{112} := \varphi_{121} &:= \varphi_{122} := \varphi_{211} := \varphi_{212} := \varphi_{221} := 0.\end{aligned}$$

Then $-\operatorname{div}^3 \varphi = 1$ and φ is an admissible right-hand side for (6.16).

The discrete solution σ_h for $k = 3$ is depicted in Figure 6.18 on a uniform mesh with 225 nodes.

Since the exact solution is not known, only the error estimators η from Section 6.5 are plotted in Figure 6.19 for $k = 0, 1, 2$ on a sequence of uniformly red-refined triangulations and on a sequence generated by Algorithm 6.22. On the sequence of uniformly refined meshes, the error estimators for $k = 1, 2$ show a convergence rate of $\texttt{ndof}^{-1/3}$, while the error estimator for $k = 0$ converges with rate $1/2$. However, this error estimator is of larger size than the error estimators for $k = 1, 2$ and it is therefore expected that the higher rate is a preasymptotic effect. Algorithm 6.22 leads to the optimal convergence rates of $\texttt{ndof}^{-1/2}$ for $k = 0$, $\texttt{ndof}^{-1}$ for $k = 1$, and $\texttt{ndof}^{-3/2}$ for $k = 2$.

Figure 6.20 displays triangulations with approximately 5000 degrees of freedom generated by Algorithm 6.22 for $k = 0, 1, 2$. The strong refinement towards the re-entrant corner is clearly visible for $k = 1, 2$, while for $k = 0$ the refinement is quasi-uniform. This is in agreement with the observed convergence rate for $k = 0$

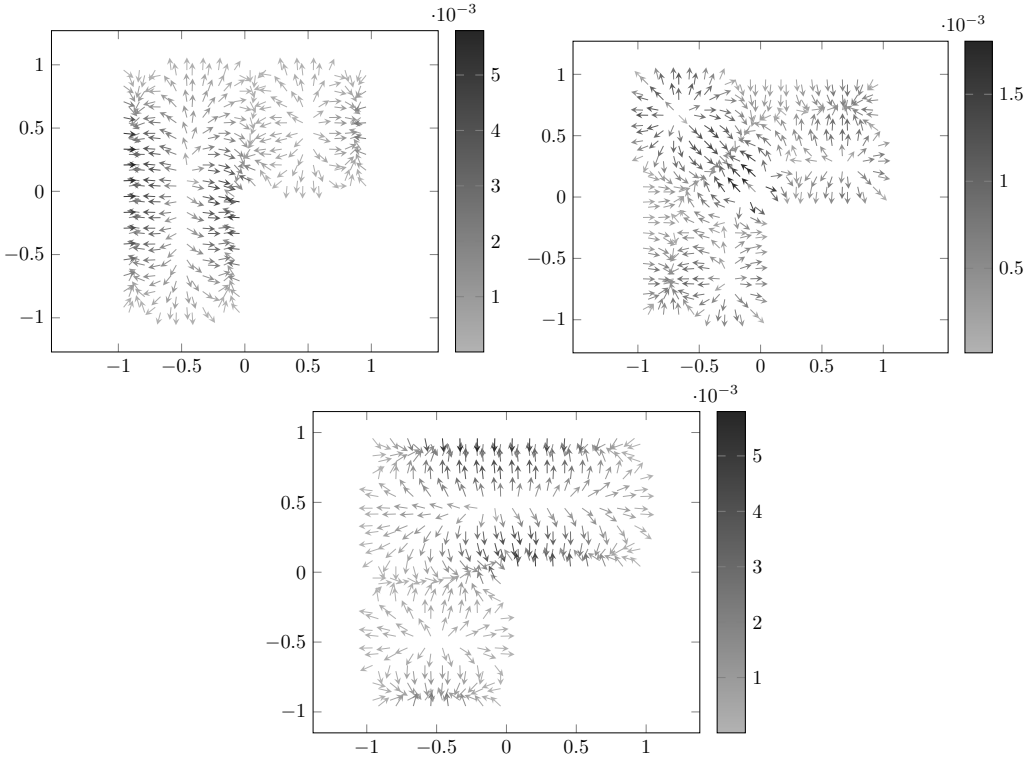

Figure 6.18.: Discrete solution for $k = 2$ for a uniform mesh with 225 nodes for the experiment from Subsection 6.7.5. The first plot shows the components $((\sigma_h)_{111}, (\sigma_h)_{112})$, the second plot contains $((\sigma_h)_{121}, (\sigma_h)_{122}) = ((\sigma_h)_{211}, (\sigma_h)_{212})$, and the third plot contains $((\sigma_h)_{221}, (\sigma_h)_{222})$.

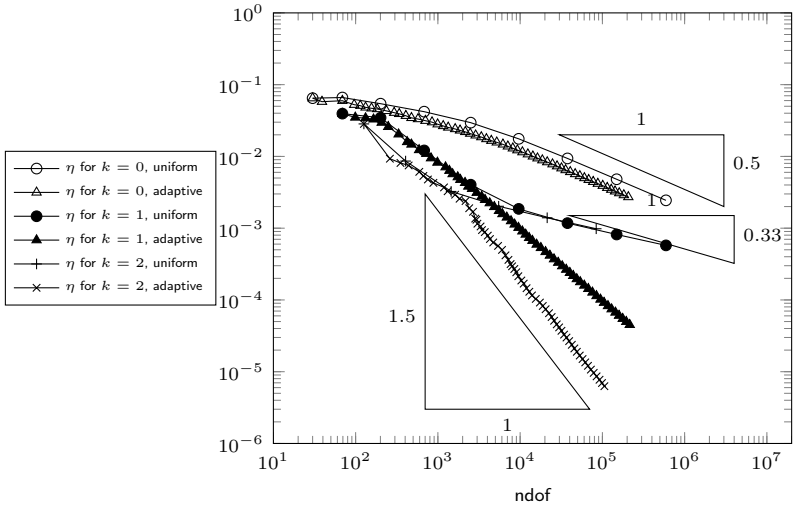

Figure 6.19.: Error estimators for the experiment on the L-shaped domain for $m = 3$ from Subsection 6.7.5.

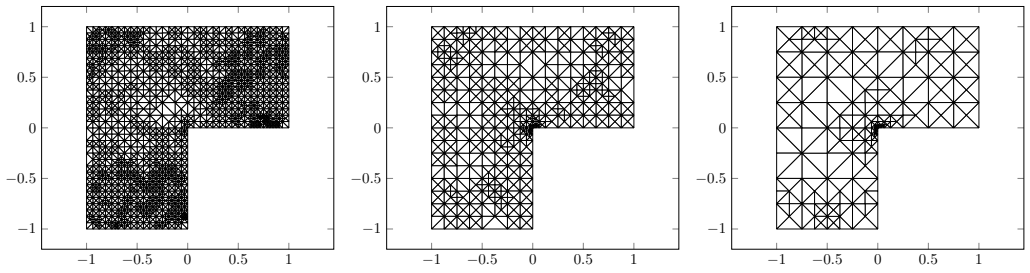

Figure 6.20.: Adaptively refined triangulations for $k = 0$ with 1730 nodes (5196 dofs), for $k = 1$ with 480 nodes (5529 dofs), and for $k = 2$ with 218 nodes (5391 dofs) for the experiment on the L-shaped domain from Subsection 6.7.5.

and the interpretation that the behaviour of the exact solution is not reflected in the discrete solution up to this number of degrees of freedom. The marking with respect to the data-approximation ($\mu_\ell^2 > \kappa\lambda_\ell^2$ in Algorithm 6.22) is only applied at levels 1 and 2 for $k = 0$. All other marking steps for $k = 0, 1, 2$ use the Dörfler marking ($\mu_\ell^2 \leq \kappa\lambda_\ell^2$).

Bibliography

A. Adini and R. Clough. Analysis of plate bending by the finite element method. NSF report g. 7337., 1961.

A. Alonso. Error estimators for a mixed method. *Numer. Math.*, 74(4):385–395, 1996.

A. Alonso Rodríguez, R. Hiptmair, and A. Valli. Mixed finite element approximation of eddy current problems. *IMA J. Numer. Anal.*, 24(2):255–271, 2004.

C. Amrouche, C. Bernardi, M. Dauge, and V. Girault. Vector potentials in three-dimensional non-smooth domains. *Math. Methods Appl. Sci.*, 21(9):823–864, 1998.

D. N. Arnold and F. Brezzi. Mixed and nonconforming finite element methods: implementation, postprocessing and error estimates. *RAIRO Modél. Math. Anal. Numér.*, 19(1):7–32, 1985.

D. N. Arnold and R. S. Falk. A uniformly accurate finite element method for the Reissner-Mindlin plate. *SIAM J. Numer. Anal.*, 26(6):1276–1290, 1989.

D. N. Arnold, F. Brezzi, and M. Fortin. A stable finite element for the Stokes equations. *Calcolo*, 21(4):337–344 (1985), 1984.

D. N. Arnold, R. S. Falk, and R. Winther. Preconditioning in $H(\mathrm{div})$ and applications. *Math. Comp.*, 66(219):957–984, 1997.

E. Bänsch, P. Morin, and R. H. Nochetto. An adaptive Uzawa FEM for the Stokes problem: convergence without the inf-sup condition. *SIAM J. Numer. Anal.*, 40 (4):1207–1229, 2002.

R. Becker and S. Mao. Quasi-optimality of adaptive nonconforming finite element methods for the Stokes equations. *SIAM J. Numer. Anal.*, 49(3):970–991, 2011.

R. Becker, S. Mao, and Z. Shi. A convergent nonconforming adaptive finite element method with quasi-optimal complexity. *SIAM J. Numer. Anal.*, 47(6):4639–4659, 2010.

L. Beirão da Veiga, J. Niiranen, and R. Stenberg. A posteriori error estimates for the Morley plate bending element. *Numer. Math.*, 106(2):165–179, 2007.

P. Binev and R. DeVore. Fast computation in adaptive tree approximation. *Numer. Math.*, 97(2):193–217, 2004.

P. Binev, W. Dahmen, and R. DeVore. Adaptive finite element methods with convergence rates. *Numer. Math.*, 97(2):219–268, 2004.

D. Boffi, F. Brezzi, and M. Fortin. *Mixed Finite Element Methods and Applications*, volume 44 of *Springer Series in Computational Mathematics*. Springer, Heidelberg, 2013.

D. Braess. *Finite Elements*. Cambridge University Press, Cambridge, third edition, 2007.

S. C. Brenner. C^0 interior penalty methods. In *Frontiers in Numerical Analysis—Durham 2010*, volume 85 of *Lect. Notes Comput. Sci. Eng.*, pages 79–147. Springer, Heidelberg, 2012.

S. C. Brenner and L. R. Scott. *The Mathematical Theory of Finite Element Methods*, volume 15 of *Texts in Applied Mathematics*. Springer Verlag, New York, Berlin, Heidelberg, 3 edition, 2008.

S. C. Brenner and L.-Y. Sung. Linear finite element methods for planar linear elasticity. *Math. Comp.*, 59(200):321–338, 1992.

F. Brezzi. On the existence, uniqueness and approximation of saddle-point problems arising from Lagrangian multipliers. *Rev. Française Automat. Informat. Recherche Opérationnelle Sér. Rouge*, 8(R-2):129–151, 1974.

F. Brezzi and M. Fortin. *Mixed and Hybrid Finite Element Methods*, volume 15 of *Springer Series in Computational Mathematics*. Springer-Verlag, New York, 1991.

F. Brezzi, M. Fortin, and R. Stenberg. Error analysis of mixed-interpolated elements for Reissner-Mindlin plates. *Math. Models Methods Appl. Sci.*, 1(2):125–151, 1991.

C. Carstensen. A posteriori error estimate for the mixed finite element method. *Math. Comp.*, 66(218):465–476, 1997.

C. Carstensen. All first-order averaging techniques for a posteriori finite element error control on unstructured grids are efficient and reliable. *Math. Comp.*, 73 (247):1153–1165, 2004.

C. Carstensen. A unifying theory of a posteriori finite element error control. *Numer. Math.*, 100(4):617–637, 2005.

C. Carstensen and G. Dolzmann. A posteriori error estimates for mixed FEM in elasticity. *Numer. Math.*, 81(2):187–209, 1998.

C. Carstensen and H. Rabus. The adaptive nonconforming FEM for the pure displacement problem in linear elasticity is optimal and robust. *SIAM J. Numer. Anal.*, 50(3):1264–1283, 2012.

C. Carstensen and H. Rabus. Axioms of adaptivity for separate marking. 2015. In preparation, private communication.

C. Carstensen and M. Schedensack. Medius analysis and comparison results for first-order finite element methods in linear elasticity. *IMA J. Numer. Anal.*, 2014. doi: 10.1093/imanum/dru048. Published online.

C. Carstensen, D. Peterseim, and M. Schedensack. Comparison results of finite element methods for the Poisson model problem. *SIAM J. Numer. Anal.*, 50(6): 2803–2823, 2012.

C. Carstensen, D. Gallistl, and M. Schedensack. Quasi-optimal adaptive pseudostress approximation of the Stokes equations. *SIAM J. Numer. Anal.*, 51(3): 1715–1734, 2013a.

C. Carstensen, D. Gallistl, and M. Schedensack. Discrete reliability for Crouzeix-Raviart FEMs. *SIAM J. Numer. Anal.*, 51(5):2935–2955, 2013b.

C. Carstensen, D. Peterseim, and H. Rabus. Optimal adaptive nonconforming FEM for the Stokes problem. *Numer. Math.*, 123(2):291–308, 2013c.

C. Carstensen, M. Feischl, M. Page, and D. Praetorius. Axioms of adaptivity. *Comput. Math. Appl.*, 67(6):1195–1253, 2014a.

C. Carstensen, D. Gallistl, and J. Hu. A discrete Helmholtz decomposition with Morley finite element functions and the optimality of adaptive finite element schemes. *Comput. Math. Appl.*, 68(12):2167–2181, 2014b.

C. Carstensen, D. Gallistl, and M. Schedensack. L^2 best-approximation of the elastic stress in the Arnold-Winther FEM. 2014c. Preprint 2014-15, Humboldt-Universität zu Berlin, Institut für Mathematik.

C. Carstensen, K. Köhler, D. Peterseim, and M. Schedensack. Comparison results for the Stokes equations. *Appl. Numer. Math.*, 2014d. doi: 10.1016/j.apnum.2013.12.005. Published online.

C. Carstensen, B. D. Reddy, and M. Schedensack. A natural nonconforming FEM for the Bingham flow problem is quasi-optimal. 2014e. Preprint 2014-28, Humboldt-Universität zu Berlin, Institut für Mathematik.

C. Carstensen, D. Gallistl, and M. Schedensack. Adaptive nonconforming Crouzeix-Raviart FEM for eigenvalue problems. *Math. Comp.*, 84(293):1061–1087, 2015.

C. Carstensen et al. AFEM software package and documentaion. Humboldt-Universität zu Berlin, unpublished, 2009.

J. M. Cascon, C. Kreuzer, R. H. Nochetto, and K. G. Siebert. Quasi-optimal convergence rate for an adaptive finite element method. *SIAM J. Numer. Anal.*, 46(5):2524–2550, 2008.

P. G. Ciarlet. *The Finite Element Method for Elliptic Problems.* Studies in Mathematics and its Applications, Vol. 4. North-Holland Publishing Co., Amsterdam-New York-Oxford, 1978.

P. Clément. Approximation by finite element functions using local regularization. *Rev. Française Automat. Informat. Recherche Operationnelle*, 9(R-2):77–84, 1975.

M. Crouzeix and R. S. Falk. Nonconforming finite elements for the Stokes problem. *Math. Comp.*, 52(186):437–456, 1989.

M. Crouzeix and P.-A. Raviart. Conforming and nonconforming finite element methods for solving the stationary Stokes equations. I. *Rev. Française Automat. Informat. Recherche Opérationnelle Sér. Rouge*, 7(R-3):33–75, 1973.

E. Dari, R. Duran, C. Padra, and V. Vampa. A posteriori error estimators for nonconforming finite element methods. *RAIRO Modél. Math. Anal. Numér.*, 30 (4):385–400, 1996.

D. A. Di Pietro and A. Ern. *Mathematical Aspects of Discontinuous Galerkin Methods*, volume 69 of *Mathématiques & Applications (Berlin).* Springer, Heidelberg, 2012.

G. Engel, K. Garikipati, T. J. R. Hughes, M. G. Larson, L. Mazzei, and R. L. Taylor. Continuous/discontinuous finite element approximations of fourth-order elliptic problems in structural and continuum mechanics with applications to thin beams and plates, and strain gradient elasticity. *Comput. Methods Appl. Mech. Engrg.*, 191(34):3669–3750, 2002.

L. C. Evans. *Partial Differential Equations*, volume 19 of *Graduate Studies in Mathematics.* American Mathematical Society, Providence, RI, second edition, 2010.

R. Falk and B. Mercier. Error estimates for elasto-plastic problems. *RAIRO Analyse Numérique*, 11(R-2):135–144, 1977.

M. Fortin. A three-dimensional quadratic nonconforming element. *Numer. Math.*, 46(2):269–279, 1985.

M. Fortin and M. Soulie. A nonconforming piecewise quadratic finite element on triangles. *Internat. J. Numer. Methods Engrg.*, 19(4):505–520, 1983.

T. Gantumur. Optimal convergence rates for an adaptive mixed finite element method for the Stokes problem. 2014. Preprint, arXiv:1403.0895v4.

V. Girault and P.-A. Raviart. *Finite Element Methods for Navier-Stokes Equations*, volume 5 of *Springer Series in Computational Mathematics.* Springer-Verlag, Berlin, 1986.

P. Grisvard. *Elliptic Problems in Nonsmooth Domains*, volume 24 of *Monographs and Studies in Mathematics*. Pitman (Advanced Publishing Program), Boston, MA, 1985.

T. Gudi. A new error analysis for discontinuous finite element methods for linear elliptic problems. *Math. Comp.*, 79(272):2169–2189, 2010.

T. Gudi and M. Neilan. An interior penalty method for a sixth-order elliptic equation. *IMA J. Numer. Anal.*, 31(4):1734–1753, 2011.

J. Guzmán and M. Neilan. Conforming and divergence-free Stokes elements on general triangular meshes. *Math. Comp.*, 83(285):15–36, 2014.

J. Hu and J. Xu. Convergence and optimality of the adaptive nonconforming linear element method for the Stokes problem. *J. Sci. Comput.*, 55(1):125–148, 2013.

J. Hu, Z. Shi, and J. Xu. Convergence and optimality of the adaptive Morley element method. *Numer. Math.*, 121(4):731–752, 2012.

J. Huang and Y. Xu. Convergence and complexity of arbitrary order adaptive mixed element methods for the Poisson equation. *Sci. China Math.*, 55(5):1083–1098, 2012.

R. Kouhia and R. Stenberg. A linear nonconforming finite element method for nearly incompressible elasticity and Stokes flow. *Comput. Methods Appl. Mech. Engrg.*, 124(3):195–212, 1995.

C. Kreuzer and M. Schedensack. Instance optimal Crouzeix-Raviart adaptive finite element methods for the Poisson and Stokes problems. 2014. Preprint, arXiv:1404.3065.

J.-L. Lions and E. Magenes. *Non-homogeneous Boundary Value Problems and Applications. Vol. I.* Die Grundlehren der mathematischen Wissenschaften, Band 181. Springer-Verlag, New York-Heidelberg, 1972.

G. Matthies and L. Tobiska. Inf-sup stable non-conforming finite elements of arbitrary order on triangles. *Numer. Math.*, 102(2):293–309, 2005.

J. M. L. Maubach and P. J. Rabier. Nonconforming finite elements of arbitrary degree over triangles. RANA : Reports on applied and numerical analysis, Technische Universiteit Eindhoven, 2003.

P. Monk. *Finite Element Methods for Maxwell's Equations*. Numerical Mathematics and Scientific Computation. Oxford University Press, New York, 2003.

L. Morley. The triangular equilibrium element in the solution of plate bending problems. *Aeronaut.Quart.*, 19:149–169, 1968.

J. Nečas. *Les Méthodes Directes en Théorie des Équations Elliptiques.* Masson et Cie, Éditeurs, Paris; Academia, Éditeurs, Prague, 1967.

J.-C. Nédélec. Mixed finite elements in $\mathbf{R}^3$. *Numer. Math.*, 35(3):315–341, 1980.

J.-C. Nédélec. A new family of mixed finite elements in $\mathbf{R}^3$. *Numer. Math.*, 50(1): 57–81, 1986.

H. Rabus. A natural adaptive nonconforming FEM of quasi-optimal complexity. *Comput. Methods Appl. Math.*, 10(3):315–325, 2010.

H. Rabus. *On the quasi-optimal convergence of adaptive nonconforming finite element methods in three examples.* PhD thesis, 2014.

R. Rannacher and S. Turek. Simple nonconforming quadrilateral Stokes element. *Numer. Methods Partial Differential Equations*, 8(2):97–111, 1992.

P.-A. Raviart and J. M. Thomas. A mixed finite element method for 2nd order elliptic problems. In *Mathematical Aspects of Finite Element Methods (Proc. Conf., Consiglio Naz. delle Ricerche (C.N.R.), Rome, 1975)*, pages 292–315. Springer, Berlin, 1977.

W. Rudin. *Principles of Mathematical Analysis.* McGraw-Hill Book Co., New York-Auckland-Düsseldorf, third edition, 1976.

J. Schöberl. A posteriori error estimates for Maxwell equations. *Math. Comp.*, 77 (262):633–649, 2008.

L. R. Scott and M. Vogelius. Conforming finite element methods for incompressible and nearly incompressible continua. In *Large-scale Computations in Fluid Mechanics, Part 2 (La Jolla, Calif., 1983)*, volume 22 of *Lectures in Appl. Math.*, pages 221–244. Amer. Math. Soc., Providence, RI, 1985.

L. R. Scott and S. Zhang. Finite element interpolation of nonsmooth functions satisfying boundary conditions. *Math. Comp.*, 54(190):483–493, 1990.

R. Stevenson. Optimality of a standard adaptive finite element method. *Found. Comput. Math.*, 7(2):245–269, 2007.

R. Stevenson. The completion of locally refined simplicial partitions created by bisection. *Math. Comp.*, 77(261):227–241, 2008.

G. Stoyan and Á. Baran. Crouzeix-Velte decompositions for higher-order finite elements. *Comput. Math. Appl.*, 51(6-7):967–986, 2006.

The MathWorks, Inc. *Matlab version 8.1.0.604 (R2013a).* Natick, Massachusetts, United States., 2013.

A. Veeser. Approximating gradients with continuous piecewise polynomial functions. 2014. Preprint, arXiv:1402.3945.

R. Verfürth. *A Review of a Posteriori Error Estimation and Adaptive Mesh-Refinement Techniques*. Advances in numerical mathematics. Wiley, 1996.

M. Wang and J. Xu. Minimal finite element spaces for $2m$-th-order partial differential equations in R^n. *Math. Comp.*, 82(281):25–43, 2013.

Wolfram Research, Inc. *Mathematica*. Wolfram Research, Inc., Champaign, Illinois, version 9.0 edition, 2012.

J. Xu and L. Zikatanov. Some observations on Babuška and Brezzi theories. *Numer. Math.*, 94(1):195–202, 2003.

E. Zeidler. *Nonlinear Functional Analysis and Its Applications. III. Variational Methods and Optimization*. Springer-Verlag, New York, 1985.

A. Ženíšek. Interpolation polynomials on the triangle. *Numer. Math.*, 15:283–296, 1970.

L. Zhong, L. Chen, S. Shu, G. Wittum, and J. Xu. Convergence and optimality of adaptive edge finite element methods for time-harmonic Maxwell equations. *Math. Comp.*, 81(278):623–642, 2012.

A. Table of notation

Elementary notation

$\bullet$, id	identity mapping
$\emptyset$	empty set
card	cardinality of a set
$A \cup B$, $\cup\mathcal{A}$	union of two sets A and B or of the sets A, $A \in \mathcal{A}$
$A \cap B$	intersection of two sets A and B
$A \subseteq B$	A is subset of B
$A \setminus B$	$= \{a \in A \mid a \notin B\}$
$A \oplus B$	direct sum of A and B, $A \cap B = \emptyset$ and $A \oplus B = \{a + b \mid a \in A, b \in B\}$
$\mathbb{N}$	positive integers, $\mathbb{N} = \{1, 2, 3, \dots\}$
$\mathbb{N}_0$	positive integers and zero, $\mathbb{N}_0 = \{0\} \cup \mathbb{N}$
$\mathfrak{S}_m$	symmetric group, i.e., the set of all permutations of $(1, \dots, m)$
$\mathbb{R}$	field of real numbers
$\mathbb{R}^{n\times m}$	space of $n \times m$ matrices with real coefficients
$I_{n\times n}$	unit matrix in $\mathbb{R}^{n\times n}$
$A^\top$	transpose of the matrix A
$\mathbb{S}$	$= \{A \in \mathbb{R}^{n\times n} \mid A = A^\top\}$
$\mathrm{sym}(A)$	symmetric part of $A \in \mathbb{R}^{n\times n}$, $\mathrm{sym}(A) = (A + A^\top)/2$
$\mathrm{tr}(A)$	trace of a matrix $A \in \mathbb{R}^{n\times n}$, $\mathrm{tr}(A) = \sum_{j=1}^n A_{jj}$
$\mathrm{dev}(A)$	deviatoric part of a matrix $A \in \mathbb{R}^{n\times n}$, $\mathrm{dev}(A) = A - (1/n)\mathrm{tr}(A) I_{n\times n}$
$\mathbb{C}$	elasticity tensor, $\mathbb{C}A = 2\mu A + \lambda \mathrm{tr}(A) I_{2\times 2}$ for all $A \in \mathbb{R}^{2\times 2}$ with Lamé parameter $0 < \mu, \lambda < \infty$
$x \cdot y$	Euclidean scalar product on $\mathbb{R}^n$, $x \cdot y = \sum_{j=1}^n x_j y_j$
$A : B$	scalar product of $A, B \in \mathbb{R}^{n\times m}$ defined by $A : B = \sum_{j=1}^n \sum_{k=1}^m A_{jk} B_{jk}$
$A \wedge B$	cross (or vector) product of two vectors $A, B \in \mathbb{R}^3$
$\lvert x\rvert$	absolute value of $x \in \mathbb{R}$, Euclidean length of a vector $x \in \mathbb{R}^n$, $\lvert x\rvert = \sqrt{x \cdot x}$, Frobenius norm of a matrix $x \in \mathbb{R}^{n\times m}$, $\lvert x\rvert = \sqrt{x : x}$, or length of a multi-index $x \in \mathbb{N}_0^n$, $\lvert x\rvert = \sum_{j=1}^n x_j$
(a, b), $[a, b]$	open (resp. closed) real interval
$\mathrm{dist}(x, \omega)$	Euclidean distance of $x \in \mathbb{R}^n$ to $\omega \subseteq \mathbb{R}^n$
$\mathrm{diam}(A)$	diameter of a set $A \subseteq \mathbb{R}^n$, $\mathrm{diam}(A) = \sup_{x,y\in A} \lvert x - y\rvert$

$B_r(x)$	open ball with radius r and centre x
$\overline{\omega}$	closure of the set $\omega \subseteq \mathbb{R}^n$ with respect to the Euclidean norm
$\operatorname{int}(\omega)$	interior of the set $\omega \subseteq \mathbb{R}^n$ with respect to the Euclidean norm
$\partial\omega$	boundary of the set $\omega \subseteq \mathbb{R}^n$ with respect to the Euclidean norm
$\operatorname{conv}\{A_1, \dots, A_n\}$	convex hull of $A_1, \dots, A_n \in \mathbb{R}^n$
$\operatorname{span}(A_1, \dots, A_n)$	linear hull of $A_1, \dots, A_n$
$\operatorname{im}(A)$	range or image of a map $A : X \to Y$, $\operatorname{im}(A) \subseteq Y$
$\ker(A)$	kernel of a map $A : X \to Y$, $\ker(A) \subseteq X$
$H^\star$	dual space of a Hilbert space H
$\langle \bullet, \bullet \rangle_H$	dual pairing for a Hilbert space $(H, (\bullet, \bullet)_H)$, $\langle \bullet, \bullet \rangle_H : H^\star \times H \to \mathbb{R}$
Π_{X_h}	projection to X_h with respect to $(\bullet, \bullet)_X$ for a Hilbert space $(X, (\bullet, \bullet)_X)$ with $X_h \subseteq X$

Differential operators

D	derivative
∇	gradient, $\nabla v = Dv^\top$
Δ	Laplacian, applied row-wise to vector fields
div	divergence, applied row-wise to vector fields
Curl	Curl operator, $\operatorname{Curl} v = (-\partial v/\partial y, \partial v/\partial x)$ for scalar-valued functions; applied row-wise to vector fields (see Definition 2.2 for scalar- and vector-valued functions and Definition 6.5 for tensor-valued functions)
curl	rotation of a vector field, $\operatorname{curl} v = -\partial v_1/\partial y + \partial v_2/\partial x$; applied row-wise to matrix-valued functions (see Definition 2.2 for vector- and matrix-valued functions and Definition 6.5 for tensor-valued functions)
ε	symmetric part of the gradient, $\varepsilon(v) = \operatorname{sym}(Dv)$

Notation related to Lebesgue and Sobolev functions

Let $\Omega \subseteq \mathbb{R}^n$.

$\operatorname{meas}_k(\omega)$	k-dimensional surface measure (Hausdorff measure) of $\omega \subseteq \mathbb{R}^n$ for $k \leq n$
$\operatorname{supp}(f)$	support of a function $f : \Omega \to \mathbb{R}^m$, $\operatorname{supp}(f) := \overline{\{x \in \Omega \mid f(x) \neq 0\}}$
$v\|_\omega$	restriction of $v : \Omega \to \mathbb{R}^m$ to $\omega \subseteq \Omega$

$C_c^\infty(\Omega)$, $C_c^\infty(\Omega;X)$	space of infinitely differentiable functions $v:\Omega\to\mathbb{R}$ (resp. $v:\Omega\to X$) with compact support in Ω, $\operatorname{supp}(v)\subseteq\Omega$
$\int_\omega f\,dx$	n-dimensional Lebesgue integral of f over $\omega\subseteq\mathbb{R}^n$
$\int_\omega f\,ds$	$(n-1)$-dimensional surface integral of f over $\omega\subseteq\mathbb{R}^n$
$\fint$	mean value integral (see Definition 2.1)
$L^2(\omega)$, $L^2(\omega;X)$	square-integrable functions over ω with values in $\mathbb{R}$ (resp. X)
$L^2_0(\omega)$	square-integrable functions with vanishing integral mean
$\|f\|_{L^2(\omega)}$	L^2 norm of f over ω
$(f,g)_{L^2(\Omega)}$	L^2 scalar product of f and g
$f\perp_{L^2(\Omega)}g$	f is orthogonal to g with respect to the L^2 scalar product $(\bullet,\bullet)_{L^2(\Omega)}$
$H^k(\omega)$, $H^k(\Omega;X)$	Sobolev space of k times weakly differentiable L^2 functions with values in $\mathbb{R}$ (resp. X) and weak derivatives in L^2
$\|f\|_{H^k(\Omega)}$	kth-order Sobolev norm
$H^k_0(\Omega)$, $H^k_0(\Omega;X)$	closure of $C_c^\infty(\Omega)$ (resp. $C_c^\infty(\Omega;X)$) with respect to $\|\bullet\|_{H^k(\Omega)}$
$H^1_\Gamma(\Omega)$, $H^1_\Gamma(\Omega;X)$	Sobolev space of (weakly) differentiable functions with vanishing trace on $\Gamma\subseteq\partial\Omega$
$H^{-m}(\Omega)$	dual space of $H^m_0(\Omega)$
$\langle\bullet,\bullet\rangle_{H^{-1}}$	duality pairing of $H^{-1}(\Omega)$ and $H^1_0(\Omega)$
$H(\operatorname{div},\Omega)$, $H(\operatorname{div},\Omega;\mathbb{R}^{n\times n})$, $H(\operatorname{div},\Omega;\mathbb{S})$	space of functions $v:\Omega\to\mathbb{R}^n$ (resp. $v:\Omega\to\mathbb{R}^{n\times n}$ or $v:\Omega\to\mathbb{S}$) with divergence in $L^2(\Omega)$ (resp. in $L^2(\Omega;\mathbb{R}^n)$)
$H(\operatorname{div}^m,\Omega;X)$	space of functions with mth weak divergence (see Definition 6.6
$P_k(\omega)$, $P_k(\omega;X)$	set of functions on ω with values in $\mathbb{R}$ (resp. X) which components are polynomials of total degree $\le k$
$Q_k(\omega)$	space of polynomials of partial degree $\le k$

Notation related to triangulations

$\mathbb{T}$	set of admissible triangulations, see Definition 2.4
$\mathcal{N}(T)$	set of vertices of a triangle T
$\mathcal{E}(T)$	set of edges of a triangle T
$\mathcal{N}=\mathcal{N}(\mathcal{T})$, $\mathcal{E}=\mathcal{E}(\mathcal{T})$	set of vertices (resp. edges) of a triangulation $\mathcal{T}$
ν_E, τ_E	unit normal and unit tangent associated with E
$[\bullet]_E$	jump across an edge E
ω_E	edge patch

$P_k(\mathcal{T})$, $P_k(\mathcal{T}, X)$	set of piecewise polynomials with values in $\mathbb{R}$ (resp. X)
$h_{\mathcal{T}}$	piecewise constant mesh-size function, $h_{\mathcal{T}}\|_T = h_T = \operatorname{meas}_n(T)^{1/n}$ for a simplex $T \subseteq \mathbb{R}^n$
h_E	length of an edge E
φ_z	continous P_1 nodal basis function of $z \in \mathcal{N}(\mathcal{T})$
D_{NC}, ∇_{NC}, $\operatorname{div}_{\mathrm{NC}}$, $\operatorname{Curl}_{\mathrm{NC}}$, $\operatorname{curl}_{\mathrm{NC}}$, $\varepsilon_{\mathrm{NC}}$	piecewise differential operators
$\operatorname{osc}(f, \mathcal{T})$	oscillations of $f \in L^2(\Omega; \mathbb{R}^m)$, $\operatorname{osc}(f, \mathcal{T}) := \|h_{\mathcal{T}}(f - \Pi_0 f)\|_{L^2(\Omega)}$

B. Implementation

This appendix chapter gives an overview of the Matlab implementation for the numerical examples from Sections 3.7, 4.4, 5.6, and 6.7. The implementation is based on the AFEM software package [Carstensen et al., 2009] maintained by the Numerical Analysis Group at HU Berlin.

B.1. Structure of the implementation

Solvers for novel discretizations

The following programs compute the solutions for the discretization (3.5) for the Poisson problem for $k = 0, 1, 2$.

```
function [p,alpha,ndof,STIMA2,rhs,conditionNumber] = ...
                                  solveHHPoissonP1(phi,graduD,c4n,n4e,~,n4sNb)
function [p,alphah,ndof,STIMA2,rhs,conditionNumber] = ...
                                  solveHHPoissonP2(phi,graduD,c4n,n4e,~,n4sNb)
function [p,alphah,ndof,STIMA2,rhs,conditionNumber] = ...
                                  solveHHPoissonP3(phi,graduD,c4n,n4e,~,n4sNb)
```

The solver for the discretization (4.6) for the Stokes equations for $k = 0, 1$ are implemented as

```
function [sigma,alpha,p,ndof,STIMA2,rhs,conditionNumber] = ...
                    solveHHstokesP1(phi,graduD,c4n,n4e)
function [sigma,alpha,p,ndof,STIMA2,rhs,conditionNumber] = ...
                    solveHHstokesP2(phi,graduD,c4n,n4e)
```

For the Navier-Lamé equations of linear elasticity, the solver for the discretization of Subsection 5.3.3 for $k = 1$ is implemented as

```
function [sigma,alpha,chi,ndof,STIMA2,b2,conditionNumber] = ...
                           solveHHLETH(phi,graduD,c4n,n4e,~,n4sNb,mu,lambda)
```

The novel FEM for the biharmonic problem (6.16) for $m = 2$ is implemented for $k = 0, 1$ as

```
function [p,alpha,ndof,STIMA2,rhs,conditionNumber] = ...
                           solveHHplateP1(phi,hessuD,c4n,n4e)
function [p,alpha,ndof,STIMA2,rhs,conditionNumber] = ...
                           solveHHplateP2(phi,graduD,c4n,n4e)
```

For linear elasticity, the standard conforming P_1 FEM is implemented as

```
function [u1,u2,ndofs,A,b,sigma4e,div4e] = ...
                 solveP1P1LinElast(f,g,u4Db,lambda,mu,c4n,n4e,n4sDb,n4sNb)
```

Error estimation

The error estimator contributions for μ and λ for the Poisson problem, the Stokes equations, the biharmonic problem, and the problem $-\Delta^3 u = f$ are implemented as

```
function eta4eSq = estimateData(k,phi,graduD,c4n,n4e)
function eta4eSq = estimateRest(k,graduD,p,c4n,n4e,n4sDb,n4sNb)
```

For linear elasticity, the error estimator contributions are computed by

```
function eta4eSq = estimateData4LE(phi,graduD,c4n,n4e,mu,lambda)
function eta4eSq = estimateRest4LE(graduD,sigma,alpha,chi,...
                                   c4n,n4e,n4sDb,n4sNb,mu,lambda)
```

For the standard conforming P_1 FEM, the error estimator contributions are implemented as

```
function eta4e = estimateP1P1EtaElementsData(f,c4n,n4e)
function eta4e = estimateP1P1EtaElementsRest(g,u1,u2,c4n,n4e,n4sDb,n4sNb,...
                                             mu,lambda,Sigma4e)
```

AFEM loops

The adaptive algorithms for the Poisson problem, the Stokes equations, the Navier-Lamé equations, the biharmonic problem, and the problem $-\Delta^3 u = f$ are implemented as

```
function afemPoissonHelmholtz(name,degree,minndof,adaptive,theta,rho,...
                              kappa,plotsol,saveinf,savefolder)
function afemStokesHelmholtz(name,degree,minndof,adaptive,theta,rho,kappa,...
                              plotsol,saveinf,savefolder)
function afemLEHelmholtz(name,E,nu,minndof,adaptive,theta,rho,...
                              kappa,plotsol,saveinf,savefolder)
function afemPlateHelmholtz(name,degree,minndof,adaptive,theta,rho,kappa,...
                              plotsol,saveinf,savefolder)
function afem6thorderHelmholtz(name,degree,minndof,adaptive,theta,rho,...
                              kappa,plotsol,saveinf,savefolder)
```

Further programs

The L^2 projection onto piecewise P_k functions for $k = 0, 1, 2$ is implemented as

```
function Pikphi4e = projectPk(c4n,n4e,phi,k)
```

The following plot routines create a quiver plot of a piecewise P_k function

```
function plotHHp(c4n, n4e, p, OPTtitle)
function plotHHpP2(c4n, n4e, pApprox, OPTtitle)
function plotHHpP3(c4n, n4e, pApprox, OPTtitle)
```

The following programs compute the errors for a piecewise P_k approximation for $k = 0, 1, 2$.

```
function error4e = error4eHHEnergy(c4n,n4e,gradExact,pApprox)
function error4e = error4eHHEnergyP2(c4n,n4e,gradExact,pApprox)
function error4e = error4eHHEnergyP3(c4n,n4e,gradExact,pApprox)
```

The following program saves informations and is applied during the AFEM loops

```
function saveInformation(folder,problem,geom,ndofList,etaListData,...
         etaListRest,conditionList,degree,minndof,adaptive,infostring,...
         casesList,errorList,errorList_p)
```

The input data of the numerical experiments are stored in

```
function [c4n,n4e,n4sDb,n4sNb,gradu4Db,phi,exsolknown,u_exact,grad_exact] ...
                  = load_data_Poisson(name)
function [c4n,n4e,n4sDb,n4sNb,gradu4Db,phi,exsolknown,u_exact,grad_exact,...
                  p_exact] = load_data_Stokes(name)
function [c4n,n4e,n4sDb,n4sNb,gradu4Db,phi,exsolknown,u_exact,grad_exact,...
                  stress_exact] = load_data_elasticity(name,mu,lambda)
function [c4n,n4e,n4sDb,n4sNb,hessu4Db,phi,exsolknown,u_exact,...
                  hess_exact] = load_data_Plate(name)
function [c4n,n4e,n4sDb,n4sNb,D3u4Db,phi,exsolknown,u_exact,...
                  grad_exact,hess_exact,D3u_exact] = load_data_6thorder(name)
```

The input data for the P_1 conforming FEM for linear elasticity are stored in

```
function [c4n,n4e,n4sDb,n4sNb,u4Db,f,g,exsolknown,u_exact,grad_exact,...
            stress_exact] = load_data_elasticityP1(name,mu,lambda)
```

B.2. Reproduction of the numerical experiments

All numerical experiments from Section 3.7 can be reproduced by the call

```
experiments_Poisson(200000)
```

All numerical experiments from Section 4.4 can be reproduced by the call

```
experiments_Stokes(1000000)
```

All numerical experiments from Section 5.6 can be reproduced by the call

```
experiments_LE(200000)
```

All numerical experiments from Section 6.7 can be reproduced by the calls

```
experiments_plate(200000)
experiments_6thorder(200000)
```

B.3. Content of the software archive

```
├── afem6thorderHelmholtz.m    afemLEHelmholtz.m        afemLEP1.m
│   afemPlateHelmholtz.m       afemPoissonHelmholtz.m   afemStokesHelmholtz.m
│   experiments_6thorder.m     experiments_LE.m         experiments_plate.m
│   experiments_Poisson.m      experiments_Stokes.m     GNUGPLv3.txt
│   LICENSE.txt                load_data_6thorder.m     load_data_elasticity.m
│   load_data_elasticityP1.m   load_data_Plate.m        load_data_Poisson.m
│   load_data_Stokes.m
├── rotL-shapeNb ..... folder contains *.dat-files with geometrical data
├── estimate_error
│   ├── error4eHHEnergy.m               error4eHHEnergyP2.m   error4eHHEnergyP3.m
│   │   estimateData4LE.m               estimateData.m        estimateP1P1EtaElementsData.m
│   │   estimateP1P1EtaElementsRest.m   estimateRest4LE.m     estimateRest.m
├── plot
│   ├── plotHHp.m   plotHHpP2.m   plotHHpP3.m
├── solveHelmholtz
│   ├── solveHH6thorderP1.m   solveHH6thorderP2.m   solveHH6thorderP3.m
│   │   solveHHLETH.m         solveHHplateP1.m      solveHHplateP2.m
│   │   solveHHPoissonP1.m    solveHHPoissonP2.m    solveHHPoissonP3.m
│   │   solveHHstokesP1.m     solveHHstokesP2.m     solveP1P1LinElast.m
├── tools
│   ├── cart2pol_neu.m   CElast.m            component.m
│   │   projectPk.m      saveInformation.m
├── separateMarking ..... Author: H. Rabus [Rabus, 2014]
│   ├── approx.m   completion.m   overlay.m   refineBi3GB_irregular.m
├── afem4thesis ..... files taken from AFEM [Carstensen et al., 2009]
│   ├── Lshape ..... folder contains *.dat-files with geometrical data
│   ├── LshapeNb ..... folder contains *.dat-files with geometrical data
│   ├── Square ..... folder contains *.dat-files with geometrical data
│   ├── closure.m            computeArea4e.m     computeE4n.m          computeE4s.m
│   │   computeLength4s.m    computeMid4e.m      computeMid4s.m        computeN4s.m
│   │   computeNormal4e.m    computeS4e.m        computeS4n.m          computeTangent4e.m
│   │   computeTangent4s.m   integrate.m         L2Norm.m              loadGeometry.m
│   │   markBulk.m           plotConvergence.m   plotTriangulation.m   refineBi3GB.m
│   │   refineUniformRed.m
```

C. Data medium containing the software

The online version of this document contains the software as embedded tar-file. Please use an appropriate pdf viewer to extract the file, such as KDE Okular or Adobe Reader. In contrast to the thesis' text, the code is provided under the terms of the GNU General Public License as published by the Free Software Foundation, either version 3 of the License, or (at your option) any later version. Refer to the file LICENSE.txt in the software archive for more information.

List of figures

Erklärung

Ich erkläre, dass ich die vorliegende Arbeit selbständig und nur unter Verwendung der angegebenen Literatur und Hilfsmittel angefertigt habe.

Berlin, den 20. März 2015 Mira Schedensack